



Investigation of the Role of Novel SGK1 Isoforms in  
Regulation of Sodium Transport in Kidney  
Epithelial Cells

Nigel Allan Daniels

**B.Sc. (Hons)**

Thesis submitted in partial fulfilment of the requirements of the regulations for the degree  
of Doctor of Philosophy

Newcastle University

Faculty of Medical Sciences

Institute of Cellular Medicine

**August 2010**

## **Abstract**

Serum/glucocorticoid regulated kinase 1 (SGK1) is a key component of the pathway that leads to activation of the epithelial sodium channel (ENaC) in the aldosterone-sensitive distal nephron (ASDN). Regulation of ENaC is a major determinant of renal Na<sup>+</sup> absorption and overall body fluid homeostasis and blood pressure. Studies from our laboratory have shown that human skin cells express multiple SGK1 isoforms (A-F) that arise from alternative transcriptional start sites and RNA splicing at the *SGK1* locus. The aim of this study was to investigate if SGK1 isoforms are also expressed in the ASDN and to assess their potential role in regulating Na<sup>+</sup> transport. For these studies the mouse cortical collecting duct cell line mpkCCD<sub>c14</sub>, was used as an *in vitro* model of the ASDN. Comparison of mouse *Sgk1* expressed sequence tags (ESTs) with genomic DNA, identified four potential *Sgk1* isoforms (*Sgk1a-1d*). Each isoform has a unique amino terminus of varying size, but otherwise an identical sequence. Using sequence specific primers, mRNA expression of all four isoforms was confirmed by RT-PCR from purified mpkCCD<sub>c14</sub> cell and mouse renal tissue RNA. mpkCCD<sub>c14</sub> cells exposed to aldosterone (Aldo) or Aldo plus insulin (Ins) showed a time-dependent increase in the endogenous expression levels of multiple *Sgk1* bands within 1 hour of treatment. These Aldo and Aldo + Ins-induced endogenous *Sgk1* bands co-migrated with overexpressed *Sgk1 a-d* isoform bands. Aldosterone also produced a significant increase in amiloride-sensitive (ENaC-mediated) equivalent short circuit current within 2 hours of exposure, peaking after 4 hours. Insulin potentiated the Aldo response, but had no effect alone. Specific inhibitors showed that the hormonal response involved both PI3Kinase and mTOR-dependent and independent pathways. Immunofluorescence studies utilising cloned and tagged SGK1 isoforms in transfected HEK293T cells revealed cytoplasmic network-like staining for all

SGK1 isoforms except for SGK1D, which produced plasma membrane staining. In mouse renal tissue, endogenous Sgk1d localised to the basolateral membrane of collecting duct epithelial cells. Furthermore co-immunoprecipitation of cloned human SGK1 and mouse Sgk1 proteins with the Aldo induced regulatory protein, glucocorticoid-induced leucine zipper protein 1 (GILZ1), showed isoform-specific interactions. Collectively, these results build upon our understanding of *SGK1* gene expression, protein localisation and function in the ASDN.

## **Acknowledgements**

I would like to thank my supervisors Dr Mike Gray, Dr John Sayer, and Dr Penny Lovat for their guidance and support during my research. I would also like to thank Dr John Sayer and Dr Fiona Oakley for advice and encouragement during their assessments of my research progress. Thanks to all members of the dermatology, epithelial research, and bioimaging laboratories during my PhD for their help, support, and friendship.

A huge thank you to my family and friends, in particular my mum Helen, my dad Pete, and my brothers James and Alex, for their support, inspiration, and love on which I constantly depend. And a very special thank you to my Natalie, for being my partner, my love, and my soul-mate.

This work was funded by the Hypertension Trust.

## **Declaration**

This thesis is submitted to the degree of Doctor of Philosophy at Newcastle University. The research was performed in the Institutes of Cell and Molecular Biosciences and Cellular Medicine under the supervision of Dr Mike Gray, Dr John Sayer, and Dr Penny Lovat and is my own work unless otherwise stated within the text. I certify that none of the material offered in this thesis has previously been submitted by me for a degree or any other qualification at this or any other university.

## **List of Contents**

<b>Chapter 1 - Introduction .....</b>	<b>1</b>
1.1 Renal regulation of sodium balance.....	1
1.1.1 Renal regulation of blood pressure .....	2
1.1.2 The renin-angiotensin-aldosterone system .....	3
1.1.3 The aldosterone-sensitive distal nephron.....	4
1.1.4 The principal cells of the collecting duct.....	4
1.2 Regulation of sodium transport in principal cells.....	6
1.2.1 The mineralocorticoid receptor.....	7
1.2.2 The phosphoinositide 3-kinase pathway.....	8
1.2.3 The mitogen-activated protein kinase/extracellular signal-regulated kinase pathway.....	11
1.2.4 The protein kinase A pathway .....	12
1.3 Serum/glucocorticoid regulated kinase 1 .....	12
1.3.1 Regulation of serum/glucocorticoid regulated kinase 1 .....	14
1.3.2 Functions of serum/glucocorticoid regulated kinase 1 .....	18
1.4 Epithelial sodium channel.....	20
1.4.1 Regulation of epithelial sodium channel .....	22
1.5 Hypertension.....	27
1.5.1 SGK1 and other diseases .....	30
1.6 Aims.....	31
<b>Chapter 2 - Materials and Methods .....</b>	<b>32</b>
2.1 Cell Culture.....	32
2.1.1 Culture of mpkCCD <sub>c14</sub> cells on Transwell supports.....	33
2.1.2 Hormone and drug treatments.....	33
2.1.3 Transient transfection of plasmid DNA.....	34
2.1.4 siRNA knockdown.....	35
2.2 Molecular Biology .....	36
2.2.1 DNA cloning.....	36
2.2.2 Restriction enzyme digests .....	39
2.2.3 Bacterial culture.....	40
2.2.4 Transformation into <i>E.coli</i> .....	40
2.2.5 Plasmid DNA extraction.....	40
2.2.6 Polymerase chain reaction (PCR).....	41
2.2.7 Reverse transcriptase (RT)-PCR.....	41
2.2.8 RNA purification, quantification and storage.....	41
2.2.9 DNA isolation, quantification and storage .....	42
2.2.10 Primers .....	42
2.2.11 Agarose gel electrophoresis .....	44
2.2.12 DNA sequencing.....	45
2.2.13 <i>In vitro</i> protein synthesis from Sgk1 isoform DNA .....	45
2.3 Western Blotting (Immunoblotting) .....	46
2.3.1 Preparation, treatments and storage of protein samples .....	46
2.3.2 Protein quantification.....	47
2.3.4 Sodium dodecyl sulphate polyacrylamide gel electrophoresis (SDS-PAGE) and protein transfer .....	47

2.3.4 Membrane immunostaining .....	48
2.3.5 Visualisation .....	49
2.3.6 Membrane stripping .....	50
2.3.7 Data analysis .....	50
2.4 Immunoprecipitation .....	51
2.5 Electrophysiology .....	52
2.5.1 Measurement of transepithelial resistance and potential difference .....	52
2.5.2 Treatments .....	52
2.5.3 Data analysis .....	53
2.6 Immunofluorescence .....	53
2.6.1 Human renal tissue collection and preparation .....	53
2.6.2 Mouse renal tissue collection and preparation .....	54
2.6.3 Tissue sectioning .....	54
2.6.4 Preparation of tissue and cells for immunofluorescence studies .....	55
2.6.5 Microscopy .....	57
2.7 Statistical analyses .....	57
<b>Chapter 3 - Identification of Multiple Isoforms of Mouse Sgk1.....</b>	<b>58</b>
3.1 Introduction .....	58
3.2 Results .....	59
3.2.1 Identification and comparisons of mouse Sgk1 variant sequences .....	59
3.2.2 Features of the mouse Sgk1 variant sequences .....	60
3.2.3 Predicted protein products for the mouse Sgk1 variants .....	62
3.2.4 Cloning of the mouse Sgk1 isoforms .....	65
3.2.5 Multiple mouse Sgk1 isoforms are expressed in mpkCCD <sub>cl4</sub> cells .....	68
3.2.6 Aldosterone stimulates endogenous expression of multiple Sgk1 isoforms in mpkCCD <sub>cl4</sub> cells .....	69
3.2.7 Co-migration of overexpressed Sgk1 isoforms with endogenous Sgk1 proteins .....	74
3.2.8 Co-migration of overexpressed Sgk1 isoform proteins with synthesised Sgk1 isoform proteins .....	75
3.2.9 Detection of multiple phosphorylated Sgk1 isoforms .....	77
3.2.10 Sensitivity of aldosterone-stimulated Sgk1 isoforms to LY294002 .....	79
3.2.11 Detection of overexpressed mouse Sgk1 isoforms with human SGK1 isoform-specific antisera .....	83
3.3 Discussion .....	87
3.3.1 Identification and features of mouse Sgk1 isoforms .....	87
3.3.3 Cloning of the mouse Sgk1 isoforms .....	89
3.3.4 Identification of multiple aldosterone-stimulated endogenous Sgk1 isoforms in mpkCCD <sub>cl4</sub> cells .....	90
3.3.5 Co-migration of overexpressed Sgk1 isoform proteins with endogenous and synthesised Sgk1 isoform proteins .....	91
3.3.6 Detection of phosphorylated Sgk1 isoforms .....	92
3.3.7 Sensitivity of aldosterone-stimulated Sgk1 isoforms to LY294002 .....	92
3.3.8 Detection of overexpressed isoforms with isoform-specific antisera .....	93
3.4 Summary .....	94
<b>Chapter 4 - Electrophysiological Studies of the Regulation of Sodium Transport</b>	<b>95</b>
4.1 Introduction .....	95
4.2 Results .....	97
4.2.1 Aldosterone and insulin stimulate ENaC-mediated sodium transport .....	97

4.2.2 LY294002 reduces aldosterone and aldosterone plus insulin -stimulated sodium transport .....	106
4.2.3 Rapamycin reduces aldosterone plus insulin-stimulated sodium transport .	108
4.2.4 Effect of overexpressing individual mouse Sgk1 isoforms a-d on ENaC-mediated sodium transport.....	111
4.2.5 Effect of Sgk1 knockdown using siRNA on transepithelial amiloride-sensitive equivalent short circuit current .....	120
4.3 Discussion.....	122
4.3.1 Aldosterone and insulin stimulate amiloride-sensitive equivalent short circuit current .....	122
4.3.2 Sensitivity of aldosterone and insulin-stimulated ENaC-mediated sodium transport to inhibition of activators of SGK1 .....	124
4.3.3 Overexpression and knockdown of Sgk1 in mpkCCD <sub>c14</sub> cells grown on permeable filter supports .....	126
4.4 Summary.....	129
<b>Chapter 5 - Localisation and Co-Immunoprecipitation Studies as Clues to Regulation of SGK1 .....</b>	<b>130</b>
5.1 Introduction.....	130
5.2 Results.....	131
5.2.1 Fluorescence microscopy of SGK1D in human renal tissue .....	131
5.2.2 Fluorescence microscopy of Sgk1d in mouse renal tissue .....	136
5.2.3 Fluorescence microscopy of immunostained FLAG-tagged human SGK1 isoforms in HEK293T cells .....	138
5.2.4 Fluorescence microscopy of immunostained FLAG-tagged mouse Sgk1 isoforms in HEK293T cells .....	145
5.2.5 Co-immunoprecipitation of human SGK1 with GILZ1 .....	149
5.2.6 Co-immunoprecipitation of mouse Sgk1 with GILZ1.....	152
5.3 Discussion.....	154
5.3.1 Fluorescence microscopy of SGK1D in human and mouse renal tissue .....	154
5.3.2 Fluorescence microscopy of FLAG-tagged SGK1 isoforms in HEK293T cells .....	156
5.3.3 Co-immunoprecipitation of SGK1 isoforms with GILZ1 .....	159
5.4 Summary.....	160
<b>Chapter 6 - Conclusions .....</b>	<b>162</b>
6.1 Achievement of aims .....	162
6.2 Review of research path.....	162
6.3 Final discussion.....	165
6.4 Relevance of findings .....	166
6.5 Future work.....	168
<b>References.....</b>	<b>171</b>
<b>Appendix - Raw DNA Sequencing Data .....</b>	<b>171</b>
<b>Publications and presentations arising from the work presented in this thesis....</b>	<b>203</b>

## **List of Tables**

<b>Table 1.1</b> A summary of the PI3K classes and their respective regulation, substrate reactions, and constituting subunits .....	9
<b>Table 2.1</b> Hormone and drug treatments.....	34
<b>Table 2.2</b> Qiagen siRNA data .....	36
<b>Table 2.3</b> Primers for identification of mouse Sgk1 isoforms .....	43
<b>Table 2.4</b> Primers for cloning into pCMV-SPORT6 .....	43
<b>Table 2.5</b> Primers for cloning into pFLAG-CMV <sup>TM</sup> -2 .....	44
<b>Table 2.6</b> Details of antibodies used in Western blotting .....	49
<b>Table 2.7</b> Primary antibodies used in immunofluorescence studies.....	56
<b>Table 3.1</b> Sgk1 isoform nucleotide data.....	60
<b>Table 3.2</b> Sgk1 isoform protein data .....	64
<b>Table 5.1</b> SGK1 isoform localisation summary .....	149

## List of Figures

<b>Figure 1.1</b>	Structure of a nephron indicating the different segments and vasculature.....	2
<b>Figure 1.2</b>	Routes of the major ion and water transport in principal cells.....	5
<b>Figure 1.3</b>	Simplified SGK1-regulated Na <sup>+</sup> transport in a CCD principal cell.....	7
<b>Figure 1.4</b>	Structure of the epithelial sodium channel (ENaC).....	22
<b>Figure 1.5</b>	A model of a principal cell highlighting the signalling pathways involved in regulation of ENaC .....	23
<b>Figure 2.1</b>	A vector map of the pLEGFP-N1 vector.....	35
<b>Figure 2.2</b>	pCMV-SPORT6 vector map .....	38
<b>Figure 2.3</b>	pFLAG-CMV-2 vector map .....	39
<b>Figure 2.4</b>	Vector map of the TNT® Luciferase SP6 control vector.....	45
<b>Figure 3.1</b>	The mouse <i>Sgk1</i> locus, showing the possible alternative splicing and the resulting mRNA.....	62
<b>Figure 3.2</b>	Full-length mouse <i>Sgk1</i> isoform proteins .....	65
<b>Figure 3.3</b>	The pCMV-SPORT6 vector map and multiple cloning site sequence.....	67
<b>Figure 3.4</b>	mpkCCD <sub>c14</sub> cells express all four isoform-specific <i>Sgk1</i> variant mRNAs ..	68
<b>Figure 3.5</b>	Native mouse kidney tissue expresses specific <i>Sgk1a, b, c, and d</i> variant mRNAs .....	69
<b>Figure 3.6</b>	Aldosterone stimulates endogenous <i>Sgk1</i> protein expression in mpkCCD <sub>c14</sub> cells in a dose-dependent manner .....	71
<b>Figure 3.7</b>	Aldosterone stimulates expression of multiple endogenous <i>Sgk1</i> proteins in mpkCCD <sub>c14</sub> cells in a time-dependent manner.....	74
<b>Figure 3.8</b>	Aldosterone plus insulin-stimulated endogenous <i>Sgk1</i> proteins co-migrate with overexpressed <i>Sgk1</i> isoforms .....	75
<b>Figure 3.9</b>	Synthesised and overexpressed <i>Sgk1</i> isoforms show similar protein products.....	77
<b>Figure 3.10</b>	No detected expression of phosphorylated <i>Sgk1</i> isoform protein in insulin-treated mpkCCD <sub>c14</sub> cells.....	78
<b>Figure 3.11</b>	Detection of phosphorylated SGK1 protein in HEK293T cells co-transfected with SGK1B and PDPK1 .....	79
<b>Figure 3.12</b>	Detection of phosphorylated SGK1 protein in HEK293T cells co-transfected with SGK1C and PDPK1 .....	79
<b>Figure 3.13</b>	LY294002 reduces aldosterone-stimulated expression of <i>Sgk1a, b, and c</i> .....	81
<b>Figure 3.14</b>	Aldosterone plus insulin-stimulated expression of endogenous <i>Sgk1</i> is partially sensitive to LY294002.....	83
<b>Figure 3.15</b>	Pre-incubation with target peptide blocked anti-SGK1B 3259 detection of overexpressed human SGK1B in lysate of transfected HEK293T cells.....	85
<b>Figure 3.16</b>	Pre-incubation with target peptide blocked anti-SGK1D 3253 detection of overexpressed human SGK1D in lysate of transfected HEK293T cells .....	85
<b>Figure 3.17</b>	Anti-SGK1B 3259 antibody specifically detected overexpressed mouse <i>Sgk1b</i> in transfected mpkCCD <sub>c14</sub> cells.....	86
<b>Figure 3.18</b>	Anti-SGK1D 3253 antibody specifically detected overexpressed mouse <i>Sgk1d</i> in transfected mpkCCD <sub>c14</sub> cells.....	86
<b>Figure 4.1</b>	Effect of aldosterone plus insulin on electrophysiology measurements of ion transport in mpkCCD <sub>c14</sub> cells .....	100

<b>Figure 4.2</b> Insulin stimulates a small and short-lived increase in transepithelial equivalent short circuit current, whereas aldosterone stimulates a larger and more sustained increase that peaks earlier when aldosterone is combined with insulin.....	102
<b>Figure 4.3</b> Aldosterone and aldosterone plus insulin stimulate significant ENaC-mediated sodium transport at 2 hours and 6 hours, whereas insulin did so only at 2 hours.....	103
<b>Figure 4.4</b> Aldosterone plus insulin-stimulated ENaC-mediated sodium transport was greater at 6 hours than at 2 hours of exposure .....	104
<b>Figure 4.5</b> Aldosterone plus insulin-stimulated ENaC-mediated $I_{eq}$ is maintained for at least 24 hours and is maximal at 6 hours .....	105
<b>Figure 4.6</b> LY294002 causes a lesser magnitude $I_{eq}$ response to aldosterone plus insulin.....	107
<b>Figure 4.7</b> LY294002 causes a significant decrease in aldosterone and aldosterone plus insulin-stimulated ENaC-mediated $I_{eq}$ at 7 hours .....	108
<b>Figure 4.8</b> Rapamycin lowers the transepithelial equivalent short circuit current response to aldosterone plus insulin .....	109
<b>Figure 4.9</b> Rapamycin significantly reduced aldosterone plus insulin-stimulated ENaC-mediated $I_{eq}$ at 6 hours .....	110
<b>Figure 4.10</b> Transepithelial equivalent short circuit current failed to stabilise after transfection of mpkCCD <sub>cl4</sub> cell monolayers .....	114
<b>Figure 4.11</b> Transiently transfected and then re-seeded mpkCCD <sub>cl4</sub> cell monolayers failed to show both aldosterone plus insulin-stimulated ENaC-mediated equivalent short circuit current and Sgk1d overexpression.....	116
<b>Figure 4.12</b> Transiently transfected and then re-seeded mpkCCD <sub>cl4</sub> cell monolayers failed to show aldosterone plus insulin-stimulated ENaC-mediated equivalent short circuit current, Sgk1a overexpression, and induction of Sgk1 expression.....	118
<b>Figure 4.13</b> Untransfected control cells also failed to show aldosterone plus insulin-stimulated ENaC-mediated equivalent short circuit current and induction of Sgk1 expression .....	119
<b>Figure 4.14</b> mpkCCD <sub>cl4</sub> cells transiently transfected with SGK1 siRNA failed to show aldosterone plus insulin-stimulated ENaC-mediated equivalent short circuit current .	121
<b>Figure 5.1</b> Immunofluorescence of SGK1D sub-apical intracellular accumulations in human renal collecting duct epithelia .....	133
<b>Figure 5.2</b> Immunofluorescence of SGK1D sub-apical intracellular accumulations and cell-cell junction localisation in human renal collecting duct epithelia. ....	135
<b>Figure 5.3</b> Immunofluorescence of Sgk1d basolateral membrane localisation in mouse renal tubule epithelia.....	137
<b>Figure 5.4</b> Intracellular localisation of FLAG-tagged human SGK1 isoforms A, B, C, D and F compared with red fluorescent protein (RFP)-labelled mitochondria in HEK293T cells .....	141
<b>Figure 5.5</b> Intracellular localisation of FLAG-tagged human SGK1 isoforms A, B, D and F compared with phalloidin-stained actin cytoskeleton in HEK293T cells.....	143
<b>Figure 5.6</b> Intracellular localisation of FLAG-tagged human SGK1 isoforms A, B, C, D and F compared with calnexin in HEK293T cells .....	145
<b>Figure 5.7</b> Intracellular localisation of FLAG-tagged mouse Sgk1 isoforms a, b, c, and d compared with red fluorescent protein (RFP)-labelled mitochondria in HEK293T cells .....	147

<b>Figure 5.8</b> Intracellular localisation of FLAG-tagged mouse Sgk1 isoforms a, b, c, and d compared with red fluorescent protein (RFP)-labelled mitochondria in HEK293T cells .....	149
<b>Figure 5.9</b> Human SGK1 isoforms A-F all co-immunoprecipitate with GILZ1, but SGK1A and SGK1B show the greatest amount of binding.....	151
<b>Figure 5.10</b> SGK1A and B also appear to co-immunoprecipitate with GILZ1 in greater amounts than SGK1 isoforms C, D and F when detected with a different anti-FLAG antibody .....	152
<b>Figure 5.11</b> Mouse Sgk1 isoforms a-d all co-immunoprecipitate with GILZ1, but Sgk1b shows the greatest amount of binding .....	153

## **List of Abbreviations**

11 $\beta$ -HSD2	11 $\beta$ -hydroxysteroid dehydrogenase 2
AC	Adenylate cyclase
ACE	Angiotensin converting enzyme
ADH	Antidiuretic hormone
ADP	Adenosine diphosphate
AF9	ALL-1 fused gene from chromosome 9
A, Aldo	Aldosterone
ANOVA	Analysis of variance
AP1	Activating protein 1
APTES	3-aminopropyltriethoxysilane
AQP2/3	Aquaporin 2/3
ASDN	Aldosterone-sensitive distal nephron
ATF6	Activating transcription factor 6
ATP	Adenosine triphosphate
AVP	Arginine vasopressin
BCA	Bicinchoninic acid
BMK	Big mitogen-activated protein kinase
BSA	Bovine serum albumin
cAMP	Cyclic adenosine monophosphate
CAP-1	Channel-activating protease 1
CCD	Cortical collecting duct
CFTR	Cystic fibrosis transmembrane conductance regulator

CHIF	Corticosterone hormone-induced factor
CMV	Cytomegalovirus
CNT	Connecting tubule
CO <sub>2</sub>	Carbon dioxide
CREB	cAMP response element binding protein
c-Rel	Reticuloendotheliosis viral oncogene homolog
CSNK2	Casein kinase 2
DCT	Distal convoluted tubule
DMEM	Dulbecco's modified Eagle's medium
DMSO	Dimethyl sulfoxide
DNA	Deoxyribonucleic acid
DOCA	Desoxycorticosterone acetate
Dot1a	Disruptor of telomeric silencing 1a
EDTA	Ethylene diamine tetraacetic acid
EGF	Epidermal growth factor
EFGR	EGF receptor
EGTA	Ethylene glycol tetraacetic acid
ENaC	Epithelial sodium channel
EST	Expressed sequence tag
ER	Endoplasmic reticulum
ERK	Extracellular signal regulated kinase
FAST	Forkhead activin signal transducer
FCS	Fetal calf serum
FGF	Fibroblast growth factor

FOXO	Forkhead box O
FXR	Farsenoid X receptor
GAPDH	Glyceraldehyde-3-phosphate-dehydrogenase
GDP	Guanine diphosphate
GFP	Green fluorescent protein
GFR	Glomerular filtration rate
GILZ1	Glucocorticoid-induced leucine zipper protein 1
GR	Glucocorticoid receptor
GRB2	Growth factor receptor-bound protein 2
GRK2	G-protein-coupled receptor kinase 2
GSK	Glycogen synthase kinase
GTP	Guanine triphosphate
HA	Hemagglutinin
HEK293T	Human embryonic kidney 293 T cells
HSF	Heat shock factor
IDV	Integrated density value
IgG	Immunoglobulin G
IGF	Insulin-like growth factor
IGF1R	IGF-1 receptor
IL	Interleukin
INPP4	inositol polyphosphate-4-phosphatase
I, Ins	Insulin
IPP5E	inositol polyphosphate-5-phosphatase E
JNK1	c-Jun N-terminal kinase 1

kbp	Kilobase pair
KCC4	$K^+, Cl^-$ cotransporter
kDa	Kilodalton
LB	Lysogeny broth
LY	LY294002
MAPK	Mitogen-activated protein kinase
MCD	Medullary collecting duct
mpkCCD <sub>c14</sub>	Mouse pyruvate kinase cortical collecting duct clone 4
MR	Mineralocorticoid receptor
MSK	Mitogen- and stress-activated protein kinase
mTOR	mechanistic target of rapamycin
mTORC1/2	mechanistic target of rapamycin complex 1/2
Na <sub>2</sub> HPO <sub>4</sub>	Disodium hydrogen phosphate
NaDC1	$Na^+$ -dicarboxylate cotransporter 1
NCC	$Na^+/Cl^-$ cotransporter
NDRG1	N-myc downstream regulated gene protein 1
Nedd4-2	neural precursor cell-expressed, developmentally down-regulated protein 4-2
NF $\kappa$ B	Nuclear factor kappa B
NHE3	$Na^+/H^+$ Exchanger
NHERF	$Na^+/H^+$ Exchanger Regulatory Factor
OSR1	Oxidative stress responsive kinase 1
PAGE	Polyacrylamide gel electrophoresis
PBS	Phosphate buffered saline

PBS/T	Phosphate buffered saline/Tween 20
PCR	Polymerase chain reaction
PCT	Proximal convoluted tubule
PDGF	Platelet-derived growth factor
PDPK1	3-phosphoinositide-dependent protein kinase 1
PDZ	PSD-95/Dlg/ZO-1
PH	Pleckstrin homology
PHA1/2	Pseudohypoaldosteronism type 1/2
PI3K	Phosphoinositide 3-kinase
PIF	PDPK1 interacting fragment
PIPES	Piperazinediethanesulfonic acid
PKA,B,C,D,G	Protein kinase A,B,C,D,G
PMM2	Phosphomannose mutase 2
PPAR- $\gamma$	Peroxisome proliferator-activated receptor gamma
PR	Progesterone receptor
PRK	Protein kinase C-related kinase
PtdIns	Phosphatidylinositol
PtdIns(3/4/5)P	Phosphatidylinositol 3/4/5-phosphate
PtdIns(3,4)P <sub>2</sub>	Phosphatidylinositol (3,4)-bisphosphate
PtdIns(4,5)P <sub>2</sub>	Phosphatidylinositol (4,5)-bisphosphate
PtdIns(3,4,5)P <sub>3</sub>	Phosphatidylinositol (3,4,5)-trisphosphate
PTEN	phosphatase and tensin homologue deleted on chromosome 10
PX	Phox (Phagocyte Oxidase) homology
qRT-PCR	Quantitative reverse transcriptase polymerase chain reaction

RAAS	Renin-angiotensin-aldosterone system
RNA	Ribonucleic acid
RTK	Receptor tyrosine kinase
RT-PCR	Reverse transcriptase polymerase chain reaction
RXR	Retinoid X receptor
SDS-PAGE	Sodium dodecyl sulphate - polyacrylamide gel electrophoresis
sem	Standard error of the mean
SGK	Serum/glucocorticoid regulated kinase
SGLT1	Sodium-glucose cotransporter 1
SH2	Src homology 2
SHIP2	SH2 domain-containing inositol 5-phosphatase type 2
siRNA	Small interfering ribonucleic acid
SOS	Guanine nucleotide exchange factor son of sevenless
SPAK	STE20-like proline and alanine-rich kinase
SPLUNC1	Short palate, lung, and nasal epithelial clone 1
SREBP	Sterol regulatory element binding protein
STAT	Signal transducers and activators of transcription
STIP1	Stress-induced phosphoprotein 1
STUB1	STIP1 homology and U-box-containing protein 1
SYVN1	Synoviolin
TBS	Tris buffered saline
TBS/T	Tris buffered saline/Tween 20
TGF	Transforming growth factor
TPA	12-O-tetradecanoylphorbol-13-acetate

Usp-45	45 kDa ubiquitin-specific protease
VDR	Vitamin D receptor
WNK	With no lysine kinase
YFP	Yellow fluorescent protein

## **Chapter 1 - Introduction**

Elevated blood pressure (hypertension) is widely considered to be a main cause of cardiovascular disease and stroke, however, the causes of hypertension and the mechanisms by which hypertension causes cardiovascular disease and stroke are poorly understood (Titze and Ritz, 2009; Staessen et al., 2003; Beevers et al., 2001). Regulation of body salt represents a major determinant of blood pressure homeostasis, and the principle regulation of salt balance occurs in the kidneys (O'Shaughnessy and Karet, 2006). The final composition of the kidney filtrate is regulated in the cortical collecting duct (CCD), where the principal cells mediate the hormone-regulated sodium reabsorption required for the fine control of salt homeostasis (Greger, 2000). Serum/glucocorticoid regulated kinase 1 (SGK1) plays a key role in regulation of transepithelial sodium transport by principal cells and for this reason is vital for the control of blood pressure (McCormick et al., 2005).

### **1.1 Renal regulation of sodium balance**

The primary function of the kidneys is to filter the blood of waste products such as urea and pass it to the urinary bladder for excretion. Additional functions of the kidneys include: regulation of plasma osmolality, long-term regulation of blood pressure, regulation of bicarbonate excretion to help regulate acid-base balance, and secretion of hormones such as calcitriol, erythropoietin, and renin (Marieb, 2000). As well as waste, the kidneys also filter water, glucose, amino acids, and ions from blood which must be reabsorbed before being excreted in urine. Every day the kidneys process approximately 180 litres of fluid, but only about 1% gets excreted as urine. A kidney is comprised of

about 1.2 million individual filtering and reabsorption/secretion units called nephrons (Figure 1.1). The nephrons are responsible for the filtration of blood and the reabsorption and secretion of electrolytes by the kidney. Connecting the nephrons to the renal pelvis is the collecting duct system, which is responsible for the final reabsorption and secretion of ions and water and thus the site of the fine regulation of body fluid homeostasis (Marieb, 2000).

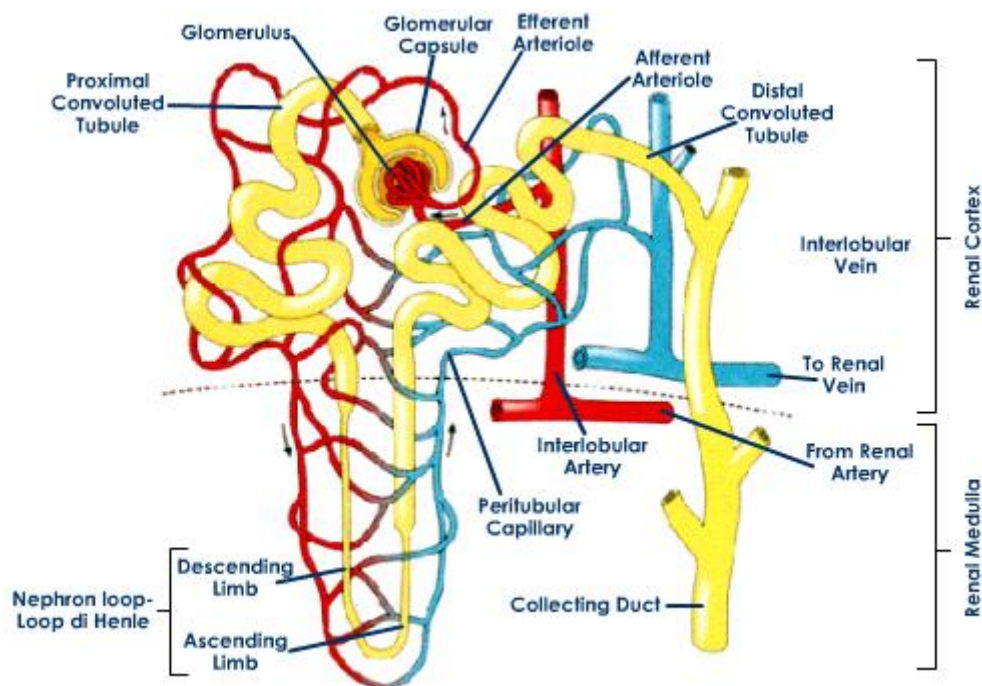


**Figure 1.1 Structure of a nephron indicating the different segments and vasculature.** Image used from (<http://www.tutorvista.com/content/biology/biology-iv/excretion/nephron-structure.php>).

### 1.1.1 Renal regulation of blood pressure

The kidneys regulate blood pressure by controlling the volume of extracellular fluid (ECF), mainly through controlling the plasma concentration of  $\text{Na}^+$ . An increase of plasma  $\text{Na}^+$  concentration increases the osmotic pressure of the blood, thereby increasing fluid retention, ECF volume and blood pressure. The renin-angiotensin-aldosterone system

(RAAS) mediates the response of the kidneys to low blood pressure and, together with the baroreceptor reflex, is responsible for long-term control of blood pressure and body fluid homeostasis. The RAAS is stimulated by sympathetic nervous system activity or in response to low arterial blood pressure, as detected by the baroreceptors or by the kidney through a lowering of glomerular filtration rate (GFR). The juxtaglomerular apparatus is a structure located at the junction of the glomerulus, distal convoluted tubule (DCT), and afferent and efferent arterioles of the renal nephrons. The macula densa of the juxtaglomerular apparatus detects changes in GFR through altered  $\text{Na}^+$  concentration in the nephron filtrate flowing through the DCT. In response to lowered DCT filtrate  $\text{Na}^+$  concentration, the macula densa stimulates granular cells, another part of the juxtaglomerular apparatus, to release renin into the bloodstream, which activates RAAS.

### **1.1.2 The renin-angiotensin-aldosterone system**

The renin-angiotensin-aldosterone system (RAAS) is activated upon the release of renin from the juxtaglomerular apparatus into the bloodstream. Renin causes hydrolysis of angiotensinogen into angiotensin I, which is then converted into angiotensin II by pulmonary and renal angiotensin converting enzyme (ACE). Angiotensin II stimulates vasoconstriction and release of arginine vasopressin (AVP) from the pituitary gland and aldosterone from the adrenal cortex. ADH acts on the collecting duct to stimulate water absorption, whereas aldosterone acts on the aldosterone-sensitive distal nephron (ASDN) to stimulate  $\text{Na}^+$  reabsorption,  $\text{K}^+$  excretion, and water retention. These effects cause an increase in plasma volume, which in turn causes increased arterial blood pressure and GFR, thereby reducing the stimulation of renin release by the macula densa in a negative feedback mechanism.

### **1.1.3 The aldosterone-sensitive distal nephron**

The aldosterone-sensitive distal nephron (ASDN) consists of the late distal convoluted tubule (DCT), connecting tubule (CNT), cortical collecting duct (CCD), and medullary collecting duct (MCD) (Meneton et al., 2004; Loffing et al., 2001). The DCT is defined by the presence of the  $\text{Na}^+/\text{Cl}^-$  cotransporter (NCC) in the apical membrane of its simple cuboidal epithelial cells. The other segments of the ASDN each contain two epithelial cell types; intercalated cells and segment-specific cells. The intercalated cells perform the acid-base homeostasis role of the kidneys. There are two intercalated cell types:  $\alpha$ ; acid absorbing and bicarbonate secreting and  $\beta$ ; bicarbonate absorbing and acid secreting. The ASDN segment-specific cells are specialised for their respective segments and are named accordingly as connecting tubule cells, principal cells of the collecting duct, or inner medullary collecting duct cells.

### **1.1.4 The principal cells of the collecting duct**

Principal cells comprise approximately 71% of the cells of the cortical collecting duct (CCD) epithelium and are solely responsible for the  $\text{Na}^+$  reabsorption and  $\text{K}^+$  secretion that occurs in the CCD (O'Neil and Hayhurst, 1985). These cells are characterised by having a large number of water channels (aquaporins) which coupled with  $\text{Na}^+$  reabsorption, are used to reabsorb water. Principal cells are responsible for the fine control of salt balance through regulated reabsorption of the remaining 2-5% of filtered  $\text{Na}^+$ . Reabsorption of  $\text{Na}^+$  occurs because of the generation of an inward  $\text{Na}^+$  electrochemical gradient into the cell by the basolateral  $\text{Na}^+/\text{K}^+$ -ATPase, which actively transports 3  $\text{Na}^+$  out of the cell and 2  $\text{K}^+$  into the cell. The  $\text{Na}^+$  electrochemical gradient allows  $\text{Na}^+$  to flow into the cell from the CCD lumen through the apical epithelial sodium channel (ENaC). ENaC is the rate

limiting step for reabsorption of  $\text{Na}^+$  and therefore is tightly regulated, as discussed later in section 1.4.1. The  $\text{Na}^+/\text{K}^+$ -ATPase also creates a  $\text{K}^+$  electrochemical gradient out of the cell, which is either used to secrete  $\text{K}^+$  via the apical ROMK  $\text{K}^+$  channel, which is also under tight regulation, or is used to transport  $\text{Cl}^-$  across the basolateral membrane via the  $\text{K}^+, \text{Cl}^-$  cotransporter (KCC4). The movement of  $\text{K}^+$  is important for the maintenance of cell membrane potential.  $\text{Cl}^-$  may also be transported across the basolateral membrane by CLC-K2, but this transporter is only present in the intercalated cells of the CCD. Water reabsorption by principal cells is mediated by water channels aquaporin 2 (AQP2) in the apical membrane and aquaporin 3 (AQP3) in the basolateral membrane. AQP2 is the rate limiting step in water reabsorption, and AQP2 channels are inserted into the membrane following stimulation by argenine vasopressin (AVP) hormone in response to dehydration. Ion transport across principal cells is summarised in Figure 1.2.

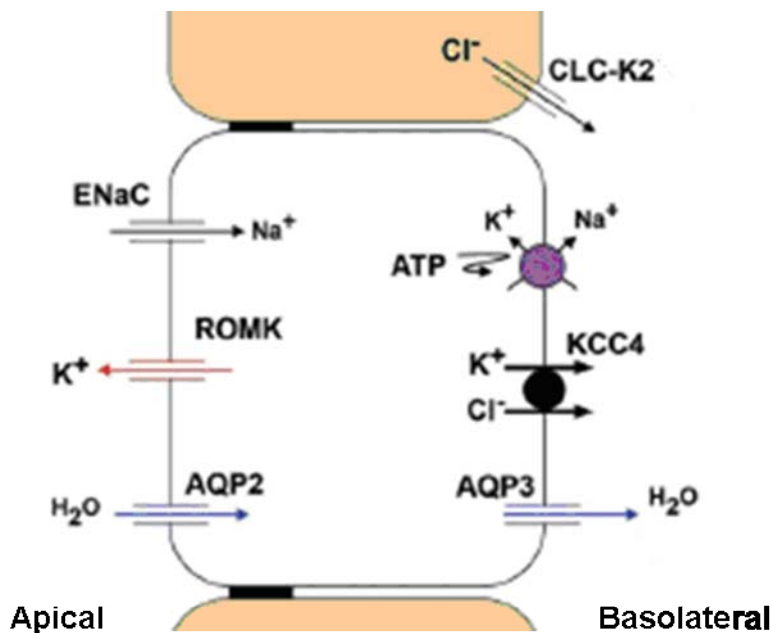


**Figure 1.2 Routes of the major ion and water transport in principal cells.** Figure adapted from (Fenton and Knepper, 2007).

## 1.2 Regulation of sodium transport in principal cells

Sodium transport in principal cells is mostly regulated at the point of  $\text{Na}^+$  entry across the apical membrane via ENaC. ENaC is controlled through various mechanisms, but the most important is the regulation by hormones such as aldosterone and insulin via SGK1. The basic pathway of aldosterone and insulin regulation of sodium transport in principal cells is summarised in Figure 1.3. Aldosterone induces expression of SGK1, whilst insulin stimulates the PI3K pathway causing phosphorylation and activation of SGK1. Active SGK1 stimulates ENaC by phosphorylating and inactivating Nedd4-2, which would otherwise cause ENaC internalisation and degradation (McCormick et al., 2005). Regulation of ENaC is reviewed in more detail in section 1.4.1. ENaC-mediated sodium transport is also sensitive to both intracellular and extracellular  $[\text{Na}^+]$ . Increased intracellular  $[\text{Na}^+]$  blocks further  $\text{Na}^+$  entry into the cell via ENaC possibly to protect the cell from osmotic damage (Anantharam et al., 2006). Increased intracellular  $[\text{Na}^+]$  has also been shown to increase the activity of  $\text{Na}^+, \text{K}^+$ -ATPase at the cell surface of isolated rat CCD cells and mpkCCD<sub>cl4</sub> cells (Vinciguerra et al., 2003). ENaC is also blocked by high extracellular  $\text{Na}^+$  which is suggested to be mediated by a  $\text{Na}^+$ -sensing self-inhibition site on ENaC (Bize and Horisberger, 2007).

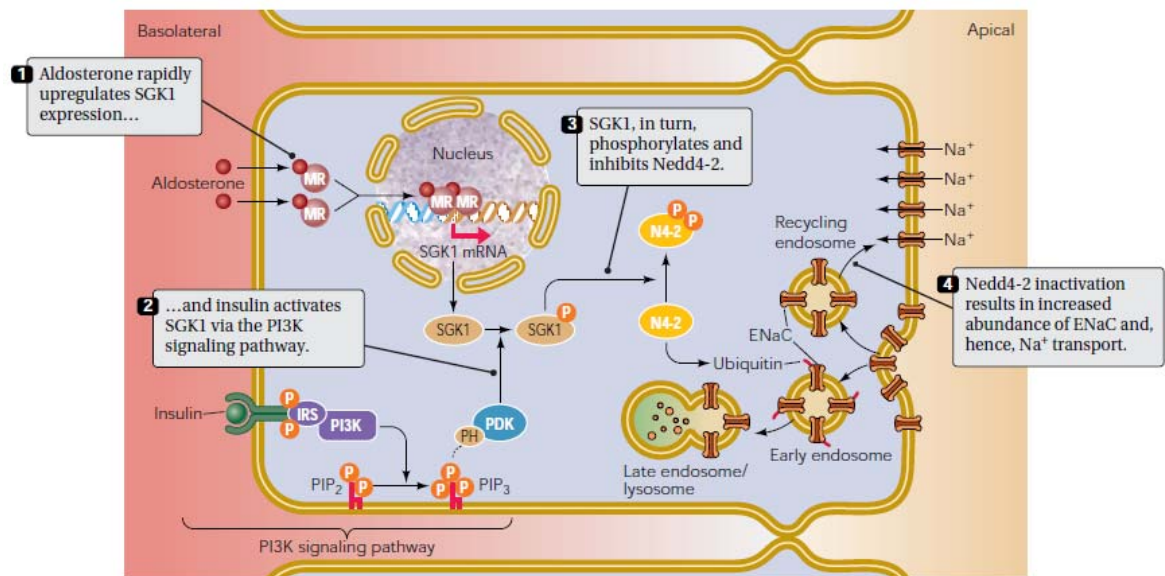


**Figure 1.3 Simplified SGK1-regulated Na<sup>+</sup> transport in a CCD principal cell.** Figure used from (McCormick et al., 2005).

### 1.2.1 The mineralocorticoid receptor

Mineralocorticoid receptors (MRs) mediate the aldosterone-induced signalling and upregulated gene expression involved in the regulation of sodium transport in principal cells. The MR is a member of the steroid hormone receptor family that has high affinity for mineralocorticoids such as aldosterone. MRs are expressed in various tissues, including kidney, brain, heart, blood vessels, adipose tissue, and circulating monocytes (Gomez-Sanchez, 2010; Urbanet et al., 2010; Fuller and Young, 2005). MRs are bound by both aldosterone and cortisol, but 11  $\beta$ -hydroxysteroid dehydrogenase 2 (11 $\beta$ -HSD2) acts to protect MRs from cortisol (Morris et al., 2000). Aldosterone enters the principal cells of the ASDN and binds to MRs present in the cytosol. The aldosterone-MR complexes then translocate from the cytosol to the nucleus, where they bind to DNA hormone response elements in order to transcriptionally upregulate various proteins such as SGK1 (Chen et al., 1999; Naray-Fejes-Toth et al., 1999), ENaC, Na<sup>+</sup>,K<sup>+</sup>-ATPase (Feraille et al., 2003; Verrey et al., 2003), K-Ras, and corticosterone hormone-induced factor (CHIF). SGK1 is

a critical component of the aldosterone-induced increase in ENaC-mediated Na<sup>+</sup> transport (Naray-Fejes-Toth and Fejes-Toth, 2000). SGK1 is also able to stimulate Na<sup>+</sup>,K<sup>+</sup>-ATPase activity, however, this is separate to the activation by aldosterone (Alvarez de la Rosa et al., 2006; Zecevic et al., 2004). Osmotic stress caused by hypertonic conditions reduces expression of MR in CCD cells (Viengchareun et al., 2009). Mice deficient in MR show impaired salt balance (Ronzaud et al., 2007).

### **1.2.2 The phosphoinositide 3-kinase pathway**

The phosphoinositide 3-kinase (PI3K) pathway regulates SGK1 activity by controlling the phosphorylation of SGK1 by phosphoinositide-dependent protein kinase 1 (PDK1) and mammalian target of rapamycin complex 2 (mTORC2) (Lu et al., 2010; Kobayashi and Cohen, 1999). The PI3K pathway can be activated by various substances including insulin, insulin-like growth factor 1 (IGF-1), and pervanadate and is involved in many cellular processes including regulation of cell proliferation, differentiation, motility, survival and intracellular trafficking (Gonzalez-Rodriguez et al., 2007; Gamper et al., 2002; Park et al., 1999; Alessi et al., 1996). The diverse functions of this pathway are mediated by the actions of the PI3Ks; a family of intracellular signalling proteins that are split into three classes based on their structure, regulation, and substrate specificity, which are summarised in Table 1.1.

<b>PI3K class</b>	<b>Activator</b>	<b>Lipid substrate and product</b>	<b>Catalytic subunit</b>	<b>Regulatory subunit</b>
I	Tyrosine kinases/G protein-coupled receptors/Ras	PtdIns(4,5)P <sub>2</sub> → PtdIns(3,4,5)P <sub>3</sub>	p110α p110β p110δ	p85α p85β p50α p55α p55γ
			p110γ	p101 p87
II	Tyrosine kinases?/G protein-coupled receptors?	PtdIns → PtdIns(3)P PtdIns(4)P → PtdIns(3,4)P <sub>2</sub>	C2α C2β C2γ	-
III	G protein-coupled receptors?	PtdIns → PtdIns(3)P	Vps34	Vps15

**Table 1.1 A summary of the PI3K classes and their respective regulation, substrate reactions, and constituting subunits.**

The PI3Ks are defined by their phosphorylation of a hydroxyl group in the 3-position of the inositol ring of phosphatidylinositol (PtdIns) in order to regulate the levels of PtdIns and its phosphorylated forms; PtdIns(3)P, PtdIns(4)P, PtdIns(3,4)P<sub>2</sub>, PtdIns(4,5)P<sub>2</sub>, and PtdIns(3,4,5)P<sub>3</sub> in cells. The PI3Ks perform their role in conjunction with various phosphatases, which dephosphorylate the 3- 4- or 5-positions of PtdIns enabling regulation of the relative levels of the different PtdIns species. The class I PI3Ks are activated by tyrosine kinases, G protein coupled receptors (GPCRs), or Ras and produce PtdIns(3,4,5)P<sub>3</sub> from PtdIns(4,5)P<sub>2</sub>. The PtdIns(3,4,5)P<sub>3</sub> product of class I PI3Ks is subject to conversion into the other lipid second messengers; PtdIns(4,5)P<sub>2</sub> and PtdIns(3,4)P<sub>2</sub>, by PtdIns 3- and PtdIns 5-phosphatases, respectively. The principle PtdIns 3-phosphatase is the phosphatase and tensin homologue deleted on chromosome 10 (PTEN), which counteracts the phosphorylation performed by the class I PI3Ks to produce PtdIns(4,5)P<sub>2</sub>. Two important PtdIns 5-phosphatases are the SH2 domain-containing inositol 5-phosphatase type 2 (SHIP2) and the inositol polyphosphate-5-phosphatase E (IPP5E), which convert

PtdIns(3,4,5)P<sub>3</sub> into PtsIns(3,4)P<sub>2</sub>. Both PtdIns(3,4,5)P<sub>3</sub> and PtdIns(3,4)P<sub>2</sub> are bound by proteins that possess a PH domain and, through this interaction, regulate the localisation and function of kinases such as PKB and PDK1. PtdIns(3,4)P<sub>2</sub> is also produced from PtdIns(4)P by class II PI3Ks, which may be activated by the same route as class I PI3Ks, but the routes of activation of class II PI3Ks are not yet fully understood. Class II PI3Ks also share production of PtdIns(3)P from PtdIns with class III PI3K, which may also be produced from phosphorylation of PtdIns(3,4)P<sub>2</sub> by inositol polyphosphate-4-phosphatase (INPP4). Class II PI3Ks are primarily present in intracellular membranes and, concurrently, basal PtdIns(3)P is localised mainly on endosomes or organelles. PtdIns(3)P is bound by proteins that possess a Phagocyte Oxidase homology (PX) domain or a Fab1, YOTB/ZK632.12, Vac1, and EEA1 (FYVE) zinc finger domain, which may involve downstream kinases, vesicle sorting proteins, or scaffold proteins (Vanhaesebroeck et al., 2010).

SGK1 has been shown to be able to bind PtdIns(3)P, PtdIns(4)P, and PtdIns(5)P, but not bind PtdIns(3,4,5)P<sub>3</sub> *in vitro* and mutation of a specific residue involved in PI binding reduced SGK1 effects on ENaC and FOXO3 (Pao et al., 2007). Interestingly, PDK1 is recruited to PtdIns(3,4,5)P<sub>3</sub> via a pleckstrin homology (PH) domain in order to maintain activity of the kinase (Komander et al., 2004; McManus et al., 2004). However, sodium hydrogen exchanger regulating factor 2 (NHERF2) has been shown to bind both SGK1 and PDK1 via a PSD-95/Dlg/ZO-1 (PDZ) domain and a 3-phosphoinositide-dependent protein kinase 1 (PDK1) interacting fragment (PIF), respectively, acting as a scaffold protein to recruit SGK1 to PDK1 for activation (Chun et al., 2002).

### **1.2.3 The mitogen-activated protein kinase/extracellular signal-regulated kinase pathway**

The mitogen-activated protein kinase/extracellular signal-regulated kinase (MAPK/ERK) pathway is an intracellular signalling pathway that typically mediates the effects of growth factors on gene transcription. Activation of the MAPK/ERK pathway by epidermal growth factor (EGF), transforming growth factor  $\alpha$  (TGF $\alpha$ ), or phorbol myristate acetate (PMA) was shown to cause decreased Na<sup>+</sup> transport in CCD cells (Shen and Cotton, 2003). The MAPK/ERK pathway is stimulated by the binding of growth factors such as epidermal growth factor (EGF) and insulin-like growth factor 1 (IGF-1) to their cell surface tyrosine kinase receptors such as EGF receptor (EGFR) and IGF-1 receptor (IGF1R). Growth factor receptor binding induces phosphorylation of the receptor substrate or autophosphorylation of the receptor itself. Phosphorylation of the receptor provides sites for recruitment of Src homology 2 (SH2) domain-containing effector proteins such as growth factor receptor-bound protein 2 (GRB2) or insulin receptor substrate 1 (IRS-1). Phosphorylated IRS-1 binds to the SH2 domain of GRB2. GRB2 forms a complex with the guanine nucleotide exchange factor son of sevenless (SOS) via an SH3 domain and recruitment of this GRB2-SOS complex causes activation of SOS. Activated SOS promotes the activation of Ras by removing bound GDP allowing Ras to bind GTP and become active. Active Ras binds and activates Raf to initiate the MAPK signalling cascade of MAPKKK (Raf)-MAPKK (MEK)-MAPK (ERK1/2)-various downstream targets, whereby each member is phosphorylated and activated by the last. ERK1/2 phosphorylate ENaC stimulating its interaction with Nedd4-2. The components of the MAPK/ERK pathway cascade exist in a multiprotein complex (Kyriakis, 2007). Interestingly, a recent study has described the existence of a complex of ENaC-Raf-Nedd4-

2, which GILZ1 and SGK1 interact with to cooperatively stimulate ENaC (Soundararajan et al., 2009).

#### **1.2.4 The protein kinase A pathway**

In principal cells, the protein kinase A (PKA) pathway mediates the response to the AVP. AVP is released into the bloodstream from the pituitary gland in response to a drop in plasma osmotic pressure as detected by the hypothalamus. AVP binds to the AVP receptor 2 (AVPR2) on the basolateral membrane of CCD principal cells. AVPR2 is a G protein coupled-receptor that activates adenylate cyclase (AC) through the  $G_s$  pathway. AC catalyses the conversion of ATP into the second messenger 3',5'-cyclic adenosine monophosphate (cAMP). The increased cAMP activates PKA, which has been shown to increase ENaC activity via phosphorylation of SGK1 (Vasquez et al., 2008; Perrotti et al., 2001). cAMP has also been suggested to phosphorylate equivalent sites on Nedd4-2 to SGK1 in order to stimulate ENaC (Snyder et al., 2004). In addition, cAMP/PKA also cause the translocation of  $Na^+,K^+$ -ATPase to the plasma membrane, thereby promoting  $Na^+$  reabsorption (Feraille et al., 2003; Verrey et al., 2003; Gonin et al., 2001). cAMP/PKA are also reported to induce SGK1 and  $\alpha$ ENaC protein expression in the rat salivary submandibular gland cell line SMG-C6 (Vasquez et al., 2008). The cAMP/PKA induction of SGK1 and  $\alpha$ ENaC in SMG-C6 cells has also been linked to the PI3K and MAPK pathways (Mustafa et al., 2008; Vasquez et al., 2008).

#### **1.3 Serum/glucocorticoid regulated kinase 1**

The serum/glucocorticoid regulated kinases (SGKs) are members of the AGC protein kinase subfamily of serine/threonine protein kinases. Other members of this subfamily

include PKA, PKB, PKC, PKG, protein kinase C related kinase (PRK), mitogen- and stress-activated protein kinase (MSK), and 3-phosphoinositide dependent protein kinase-1 (PDPK1) (Pearce et al., 2010). SGK1 was originally characterised as a 49 kDa protein kinase whose mRNA was rapidly induced by serum and dexamethasone in a rat mammary tumour cell line and was therefore named serum/glucocorticoid regulated kinase (SGK) (Webster et al., 1993a; Webster et al., 1993b). The later discovery of the SGK paralogues SGK2 and SGK3 led to the original SGK being renamed SGK1. SGK2 and SGK3 were discovered as products of distinct genes, but with 80% amino acid identity between the catalytic domains of the three SGK paralogues (Kobayashi et al., 1999). In humans, the *SGK1* gene locus is on chromosome 6q23, the *SGK2* gene locus is on chromosome 20q12, and the *SGK3* gene locus is on chromosome 8q12.3. SGKs are broadly conserved and are present in mammals, shark, chicken, *C. elegans*, and two orthologues also exist in yeast. The human *SGK1* gene consists of 12 exons separated by relatively short introns (Waldegger et al., 1998). SGK1 consists of an N-terminus domain of ~100 residues; which is thought to be responsible for regulating localisation, and the remaining ~330 residues constitute a kinase domain containing various putative binding sites and motifs. In mammals, SGK1 and SGK3 are expressed in most tissues including brain, heart, intestine, kidney, liver, lung, and muscle, whereas SGK2 is expressed more exclusively in epithelial tissues of the kidney, liver and pancreas (Lang et al., 2006). SGK1, 2, and 3 are all expressed in cortical collecting duct cells, however, only expression of SGK1 is induced by aldosterone and dexamethasone (Naray-Fejes-Toth et al., 2004a). To date, most research has focussed on SGK1 due to its regulation by hormones and comparatively little is known about SGK3 and particularly SGK2 because of their less obvious regulation. SGK1 is involved in regulation of many different cellular processes including proliferation, signalling, survival, and trafficking (Leong et al., 2003; Mikosz et al., 2001). SGK1

performs its roles through acting on ion channels and transporters, other enzymes, and transcription factors as discussed further in section 1.3.2. SGK2 and SGK3 are also thought to be involved in regulation of transport and transcription, but their exact roles remain to be established. SGK1 has recently been shown to be expressed as multiple isoforms in humans and are thought to confer functional diversity and specificity to SGK1 (Hall, 2007; Simon et al., 2007), which is discussed further in chapter 3.

### **1.3.1 Regulation of serum/glucocorticoid regulated kinase 1**

Following its characterisation as a serum and glucocorticoid regulated kinase in 1993, *sgk1* was later shown to be upregulated by aldosterone in A6 cells, rat kidney distal nephron, and rabbit cortical collecting duct cells (Chen et al., 1999; Naray-Fejes-Toth et al., 1999). The induction of *sgk1* by aldosterone was confirmed *in vivo* by other researchers studying rat kidney and colon (Bhargava et al., 2001; Brennan and Fuller, 2000; Shigaev et al., 2000). These studies of aldosterone action on *sgk1* also showed that *sgk1* increased activity of ENaC, suggesting *sgk1* involvement in regulation of sodium reabsorption. This led to the investigation of the possible involvement of *sgk1* in other diseases associated with hypertension. *Sgk1* was shown to be upregulated by transforming growth factor B (TGF- $\beta$ ), increased extracellular glucose concentration, osmotic cell shrinkage, and thrombin, suggesting *Sgk1* may have a role in the pathogenesis of diabetic nephropathy (Hills et al., 2006; Lang et al., 2000; Kumar et al., 1999). SGK1 has also been shown to be induced by endothelin-1 (ET-1) and suggested to be involved in blood pressure changes during renal failure (Wolf et al., 2006). Peroxisome proliferator-activated receptor gamma (PPAR- $\gamma$ ) agonists, which sensitise cells to insulin and are used clinically in treatment of type 2 diabetes, stimulated SGK1 activity in a human CCD cell line (Vallon and Lang,

2005; Hong et al., 2003). The MAPK/ERK pathway is known to regulate SGK1 and mediates induction of SGK1 in response to cell stress allowing SGK1 to protect cells from stress-induced apoptosis by negatively regulating forkhead box protein O3 (FOXO3) (Leong et al., 2003; Brunet et al., 2001). The MAPK/ERK pathway also mediates fibroblast growth factor (FGF), platelet-derived growth factor (PDGF) and 12-O-tetradecanoylphorbol-13-acetate (TPA) induction of Sgk1 (Mizuno and Nishida, 2001). Sgk1 has also been shown to be induced by follicle stimulating hormone (FSH) in granulosa cells via a cAMP-dependent pathway (Gonzalez-Robayna et al., 2000).

Transcriptional regulation of SGK1 occurs through several intracellular signalling pathways and as such a number of different signalling proteins have been shown to be involved. In addition to components of the PI3K, MAPK/ERK, and cAMP/PKA pathways discussed earlier, SGK1 expression is also induced by PKC increases of intracellular  $[Ca^{2+}]$  in endothelial cells (Lang et al., 2000). SGK1 may also be transcriptionally regulated by changes in nitric oxide, and interleukin 2 (IL-2) (Amato et al., 2007). However, the transcriptional regulation of SGK1 probably involves many more potential players as the *SGK1* promoter region in rat has been suggested to contain various transcription factor binding sites such as for progesterone receptor (PR), vitamin D receptor (VDR), retinoid X receptor (RXR), farnesoid X receptor (FXR), sterol regulatory element binding protein (SREBP), p53, Sp1 transcription factor, activating protein 1 (AP1), activating transcription factor 6 (ATF6), heat shock factor (HSF), reticuloendotheliosis viral oncogene homolog (c-Rel), NFkB, signal transducers and activators of transcription (STAT). As well as binding sites for GR, MR, cAMP response element binding protein (CREB), PPAR $\gamma$ , TGF- $\beta$ -dependent transcription factors SMAD3 and SMAD4, and forkhead activin signal transducer (FAST) (Lang et al., 2006; Itani et al.,

2002). Not all of these binding sites may be used universally, but this does suggest that transcription regulation of SGK1 is complex.

The activity of SGK1 inside the cell is governed by its phosphorylation, which may occur at various phosphorylation sites that are each substrate for different activators. The most well documented phosphorylation of SGK1 is performed by 3-phosphoinositide-dependent protein kinase 1 (PDK1) at threonine 256 and by mechanistic target of rapamycin complex 2 (mTORC2) at serine 422, which promotes its actions in inhibiting Nedd4-2 (Lu et al., 2010; Garcia-Martinez and Alessi, 2008; Kobayashi and Cohen, 1999). Activation of SGK1 via the PI3K pathway may be stimulated by hormones such as insulin (Fuster et al., 2007). Phosphorylation of SGK1 at threonine 256 is first dependent on the phosphorylation of serine 422 (Kobayashi and Cohen, 1999). The interaction of SGK1 with PDK1 is enabled by Na<sup>+</sup>/H<sup>+</sup> Exchanger Regulatory Factor 2 (NHERF2), which contains two PDZ binding domains that are able to interact with PDZ binding motifs such as is found at the C-terminus of SGK1 (DSFL) 6 residues away from serine 422 (Chun et al., 2002). Also, PDK1 contains a PDK interacting fragment (PIF)-binding pocket which may bind SGK1 directly or require NHERF2 as a scaffold protein for interaction with SGK1. PDK1 is activated by the PI3K pathway and binds to PtdIns(3,4,5)P<sub>3</sub> via its PH domain. SGK1 has also been shown to bind to phosphoinositides, possibly due to being localised with PDK1 by NHERF2 (Pao et al., 2007). The findings of these studies suggest that activation of SGK1 by via the PI3K pathway may occur at the plasma membrane. The activity of SGK1 has been shown to be dependent on its N-terminal domain, which may contain amino-acid sequence required for specific localisation (Pao et al., 2007; Naray-Fejes-Toth et al., 2004a).

SGK1 is also phosphorylated by big mitogen-activated protein kinase 1/extracellular signal regulated kinase 5 (BMK1/ERK5) at serine 78 during growth-factor-induced cell

proliferation as part of the MAPK/ERK signalling pathway (Hayashi et al., 2001). The cAMP/PKA pathway is also involved in regulating activity of SGK1 as PKA has been shown to phosphorylate SGK1 at threonine 369 (Perrotti et al., 2001). The study by Perrotti et al. (2001) also showed that phosphorylation and activation of SGK1 by PKA is dependent on the prior phosphorylation of threonine 256 or serine 422. Additionally, phosphorylation of SGK1 at threonine 369 by NIMA (never in mitosis, gene A)-related kinase-6 (NEK6) links SGK1 with cell-cycle progression, however, this study also found that this phosphorylation was unlikely *in vivo* (Lizcano et al., 2002). Recently, it has also been argued that phosphorylation of SGK1 at serine 397 and serine 401 is required for maximum SGK1 activity, which was dependent on co-expression with active PKB and with no lysine kinase 1 (WNK1) (Chen et al., 2009).

SGK1 has a half life of ~30 min in the cell and is degraded through being ubiquitin-tagged at a specific six-amino-acid motif in its N-terminal domain, signalling it for degradation by the 26S proteasome (Brickley et al., 2002). The ubiquitin-binding motif of SGK1 consists of amino acids 19-24 (GMVAIL) and is required for correct regulation of SGK1 (Bogusz et al., 2006). Ubiquitination of SGK1 is performed by phosphorylated Nedd4-2, which itself is produced by SGK1 forming a negative feedback loop of regulation of SGK1 (Zhou and Snyder, 2005). SGK1 has also been shown to be ubiquitinated *in vitro* by Nedd4-2 (Zhou and Snyder, 2005), stress-induced-phosphoprotein 1 (STIP1) homology and U-box containing protein 1 (STUB1) (Belova et al., 2006) and synoviolin (SYVN1) (Arteaga et al., 2006).

### 1.3.2 Functions of serum/glucocorticoid regulated kinase 1

The SGK1 kinase consensus sequence has been identified as R-X-R-X-X-(S/T)- $\phi$ , containing arginine (R), any amino acid (X), and a hydrophobic amino acid ( $\phi$ ) (Lang et al., 2006). This sequence is shared with the other SGK isoforms SGK2 and SGK3 as well as with PKB. SGK1 has been shown to be involved in regulation of Na<sup>+</sup> reabsorption in the distal nephron, primarily via stimulating ENaC (Chen et al., 1999; Naray-Fejes-Toth et al., 1999), which is discussed in more detail later in section 1.4.2. SGK1 also increases activity and cell-surface expression of the renal Na<sup>+</sup>/K<sup>+</sup>-ATPase, suggesting an additional stimulation of sodium reabsorption in the distal nephron by SGK1 separate to the stimulation of ENaC (Alvarez de la Rosa et al., 2006; Verrey et al., 2003). The renal K<sup>+</sup> channel (ROMK1), which is important for the secretion of K<sup>+</sup> into the nephron filtrate, is also stimulated by SGK1 via interaction with sodium hydrogen exchanger regulating factor 2 (NHERF2) (Palmada et al., 2005; Vallon and Lang, 2005; Yun et al., 2002). SGK1 and NHERF2 are also involved in regulation of the renal Ca<sup>2+</sup> channels, TRPV5 and TRPV6 that are important for reabsorption of Ca<sup>2+</sup> (Bohmer et al., 2007; Palmada et al., 2005; Embark et al., 2004b) and also regulate the renal Na<sup>+</sup>-dicarboxylate cotransporter (NaDC1) (Boehmer et al., 2004). NHERF2 acts as a scaffold protein by binding SGK1 and regulating/effector proteins to facilitate their interaction.

Sodium transport across the apical membrane of the proximal tubule by the Na<sup>+</sup>/H<sup>+</sup> exchanger (NHE3) is stimulated by insulin and SGK1 (Fuster et al., 2007). Sodium is also reabsorbed in the proximal tubule with glucose via the Na<sup>+</sup>-glucose cotransporter (SGLT1) and SGK1 has been shown to stimulate SGLT1 activity via phosphorylation of Nedd4-2 in a mechanism similar to regulation of ENaC (Dieter et al., 2004). SGK1 and Nedd4-2 regulation has also been shown for the renal and inner ear Cl<sup>-</sup> channel (ClC-Ka) (Embark et al., 2004a) and the ubiquitous Cl<sup>-</sup> channel (ClC2) (Palmada et al., 2004a). NHE3 and

SGLT1 are also used in absorption of Na<sup>+</sup> and glucose in the intestine and their dysregulation by SGK1 may cause diarrhoea or underlie obesity. SGK1 stimulates activity of the intestinal Na<sup>+</sup>-phosphate cotransporter (NAPiIb), also through phosphorylation of Nedd4-2 (Palmada et al., 2004b).

SGK1 is also suggested to be involved in the maintenance of cardiac function via regulation of the cardiac voltage-gated Na<sup>+</sup> channel (SCN5A) (Boehmer et al., 2003) and the cardiac K<sup>+</sup> channels (KCNE1 and KCNQ1) (Busjahn et al., 2004). SGK1 also regulates other KCNQ channels involved in neuronal excitability (Schuetz et al., 2008).

SGK1 has also been shown to play a role in regulation of insulin secretion from glucose-sensitive cells, in part through regulation of voltage-gated K<sup>+</sup> channels (Kv1.3, Kv1.5, and Kv4.3) (Laufer et al., 2009; Boehmer et al., 2008a; Vallon and Lang, 2005). SGK1 also increased the abundance of glucose transporter (GLUT1) in plasma membrane suggesting that SGK1 has a role in regulating glucose uptake by cells (Palmada et al., 2006).

Further transporters that have been shown to be regulated by SGK include the cystic fibrosis transmembrane conductance regulator Cl<sup>-</sup> channel (CFTR) (Sato et al., 2007), various amino acid transporters (Boehmer et al., 2006; Boehmer et al., 2005; Bohmer et al., 2004), the creatinine transporter (SLC6A8) (Strutz-Seebohm et al., 2007), and the peptide transporter (PEPT2) (Boehmer et al., 2008b).

SGK1 mediates its effects through phosphorylation of downstream targets such as regulatory proteins and transcription factors. An important role for SGK1 in regulation of many channels and transporters including ENaC is SGK1 regulation of the ubiquitin ligase Nedd4-2. Nedd4-2 regulates its target proteins through ubiquitination, signalling the target protein for degradation by the proteasome. SGK1 phosphorylation of Nedd4-2 induces binding of Nedd4-2 by members of the 14-3-3 family of regulatory proteins which block the tryptophan-rich WW domains of Nedd4-2 that are involved in PY motif interactions

such as Nedd4-2 uses to bind and inhibit ENaC (Bhalla et al., 2005; Debonneville et al., 2001).

N-myc downstream-regulated gene proteins 1 and 2 (NDRG1 and 2) have been identified as substrates for SGK1 phosphorylation and NDRG1 phosphorylation has since been used as an assay for SGK1 activity (Inglis et al., 2008; Murray et al., 2004). SGK1 also phosphorylates and inactivates the proapoptotic enzyme glycogen synthase kinase 3 $\beta$  (GSK3 $\beta$ ), which is involved in regulation of  $\beta$ -Catenin (Failor et al., 2007; Aoyama et al., 2005; Kobayashi and Cohen, 1999). SGK1 also phosphorylates members of the MAPK/ERK signalling pathway in regulation of cell proliferation including mitogen-activated kinase kinase kinase 3 (MEKK3) (Chun et al., 2003) and B-Raf (Zhang et al., 2001). Microtubule-associated protein tau interacts with microtubules as part of being involved in cell proliferation and apoptosis and is inhibited upon phosphorylation by SGK1 (Chun et al., 2004). SGK1 also showed possible regulatory effects on insulin stimulated glycosylation of glycoproteins involving phosphomannose mutase 2 (PMM2) (Menniti et al., 2005). SGK1 also acts to enhance transcription factors such as cAMP responsive element binding protein (CREB) (Tyan et al., 2007), NF $\kappa$ B (Leroy et al., 2008), and FOXO3a (Dehner et al., 2008; You et al., 2004; Brunet et al., 2001) to mediate cell survival and rescue from apoptosis.

#### **1.4 Epithelial sodium channel**

The epithelial sodium channel (ENaC) is a member of the degenerin/epithelial sodium channel (DEG/ENaC) family of ion channels. It constitutes the rate-limiting step in Na<sup>+</sup> transport across many epithelia, such as the kidney distal nephron, airway, colon, sweat glands, and salivary ducts. ENaC mediates the final regulation of Na<sup>+</sup> reabsorption by the

kidney in the aldosterone-sensitive distal nephron (ASDN) (Bachmann et al., 1999; Duc et al., 1994). Principal cells of the cortical collecting duct (CCD) express apical ENaC, allowing entry of Na<sup>+</sup> into the cell, which is then extruded across the basolateral membrane by the Na<sup>+</sup>/K<sup>+</sup>-ATPase (Garty and Palmer, 1997). ENaC is a heterotrimeric Na<sup>+</sup> channel made up of three homologous subunits named  $\alpha$ ,  $\beta$ , and  $\gamma$  (Butterworth et al., 2008) (Figure 1.4). A fourth subunit has been identified named  $\delta$ , which replaces the  $\alpha$ ENaC subunit to create a Na<sup>+</sup> channel with different functional properties, and is present in brain, pancreas, ovaries, and testes (Ji et al., 2006). Channels of  $\delta\beta\gamma$ ENaC had increased channel activity and much reduced sensitivity to amiloride compared to  $\alpha\beta\gamma$ ENaC (Haerteis et al., 2009). In humans, the four genes that encode the ENaC subunits are named *SCNN1A* ( $\alpha$ ENaC), *SCNN1B* ( $\beta$ ENaC), *SCNN1G* ( $\gamma$ ENaC), and *SCNN1D* ( $\delta$ ENaC). Each of the ENaC subunits consists of two transmembrane helices with a large extracellular loop and intracellular N- and C-termini (Canessa et al., 1994a). PY motifs (xPPxY) at the C-termini of the ENaC subunits just distal to the second transmembrane domain have been identified and are required for normal channel regulation (Booth et al., 2003; Abriel et al., 1999). Mutations of the PY motifs of ENaC subunits cause dysregulation of ENaC activity and Liddle's syndrome (Schild et al., 1996). Formation of a fully functional channel requires all  $\alpha$ ,  $\beta$ , and  $\gamma$  subunits, however, the  $\alpha$  subunit appears to be most important for channel activity and can form partially functional channels when expressed alone or with  $\beta$ ENaC or  $\gamma$ ENaC (Harris et al., 2008; Cheng et al., 1998; Firsov et al., 1998; Canessa et al., 1994b).

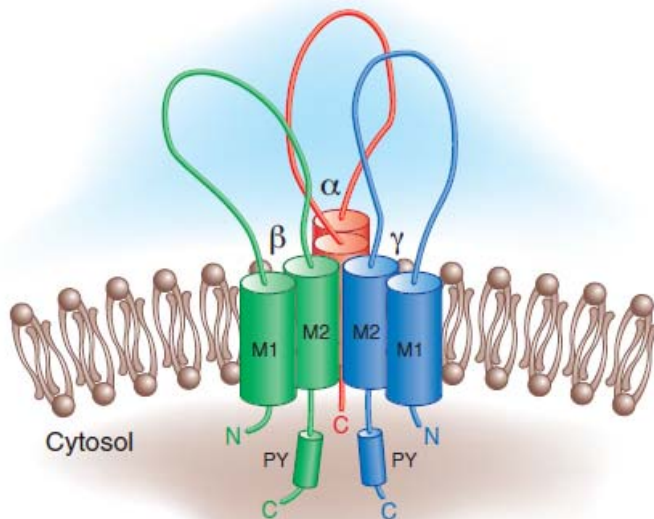


**Figure 1.4 Structure of the epithelial sodium channel (ENaC).** ENaC consists of three homologous subunits ( $\alpha$ ,  $\beta$ , and  $\gamma$ ), each of which has two transmembrane domains (M1 & M2), a large extracellular loop, and cytosolic N- and C-termini with PY motifs close to the C-terminus. Figure used from (Bhalla and Hallows, 2008).

### 1.4.1 Regulation of epithelial sodium channel

ENaC is regulated through changes in expression, trafficking, and channel open probability ( $P_o$ ). ENaC protein expression is upregulated hormonally by aldosterone (Mick et al., 2001), AVP (Perlewitz et al., 2010), and insulin. Aldosterone induces expression of SGK1 and  $\alpha$ ENaC in the ASDN and causes ENaC translocation to the apical membrane in principal CCD cells (Loffing et al., 2001). Aldosterone stimulates  $\alpha$ ENaC expression in part by relieving gene repression by a repressor complex of disruptor of telomeric silencing 1a (Dot1a) and ALL-1 fused gene from chromosome 9 (AF9) via a) downregulating expression of Dot1a and AF9 and b) upregulating SGK1, which phosphorylates AF9 preventing its interaction with Dot1a to form the repression complex (Reisenauer et al., 2010; Zhang et al., 2007). In mouse kidney ASDN,  $\alpha$ ENaC was upregulated in response to

low salt diet or aldosterone and this caused translocation of cytosolic  $\beta$ ENaC and  $\gamma$ ENaC to the apical membrane (Loffing et al., 2000).

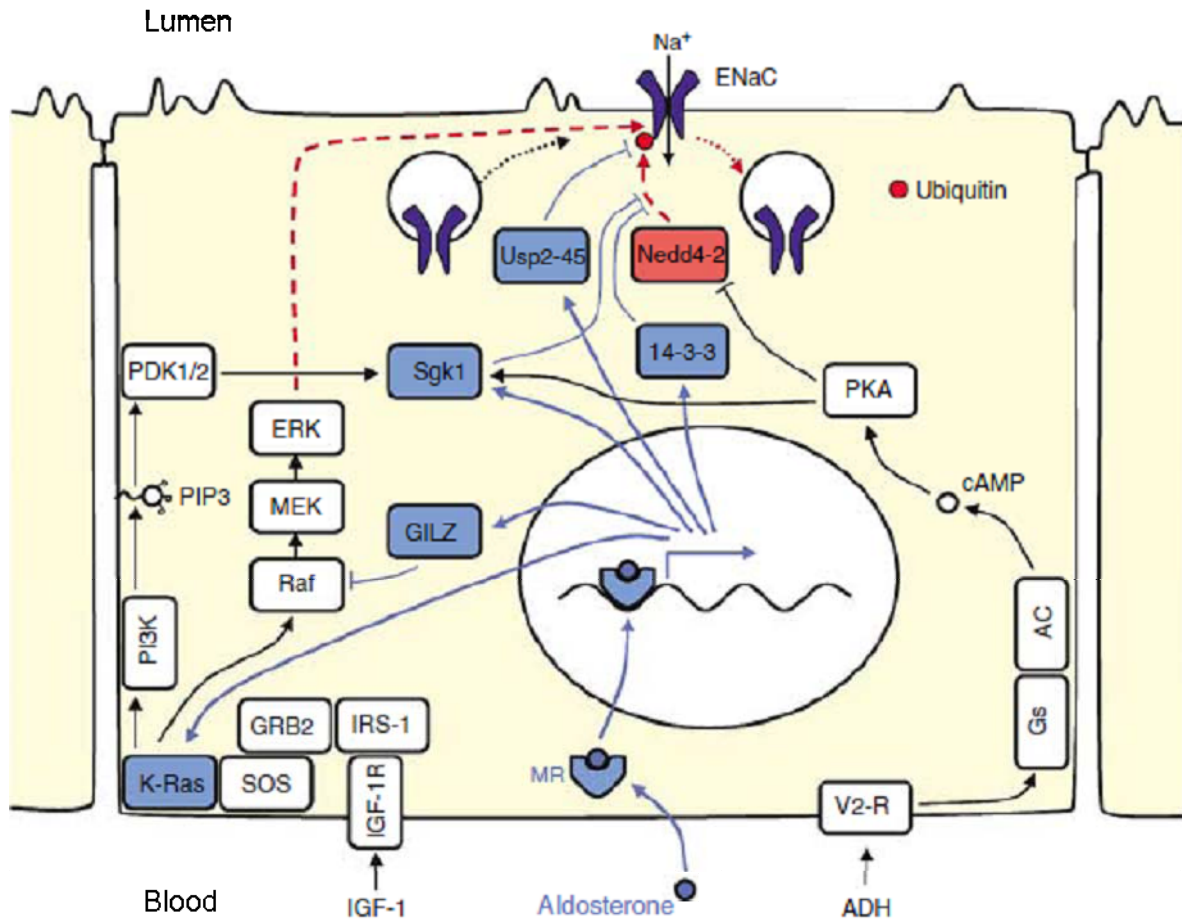


**Figure 1.5 A model of a principal cell highlighting the signalling pathways involved in regulation of ENaC.** Aldosterone and the signalling components that are upregulated by aldosterone are coloured blue. Components and actions that cause reduced expression of ENaC at the apical membrane are coloured red. Figure adapted from (Verrey et al., 2007).

ENaC is bound to and requires PtdIns(4,5)P<sub>2</sub> for normal channel gating, whilst ENaC binding to PtdIns(3,4,5)P<sub>3</sub> via PY motifs caused increased activity of ENaC (Zhang et al., 2009; Pochynyuk et al., 2005). ENaC may also be regulated through mechanosensitivity associated with laminar shear stress. In isolated rabbit CCDs and *Xenopus* oocytes, increasing shear stress associated with fluid flow caused an increase in ENaC  $P_o$  that was

sensitive to temperature (Carattino et al., 2007). The large extracellular loops in the structure of ENaC subunits are also involved in Na<sup>+</sup> self-inhibition (Sheng et al., 2007).

The large extracellular loops of the ENaC subunits play a considerable role in limiting channel  $P_o$ , however, cleavage of the loops by intra and extracellular proteases greatly increases ENaC  $P_o$  and subsequent Na<sup>+</sup> transport. Prostasin/channel-activating protease 1 (CAP1) increased ENaC currents when coexpressed in oocytes and other systems (Planes et al., 2010; Andreasen et al., 2006; Vuagniaux et al., 2000). Trypsin has also been shown to increase ENaC activity (Nesterov et al., 2008). Proteolytic cleavage of an inhibitory peptide out of the extracellular loop of  $\alpha$ ENaC by furin and of  $\gamma$ ENaC by prostasin caused a step-wise increase in ENaC open probability (Carattino et al., 2008). Prostasin is regulated itself by PN-1, which is upregulated by aldosterone and TGF $\beta$  (Wakida et al., 2006). Extracellular proteolytic cleavage of ENaC removed the self-inhibition caused by extracellular [Na<sup>+</sup>] (Chraïbi and Horisberger, 2002). Short palate, lung, and nasal epithelial clone 1 (SPLUNC1) has been identified as an anti-protease regulatory protein of extracellular ENaC cleavage in airway surface fluid volume (Garcia-Caballero et al., 2009). The extracellular protein SPLUNC binds to the extracellular loops of non-cleaved ENaC and prevents ENaC cleavage and thereby reducing ENaC currents.

ENaC apical membrane half-life is estimated to be approximately 20-30 min from various studies (Kabra et al., 2008; Lu et al., 2007; Alvarez de la Rosa et al., 2002). It has been suggested that ENaC is present in a large sub-apical pool and its recycling or degradation from this pool is dependent on PY motifs near the C-termini of each subunit (Lu et al., 2007). ENaC endosomes (recycling and late) are coordinated by sorting proteins syntaxin and Rab GTPases (Saxena et al., 2007). The ubiquitin ligase Nedd4-2 binds and ubiquitinates ENaC, causing it to be internalised by endocytosis. SGK1 phosphorylates

Nedd4-2, preventing its ubiquitination of ENaC (Flores et al., 2005; Kamynina and Staub, 2002).

SGK1 binds via a PY motif to WW domains of Nedd4-2 and phosphorylates it primarily at serine 444, but also at serine 338, causing its reduced interaction with ENaC (Debonneville et al., 2001). Another protein upregulated by aldosterone, 14-3-3 $\beta$ , binds to the phosphorylated Nedd4-2 blocking its interaction with ENaC (Liang et al., 2006; Nagaki et al., 2006) (Figure 1.5). Dysregulated ubiquitination and internalisation of ENaC by Nedd4-2 is linked to Liddle's syndrome (Abriel et al., 1999; Goulet et al., 1998), which is characterised by increased Na<sup>+</sup> transport due to increased apical membrane half-life of ENaC. ENaC subunits may be either polyubiquitinated or multi-monoubiquitinated at the cell surface (Butterworth et al., 2007; Wiemuth et al., 2007). Polyubiquitination through ubiquitin lysine 48 targets ENaC for degradation by the proteasome, whereas monoubiquitination or polyubiquitination through ubiquitin lysine 63 targets ENaC for internalisation (Abriel and Staub, 2005). ENaC recycling following ubiquitination and internalisation is associated with deubiquitination by enzymes such as Usp-45 (Fakitsas et al., 2007) and UCH-L3 (Butterworth et al., 2007). Ubiquitin-specific protease Usp2-45 is induced by aldosterone in vivo and has been shown to deubiquitinate ENaC and cause increased ENaC-mediated sodium transport in HEK293, *Xenopus* oocytes, and mpkCCD<sub>cl4</sub> cells (Fakitsas et al., 2007) (Figure 1.5). Another deubiquitinating enzyme USP10 requires sorting nexin 3 (SNX3) for upregulation of ENaC (Butterworth and Johnson, 2008).

ENaC is subject to feedback inhibition by increased intracellular [Na<sup>+</sup>] causing binding of Nedd4-2 and Nedd4 to PY motifs present in the C-terminal domains of  $\beta$  and  $\gamma$ ENaC (Rauh et al., 2006). In addition to indirect effects of SGK1 on ENaC via Nedd4-2, SGK1 can also directly phosphorylate and stimulate  $\alpha$ ENaC activity. ENaC regulation can also occur via Nedd4-2 phosphorylation and inactivation by I $\kappa$ B kinase- $\beta$  (IKK $\beta$ ) (Edinger et

al., 2009). A recent publication by Hallows et al. (2010) has shown that c-Jun N-terminal kinase 1 (JNK1) of MAPK/ERK signalling phosphorylates Nedd4-2 at several novel phosphorylation sites causing increased interaction and inhibition of ENaC (Hallows et al., 2010).

In an opposing system to SGK1 stimulation of ENaC, MAPK/ERK phosphorylates  $\beta$  and  $\gamma$ ENaC C-termini increasing their interaction with Nedd4-2 and subsequent internalisation. MAPK/ERK inhibition of ENaC has also been shown to be induced by PKC. Casein kinase 2 (CSNK2) has also been shown to phosphorylate Nedd4-2 removing its inhibition of ENaC (Bachhuber et al., 2008). ENaC has been shown to be maintained in its active state by G-protein-coupled receptor kinase 2 (GRK2), an enzyme implicated in the development of essential hypertension. Also, GRK2 binds and phosphorylates  $\beta$ ENaC, Nedd4 and Nedd4-2, but only the phosphorylation of the C-terminus of  $\beta$ ENaC inhibits binding of Nedd4-2 (Sanchez-Perez et al., 2007). cAMP/protein kinase A can induce phosphorylation and inhibition of Nedd4-2 independently of SGK1 (Vallon and Lang, 2005). Protein Kinase D1 also modulates aldosterone-induced ENaC activity in M1-CCD cells (McEneaney et al., 2010).

ENaC has also been shown to be regulated by members of the With No Lysine (WNK) kinase family, which are structurally classified as MAPKKK that lack a conserved lysine residue within their kinase domain. There are four WNK kinases in mammals, named WNK1, WNK2, WNK3, and WNK4. WNK kinases phosphorylate and activate oxidative stress responsive kinase 1 (OSR1) and STE20-like proline and alanine-rich kinase (SPAK), which, in turn, phosphorylate and activate the  $\text{Na}^+/\text{Cl}^-$  cotransporter (NCC) (Moriguchi et al., 2005). Mutations in WNK1 and WNK4 have been identified as causing pseudohypoaldosteronism type 2 (PHA2) – an autosomal dominant disorder resulting in hypertension and hyperkalemia (Wilson et al., 2001). Both WNK1 and WNK4 are

expressed in the distal nephron (Wilson et al., 2001), however, in situ hybridisation (ISH) studies have shown that the kidney-specific WNK1-S (short WNK1) is the primary WNK isoform expressed in kidney (O'Reilly et al., 2003). ISH studies have also shown that WNK1-S is predominantly expressed in DCT, but WNK4 is expressed throughout the distal nephron (O'Reilly et al., 2006). WNK1 activates SGK1 resulting in increased ENaC activity in a SGK1 and Nedd4-2 dependent manner (Xu et al., 2005a). WNK1 activation of SGK1 is PI3K-dependent and requires the N-terminal 220 residues of WNK1, but not its kinase domain (Xu et al., 2005b). WNK1 has been shown to be induced by hyperosmotic stress and to redistribute from cytosol to vesicles that could be recycling endosomes (Zagorska et al., 2007). Aldosterone rapidly increases the expression of (the short kidney-specific) WNK1-S isoform and overexpression of this isoform results in increased activity of ENaC (Naray-Fejes-Toth et al., 2004b). In *Xenopus* oocytes, coexpression of WNK4 with ENaC caused inhibition of sodium transport, whereas coexpression with WNK4 carrying a mutation that causes PHAII did not inhibit ENaC (Ring et al., 2007a). SGK1 phosphorylates wild-type WNK4 preventing its inhibitory effect on ENaC and ROMK (Ring et al., 2007b).

## **1.5 Hypertension**

Hypertension is a chronic condition of elevated blood pressure that causes an increased risk of heart attack, heart disease, kidney disease, and stroke. In the UK, guidelines state that a patient should be treated for hypertension if their blood pressure readings are consistently 140 mm Hg systolic and 90 mm Hg diastolic or higher (Higgins and Williams, 2007). However, changes in blood pressure by as little as 1 to 3 mm Hg systolic can alter the risk of stroke by up to 20 to 30% (Staessen et al., 2003). In 2001, approximately

13.5% of total global premature deaths were attributed to high blood pressure (Lawes et al., 2008).

Several studies have found polymorphisms in the *SGK1* gene that are linked to increased risk of hypertension. Studies by von Wovern et al. (2005) and Busjahn et al. (2002) found that polymorphisms in intron 6 and exon 8 of the *SGK1* gene were linked to increased diastolic and systolic blood pressure and also caused greater blood pressure increase in response to insulin (von Wovern et al., 2005; Busjahn et al., 2002). However, a conflicting report published by Trochen et al. (2004) demonstrated that SGK1 polymorphisms did not show increased prevalence in hypertensive or renal disease patients and showed no relation to blood pressure (Trochen et al., 2004). Despite the conflicting reports in links between SGK1 and hypertension, it is still highly likely that SGK1 is involved in hypertension, as Nedd4-2 deficient mice show salt-sensitive hypertension (Shi et al., 2008). Also, SGK1 knockout and double SGK1/SGK3 knockout mice display an inability to restrict salt excretion when given a low-salt diet (Grahammer et al., 2006; Wulff et al., 2002) and SGK1 knockout mice were also protected against high salt and desoxycorticosterone acetate (DOCA)-induced renal fibrosis and albuminuria (Artunc et al., 2006).

In humans, the majority of inherited genetic disorders that cause hypertension do so by causing dysregulation of renal Na<sup>+</sup> reabsorption. Liddle's syndrome is an autosomal dominant condition that causes early-onset hypertension with low potassium, alkalosis and reduced plasma aldosterone concentration. Liddle's syndrome is caused by gain-of-function mutations in ENaC subunits through deletion or disruption of the PY motifs resulting in reduced channel downregulation by Nedd4-2, increased number and activity of ENaC, and increased Na<sup>+</sup> reabsorption (Knight et al., 2006; Schild et al., 1996).

Pseudohypoaldosteronism type 1 (PHA1) causes renal salt wasting with metabolic acidosis, high potassium levels and high renin and aldosterone. Autosomal recessive PHA1 is caused by loss-of-function mutation of any ENaC subunit, causing reduced  $\text{Na}^+$  reabsorption in the CCD (Riepe, 2009). The reduced  $\text{Na}^+$  reabsorption also removes the driving force for  $\text{K}^+$  and  $\text{H}^+$  excretion in the CCD causing hyperkalemia and acidosis. The hyperkalemia and decreased hydration/blood pressure stimulates the RAAS causing the high levels of renin and aldosterone, but without effects of functional ENaC. Autosomal dominant PHA1 also exists and causes milder salt wasting than the autosomal recessive form through loss-of-function mutations in the mineralocorticoid receptor (Uchida et al., 2009).

Pseudohypoaldosteronism type 2 (PHA2) is an autosomal dominant condition causing hypertension, high potassium, hyperchloremic acidosis and low renin and aldosterone. PHA2 is caused by mutations in WNK1 and WNK4, which regulate  $\text{Na}^+$  transport in the distal nephron primarily via NCC and ROMK (Vitari et al., 2005). WNK4 acts as a negative regulator of NCC and ROMK, whereas WNK1 acts as a negative regulator of WNK4 (Kahle et al., 2005; Choate et al., 2003). Loss-of-function mutations of either WNK1 or WNK4 therefore cause increased NCC and ROMK activity, and then lead to enhanced  $\text{Na}^+$  and  $\text{K}^+$  retention. Additional conditions affecting renal electrolyte regulation include Bartter and Gitelman syndromes, both of which cause hypotension, are autosomal recessive, and occur through dysregulated calcium handling (O'Shaughnessy and Karet, 2006).

### **1.5.1 SGK1 and other diseases**

Sgk1 is involved in pulmonary vascular remodelling (BelAiba et al., 2006). SGK1 upregulated CFTR in a kinase-dependent manner in *Xenopus* oocytes (Sato et al., 2007). ENaC has been linked to regulation of the cystic transmembrane conductance regulator (CFTR) associated with cystic fibrosis (CF) (Fajac et al., 2009; Mall, 2008). Recently novel gain-of-function or loss-of-function mutations were identified in the  $\alpha$ ENaC of atypical CF patients that possibly contribute to the symptoms of CF (Huber et al., 2010; Rauh et al., 2010).

SGK1 contributes to tissue fibrosis during diabetic neuropathy (Feng et al., 2005; Wang et al., 2005; Kumar et al., 1999). Polymorphisms in the SGK1 gene have been linked to type 2 diabetes (Schwab et al., 2008) and SGK1 has been shown to mediate salt-sensitive cellular uptake of glucose (Boini et al., 2006). In patients suffering from type 2 diabetes, it has been suggested that SGK1 enhances hypertension and tissue fibrosis (Lang et al., 2009). A role for SGK1 in stress induced tissue fibrosis was further confirmed in doxorubicin-induced nephrotic syndrome (Artunc et al., 2008). SGK1 is also involved in cardiac fibrosis as a result of high mineralocorticoid levels (Vallon et al., 2006). SGK1 is also expressed in brain and is involved in neuronal function as well as Parkinson's disease, neuronal damage and neurodegenerative diseases (Lang et al., 2010; Schoenebeck et al., 2005; Stichel et al., 2005).

## **1.6 Aims**

The primary aim of this thesis was to determine which of the sodium/glucocorticoid regulated kinase 1 (SGK1) isoforms identified in human are expressed in renal cortical collecting duct epithelial cells. Following identification of the SGK1 isoforms expressed in CCD cells, the requirements for SGK1 isoforms in regulation of ENaC-mediated sodium transport would be investigated. The mouse cortical collecting duct model cell line (mpkCCD<sub>cl4</sub>) was used for this project as a model of CCD cells in which ENaC is known to be regulated by aldosterone-stimulated Sgk1 (Flores et al., 2005; Bens et al., 1999). The aim therefore became to investigate the requirements for Sgk1 isoforms in regulation of ENaC-mediated sodium transport in mpkCCD<sub>cl4</sub> cells including investigation of the subcellular distribution of human and mouse SGK1 isoforms in regulation of sodium transport in renal epithelial cells.

## **Chapter 2 - Materials and Methods**

### **2.1 Cell Culture**

The mpkCCD<sub>cl4</sub> transimmortalized mouse cortical collecting duct cell line was a gift from Prof. Alain Vandewalle (Institut National de la Santé et de la Recherche Médicale (INSERM), Paris, France). mpkCCD<sub>cl4</sub> cells were maintained in growth medium consisting of: Dulbecco's modified Eagle's medium (DMEM) minus phenol red (Sigma-Aldrich Ltd., Gillingham, UK):HAM's F12 (Sigma-Aldrich) at 1:1 vol/vol, supplemented with: 60 nM sodium selenate (Sigma-Aldrich); 5 mg/ml transferrin (Sigma-Aldrich); 2 mM L-glutamine (Lonza Biologics plc, Slough, UK); 50 nM dexamethasone (Sigma-Aldrich); 1 nM triiodothyronine (Sigma-Aldrich); 10 nM epidermal growth factor (EGF) (Sigma-Aldrich); 5 mg/ml insulin (Sigma-Aldrich); 20 mM D-glucose (Sigma-Aldrich); 2% fetal calf serum (FCS) (Biosera, Ringmer, East Sussex, UK) and 20 mM HEPES (Sigma-Aldrich/Invitrogen Ltd., Paisley, UK) (Bens et al., 1999). HEK293T cell growth medium was DMEM (Lonza) supplemented with 10% FCS (Biosera) (Tai et al., 2009).

Cells were grown to ~90% confluency in T25 or T75 tissue culture flasks (TPP AG, Trasadingen, Switzerland/SARSTEDT Ltd., Leicester, UK) containing 10 or 20 ml growth medium at 37°C and 5% CO<sub>2</sub>. For passage, cells were detached using 2.5 ml (T25) or 5 ml (T75) trypsin-EDTA solution (21.5 mM porcine trypsin and 685 mM EDTA in Hank's Balanced Salt Solution with phenol red) (Sigma-Aldrich) incubated at 37°C and 5% CO<sub>2</sub>. Once detached, an equal volume of growth medium was used to neutralise the enzyme prior to centrifugation at 300 x g for 3 minutes and resuspension in 5 ml growth medium and transfer to new tissue culture flasks. Cells were then seeded at the following densities depending on application: 4 x 10<sup>3</sup> cells/cm<sup>2</sup> in tissue culture flasks for cell line

maintenance,  $5 \times 10^4$  cells/cm<sup>2</sup> on cell culture-treated polystyrene plates (TPP/Corning B.V. Life Sciences, Amsterdam, The Netherlands) for transfection studies,  $2.5 \times 10^4$  cells/cm<sup>2</sup> on glass coverslips for use in immunofluorescence microscopy, or  $1 \times 10^6$  cells/cm<sup>2</sup> on Transwell<sup>®</sup> permeable supports (Corning) for equivalent short circuit current experiments. All experiments in this thesis were performed on cells of between passage 30 and 50 for mpkCCD<sub>cl4</sub> cells and between passage 20 and 50 for HEK293T cells.

### **2.1.1 Culture of mpkCCD<sub>cl4</sub> cells on Transwell supports**

mpkCCD<sub>cl4</sub> cells were seeded at high density ( $1 \times 10^6$  cells/cm<sup>2</sup>) onto 12-well Transwell<sup>®</sup> permeable supports containing 12 mm diameter (1.12 cm<sup>2</sup> surface area) polyester (PET) insert membranes of 0.4 µm pore size (Corning). Cells were seeded in growth medium, which was replaced every 2 days until transepithelial resistance had stabilised at >2 kilohms (kΩ) after 6-8 days ((Bens et al., 1999)). Prior to being used for equivalent short circuit current experiments, cell monolayers were washed in phosphate buffered saline (PBS) (Sigma-Aldrich) and then cultured for 24 hours in starvation medium (DMEM:HAM's F12 at 1:1 vol/vol) to remove the stimulatory effects of the serum, hormones and EGF that are present in growth medium.

### **2.1.2 Hormone and drug treatments**

Prior to hormone or drug treatment, mpkCCD<sub>cl4</sub> cells grown to ~80% confluency were washed in PBS and then cultured for 24 hours in starvation medium. Unless otherwise stated, hormone and drug treatments were for 24 hours in starvation medium at the final concentrations indicated in Table 2.1.

<b>Hormone/drug name</b>	<b>Stock solution</b>	<b>Final concentration</b>
Aldosterone (Sigma-Aldrich/Fisher Scientific UK Ltd., Loughborough, UK)	1 mM in ethanol	10 nM
Amiloride (Sigma-Aldrich)	10 mM in dimethyl sulfoxide (DMSO)	1 $\mu$ M
Insulin (Sigma-Aldrich)	10 mg/ml or 1.72 mM in acidified H <sub>2</sub> O (1% acetic acid)	1 $\mu$ M
Rapamycin (Enzo Life Sciences (UK) Ltd., Exeter, UK)	20 $\mu$ M in DMSO	20 nM
LY294002 (Merck Chemicals Ltd., Nottingham, UK/Promega UK Ltd., Southampton, UK)	10 mM in DMSO	10 $\mu$ M
Spirolactone (Sigma-Aldrich)	10 mM in DMSO	10 $\mu$ M
Mifepristone (Sigma-Aldrich)	10 mM in DMSO	10 $\mu$ M

**Table 2.1 Hormone and drug treatments.**

### **2.1.3 Transient transfection of plasmid DNA**

The following transfection reagents: Lipofectamine<sup>TM</sup>, Lipofectamine<sup>TM</sup> 2000, Lipofectamine PLUS<sup>TM</sup> (Invitrogen) and FuGENE<sup>®</sup> 6 (Roche Diagnostics Ltd., Burgess Hill, UK) were tested for their ability to transiently transfect mpkCCD<sub>cl4</sub> cells, used according to manufacturer's instructions. Transfection efficiency was assessed using the pLEGFP-N1 plasmid (Clontech-Takara Bio Europe, Saint-Germain-en-Laye, France) (Figure 2.1) and fluorescence microscopy. Lipofectamine<sup>TM</sup> 2000 was found to give the highest transfection efficiency, which was estimated to be 10%, for mpkCCD<sub>cl4</sub> cells grown on glass coverslips. The same transfection procedure was used for HEK293T cells, and using these cells was estimated to achieve around 65% transfection efficiency.

Using cells grown on a tissue culture 6-well plate, 4  $\mu$ g of plasmid DNA (0.2-2 mg/ml in Buffer TE (Qiagen Ltd., Crawley, UK) or H<sub>2</sub>O) and 10  $\mu$ l of Lipofectamine<sup>TM</sup> 2000 were each added to 250  $\mu$ l of serum-free medium and incubated at room temperature for 5 min.

The diluted DNA and Lipofectamine™ 2000 were then combined and incubated for a further 20 min before being added to wells containing the cells and 2 ml of growth medium. Cells were then incubated for 6 hours at 37°C and 5% CO<sub>2</sub>, at which point they were given fresh growth medium and incubated for a further 24 hours before lysis.

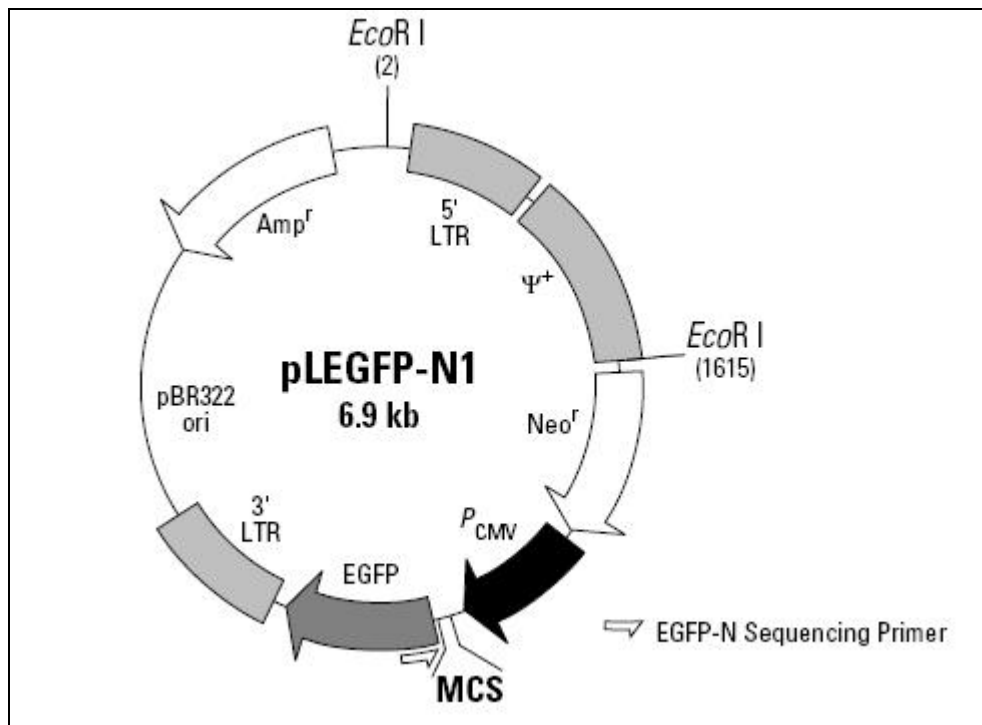


**Figure 2.1** A vector map of the pLEGFP-N1 vector. Image used from ([http://www.clontech.com/images/pt/dis\\_vectors/PT3233-5.pdf](http://www.clontech.com/images/pt/dis_vectors/PT3233-5.pdf)).

#### 2.1.4 siRNA knockdown

Cells grown on cell culture-treated polystyrene plates were transiently transfected with siRNA using Lipofectamine™ 2000 according to manufacturer's instructions. mpkCCD<sub>c14</sub> cells were seeded at  $5 \times 10^4$  cells/cm<sup>2</sup> on cell culture-treated polystyrene 6-well plates (TPP/Corning) and grown for 24 hours prior to transfection with siRNA. To prepare the transfection mix, 30  $\mu$ l of 20  $\mu$ M siRNA stock solution and 30  $\mu$ l of Lipofectamine 2000 were each diluted in 250  $\mu$ l of serum-free cell culture medium. The diluted siRNA and

Lipofectamine 2000 were incubated for 5 min at 21°C before being combined and incubated for a further 20 min. Transfection mix was then added to cells containing 2 ml growth medium so the final concentration of siRNA exposed to cells was 40 nM. Cells were then incubated for 24 hours at 37°C, 5% CO<sub>2</sub> before being lysed and knockdown assessed by Western blotting. Mouse Sgk1-specific and scrambled controls siRNAs were purchased from Qiagen. The Sgk1 siRNA targets a sequence that is conserved in all mouse Sgk1 isoform mRNAs and therefore should knockdown all Sgk1 isoforms (Table 2.2). For experiments using Transwell permeable supports, cells were first transfected on cell culture-treated 6-well plates before being washed with PBS, detached using trypsin-EDTA solution, resuspended in growth medium, and then seeded onto the Transwell membranes. These cells were then treated as described in section 2.1.2. The siRNA transfection procedure was adapted from the procedure described for siRNA transfection using Lipofectamine 2000 in Hallows et al. (2009).

siRNA Name	Target sequence	Target gene
Mm Sgk 2 HP	CTG GGA TGA TCT CAT CAA TAA	<i>Sgk1</i>
Allstars Negative Control	Scrambled	n/a

**Table 2.2 Qiagen siRNA data.**

## **2.2 Molecular Biology**

### **2.2.1 DNA cloning**

Mouse Sgk1a was purchased from Geneservice (Source BioScience, Cambridge, UK) cloned in the pCMV-SPORT6 expression vector between the *SalI* (5') and *NotI* (3') restriction sites in its multiple cloning site (Figure 2.2). Sgk1b was cloned into pCMV-SPORT6 through replacement of the N-terminus of Sgk1a in pCMV-SPORT6 with that of

Sgk1b. The N-terminus of Sgk1b was generated by RT-PCR from purified mpkCCD<sub>c14</sub> cell RNA using the primers MmSGK1bSalIF and MmSGK1PacIR, which are described in Table 2.4. These primers encompass the N-terminus of Sgk1b from an introduced *SalI* restriction site at its 5' end to a *PacI* restriction site at its 3' end. Digestion of Sgk1a in pCMV-SPORT6 and the Sgk1b RT-PCR product at these restriction sites produced the 2-4 base overhanging ends required for ligation. The digestion fragments were separated, according to size, in an agarose gel using electrophoresis. The fragments desired for ligation were then extracted using a QIAquick Gel Extraction Kit (Qiagen). T4 DNA Ligase (Promega) was then used according to the manufacturer's instructions to ligate the Sgk1b DNA fragment into the expression vector.

Sgk1c was also cloned into pCMV-SPORT6 through replacement of the Sgk1a sequence in pCMV-SPORT6, but, due to difficulties in its production by RT-PCR, Sgk1c was generated by combinatorial PCR. This first involved generating the Sgk1c N-terminus by PCR from purified mpkCCD<sub>c14</sub> cell DNA using the primers New MmSGK1cSalIF and MmSgk1cCombiR, described in Table 2.4. Then the Sgk1 common sequence was generated by PCR from the Sgk1a in pCMV-SPORT6 plasmid DNA, using the primers MmSgk1cCombiF and New MmSgk1cR, described in Table 2.4. And, finally, the purified PCR products from these two reactions were combined, to form complete Sgk1c, using PCR with the primers New MmSGK1cSalIF and New MmSgk1cR, which generated the full-length Sgk1c DNA due to a complimentary overlap of the two preliminary DNAs. The insertion of this DNA into pCMV-SPORT6 was then performed as described for Sgk1b.

Sgk1d was subcloned from pYX-Asc (in which it was purchased from Geneservice) into pCMV-SPORT6 by digestion of both vectors at *NotI* and *EcoRI* restriction sites before ligation of the purified Sgk1d and pCMV-SPORT6 fragments as described previously.

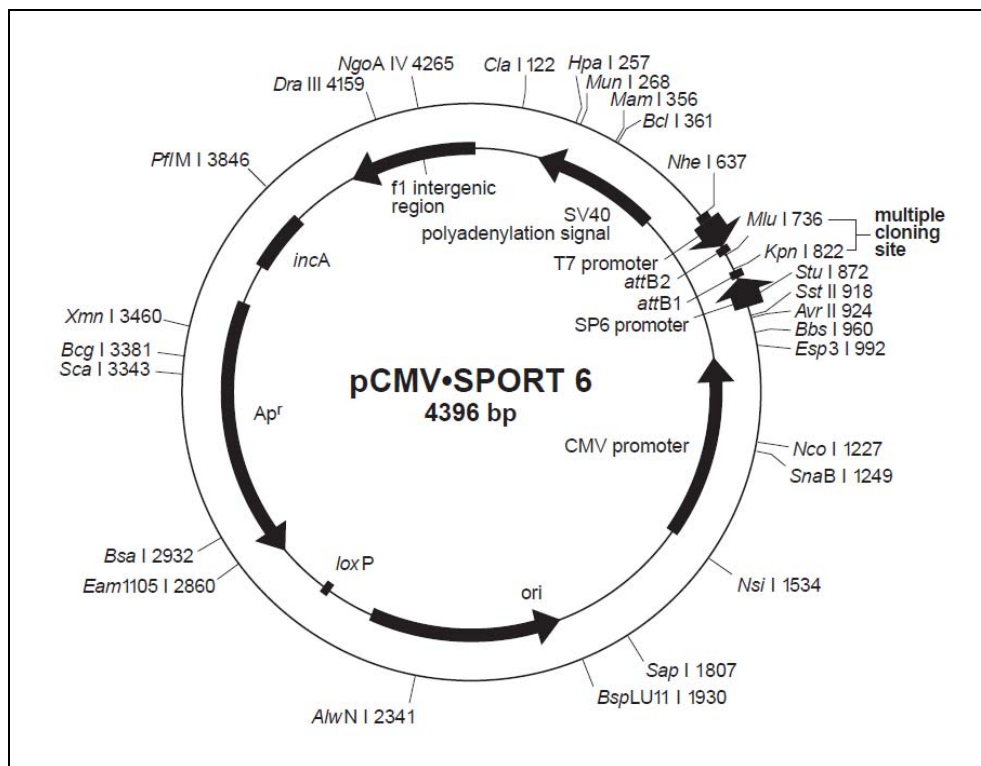


**Figure 2.2 pCMV-SPORT6 vector map.** Image used from ([http://tools.invitrogen.com/content/sfs/vectors/pcmvsport6\\_map.pdf](http://tools.invitrogen.com/content/sfs/vectors/pcmvsport6_map.pdf)).

Cloning of the mouse Sgk1 isoforms into pFLAG-CMV-2 (Sigma-Aldrich) (Figure 2.3) involved PCR of each isoforms complete sequence from their respective plasmid DNA using the primers described in Table 2.5. The resulting PCR products and empty pFLAG-CMV-2 vector were then digested using *NotI* and *SalI* before ligation of the desired fragments as described previously. All cloned DNA vectors were sequenced to confirm fragments as being in the correct orientation, in-frame and error-free (see appendix).

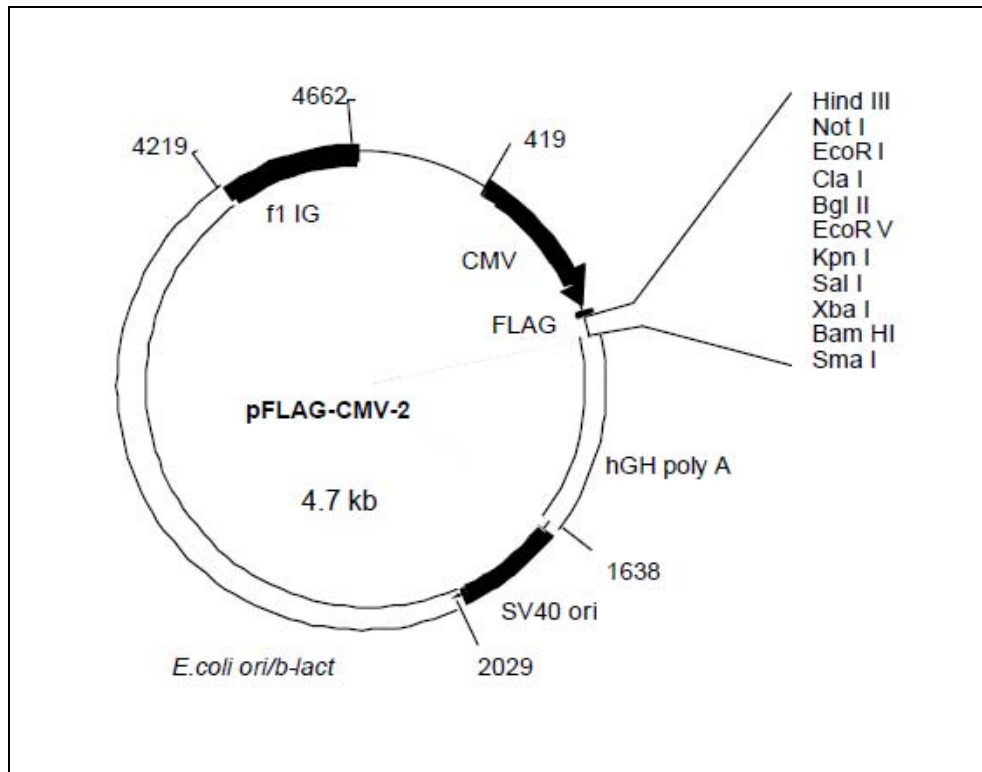


**Figure 2.3 pFLAG-CMV-2 vector map.** Image used from (<http://www.Sigma-Aldrich.com/etc/medialib/docs/Sigma-Aldrich/Datasheet/e7033dat.Par.0001.File.tmp/e7033dat.pdf>).

Additional constructs referred to in this thesis include a myr and myc-tagged constitutively active 3-phosphoinositide-dependent protein kinase 1 (PDPK1) construct (pCMV3-myr-PDPK1-myc) from Dr. K. Anderson (Babraham Institute, Cambridge) and a FLAG-tagged kinase-dead SGK1A construct (pFLAG-CMV-2-SGK1A(K127M)), which was created in-house by Dr Quan Long.

### 2.2.2 Restriction enzyme digests

Restriction enzymes were bought from NEB (New England Biolabs, Hitchin, Hertfordshire, UK), Promega or Fermentas (Fermentas GmbH, St. Leon-Rot, Germany). Restriction enzyme digests were conducted according to manufacturer's instructions, in recommended buffer with 0.1 µg/µl bovine serum albumin (BSA) (Sigma-Aldrich) and 2

units of enzyme per  $\mu\text{g}$  of DNA. Reactions were incubated for 2 hours at  $37^\circ\text{C}$  then inactivated by incubation at  $60^\circ\text{C}$  for 10 min.

### **2.2.3 Bacterial culture**

*E.coli* was grown in Lysogeny broth (LB) or on LB agar plates containing carbenicillin antibiotic (Sigma-Aldrich) (a more stable analogue of ampicillin). Small 5 ml and large 350 ml LB cultures were incubated overnight at  $37^\circ\text{C}$ , 5%  $\text{CO}_2$  swirling at 300 rpm. LB consisted of 10 g/L tryptone (Fisher), 5 g/L yeast extract (Fisher), 10 g/L NaCl (Fisher), pH 7. LB agar contained LB, but with 5 g/L NaCl and 15 g/L agar (Fisher).

### **2.2.4 Transformation into *E.coli***

Transformation of an expression vector into One Shot<sup>®</sup> TOP10 chemically competent *E.coli* (Invitrogen) was carried out using the manufacturer's rapid chemical transformation procedure. This involved addition of 1-5  $\mu\text{l}$  of ligation reaction to a 50  $\mu\text{l}$  vial of One Shot<sup>®</sup> cells, followed by incubation on ice for 5 min. The 50  $\mu\text{l}$  of cells was then spread onto a LB agar plate containing carbenicillin that had been pre-warmed to  $37^\circ\text{C}$ , which was then incubated overnight at  $37^\circ\text{C}$ , 5%  $\text{CO}_2$ . Successful colonies were picked and used to seed LB cultures for cultivating plasmid DNA.

### **2.2.5 Plasmid DNA extraction**

Plasmid DNA was then extracted from the culture using either a QIAprep<sup>®</sup> spin Miniprep Kit (Qiagen) for the 5 ml culture or a HiSpeed<sup>®</sup> Plasmid Maxiprep Kit (Qiagen) for the 350 ml culture according to the manufacturer's instructions.

### **2.2.6 Polymerase chain reaction (PCR)**

Successful bacterial colonies showing antibiotic resistance were picked and seeded into 0.5 ml PCR tubes (STARLAB (UK) Ltd., Milton Keynes, UK). The Expand High Fidelity PCR System (Roche) was then used according to the manufacturer's instructions with the appropriate primers to amplify expected insert DNA product. The amplification products were then separated by agarose gel electrophoresis (section 2.2.11) and visualised to assess which samples had the expected amplified product and, therefore, which colonies possessed the insert DNA.

### **2.2.7 Reverse transcriptase (RT)-PCR**

RT-PCR was performed using the Qiagen<sup>®</sup> OneStep RT-PCR Kit according to the manufacturer's protocol. Reactions contained: kit buffer, 400  $\mu$ M dNTP mix, 0.6  $\mu$ M of each primer, 4% kit enzyme mix (Omniscript Reverse Transcriptase, Sensiscript Reverse Transcriptase, and HotStarTaq DNA Polymerase) and 200 ng template RNA. Incubations consisted of: 50°C for 30 min, 95°C for 15 min, 30 cycles of 94°C for 1 min, 55°C for 1 min, and 72°C for 1 min followed by a final extension step of 72°C for 10 min. The completed reactions were stored at 4°C before being analysed using agarose gel electrophoresis.

### **2.2.8 RNA purification, quantification and storage**

mpkCCD<sub>c14</sub> cells were grown to confluency in complete cell culture media before a wash with PBS then treatment with trypsin/EDTA to detach the cells from their growth surface. The trypsin was then neutralised by the addition of complete media containing FCS and

cells were pelleted by centrifugation at 300 x g for 3 min. Cells were then resuspended in Buffer RLT (Qiagen RNeasy kit) and homogenised by passing the lysate through a QIAshredder spin column by centrifugation. RNA was then extracted and purified from the cell lysate using the RNeasy Mini Kit (Qiagen) according to the manufacturer's protocol. RNA was quantified by measuring sample absorbance at 260 nm using a BioPhotometer spectrophotometer (Eppendorf UK Ltd., Cambridge, UK). Purified RNA was stored in RNase-free water at -80°C.

### **2.2.9 DNA isolation, quantification and storage**

mpkCCD<sub>cl4</sub> cells prepared as described for RNA purification (section 2.2.8) were used for DNA isolation using TRIzol<sup>®</sup> Reagent (Invitrogen) according to the manufacturers instructions. Isolated DNA was stored at -20°C in 8 mM NaOH and quantified by measuring sample absorbance at 260 nm using a BioPhotometer spectrophotometer (Eppendorf).

### **2.2.10 Primers**

Sgk1 isoform specific primers, shown in Table 2.3, were designed to encompass unique isoform sequence at the first exon boundary using an online primer design tool Primer 3 (Rozen Steve, 2000).

Primer Name	Sequence (5'-3')	Length	Function
MmSGK1aF	TTC ACT GCT CCC CTC AGT CT	20-mer	Identification
MmSGK1aR	GGA CCC AGG TTG ATT TGT TG	20-mer	Identification
MmSGK1bF	GCT CAG AAA AGG AGC GAG TC	20-mer	Identification
MmSGK1b+cR	CCC TTT CCG ATC ACT TTC AA	20-mer	Identification
MmSGK1cF	AAA GTA ACC CCA GCC TCC AC	20-mer	Identification
MmSGK1dF	TGA GGC CAT GTG TCA ATC AT	20-mer	Identification
MmSGK1dR	GAG GAG AGG GGT TAG CGT TC	20-mer	Identification
GAPDHF	TGACATCAAGAAGGTGGTGAAG	22-mer	Control
GAPDHR	TCTTACTCCTTGGAGGCCATGT	22-mer	Control

**Table 2.3 Primers for identification of mouse Sgk1 isoforms.** Mm = *Mus musculus*, F = Forward, R = Reverse.

Primers were designed for cloning of the mouse Sgk1 isoforms b, c, and d, into the pCMV-SPORT6 expression vector, incorporating a restriction enzyme site in each primer to facilitate insertion of the PCR product into an expression vector (Table 2.4).

Primer name	Sequence (5'-3')	Length	Function
MmSGK1bSalIF	GGAGTCGACGGTTTTGGGACTGG	23-mer	Cloning
New MmSGK1cSalIF	AGTCGACGGAGGCTAACTTTTTCCG TA	27-mer	Cloning
New MmSgk1cR	CAAGTGTCACATTGATGCTC	20-mer	Cloning
MmSgk1cCombiF	CCTTGGAAGCTTTTATGAAACAGA	25-mer	Cloning
MmSgk1cCombiR	TCATAAAAGCTTTCCAAGGGGATCT	25-mer	Cloning
MmSGK1PacIR	CCAGTTAATTAAGAGAAGAAAAT ATG	27-mer	Cloning

**Table 2.4 Primers for cloning into pCMV-SPORT6.**

Similar primers were also designed for cloning mouse Sgk1 isoforms a, b, c, and d into pFLAG-CMV<sup>TM</sup>-2 (Sigma-Aldrich) and are shown in Table 2.5. These primers were designed to encompass the entire ORF for each isoform whilst adding restriction sites to allow the in-frame insertion of the product into the expression vector.

<b>Primer Name</b>	<b>Sequence (5'-3')</b>	<b>Length</b>	<b>Function</b>
MmSGK1aFLAGF	GCAGCGGCCGCAGCAACCGTCAA AGCCGAGG	31-mer	Cloning
MmSGK1bFLAGF	GCAGCGGCCGCAGCAGGCGAGTT ACAGGGCG	31-mer	Cloning
MmSGK1cFLAGF	GCAGCGGCCGCAGCAAAAGAGGA GACCTTAAGATC	35-mer	Cloning
FLAGMmSgk1dF2	GCAGCGGCCGCAGCAGTAAACAA AGACGCAAATGGA	36-mer	Cloning
MmSGK1FLAGR	CGCGTCGACTCAGAGGAAGGAAT CCACAG	29-mer	Cloning

**Table 2.5 Primers for cloning into pFLAG-CMV<sup>TM</sup>-2.**

### 2.2.11 Agarose gel electrophoresis

DNA samples were separated according to size by electrophoresis in 1% agarose gels. 0.75 g DNase/RNase-free agarose (Bioline, London, UK) was mixed with 75 ml Tris-Acetate-EDTA (TAE) buffer and heated in a microwave on full power until completely dissolved. TAE buffer consisted of 40 mM Tris acetate and 1 mM EDTA in water. The mixture was then cooled to ~50°C before 1.25 µM ethidium bromide was added. The mixture was then poured into a sealed tray and a comb suspended into the gel to form wells. Once the gel had polymerised, the ends of the tray were unsealed and the comb removed before use. The tray was placed in an electrophoresis chamber so that it was immersed in TAE. DNA samples were then mixed with the appropriate amount of 10x loading buffer and loaded into the wells. 5 µl of DNA size marker Hyperladder I (Bioline) was loaded with the DNA samples for comparison indicating sample DNA size and concentration. Electrophoresis occurred over 1-2 hours at 85 V and the resulting gel was visualized using a FluorChem<sup>®</sup> gel imager (Cell Biosciences Inc., Santa Clara, CA, USA). DNA separated according to size by electrophoresis in an agarose gel was purified using a QIAquick Gel extraction kit (Qiagen) according to the manufacturer's protocol.

### 2.2.12 DNA sequencing

Sequencing of DNA samples was done by postal order to MWG (Eurofins MWG Operon, Ebersberg, Germany). All sequencing results are included in the appendix.

### 2.2.13 *In vitro* protein synthesis from Sgk1 isoform DNA

Synthetic protein was generated from cloned Sgk1 isoform expression vectors using a TNT<sup>®</sup> SP6 Coupled Transcription/Translation System (Promega). This system was used according to manufacturer's instructions to (1) generate Sgk1 isoform mRNA using SP6 RNA polymerase and (2) translate that mRNA into protein using rabbit reticulocyte lysate. A Luciferase SP6 control DNA reaction was included in the procedure as a functional control for the system (Figure 2.4).

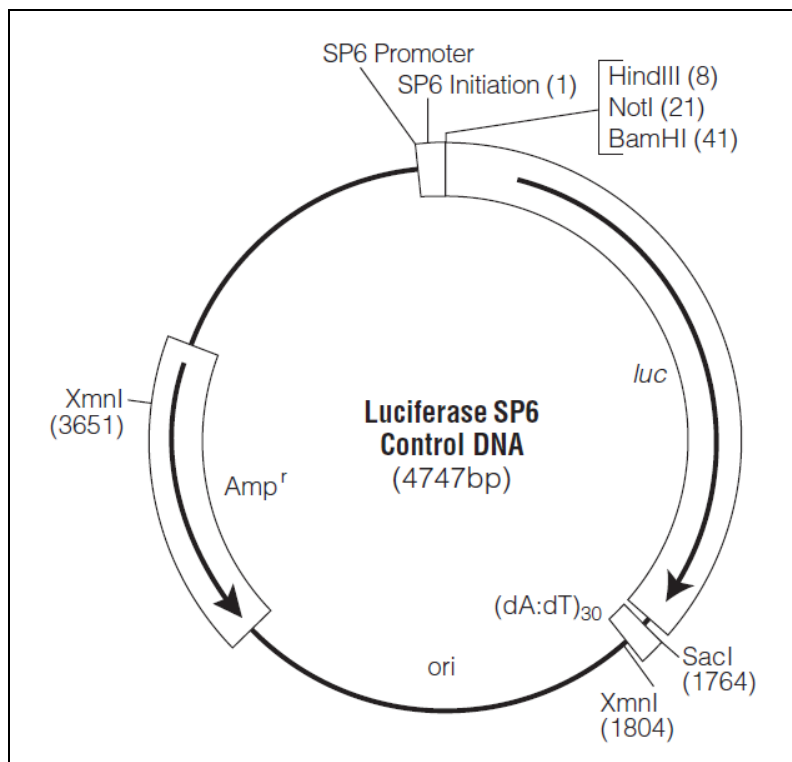


**Figure 2.4** Vector map of the TNT<sup>®</sup> Luciferase SP6 control vector. Image taken from (<http://www.promega.com/tbs/tb126/tb126.pdf>).

## **2.3 Western Blotting (Immunoblotting)**

### **2.3.1 Preparation, treatments and storage of protein samples**

Cells were washed once with ice cold PBS followed by 5 min incubation on ice with modified radio immunoprecipitation assay (RIPA) buffer. Modified RIPA buffer consisted of: 50 mM Tris buffer pH 7.5, 1% Nonidet P-40 (Sigma-Aldrich), 0.25% sodium deoxycholate (Sigma-Aldrich), 150 mM sodium chloride (Fisher), 1 mM sodium fluoride (Sigma-Aldrich), 5 mM B-glycerolphosphate (Sigma-Aldrich), 1 Complete<sup>®</sup> protease inhibitor cocktail tablet + EDTA (Roche), 0.5 mM phenylmethylsulphonylfluoride (PMSF) (Sigma-Aldrich), 1 mM sodium orthovanadate (Sigma-Aldrich), and to 50 ml final volume with water. Modified RIPA buffer minus phosphatase inhibitors was made to the same recipe only without the sodium fluoride, sodium orthovanadate, and B-glycerolphosphate. PMSF and sodium orthovanadate were made up and added to aliquots of modified RIPA buffer just before use as these components have short half-lives in solution. After incubation with modified RIPA buffer, cells were scraped off the growth surface using a cell scraper (SARSTEDT). The cell lysate was then centrifuged at 21,000 x g and 4°C for 10 min to remove cell debris and DNA. Protein samples were stored at -80°C. Protein lysates to be used as negative controls for testing the presence of phosphorylated protein forms (lysed using RIPA buffer minus phosphatase inhibitors) were treated with calf intestinal alkaline phosphatase (CIAP) (NEB). Lysates were treated with CIAP according to the manufacturer's instructions.

### **2.3.2 Protein quantification**

Concentration of total protein in samples was determined using a bicinchoninic acid (BCA) assay (Smith et al., 1985). A BCA™ Protein Assay Kit (Thermo Fisher Scientific, Cramlington, UK/Cheshire Sciences Ltd., Chester, UK) was used according to the manufacturer's instructions. A standard curve of protein concentration against absorbance at 562 nm was created using known concentrations (ranging from 2-0.025 mg/ml) of bovine serum albumin (BSA) (Sigma-Aldrich). Samples were analysed using a SpectraMax 250 microplate reader and SOFTmax® Pro analysis software (Molecular Devices, Sunnyvale, CA, USA).

### **2.3.4 Sodium dodecyl sulphate polyacrylamide gel electrophoresis (SDS-PAGE) and protein transfer**

Polyacrylamide gels for electrophoresis were prepared from liquid polyacrylamide before being poured between glass plates that were clamped together with a 1 mm divide. Separating gel consisted of: 375 mM Tris pH 8.8, 10% Acrylamide/Bis 19:1 solution, 0.1% SDS. Stacking gel consisted of: 125 mM Tris pH 6.8, 4% Acrylamide/Bis 19:1 solution, 0.1% SDS. Stacking gel was laid on top of the separating gel and had a comb inlaid to form wells. Protein samples were prepared to contain equal amounts of total protein and SDS sample buffer before being incubated at 95°C for 5 min then loaded into the gel wells. In each gel were lanes reserved for prestained and/or biotinylated protein standards. SDS sample buffer consisted of: 50 mM Tris HCl pH 6.8, 2% SDS, 6% glycerol, 0.02% bromophenol blue, and 1% β-mercaptoethanol.

Gels were immersed in SDS-PAGE running buffer which is: 25 mM Tris Base, 192 mM glycine, 3.5 mM SDS in water. Electrophoresis occurred over 1-2 hours running at 100 V

increasing to 180 V when the loading dye had entered the separating gel. When the protein samples had run far enough through the gel (assessed using the prestained protein standards) the protein was transferred to a nitrocellulose membrane (Fisher). The gel was placed in a sandwich between blotting paper against the nitrocellulose membrane and immersed in transfer buffer. Transfer buffer consists of: 25 mM Tris Base, 192 mM glycine, 0.35 mM SDS, and 20% methanol in water. Transfer occurred over 1 hour at 100 V incubated at 4°C. The protein-bound membrane was then removed from the sandwich and stored at 4°C in Tris-buffered saline with Tween20 (TBS/T), which consisted of 20 mM Tris Base, 137 mM sodium chloride, and 0.1% Tween20 in water.

#### **2.3.4 Membrane immunostaining**

Membranes were blocked by incubation in 4% milk TBS/T with mild agitation overnight at 4°C. Primary antibody was then incubated on the membrane at the appropriate dilution, as shown in Table 2.6, in TBS/T for 2 hours at room temperature or overnight at 4°C, inside a tube with constant rolling. After primary antibody incubation the membrane was washed three times with TBS/T before incubation with the secondary antibody. Secondary antibody was incubated on the membrane under the same conditions as the primary antibody.

<b>Antibody Name</b>	<b>Type</b>	<b>Epitope</b>	<b>Dilution</b>
Anti-SGK (Sigma-Aldrich)	Polyclonal IgG	vkeaaeaflgfsyapptdsfl	1:2000
Anti-DDDDK tag (Abcam plc, Cambridge, UK)	Polyclonal IgG	xxxDDDDK	1:1000
Anti-DYKDDDK (Chemicon (Millipore), Billerica, MA, USA)	Monoclonal IgG1 Kappa	DYKDDDK	1:1000
Anti-TSC22D3 (Abnova Corporation, Taipei City, Taiwan)	Monoclonal IgG2a Kappa	TSC22D3 (GILZ)	1:400
Anti-SGK1 (phospho S422) (Abcam)	Polyclonal IgG	GFS <sup>P</sup> YA	1:500
Anti-p-SGK (Ser 422) (Santa Cruz Biotechnology, Inc., Santa Cruz, CA, USA)	Polyclonal	p-SGK (Ser 422)	1:500
Anti-p-SGK (Thr 256) (Santa Cruz)	Polyclonal	p-SGK (Thr 256)	1:500
Anti-SGK1B 3259 (Cambridge BioScience Ltd., Cambridge, UK)	Polyclonal	SLLRPRHKKRAEAQKRS	1:500
Anti-SGK1D 3253 (Cambridge BioScience)	Polyclonal	CNHANILTKPDPRTF WTNDDP	1:500
Anti-Rabbit IgG (H&L) (HRP) (Abcam)	HRP conjugated Polyclonal IgG	Rabbit IgG	1:5000
Anti-Mouse IgG (H&L) (HRP) (Abcam)	HRP conjugated Polyclonal IgG	Mouse IgG	1:1000
Biotinylated anti-Rabbit (Vector Laboratories Ltd., Peterborough, UK)	Biotinylated Polyclonal IgG	Rabbit IgG	1:500
Anti-GAPDH (14C10) (Cell Signaling Technology, Inc., Danvers, MA, USA)	Monoclonal IgG	GAPDH	1:10000

**Table 2.6 Details of antibodies used in Western blotting.**

### **2.3.5 Visualisation**

To visualise immunostained protein, membranes were first washed for 5 min three times with TBS/T. For biotinylated secondary antibodies an Avidin-Biotin Complex solution (VECTASTAIN (Vector Laboratories)) was prepared according to the manufacturer's instructions and incubated on the membrane for 30 min. After a further three washes with

TBS/T, the membrane was stained for 5 min with a chemiluminescence solution (ECL Plus™ Western Blotting Detection Reagent (GE Healthcare Life Sciences, Little Chalfont, Buckinghamshire, UK)) prepared just before use according to the manufacturer's instructions. The membranes were then imaged using a FLA-3000 fluorescent image analyser (Fujifilm UK Ltd., Bedford, UK).

### **2.3.6 Membrane stripping**

To strip antibodies from the nitrocellulose in order that staining of the sample membrane by other antibodies could be performed, stripping buffer consisting of the following was used: 200 mM glycine (Fisher), 3.5 mM SDS (Fisher), 1% Tween 20 in H<sub>2</sub>O with pH adjusted to 2.2. Nitrocellulose was immersed in stripping buffer for two sequential 10 min incubations, before two 5 min washes in TBS/T, with mild agitation, and at room temperature. Membranes were then re-blocked ready for re-probing.

### **2.3.7 Data analysis**

Western blot images were analysed using AlphaEase<sup>®</sup>FC 5.0 Software (Cell Biosciences). For quantification of band densities, bands of interest and a reference background area for each were manually selected and from these, an integrated density value (IDV) was generated for each band based on the size of the selection areas, average pixel intensities within those areas, and correction for intensity of the background. Predicted molecular weights for bands of interest were also generated using this software, by comparison with bands of known molecular weight in size marker lanes. Graphs and statistical analyses of band IDVs normalised to GAPDH were done using Microsoft<sup>®</sup> Office Excel 2003 or GraphPad Prism<sup>®</sup> 4.0.

## 2.4 Immunoprecipitation

Immunoprecipitation (IP) of transfected FLAG-tagged SGK1 isoforms or GILZ was performed with anti-FLAG (Abcam/Chemicon) and anti-GILZ (Abnova) antibodies (Table 2.6). Transfected cells were lysed for IP as described by Soundararajan et al. (2005) (Soundararajan et al., 2005). Cell lysis buffer consisted of: 50 mM HEPES, 150 mM NaCl, 1.5 mM MgCl<sub>2</sub>, 1 mM EGTA, 10% glycerol, 1% Triton X-100. Antibody was added to cell lysates diluted 1:500 and incubated with mild agitation overnight at 4°C. Protein G Sepharose beads (Sigma-Aldrich) were added to the cell lysate and antibody mix (100 µl of bead suspension per 400 µg of total protein) and incubated with mild agitation overnight at 4°C for both the pre-clear and precipitation stages. After immunoprecipitation, mixes were centrifuged to pellet the beads and supernatants collected for analysis by Western blotting. Beads were washed four times to remove non-immunoprecipitated residue using 50 mM Tris-HCl pH 7.4, 150 mM NaCl wash buffer. For analysis by Western blotting, beads were boiled at 95°C with SDS-sample buffer for 5 min.

Crosslinked IP was performed using a Pierce<sup>®</sup> Crosslink IP kit (Thermo Scientific) according to manufacturer's instructions. This kit uses Disuccinimidyl suberate (DSS) to crosslink the antibody to the agarose beads to prevent antibody fragments contaminating the immunoprecipitation product. The kits standard protocol was followed, but using 2 µg of antibody and 400 µg of total protein per reaction.

## **2.5 Electrophysiology**

### **2.5.1 Measurement of transepithelial resistance and potential difference**

To measure the electrical resistance and potential difference of mpkCCD<sub>cl4</sub> cells grown on Transwell<sup>®</sup> membranes, an EVOMX meter and STX2 electrodes (World Precision Instruments UK, Stevenage, UK) were used (Bens et al., 1999). This equipment uses pairs of silver and silver/silver chloride electrodes and two different recording modes to measure: (1) transepithelial resistance of the membrane and (2) potential difference across the membrane. Transepithelial resistance is measured by the EVOMeter by application of an AC current through the membrane. Prior to use, electrodes were sterilised by immersion in 70% ethanol then pre-conditioned by immersion in mpkCCD<sub>cl4</sub> starvation medium for 1 hour. When taking readings from each well of a 12-well plate, the electrodes were positioned at the same point in each well to reduce error.

Resistance readings were taken every 2 days from seeding of mpkCCD<sub>cl4</sub> cells onto Transwell<sup>®</sup> membranes to assess the health and stability of the monolayer. For equivalent short circuit current experiments, resistance and potential difference readings were taken every hour from the time immediately before the first condition change unless stated otherwise.

### **2.5.2 Treatments**

Hormones and drugs or their respective vehicle solutions were added to cells grown on Transwell membranes, diluted in starvation medium to 100 x final concentration, allowing for a 1:100 final dilution in the culture medium. Cells were allowed to stabilise for 1 hour after any addition to the culture medium.

### **2.5.3 Data analysis**

Resistance and potential difference measurements were entered into Microsoft® Office Excel 2003 and used to calculate the equivalent short circuit current according to Ohm's Law:  $I$  (current (amperes)) =  $V$  (potential difference (volts)) /  $R$  (resistance (ohms)). Values were then converted to ohms-centimetre squared ( $\Omega\text{cm}^2$ ), millivolts per centimetre squared ( $\text{mV}/\text{cm}^2$ ) and microamperes per centimetre squared ( $\mu\text{A}/\text{cm}^2$ ) before being transferred to GraphPad Prism® 4.0 to generate graphs and perform statistical analyses.

## **2.6 Immunofluorescence**

### **2.6.1 Human renal tissue collection and preparation**

Human renal tissue was collected, prepared, and supplied to this investigation by Dr Shabbir Moochala (Institute for Cell and Molecular Biosciences, Newcastle University). Tissue was collected from the normal pole of nephrectomised specimens at the Freeman Hospital, Newcastle upon Tyne. Ethical approval was obtained from the Sunderland Local Research Ethics Committee. Kidney tissue was obtained after informed consent from patients undergoing nephrectomy for renal cell carcinoma subject to the following exclusion criteria: serum creatinine > 140  $\mu\text{mol}/\text{l}$ , or any evidence of renal scarring.

Tissue was immediately removed to a renal preservation solution (Ahmad et al., 2006) at 4 °C and transported to the laboratory on ice. The solution consisted of: 140 mM sucrose, 42.3 mM  $\text{Na}_2\text{HPO}_4$ , and 26.7 mM  $\text{NaH}_2\text{PO}_4$  in distilled water. This was pH corrected to 7.4, then autoclaved, aliquoted into sterile containers, and stored at 4 °C until use.

Human tissue on ice was cut into blocks of 5 mm x 5 mm in a Class II ventilation hood before being embedded, as a small volume of tissue enabled quicker and more even

freezing. Tissue blocks were embedded in OCT embedding medium (RA Lamb Ltd., Eastbourne, UK/Thermo Fisher Scientific) and then snap-frozen, attached to a cork mounting block, by immersion in liquid nitrogen-chilled isopentane (2-methylbutane). Once frozen, tissue blocks were stored in a sealed container at -80 °C.

### **2.6.2 Mouse renal tissue collection and preparation**

Normal mouse renal tissue was supplied by Newcastle University Comparative Biology Centre and was immediately immersed in DMEM/HAM's F12 1:1 vol/vol at 4 °C to preserve the tissue for transportation to the laboratory on ice. As with the human tissue preparation, mouse tissue was cut into blocks of 5 mm x 5 mm before being embedded. Tissue blocks were embedded in OCT embedding medium (RA Lamb/Thermo Fisher Scientific) and then snap-frozen, attached to a cork mounting block, by immersion in liquid nitrogen-chilled isopentane (2-methylbutane). Once frozen, tissue blocks were stored in a sealed container at -80°C.

### **2.6.3 Tissue sectioning**

Blocks of embedded tissue were removed from storage and allowed to acclimatise in a Cryostat chilled to -20°C before tissue sections of 6 µm thickness were cut. Cut sections were immediately applied to Superfrost Plus microscope slides (VWR International Ltd., Leighton Buzzard, UK) or to standard Superfrost microscope slides (Thermo Fisher Scientific) that had been pre-coated with 3-aminopropyltriethoxysilane (APTES) (Sigma-Aldrich). Tissue slides were stored at 4°C until they were prepared for immunofluorescence studies.

#### **2.6.4 Preparation of tissue and cells for immunofluorescence studies**

Tissue sections attached to slides were ringed with a hydrophobic pen before being fixed in cytoskeletal fixative solution for 10 min. Cytoskeletal fixative consisted of: 4% paraformaldehyde (Sigma-Aldrich), 100 mM PIPES pH 6.8 (Sigma-Aldrich), 2 mM EGTA (Sigma-Aldrich) and 2 mM MgCl<sub>2</sub> in H<sub>2</sub>O. Sections were then washed with 150 mM Tris HCl to quench fixative before permeabilisation of tissue using 0.2% Triton X100 for 10 min. Sections were washed with Phosphate-buffered saline with Tween20 (PBS/T) three times and blocked with 3% horse serum for 1 hour at room temperature. PBS/T consisted of: 137 mM NaCl, 2.7 mM KCl, 10 mM Na<sub>2</sub>HPO<sub>4</sub>, 1.8 mM KH<sub>2</sub>PO<sub>4</sub>, and 0.05% Tween20 in water. Sections were then washed another three times with PBS/T before treatment with primary antibody (Table 2.7) at the appropriate dilution in block solution for 2 hours at room temperature or overnight at 4°C. After primary antibody incubation, sections were washed and then blocked again, as before, by incubation with 3% secondary antibody host serum for 1 hour, with mild agitation, and at room temperature. Secondary antibody incubation was under the same conditions as for primary. Finally, sections were washed three times in PBS/T and once in ultrapure H<sub>2</sub>O before coverslips were affixed over the sections using fluorescence mounting medium (Dako UK Ltd., Ely, UK). Slides were kept in the dark and at room temperature until mounting medium was set, after which, slides were stored in the dark at 4°C.

<b>Antibody Name</b>	<b>Type</b>	<b>Epitope</b>	<b>Dilution</b>
Anti-DYKDDDK (Chemicon)	Monoclonal IgG	DYKDDDK	1:1000
Anti-AQP2 (C-17) (Santa Cruz)	Polyclonal	AQP2 C-terminus	1:250
Anti-SGK1D 3253 (Cambridge Biosciences)	Polyclonal	CNHANILTKPDPRTF WTNDDP	1:100
Anti- $\gamma$ tubulin (Abcam)	Monoclonal IgG1	$\gamma$ tubulin 38-53	1:200
Anti-acetylated $\alpha$ tubulin (Sigma-Aldrich)	Monoclonal IgG2b	Acetylated $\alpha$ tubulin Lys 40	1:200
Anti-ZO-1 (Zymed (Invitrogen))	Monoclonal IgG1 k	Human ZO-1 334-364.	1:200
Anti-Calnexin (H-70) (Santa Cruz)	Polyclonal	Human Calnexin 1-70.	1:100

**Table 2.7 Primary antibodies used in immunofluorescence studies.**

Cells grown on coverslips were treated in exactly the same way as tissue, except that, after staining, they were attached face-down onto Superfrost microscopy slides (Thermo Scientific). In some experiments, the actin cytoskeleton of cells was stained using Alexa Fluor 633 Phalloidin (Molecular Probes, Invitrogen) at a concentration of 1:500. Secondary antibodies for all experiments were from Molecular Probes, Invitrogen and were used at a concentration of 1:300 for 2 hours. For tissue staining, secondary antibodies raised in donkey were used, whereas for cells, secondary antibodies raised in goat or rabbit were used. Nuclei were stained by using Hoechst 33258 at a concentration of 1:1000 for 10 min. The following fluorophores and their representative colours were used: Hoechst (blue), Alexa Fluor 488 (green), Oregon Green 488 (green) Alexa Fluor 568 (red), Alexa Fluor 633 (red).

### **2.6.5 Microscopy**

Slides were imaged using either a Leica TCS SP2 UV Upright Confocal System or a Zeiss LSM 510 META laser scanning confocal microscope. The lenses used for each system were a 63x HCX PL APO oil immersion lens and a Plan-Neofluar 40x/1.3 Oil Ph3 lens, respectively. Images where nuclei are shown were taken with the Leica microscope and consist of collapsed Z-stacks. Images that are two-channel only were taken using the Zeiss microscope and are single Z-sections. Images were collected sequentially to avoid emission signal bleed-through. For multiple slides from a single experiment channel settings were kept the same except for slight alterations of the gain and offset to reduce the appearance of non-specific staining. Z-section images were captured at  $\sim 1 \mu\text{m}$  intervals. For each experiment, positive signals were verified by comparison with controls.

### **2.7 Statistical analyses**

Statistical analyses were performed using GraphPad Prism<sup>®</sup> 4.0. All data is presented as mean values  $\pm$  standard error of the mean (sem). Statistical differences among different groups were determined using one-way or two-way analysis of variance (ANOVA) with Tukey's Multiple Comparison or Bonferroni Multiple Comparison posttests, respectively. P values of  $\leq 0.05$  were considered to be statistically significant.

## **Chapter 3 - Identification of Multiple Isoforms of Mouse Sgk1**

### **3.1 Introduction**

Hypertension of unknown cause (essential hypertension) affects a significant proportion of the population (Beevers et al., 2001). Salt imbalance in the body, as a result of dysregulated sodium reabsorption in the aldosterone-sensitive distal nephron (ASDN), is a known cause of hypertension (Meneton et al., 2005). Regulation of epithelial sodium channel (ENaC) activity in the ASDN is a major determinant of renal Na<sup>+</sup> reabsorption and, consequently, overall body fluid homeostasis and blood pressure (Butterworth, 2010; Jin et al., 2010). Historically, a single isoform of SGK1 was identified as a key mediator of aldosterone-stimulated sodium transport via its regulation of ENaC (Chen et al., 1999). The importance of ENaC and SGK1 in sodium transport has been shown by their roles in various disease states in addition to hypertension, such as Liddle's syndrome, diabetes, and cystic fibrosis (Berdiev et al., 2009; Lang et al., 2009b; Lu et al., 2007) as reviewed in chapter 1. This has led to both proteins becoming key pharmacological targets. Research, thus far, is based on an incomplete knowledge of the identity, regulation, and roles of SGK1 and its relation to ENaC. Over the past 3 years, successive studies have identified additional isoforms of SGK1, some of which have been shown to display specificity in their regulation of ENaC. Since the start of the present study, two publications appeared which described the expression of isoforms of human SGK1. A study by Simon et al. (2007) into sequence variations in SGK1 transcripts has described two novel human SGK1 isoforms, in addition to the original SGK1, arising from alternative initiation of transcription and splicing. In a second study around the same time, a study by Hall (2007) on SGK1 signalling in skin identified the same two novel human SGK1 isoforms as well as

two additional novel isoforms, which were collectively named SGK1B, SGK1C, SGK1D, and SGK1F. The work described in this thesis was thus initiated based on the findings of Simon et al. (2007) and Hall (2007), with the aim of examining the role of SGK1 isoforms in regulating ENaC in renal cortical collecting duct (CCD) cells. Through differences in their expression, regulation, subcellular distribution, degradation, kinase activity, or substrate specificity, the SGK1 isoforms may differ greatly in their physiological consequences for renal sodium reabsorption. The approach to identify and investigate the regulated expression of multiple isoforms of mouse *Sgk1* in the present study uses the mpkCCD<sub>c14</sub> mouse CCD model cell line as it displays aldosterone-sensitive, SGK1-regulated, and ENaC-mediated sodium transport (Flores et al., 2005; Bens et al., 1999), thus providing the basis for the investigation of the role of mouse *Sgk1* isoforms in regulating ENaC.

## **3.2 Results**

### **3.2.1 Identification and comparisons of mouse *Sgk1* variant sequences**

Gene homology between the human *SGK1* and the mouse *Sgk1* gene suggests that the mouse *Sgk1* gene may also produce multiple isoforms. To investigate this possibility, mouse Expressed Sequence Tags (ESTs) from the EST database, dbEST (Boguski et al., 1993), were compared to the human *SGK1* splice variant sequences before being considered as potentially encoding isoforms of *Sgk1*. Putative mouse *Sgk1* splice variant EST sequences were then entered into the Spidey mRNA-to-genomic alignment program (Wheelan et al., 2001) and compared to the NCBI *Mus musculus* genome sequence around the *Sgk1* locus on chromosome 10 A3. From these searches, four putative mouse isoforms were identified. These mouse isoforms were then named according to their equivalent

human isoforms as Sgk1a, b, c, and d. Table 3.1 shows the differences in N-terminal nucleotide sequence between each of the identified isoforms.

<b>Name</b>	<b>GenBank accession number</b>	<b>Unique N-terminal coding nucleotide sequence</b>	<b>Size of the unique N-terminus compared to each complete coding mRNA (base pairs)</b>
Sgk1a	NM_011361	atgaccgtcaaagccgaggetgctcgaagcaccctta cctactccagaatgaggggaatggtagcgattctcatc	75 of 1296
Sgk1b	NM_001161850	atgggcgagatgcagggcgcgctggctcgggctcgg ctcgagtcctgtctccggccccgccacaaaaagcggg cggaggctcagaaaaggagcgagtcctctctgctga gcggactg	117 of 1338
Sgk1c	NM_001161849	atgaaagaggagaccttaagatccccttgaaa	33 of 1254
Sgk1d	NM_001161845	atggtaaacaagacatgaatggattcccgtcaagaa atgctcagcgttccaatTTTTAagaacgggtacgaag atggatcaagagccccatggctcagcgtggacaagcat cagagccccaactgaagtacactggccctgctggggt gcatctccccctggggagtcagactttgaggccatgtg tcaatcatgcctgggtgaccatgcttccaagggggat gtcctccagaggagtctgttctgggagatccaac ctgggtgtgaagtgaagaacaatgaatcatgccaac atcctgaccaagccggaccaagaaccttctggactaa tgatgatgca	354 of 1575

**Table 3.1 Sgk1 isoform nucleotide data.**

### **3.2.2 Features of the mouse Sgk1 variant sequences**

Genomic alignment of the variant sequences revealed unique alternative exons 1-5, whose addition to the *Sgk1* locus expanded its size from 5 to 120 kbp (Figure 3.1). Exons 7-17 are conserved between all isoforms, whereas exons 1-6 are isoform-specific. Exons 1-3 encode the unique N-terminus of Sgk1d (the longest Sgk1 isoform), whereas exons 4, 5, and 6 encode the unique N-termini of Sgk1c, b, and a, respectively. The increase in size of

the *Sgk1* locus, from 5 to 120 kbp, meant an expansion of genetic sequence that could contain promoter regions or regulatory binding sites. Also, because unique exons were attributed to each *Sgk1* isoform, any promoter and regulatory domains may be isoform-specific. To test this hypothesis the genomic sequence 5' of each isoforms primary exons was searched for common promoter element binding sites. Different transcription factor binding sites were found in close proximity to the *Sgk1* isoforms primary exons. *Sgk1a* and *c* had potential TATA box binding sites (TATAAA) at -44 bp and -22 bp positions, respectively, whereas *Sgk1b* and *d* were closest to potential E-box binding sites, CATTG and CAGCTG at -3 bp and -19 bp, respectively.

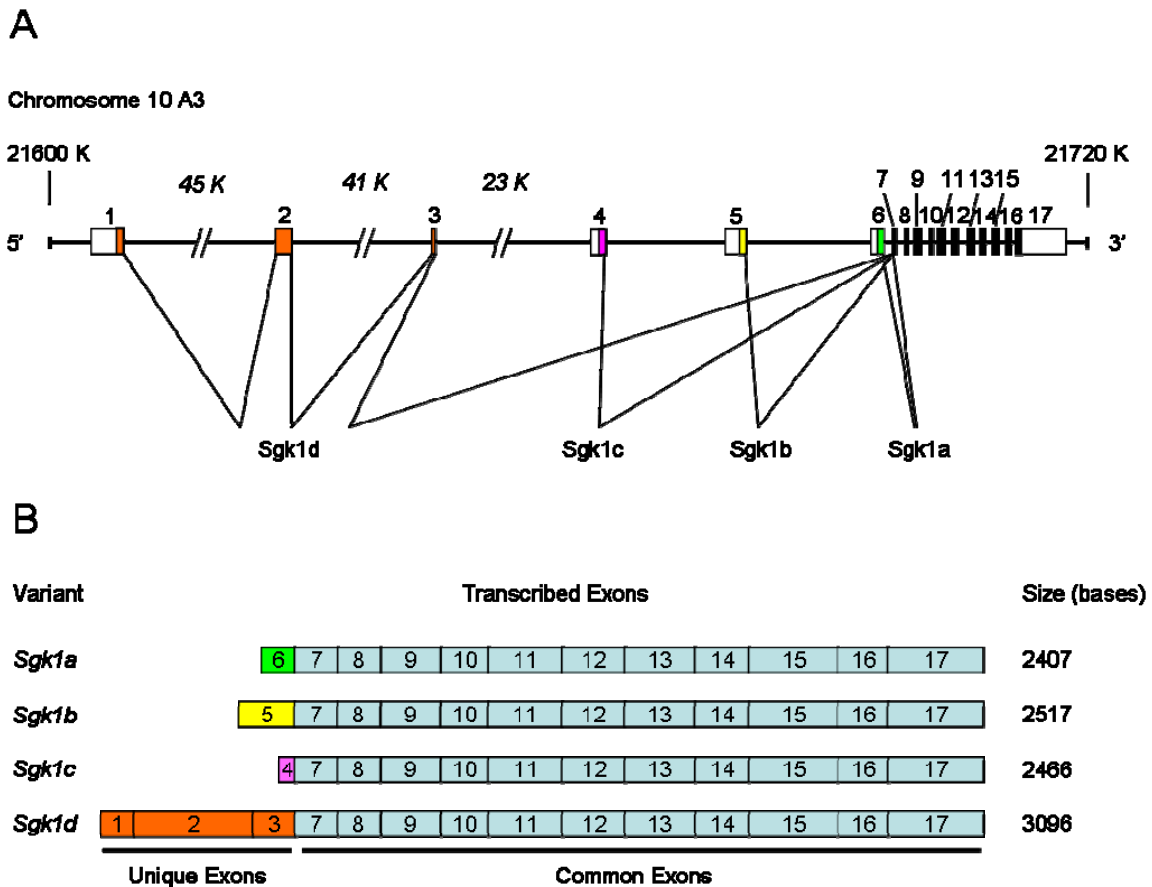


**Figure 3.1 The mouse *Sgk1* locus, showing the possible alternative splicing and the resulting mRNAs.** A depicts the 120 kbp mouse *Sgk1* locus. Genomic sequence is represented by a black horizontal line, onto which exons are marked by coloured (isoform specific) or black (conserved) bars. Untranslated regions (UTRs) are shown as colourless sections of the exon bars. Where the genomic sequence is shortened, between exons 2, 3 and 4, the actual intron sizes are given, above, in italics. Drawn below the locus are the alternative splicing variations for each isoforms unique exons showing how each isoform arises. B shows the different *Sgk1* isoform mRNAs, showing their unique and common exons (UTRs are not shown).

### 3.2.3 Predicted protein products for the mouse *Sgk1* variants

To investigate the proteins encoded by the four mouse *Sgk1* splice variants described in section 3.2.1, their nucleotide sequences were analysed using the sequence manipulation suite open reading frame (ORF) finder (<http://www.bioinformatics.org/sms/>) (Stothard, 2000). This showed all the longest ORF sequences encoded by each variant mRNA, allowing the full-length amino acid sequences to be determined. The amino acid

sequences were then entered into the sequence manipulation suite protein molecular weight calculator giving a predicted molecular weight for each full-length Sgk1 isoform protein (Stothard, 2000). However, Arteaga et al. (2007) showed that mouse Sgk1a is endogenously expressed as four, progressively shorter, isoforms resulting from alternative initiation of translation at alternative, in-frame, downstream methionines (Arteaga et al., 2007), which suggested that Sgk1b, c, and d may also be expressed as multiple alternative initiation of translation products (AITPs). The amino acid sequences of the unique N-termini and common region of the Sgk1 isoforms were searched for alternative start methionines followed by prediction of the molecular weights of the resulting isoforms (Table 3.2). Isoform-specific AITPs are named by a delta symbol ( $\Delta$ ) followed by the number of amino acids missing from the full-length isoform protein and then the name of the isoform (e.g.  $\Delta$ 16Sgk1a). Common AITPs are named by a delta symbol ( $\Delta$ ) followed by the number of amino acids missing from the common sequence then 'Sgk1' (e.g.  $\Delta$ 2Sgk1). The Sgk1 isoforms identified previously by Arteaga et al. (2007) had molecular weights of 49, 47, 45, and 42 kDa, corresponding to isoforms Sgk1a,  $\Delta$ 16Sgk1a,  $\Delta$ 19Sgk1a (both 47 kDa),  $\Delta$ 7Sgk1, and  $\Delta$ 34Sgk1, respectively (Arteaga et al., 2007).

<b>Isoform name</b>	<b>Amino acid sequence (with potential alternative start methionines in bold)</b>	<b>Size (no. of amino acids)</b>	<b>Predicted molecular weight (kDa)</b>
Sgk1a	<b>MTV</b> KAEAAARSTLTYSRMRGMVAILI*	25	49
Δ16Sgk1a		9	47
Δ19Sgk1a		6	47
Sgk1b	<b>MGEM</b> QGALARARLESLLRPRHKKRAE	39	51
Δ3Sgk1b	AQKRSESVLLSGL*	36	50
Sgk1c	<b>MKEET</b> LRSPWK*	11	48
Sgk1d	<b>MVN</b> KDMNGFPVKKCSAFQFFKKRVR	118	60
Δ5Sgk1d	RWIKSPMVSVDKHQSPNLKYTGPA	113	59
Δ31Sgk1d	GVHLPPGESDFEAM <b>CQ</b> SCLGDHAFQ <b>RGM</b>	87	56
Δ62Sgk1d	LPPEESCSWEIQPGCEVKEQCNHANILT	56	53
Δ76Sgk1d	KDPDRTFWTNDDA*	42	51
Δ2Sgk1	* <b>AFMK</b> QRRMGLNDFIQKIASNTYACK	404	46
Δ7Sgk1	HAEVQSILK <b>MSHP</b> QEPELMNANPSPPP	399	45
Δ34Sgk1	SPSQQINLGPSSNPHAKPSDFHFLK	372	42
Δ43Sgk1	VIGKGSFGKVLLARHKAEEVFYAVKVLQK	363	41
	KAILKKKEEKHIMSERNVLLKNVKHPF		
	LVGLHFSFQTADKLYFVLDYINGGELF		
	YHLQRERCFLEPRARFYAAEIASALGY		
	LHSLNIVYRDLKPENILLDSQGHIVLTD		
	FGLCKENIEHNGTTSTFCGTPEYLAPEV		
	LHKQPYDRTVDWWCLGAVLYEMLYG		
	LPPFYSRNTAEMYDNILNKPLQLKPNIT		
	NSARHLLEGLLQKDRTKRLGAKDDFM		
	EIKSHIFFSLINWDDLINKKITPPFNPV		
	SGPSDLRHFDPEFTEEPVPSSIGRSPDSI		
	LVTASVKEAAEAFLGFSYAPPVDSFL		

**Table 3.2 Sgk1 isoform protein data.** \* indicates where unique N-termini sequence and common sequence attach.

The SGK1 protein that, prior to the publications describing other isoforms by Simon et al. (2007) and Arteaga et al. (2007), was thought to be the sole isoform of SGK1 is equivalent to SGK1A (Webster et al., 1993b). A specific six-amino-acid motif (GMVAIL) that was identified in human SGK1A is also present in mouse Sgk1a. A Phox homology (PX)

domain identified in the N-terminal region of human SGK1D is conserved in mouse Sgk1d, identified by SMART and Pfam database searches (Hall, 2007). The human SGK1 PDZ binding motif (DSFL) present at its C-terminal end is also conserved in the mouse isoforms. The phosphorylation sites reported for human SGK1 at Serine 78 (Hayashi et al., 2001), Threonine 256 (Kobayashi and Cohen, 1999), Threonine 369 (Perrotti et al., 2001), Serine 377 (Lizcano et al., 2002), and Serine 422 (Kobayashi and Cohen, 1999) are also all conserved in mouse Sgk1 (numbers reflect amino acid positions in SGK1A). The distribution of some of these domains on the Sgk1 isoforms is shown in Figure 3.2.

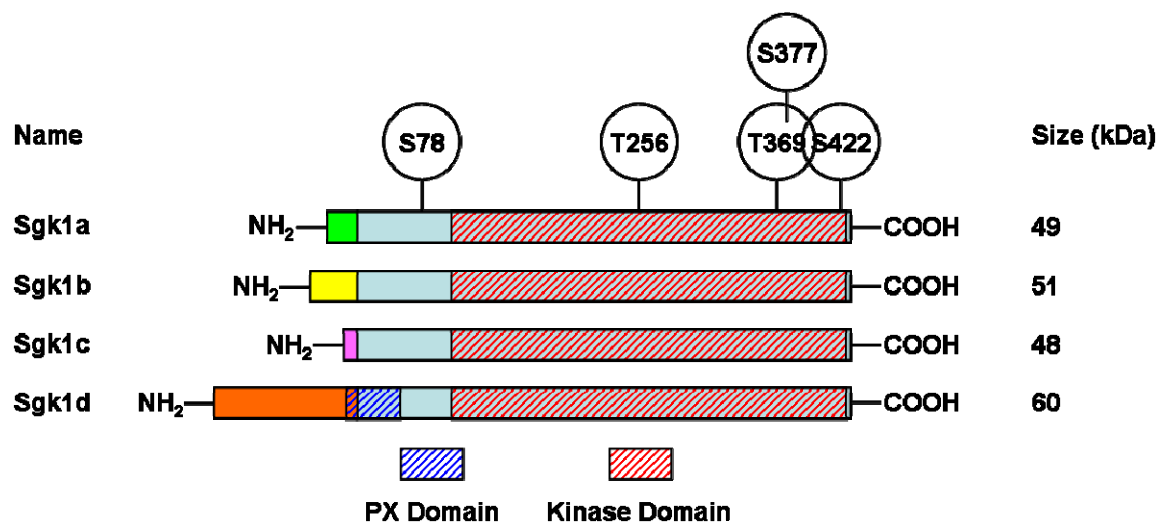


**Figure 3.2 Full-length mouse Sgk1 isoform proteins.**

### 3.2.4 Cloning of the mouse Sgk1 isoforms

In order to help identify and investigate expression of the mouse Sgk1 isoforms using molecular biology techniques such as transient transfection, mouse Sgk1 isoform cDNAs were obtained or cloned in expression vectors. Mouse Sgk1a was purchased from Geneservice ([www.geneservice.co.uk](http://www.geneservice.co.uk)) cloned in the pCMV-SPORT6 expression vector between the *SaI*I (5') and *Not*I (3') restriction sites in its multiple cloning site (MCS)

(Figure 3.3). This expression vector contains several useful features for molecular biology including: an ampicillin resistance gene appropriate for its selective generation in bacteria; a powerful cytomegalovirus (CMV) promoter upstream of its MCS for enhanced transcription of inserted DNA; T7 and SP6 promoters either side of its MCS, suitable for artificial generation of mRNA. Based on its favourable characteristics, the remaining Sgk1 isoforms were also cloned into pCMV-SPORT6. Sgk1b was cloned into pCMV-SPORT6 through replacement of the N-terminus of Sgk1a in pCMV-SPORT6 with that of Sgk1b. The N-terminus of Sgk1b was amplified from whole mpkCCD<sub>cl4</sub> cell RNA by RT-PCR using primers that introduced a *SalI* restriction site at the 5' end and a *PacI* restriction site at the 3' end of the product. The Sgk1b RT-PCR product and the Sgk1a plasmid were then digested with *SalI* and *PacI* to produce fragments that had corresponding 2-4 base overhangs. The Sgk1b N-terminus fragment was then ligated into the pCMV-SPORT6 fragment in place of the Sgk1a N-terminus to create complete Sgk1b in pCMV-SPORT6. Due to its unavailability from Geneservice and difficulties in its production by RT-PCR, mouse Sgk1c was generated by combinatorial PCR, as described in section 2.2.1. The Sgk1c PCR product was cloned into pCMV-SPORT6 by the same process using the *SalI* and *PacI* restriction sites as described for Sgk1b. Mouse Sgk1d was also obtained from Geneservice and was sub-cloned from its original vector (pYX-Asc) into pCMV-SPORT6, by digestion using *NotI* and *EcoR1* restriction enzymes. The amino acid sequence of each clone was confirmed by sequencing carried out by Eurofins MWG Operon (<http://www.eurofinsdna.com/>). Evidence that the cloned Sgk1 vectors were able to code for the expression of Sgk1 protein in cells is presented in Figure 3.8.

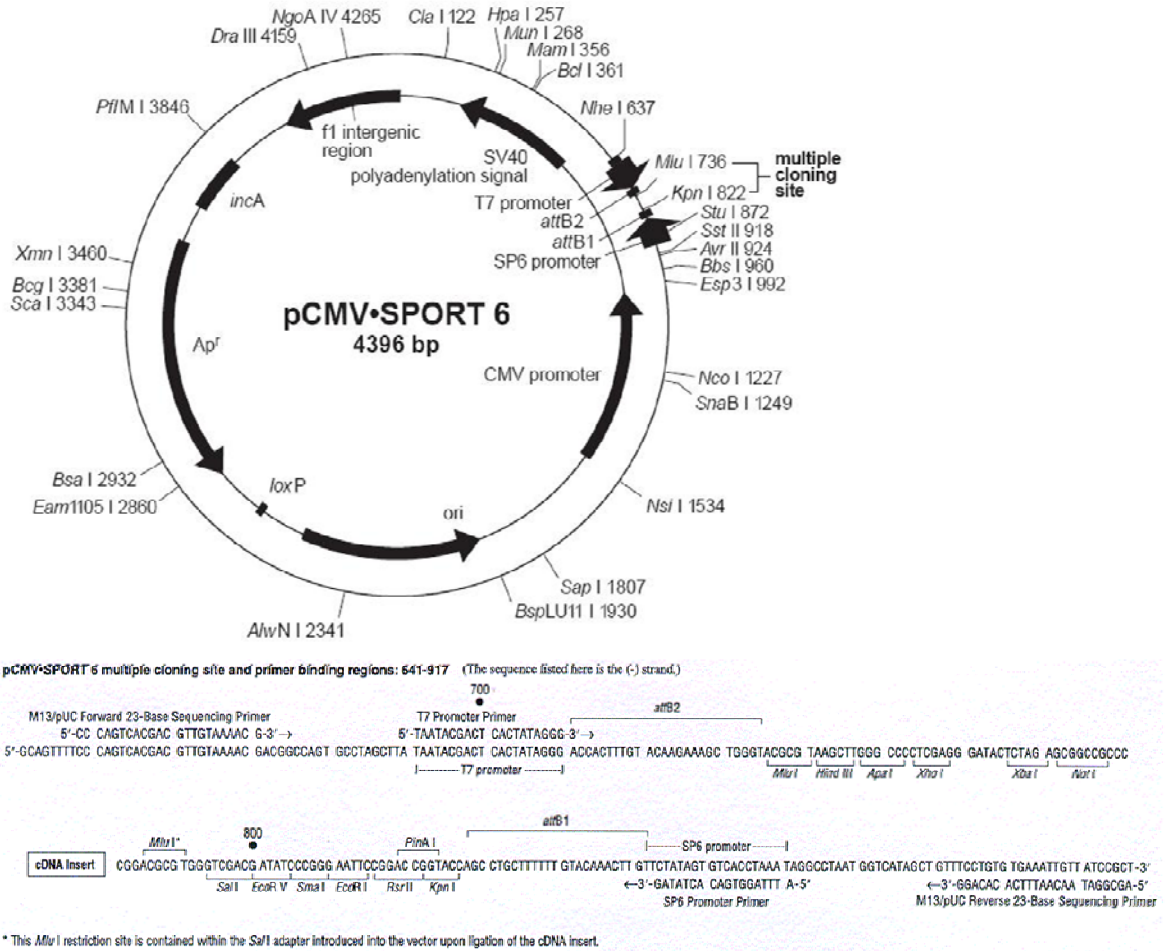


**Figure 3.3 The pCMV-SPORT6 vector map and multiple cloning site sequence.** Mouse *Sgk1a* was obtained in this vector, whilst *Sgk1b*, *c*, and *d* were cloned into this vector using RT-PCR, combinatorial PCR and sub-cloning, respectively.

In order to distinguish overexpressed *Sgk1* isoform protein from endogenous protein, the mouse *Sgk1* isoforms were also cloned into the pCMV-FLAG2 vector (Figure 2.3). This cloning was carried out as described in section 2.2.1. When transiently transfected into cells, these clones produced overexpressed FLAG-tagged *Sgk1* isoforms, which could then be detected using FLAG-specific antibodies. The FLAG-tagged *Sgk1* isoforms could also be used with other techniques such as co-immunoprecipitation and immunofluorescence.

### 3.2.5 Multiple mouse Sgk1 isoforms are expressed in mpkCCD<sub>cl4</sub> cells

To determine which mouse Sgk1 isoforms were being expressed in mpkCCD<sub>cl4</sub> cells, isoform-specific primers were designed (Table 2.3) and, together with RT-PCR, were used to amplify specific cDNA products from purified mpkCCD<sub>cl4</sub> cell RNA. Data demonstrated the expression of all four mouse Sgk1 mRNAs was detectable in mpkCCD<sub>cl4</sub> cells (Figure 3.4). Sequencing analysis then confirmed the Sgk1 isoform identities of the products (see appendix).

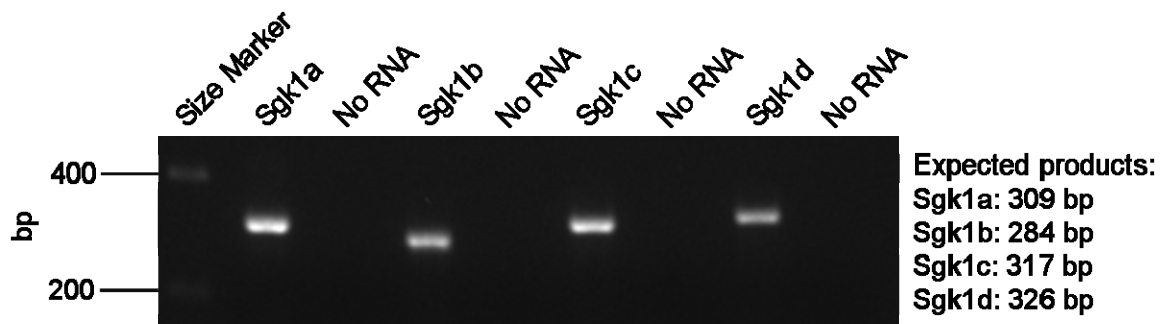


**Figure 3.4 mpkCCD<sub>cl4</sub> cells express all four isoform-specific Sgk1 variant mRNAs.**

RNA was purified from mpkCCD<sub>cl4</sub> cells that were grown on plastic for 24 hours in growth medium using an RNeasy kit. Specific mouse isoform cDNAs were amplified using the OneStep RT-PCR kit in reactions containing 400 ng of the purified RNA and Sgk1 isoform specific primers (Table 2.3). Reaction products were size separated via electrophoresis and visualised with ethidium bromide by UV imaging. No RNA controls showed no amplified product.

To verify that the expression of isoform RNA was the same in both mpkCCD<sub>cl4</sub> cells and native mouse kidney tissue, the same RT-PCR was performed using RNA purified from whole mouse kidneys. Kidneys were obtained from three different mice and results showed that all four isoforms were expressed in each of the three kidneys (Figure 3.5).

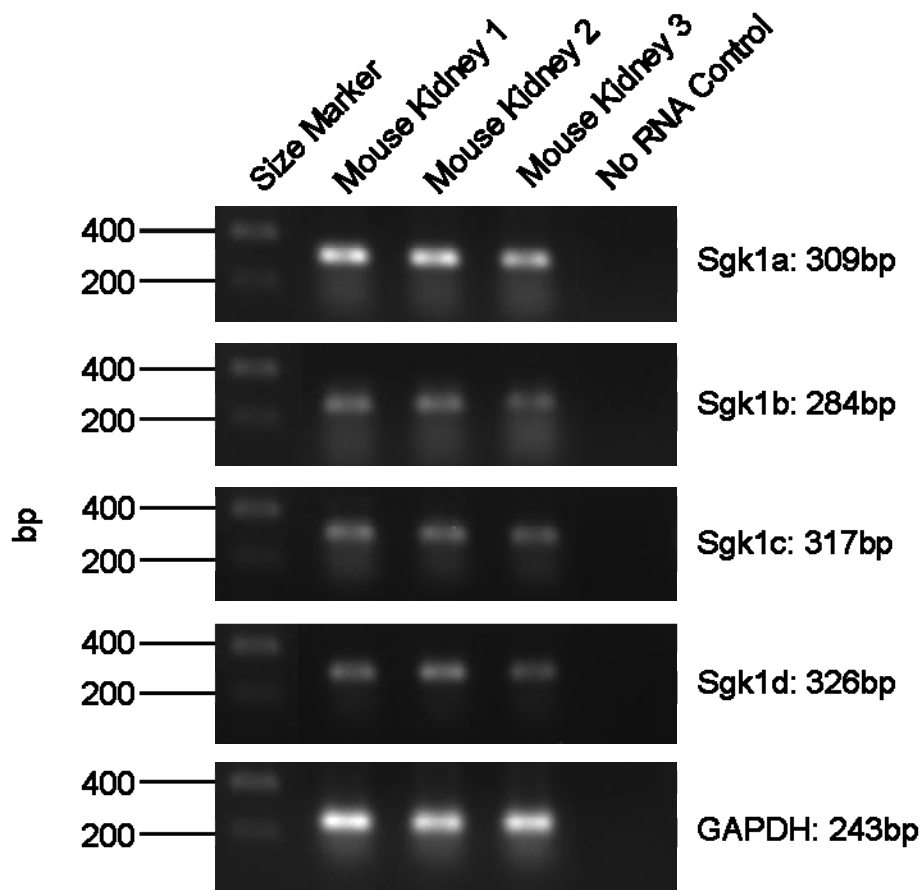


**Figure 3.5 Native mouse kidney tissue expresses specific *Sgk1a*, *b*, *c*, and *d* variant mRNAs.** RNA was purified from 3 whole mouse kidneys from different mice using TRIzol reagent (Invitrogen) according to the manufacturer's instructions. Specific mouse isoform and GAPDH cDNAs were amplified from the tissue RNA and imaged using the procedure described in Figure 3.4. No RNA controls showed no amplified product.

### **3.2.6 Aldosterone stimulates endogenous expression of multiple *Sgk1* isoforms in mpkCCD<sub>cl4</sub> cells**

Although results from the present study showed that multiple mouse *Sgk1* variant mRNAs are expressed in mpkCCD<sub>cl4</sub> cells and native mouse kidney tissue (section 3.2.5), the translation and endogenous expression of multiple mouse *Sgk1* isoforms required further investigation. Previous studies in mpkCCD<sub>cl4</sub> cells have shown that aldosterone treatment caused an increase in endogenous *Sgk1* expression levels (Wang et al., 2008; Flores et al.,

2005). The effect of different concentrations of aldosterone on Sgk1 expression levels in serum and hormone-starved mpkCCD<sub>cl4</sub> cells was therefore investigated. Cells were starved for 24 hours in starvation medium before exposure to different aldosterone concentrations ranging between 0.3-300 nM, or vehicle control, for a further 24 hours and prior to lysis in RIPA buffer.

Western blotting detected three Sgk1 protein bands which, although poorly resolved, were of the correct approximate size to correspond to the predicted mouse Sgk1 isoforms Sgk1b (51 kDa), Sgk1c (48 kDa), and Sgk1d (60 kDa) (Figure 3.6A). Due to the poor resolution Sgk1a could not be specifically identified, but probably overlapped with Sgk1b. Regarding the Sgk1 protein bands, very little expression of Sgk1b/a and Sgk1c was detected in serum and hormone-starved cells, but surprisingly Sgk1d was clearly detected. Furthermore, Sgk1b/a and Sgk1c were only detected following treatment of cells with between 0.3-100 nM aldosterone (Figure 3.6A).

After the detection of Sgk1 protein bands, the Western blot was stripped and reprobed for GAPDH expression as a control for equal protein loading. The images of the Sgk1 and GAPDH Western blots were then analysed by densitometry to compare the densities of the Sgk1 bands between treatments. The results of the densitometric analysis indicated that in starved cells Sgk1d was expressed at a high basal level, which appeared not to change in response to 0.3-1 nM aldosterone, but 3 nM aldosterone did increase expression (~1.75-fold) (Figure 3.6B). Increasing the concentration of aldosterone from 0 up to 3 nM caused a dose-dependent increase in expression of Sgk1b/a and Sgk1c to a peak of 2.25-fold basal Sgk1d expression at 3 nM aldosterone. Increasing aldosterone concentrations from 3-300 nM caused a dose-dependent decrease in expression of Sgk1b/a, c, and d, reaching starvation levels or below at 100 nM for Sgk1d and 300 nM for Sgk1b/a and c. These data suggest that expression of Sgk1d in renal epithelial cells was at a higher basal level than

Sgk1b and c, but was less sensitive to aldosterone. In contrast, Sgk1 isoforms b/a and c were present at very low levels in starved cells, but both isoforms were induced by 0.3-100 nM aldosterone.

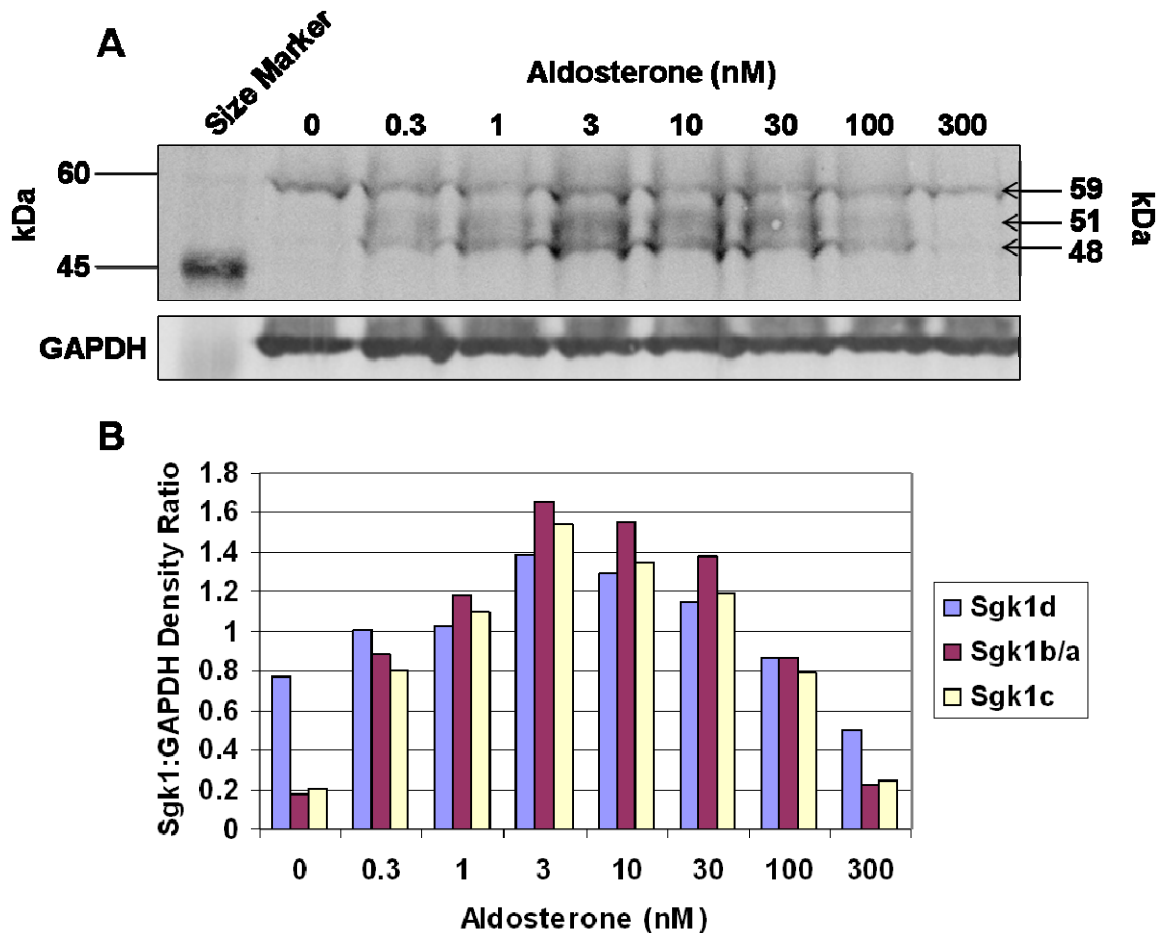


**Figure 3.6 Aldosterone stimulates endogenous Sgk1 protein expression in mpkCCD<sub>cl4</sub> cells in a dose-dependent manner.** A shows Sgk1 protein expression in cells that were starved for 24 hours then treated for 24 hours to a range of concentrations of aldosterone. Cells grown on plastic were starved for 24 hours before being treated for 24 hours with vehicle or 0.3-300 nM aldosterone. After treatment, cells were lysed and Sgk1 expression analysed by Western blotting using a SGK1 antibody. Arrows indicate the Sgk1 bands and corresponding sizes used for quantification. Due to poor resolution only single bands are present for Sgk1d and Sgk1a&b combined. B shows the mean Sgk1 protein band density as a ratio versus GAPDH for the untreated and aldosterone treated cells from two experiments. Results are representative of two separate experiments.

Based on the results presented in Figure 3.6, together with previous studies describing normal physiological plasma aldosterone concentration (Gonzalez-Rodriguez et al., 2007; Hollenberg et al., 2004) and aldosterone-stimulated changes in sodium transport by mpkCCD<sub>cl4</sub> cells (Bens et al., 1999), 10 nM aldosterone was therefore employed as a standard treatment for further study. Previous studies using mpkCCD<sub>cl4</sub> cells have shown that aldosterone treatment caused a time-dependent increase in sodium transport (Bens et al., 1999). Therefore, the effect of aldosterone treatment on starved mpkCCD<sub>cl4</sub> cell expression of Sgk1 isoforms over a similar time period was investigated. Cells grown on cell-culture plastic were serum and hormone-starved for 24 hours in starvation medium before being treated with 10 nM aldosterone. At different time points, cells were lysed and processed for Western blotting to detect Sgk1 protein expression.

Figure 3.7A shows that 10 nM aldosterone increased expression of multiple Sgk1 immunoreactive protein bands of the appropriate sizes corresponding to isoforms a (49 kDa), b (51 kDa), c (48 kDa) and d (60 kDa). An additional Sgk1 band was present that was the correct size corresponding to the  $\Delta$ 31Sgk1d isoform (~56 kDa). As was seen in Figure 3.6, a protein band for Sgk1d was detected in serum and hormone-starved cells, but the other isoforms were not. However, in the presence of 10 nM aldosterone, detection of Sgk1a, b, and c were visible after 1 hour and intensity increased after 4 and up to 24 hours. Densitometric analysis of aldosterone-induced Sgk1 isoform bands indicated that expression of Sgk1a, b, and c in starved cells was gradually increased ~25-fold in a time-dependent manner over 6 hours (Figure 3.7C). Expression of Sgk1d and  $\Delta$ 31Sgk1d was ~5-fold higher than the other Sgk1 isoforms in starved cells and aldosterone treatment only significantly increased the 60 kDa Sgk1d band after 6 hours of exposure, by ~2.5-fold. In contrast, there was a significant increase in the expression of Sgk1a, b, and c bands by 4

hours of aldosterone treatment. From 6 hours up to 24 hours exposure to aldosterone, no further change was detected in expression of Sgk1a, b, c, or d (Figure 3.7C).

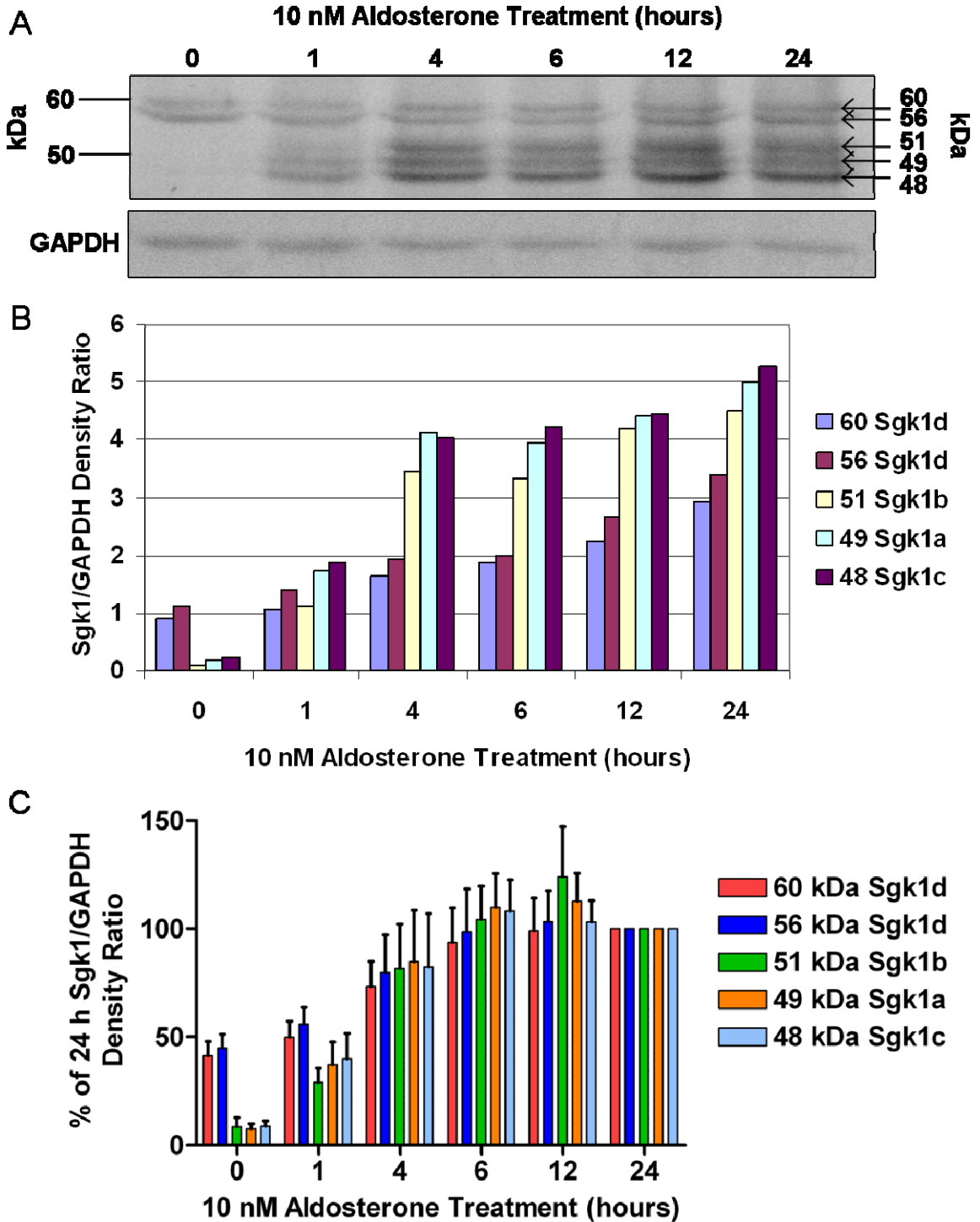


**Figure 3.7 Aldosterone stimulates expression of multiple endogenous Sgk1 proteins in mpkCCD<sub>c14</sub> cells in a time-dependent manner.** A shows Sgk1 protein expression in cells that were starved for 24 hours then treated with 10 nM aldosterone. Cells that were untreated or treated for 1, 4, 6, 12, and 24 hours were lysed and analysed by Western blotting using a SGK1-specific antibody. B shows the Sgk1 protein band density as a ratio versus GAPDH for the Western blot shown in A. C shows summary data from 3 independent experiments. Because of variation in protein density between different experiments the summary data is expressed as a percentage of the 24 h time point Sgk1/GAPDH band density ratio for each individual isoform (24 h time point designated as 100 %). Values are means  $\pm$  sem and are significantly different to 0 hours ( $P = <0.05$ ) from 6 hours for 60 kDa Sgk1d and from 4 hours for 51 kDa Sgk1b, 49 kDa Sgk1a, and 48 kDa Sgk1c. However, there was no significant change in the 56 kDa Sgk1d band over 24 hours.

### **3.2.7 Co-migration of overexpressed Sgk1 isoforms with endogenous Sgk1 proteins**

The estimated sizes of the aldosterone-induced Sgk1 bands could only be used to suggest their corresponding Sgk1 isoform identities. To better identify the aldosterone-induced Sgk1 bands, cloned Sgk1 isoforms were overexpressed in mpkCCD<sub>c14</sub> cells and lysates compared to endogenous Sgk1 proteins in aldosterone plus insulin-treated mpkCCD<sub>c14</sub> cell lysates by Western blotting. Insulin was added to aldosterone treatment of cells in order to try and maximise detection of Sgk1.

Aldosterone plus insulin-responsive bands of estimated sizes 51, 49, and 48 kDa, co-migrated with intense overexpressed Sgk1 isoforms (Figure 3.8). In addition to this, a 60 kDa endogenous Sgk1 band was detected corresponding to and co-migrating with Sgk1d. It is clear from Figure 3.8 that there were a number of additional lower molecular weight Sgk1 immunoreactive bands visible below the most intense bands. These additional bands have not been formally identified, but could be endogenous Sgk1 isoforms resulting from alternative translational start sites, such as those described by Arteaga et al. (2007). The shortened isoforms that resulted from translation initiation at alternative start methionines are described in section 3.2.3. Other possible explanations for additional bands include the

presence of phosphorylated, partially degraded, ubiquitinated or post-translationally modified forms of Sgk1. The overexpression of each individual isoform may also have altered the expression levels of the endogenous isoforms causing induction of Sgk1 bands of other predicted sizes. Nonetheless, it is clear from Figure 3.8 that A+I treatment of mpkCCD<sub>c14</sub> cells induced the expression of bands which co-migrate with exogenously expressed Sgk1a, b, c, and basally expressed 1d.

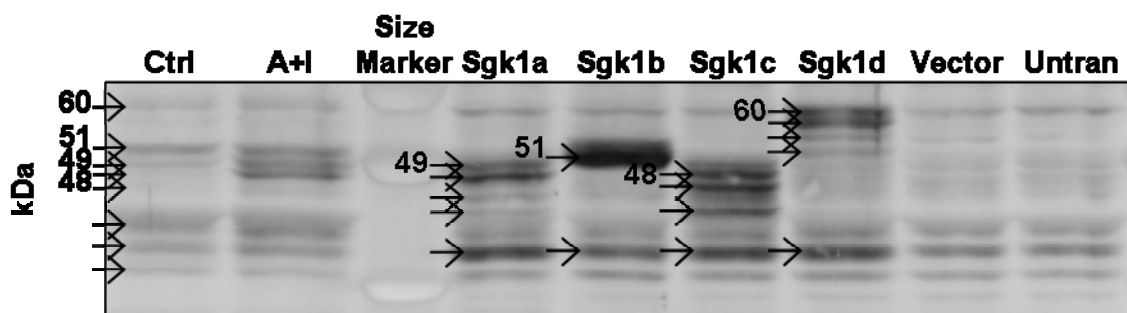


**Figure 3.8 Aldosterone plus insulin-stimulated endogenous Sgk1 proteins co-migrate with overexpressed Sgk1 isoforms.** mpkCCD<sub>c14</sub> cells grown on plastic were incubated for 24 hours in starvation medium before being exposed to A+I for 24 hours, then lysed. Other mpkCCD<sub>c14</sub> cells were transfected with Sgk1 isoforms, empty vector control (Vector), or no DNA (Untran) and incubated for 24 hours to allow plasmid protein expression before being lysed. Arrows with estimated sizes indicate full-length Sgk1 isoforms. Arrows without sizes in the Ctrl lane indicate other endogenous immunoreactive Sgk1 isoform bands. Arrows without sizes in the overexpressed lanes indicate Sgk1 isoform bands induced by the transfection. Results are representative of five separate experiments.

### 3.2.8 Co-migration of overexpressed Sgk1 isoform proteins with synthesised Sgk1 isoform proteins

In order to further improve identification of the multiple Sgk1 protein bands detected in overexpression lysates by Western blotting, Sgk1 plasmid protein was synthesised *in vitro* for comparison. This also allowed detection of the Sgk1 isoform Western blot bands specifically produced by the individual Sgk1 splice variant mRNAs. Whole TNT kit

reaction was added to SDS sample buffer and boiled according to the standard preparation of Western blotting samples described in section 2.3.4. The synthesised protein samples were run alongside samples of mpkCCD<sub>c14</sub> cell lysate transfected with Sgk1 isoforms in a Western blot (Figure 3.9).

Multiple intense Sgk1 protein bands were detected for synthesised Sgk1a of estimated sizes; 49, 45, and 42 kDa, which corresponded to Sgk1a,  $\Delta 7$ Sgk1, and  $\Delta 34$ Sgk1, respectively (Figure 3.9). For synthesised Sgk1b, two intense Sgk1 protein bands were detected of estimated sizes; 58 and 51 kDa, of which the 58 kDa isoform was unidentified, whilst the 51 kDa isoform was Sgk1b (Figure 3.9). Synthesised Sgk1c produced intense bands of estimated sizes 48, 45, and 42 kDa, which corresponded to Sgk1c,  $\Delta 7$ Sgk1, and  $\Delta 34$ Sgk1, respectively (Figure 3.9). Synthesised Sgk1d produced a single intense band of 60 kDa, the correct size corresponding to Sgk1d (Figure 3.9). The equivalent overexpressed full-length Sgk1 plasmid protein bands from transfected mpkCCD<sub>c14</sub> cells co-migrated with the synthesised protein bands, except for the unidentified 58 kDa band of synthesised Sgk1b.

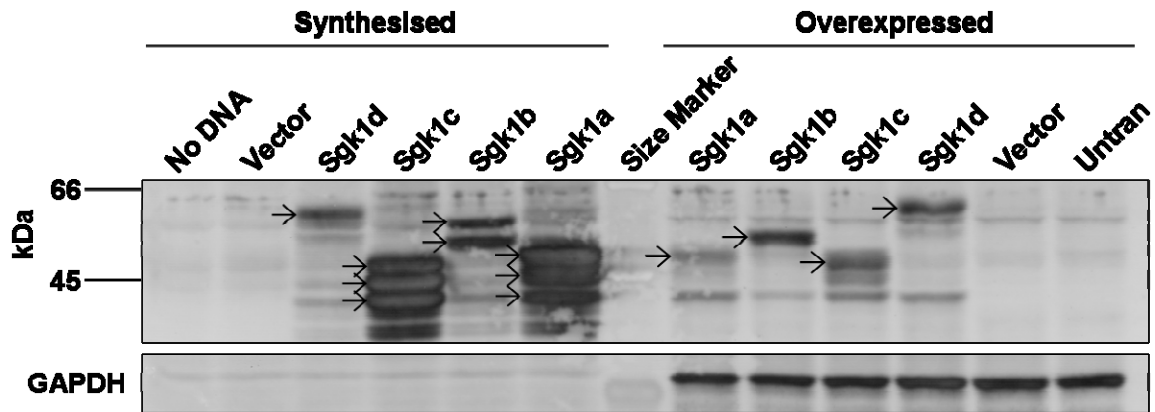


**Figure 3.9 Synthesised and overexpressed Sgk1 isoforms show similar protein products.** mpkCCD<sub>c14</sub> cells grown on plastic were transfected with Sgk1 isoforms, empty vector control (Vector), or no DNA control (Untran), grown for 24 hours to allow plasmid protein expression, then lysed. Sgk1 isoform plasmid protein, empty vector control protein (Vector), or no DNA control protein (No DNA) was synthesised *in vitro* in reactions with reticulocyte lysate using a TNT kit. Reaction product and lysates were analysed for Sgk1 protein by Western blotting using anti-SGK1 antibody. Arrows indicate strongly detected Sgk1 protein bands. Representative of two separate experiments.

### 3.2.9 Detection of multiple phosphorylated Sgk1 isoforms

To mediate any effects on the cell, Sgk1 must first be activated by phosphorylation at one or more of the sites described in section 3.2.3. Therefore, changes in total Sgk1 protein levels can only suggest possible changes in the level of Sgk1 activity. To gain a better understanding of the levels of active Sgk1 in mpkCCD<sub>c14</sub> cells, and how aldosterone and insulin treatments affect phosphorylated Sgk1 protein levels, cell lysates were analysed by Western blotting using phosphorylated Sgk1-specific antibodies. Insulin was used because it has been shown to activate SGK1 via the PI3K pathway and 3-phosphoinositide dependent protein kinase-1 (PDK1) (Wang et al., 2001). Antibodies that targeted phosphorylated Sgk1 at either threonine 256 or serine 422 were used for these experiments. Despite many attempts to detect endogenous phospho-Sgk1 protein in aldosterone and insulin stimulated mpkCCD<sub>c14</sub> cells, none were successful. Even combining

overexpression of Sgk1 isoforms with insulin treatment in mpkCCD<sub>cl4</sub> cells did not lead to detectable phosphorylated Sgk1 (Figure 3.10).

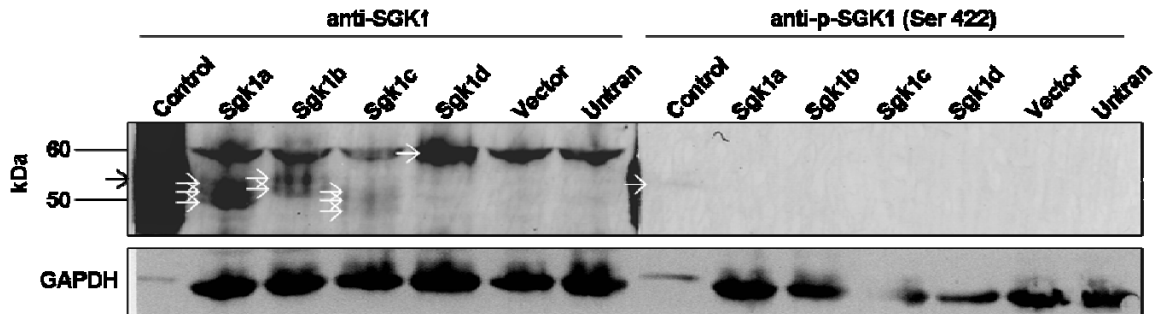


**Figure 3.10 No detected expression of phosphorylated Sgk1 isoform protein in insulin-treated mpkCCD<sub>cl4</sub> cells.** Cells grown on plastic were transfected with Sgk1 isoforms, empty vector control (Vector), or no DNA (Untran) and incubated for 24 hours to allow plasmid protein expression. Cells were then given 1  $\mu$ M insulin in grown medium for 24 hours to stimulate Sgk1 phosphorylation before cells were lysed. Cells lysates were analysed for total and phosphorylated Sgk1 protein by Western blotting using anti-SGK1 and anti-p-SGK1 (Ser 422) antibodies. A positive control lysate of HEK293T cells that were co-transfected with SGK1C and PDPK1 was included (Control) to verify functioning of the Abcam antibody. Arrows indicate detected SGK1 immunoreactive bands. Representative of four separate experiments.

The only experiment that detected phosphorylated Sgk1 isoforms used transfected HEK293T cells, which overexpress protein at very high amounts compared to the mpkCCD<sub>cl4</sub> cells. These cells were transfected with a combination of Sgk1 isoforms and human PDPK1 to ensure high expression levels of both Sgk1 and the activating kinase PDPK1. The human SGK1 isoforms were also included, in order to compare phosphorylation profiles with the mouse Sgk1 isoforms. SGK1 isoform expression was verified using anti-SGK1 antibody. Results showed that a single band of phosphorylated human SGK1B and multiple bands of phosphorylated human and mouse SGK1C were detected under these conditions, as shown in Figure 3.11 and Figure 3.12, respectively. The equivalent experiments using human and mouse SGK1A and D failed to show any phosphorylated bands.

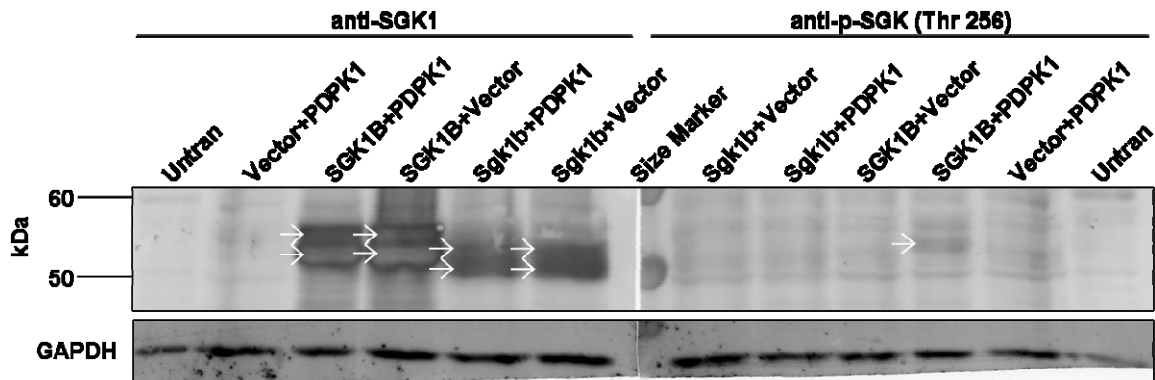


**Figure 3.11 Detection of phosphorylated SGK1 protein in HEK293T cells co-transfected with SGK1B and PDPK1.** Cells grown on plastic were co-transfected with mouse Sgk1b plus PDPK1 (Sgk1b+PDPK1), human SGK1B plus PDPK1 (SGK1B+PDPK1), empty vector plus PDPK1 (Vector+PDPK1), or no DNA (Untran). After 24 hours growth to allow plasmid protein expression, cells were lysed and cell lysates analysed for total SGK1 and phosphorylated SGK1 protein expression by Western blotting using anti-SGK1 and anti-p-SGK (Thr 256) antibodies. Arrows indicate detected SGK1 immunoreactive bands.

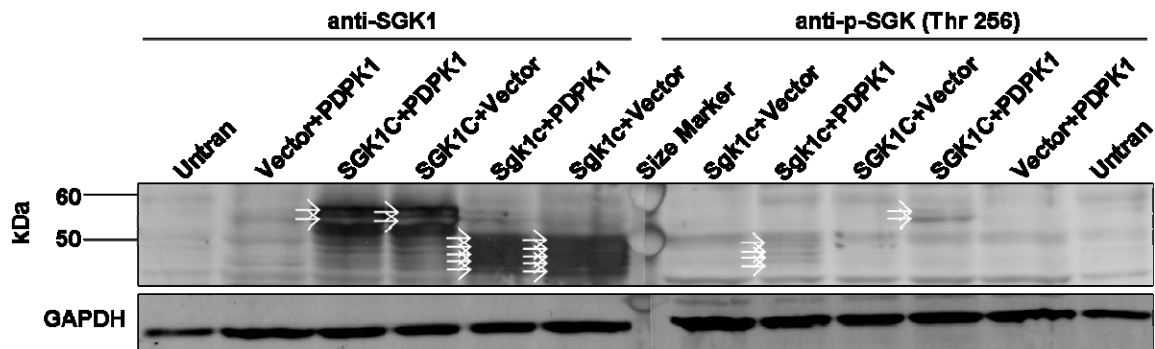


**Figure 3.12 Detection of phosphorylated SGK1 protein in HEK293T cells co-transfected with SGK1C and PDPK1.** Cells grown on plastic were co-transfected with mouse Sgk1c plus PDPK1 (Sgk1c+PDPK1), human SGK1C plus PDPK1 (SGK1C+PDPK1), empty vector plus PDPK1 (Vector+PDPK1), or no DNA (Untran). After 24 hours growth to allow plasmid protein expression, cells were lysed and cell lysates analysed for total SGK1 and phosphorylated SGK1 protein expression by Western blotting using anti-SGK1 and anti-p-SGK (Thr 256) antibodies. Arrows indicate detected SGK1 immunoreactive bands. Representative of two separate experiments.

### 3.2.10 Sensitivity of aldosterone-stimulated Sgk1 isoforms to LY294002

Previous studies have shown that inhibition of phosphoinositide 3-kinase (PI3K) abrogates aldosterone-induced Sgk1 expression and ENaC-mediated sodium transport (Shane et al.,

2006; Flores et al., 2005). Therefore, to investigate which aldosterone-induced Sgk1 isoforms are dependent on PI3K, mpkCCD<sub>cl4</sub> cells were treated with LY294002 to inhibit PI3K and then treated with aldosterone before being examined for Sgk1 isoform expression by Western blotting. Cells grown on plastic were starved for 24 hours before being exposed to 10  $\mu$ M LY294002 or vehicle control for 30 mins followed by addition of a range of aldosterone concentrations or vehicle control for an additional 24 hours. Figure 3.13 shows that LY294002 (LY) caused a decrease in expression of all isoforms, but particularly in the Sgk1b and c expression induced by aldosterone. Basal expression of Sgk1d in starved cells was ~4-fold higher than the other isoforms in both untreated and LY294002 treated cells. However, Sgk1d expression in starved cells and cells treated with 1 or 10 nM aldosterone was ~1.5-fold greater in the absence of LY294002.

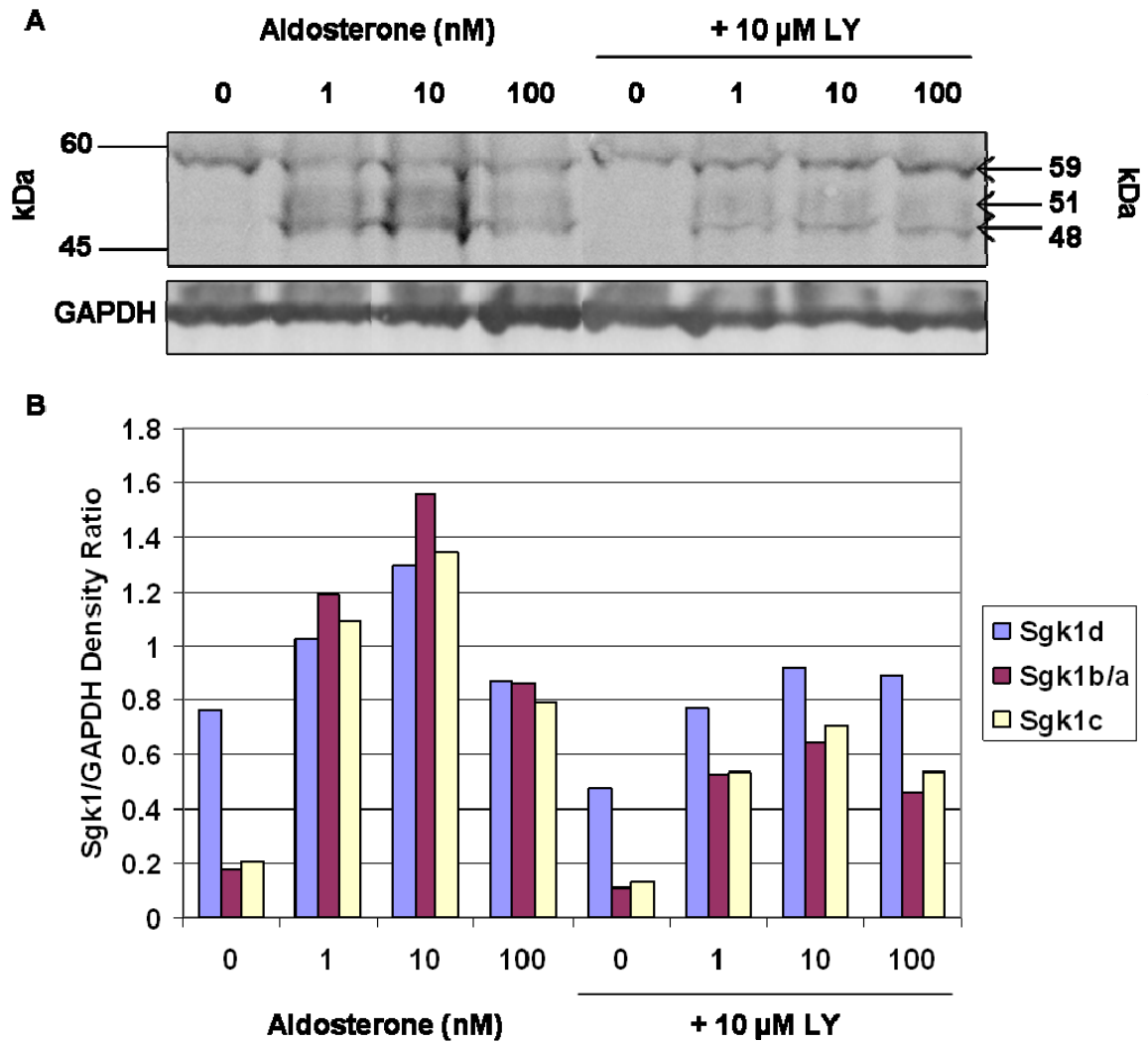


**Figure 3.13 LY294002 reduces aldosterone-stimulated expression of Sgk1a, b, and c.** A and B show additional data from the experiment described in Figure 3.6. mpkCCD<sub>c14</sub> cells were treated with a range of concentrations of aldosterone in the absence or presence of 10  $\mu$ M LY294002. Lysates were analysed for Sgk1 expression by Western blotting using a SGK1 antibody. Arrows indicate the Sgk1 bands and corresponding sizes used for quantification. Due to poor resolution only a single band is present for Sgk1d and Sgk1a&b combined. B shows the mean Sgk1 protein band density as a ratio versus GAPDH for the untreated and aldosterone treated cells from two experiments. Results are representative of two separate experiments.

Additionally, insulin has been shown to increase phosphorylated Sgk1 and ion transport in mpkCCD<sub>c14</sub> cells in a PI3K-dependent manner (Wang et al., 2008). Therefore, to investigate if any of the Sgk1 bands were induced by insulin (and were therefore due to

phosphorylated Sgk1), treatments of 1  $\mu$ M insulin and combined 10 nM aldosterone plus 1  $\mu$ M insulin were included.

Western blotting showed that aldosterone and aldosterone plus insulin, but not insulin alone, increased expression of Sgk1a, b, and c, whereas Sgk1d was expressed at a high level regardless of treatment (Figure 3.14). LY294002 reduced the aldosterone plus insulin-stimulated expression of Sgk1a, b, and c, but did not affect Sgk1d expression. These results therefore suggest that Sgk1a, b, and c are expressed at low levels in unstimulated cells and are upregulated by aldosterone and insulin, but Sgk1d is expressed at high basal levels by a process that is insensitive to aldosterone, insulin and PI3K inhibition.

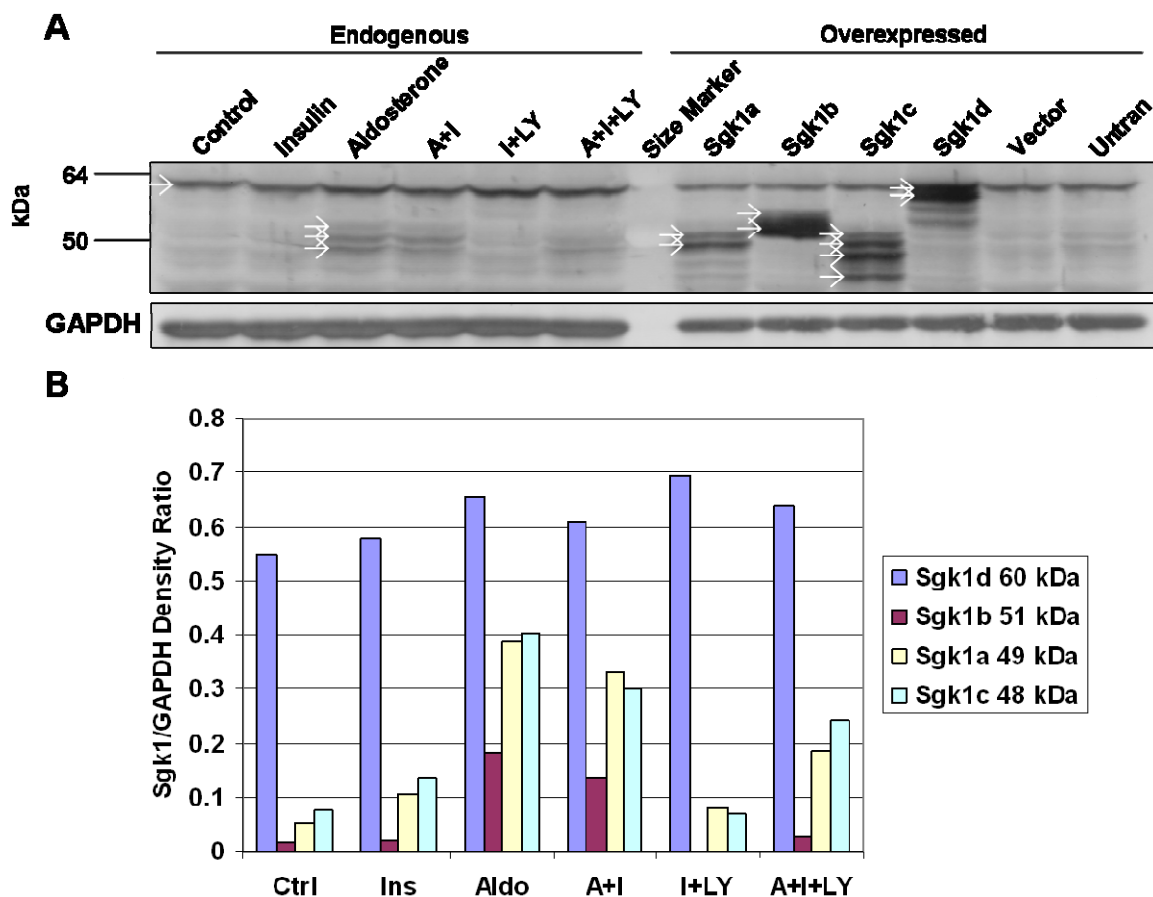


**Figure 3.14 Aldosterone plus insulin-stimulated expression of endogenous Sgk1 is partially sensitive to LY294002.** A shows a Western blot comparing the expression of Sgk1 in insulin, aldosterone, aldosterone plus insulin, and LY294002 treated mpkCCD<sub>c14</sub> cells including cells that were transfected with Sgk1 isoforms to show co-migration. The endogenous Sgk1 protein bands, detected using anti-SGK1 antibody, corresponding to the different Sgk1 isoforms, are indicated by arrows. Sgk1 immunoreactive bands in the overexpressed Sgk1 isoform cells are also indicated by arrows. B shows the quantification of the endogenous Sgk1 protein bands as a density ratio versus GAPDH.

### 3.2.11 Detection of overexpressed mouse Sgk1 isoforms with human SGK1 isoform-specific antisera

To address the need to detect and identify specific SGK1 isoforms in Western blotting and other applications, human SGK1 isoform-specific antisera were generated in collaboration with Cambridge BioScience Ltd, Cambridge, UK (Table 2.6). However, to use these antibodies to detect the mouse Sgk1 isoforms first required testing their specificity and

sensitivity with this different species. To address this, the isoform-specific antibodies were individually assessed for their ability to specifically detect overexpressed human SGK1 isoforms and mouse Sgk1 isoforms in lysate of transfected HEK293T and mpkCCD<sub>c14</sub> cells.

Six peptides were used in generation of the antibodies, four corresponding to amino acid sequence within the unique N-termini of SGK1A, B, C and F and two from within the longer N-terminus of SGK1D. Two rabbits were immunized per peptide, giving two antibody purifications for each isoform. Purified antibodies were initially tested for their ability to detect overexpressed human SGK1 isoforms in transfected HEK293T cell lysate by Western blotting. In addition to each isoform-specific antibody, anti-SGK1 antibody and peptide-blocked isoform-specific antibody were used as positive and negative controls, respectively.

The only isoform-specific antibodies that were found to specifically detect their target overexpressed human SGK1 isoforms were anti-SGK1B 3259 and anti-SGK1D 3253. Anti-SGK1B 3259 detected a single band in SGK1B transfected cell lysate of estimated size 51 kDa that co-migrated with the corresponding anti-SGK1-detected band and was removed by peptide-blocking (Figure 3.15). Similarly, anti-SGK1D 3253 also detected a single band in SGK1D transfected cell lysate of estimated size 60 kDa that co-migrated with the corresponding anti-SGK1-detected band and was removed by peptide-blocking (Figure 3.16).

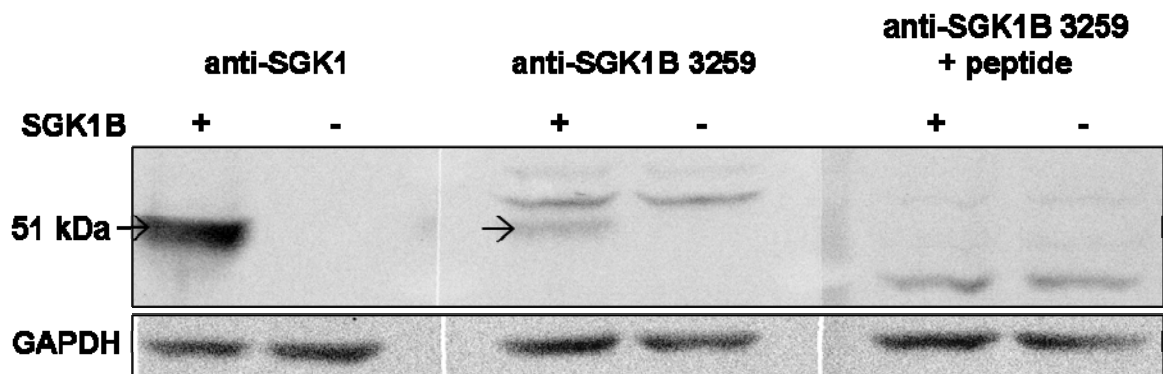


**Figure 3.15 Pre-incubation with target peptide blocked anti-SGK1B 3259 detection of overexpressed human SGK1B in lysate of transfected HEK293T cells.** HEK293T cells grown on plastic were transfected with SGK1B or control plasmid, grown for 24 hours to allow plasmid protein expression, then lysed. Lysates were co-analysed by Western blotting using anti-SGK1 antibody, anti-SGK1B 3259 antibody, and peptide-blocked anti-SGK1B 3259 antibody. Arrows indicate SGK1B bands in both the SGK1 and SGK1B-specific blots that was absent on the peptide-blocked blot.

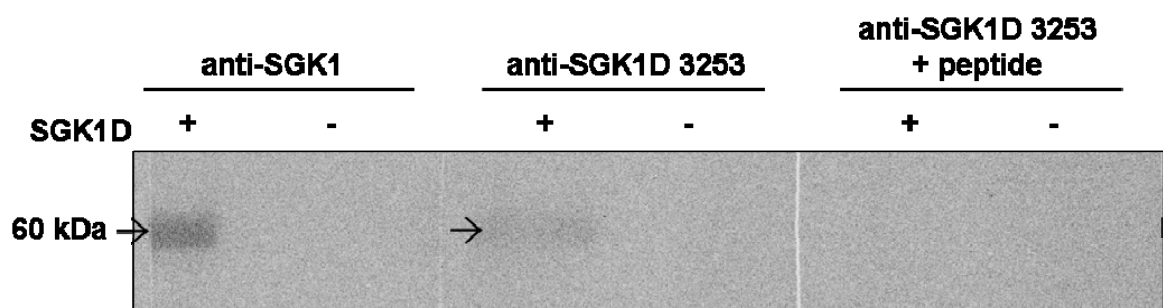


**Figure 3.16 Pre-incubation with target peptide blocked anti-SGK1D 3253 detection of overexpressed human SGK1D in lysate of transfected HEK293T cells.** HEK293T cells grown on plastic were transfected with SGK1D or control plasmid, grown for 24 hours to allow plasmid protein expression, then lysed. Lysates were co-analysed by Western blotting using anti-SGK1 antibody, anti-SGK1D 3253 antibody, and peptide-blocked anti-SGK1D 3253 antibody. Arrows indicate SGK1D bands in both the SGK1 and SGK1D-specific blots that was absent on the peptide-blocked blot.

Once an isoform-specific antibody had been verified against human SGK1 isoforms, it was then tested on overexpressed mouse Sgk1 isoforms from transfected mpkCCD<sub>c14</sub> cell lysate. To ensure antibodies remained specific in the detection of their target isoform, despite the presence of other overexpressed isoforms, antibodies were tested in the presence of overexpressed Sgk1a, b, c, and d. This testing showed that both anti-SGK1B

3259 (Figure 3.17) and anti-SGK1D 3253 (Figure 3.18) successfully detected mouse Sgk1b and Sgk1d, respectively.

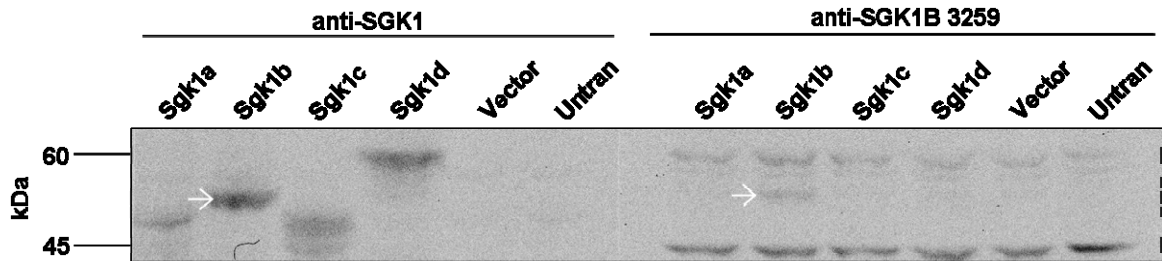


**Figure 3.17 Anti-SGK1B 3259 antibody specifically detected overexpressed mouse Sgk1b in transfected mpkCCD<sub>cl4</sub> cells.** mpkCCD<sub>cl4</sub> cells grown on plastic were transfected with Sgk1 isoforms, grown for 24 hours to allow plasmid protein expression, then lysed. Lysates were co-analysed by Western blotting using anti-SGK1 antibody to confirm Sgk1 expression and anti-SGK1B 3259 antibody. Arrows indicate Sgk1b bands in both the SGK1 and SGK1B-specific blots.

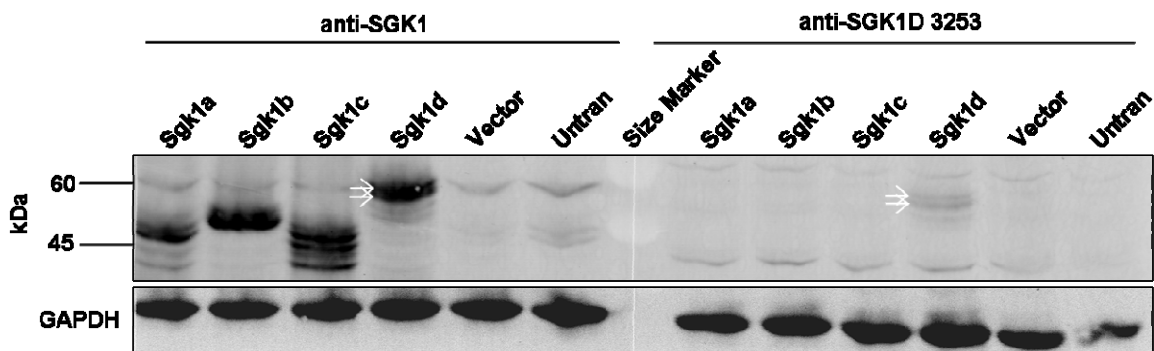


**Figure 3.18 Anti-SGK1D 3253 antibody specifically detected overexpressed mouse Sgk1d in transfected mpkCCD<sub>cl4</sub> cells.** mpkCCD<sub>cl4</sub> cells grown on plastic were transfected with Sgk1 isoforms, grown for 24 hours to allow plasmid protein expression, then lysed. Lysates were co-analysed by Western blotting using anti-SGK1 antibody to confirm Sgk1 expression and anti-SGK1D 3253 antibody. Arrows indicate Sgk1d bands in both the SGK1 and SGK1D-specific blots.

### 3.3 Discussion

#### 3.3.1 Identification and features of mouse Sgk1 isoforms

Results from the present study show that four different splice variants of mouse *Sgk1* are expressed in kidney and produce multiple mouse Sgk1 isoforms named Sgk1a, Sgk1b, Sgk1c, and Sgk1d. Conserved amino acid sequence between the mouse Sgk1 isoforms meant that all four isoforms contain a serine/threonine kinase domain, a C-terminal PDZ-binding motif (DSFL), and multiple phosphorylation sites. However, each Sgk1 isoform has a unique N-terminus creating some isoform-specific domains. For example, mouse Sgk1a contains an ubiquitin tagging domain (GMVAIL) and mouse Sgk1d contains a Phox homology (PX) domain.

The domains of the different Sgk1 isoforms could confer pan or isoform-specific roles. The C-terminal PDZ-binding motif (DSFL) is involved in phosphorylation of SGK1, as it is where the Na<sup>+</sup>/H<sup>+</sup> exchanger regulatory factor 2 (NHERF2) binds to recruit PDPK1 to SGK1, inducing phosphorylation at threonine 256 (Chun et al., 2002). The phosphorylation and activity profiles of the different Sgk1 isoforms are yet to be determined, but future work on this could lead to identification of a predominantly active isoform. Although conserved phosphorylation sites between the isoforms suggest that all four isoforms may be activated by similar routes Mouse Sgk1 displays conserved phosphorylation sites at serine 78, threonine 256, threonine 369, serine 377, and serine 422 (Kobayashi and Cohen, 1999). Serine 78 is phosphorylated by big mitogen-activated kinase 1 (BMK1) in a pathway regulating cell proliferation (Hayashi et al., 2001). As mentioned earlier, threonine 256 of Sgk1 is phosphorylated by PDPK1 (Kobayashi and Cohen, 1999). Threonine 369 is phosphorylated by protein kinase A (PKA) as part of cAMP-mediated effects of vasopressin (Perrotti et al., 2001). Serine 377 is phosphorylated

by NIMA (never in mitosis, gene A)-related kinase-6 (NEK6) (Lizcano et al., 2002). Serine 422 is phosphorylated by mechanistic target of rapamycin (mTOR) complex 2 (mTORC2) (Lu et al., 2010).

Of the Sgk1 isoform-specific domains, the GMVAIL motif of Sgk1a is a site of ubiquitin tagging of SGK1, signalling it for degradation by the 26S proteasome and is probably the site ubiquitinated by phosphorylated Nedd4-2 as part the negative feedback regulation of Sgk1 (Bogusz et al., 2006). However, the GMVAIL motif is only present in Sgk1a and none of the other SGK1 isoforms, suggesting that SGK1A may be the only isoform subject to negative feedback regulation by ubiquitination (Zhou and Snyder, 2005). Another Sgk1 isoform-specific domain, the PX domain of Sgk1d, is involved in targeted binding to phosphoinositides, suggesting that Sgk1d may have a role particularly linked to PI3K, ENaC or other plasma membrane proteins (Ellson et al., 2002; Wishart et al., 2001). The potential interactions of the PX domain of Sgk1d are discussed further in section 5.3.2.

The mouse Sgk1 isoforms share considerable sequence identity to their human equivalents and many features are conserved, which was expected considering the similar roles of Sgk1 described for both humans and mice. The mouse Sgk1 locus at chromosome position 10 A3 was extended from ~5 to ~120 kbp due to the addition of the alternative splice variant exons. This is highly similar to the human SGK1 locus at chromosome position 6q23, which was expanded from ~5 to ~150 kbp by the addition of splice variant exons. The main SGK1 splice variant responsible for the locus extension in both humans and mice is SGK1D, as it has 3 unique exons compared to 1 unique exon for each of the other isoforms. As the isoforms were named according to their proximity to the original locus, the exons of SGK1D stretch the furthest upstream (5') in both humans and mice. The next closest in proximity are the unique exons of SGK1C, SGK1B, and SGK1A, respectively. Interestingly, human SGK1F is the exception to the naming rule because it is produced by

a combination of the exon and intron sequence immediately upstream of the common human SGK1 exons, however, there is no mouse Sgk1 isoform equivalent to human SGK1F.

The discovery of mouse Sgk1 isoforms, in addition to the human SGK1 isoforms, renders much of the current research on mouse Sgk1 as too limited, but enables future investigation into the roles of these isoforms and of the evolution of SGK1 and its conservation and possible roles in other species. Regarding this project, the profiling of Sgk1 isoforms expression in mouse allowed further investigation into their roles in renal sodium transport.

### **3.3.3 Cloning of the mouse Sgk1 isoforms**

Sgk1a and Sgk1d were purchased from Geneservice in the pCMV-SPORT6 and pYX-Asc expression vectors, respectively. Sgk1 isoforms b, c, and d were cloned into the pCMV-SPORT6 vector by RT-PCR, combinatorial PCR, and sub-cloning, respectively. Once cloned, sequencing was used to confirm the identity and accuracy of the products. The cloning of Sgk1b and Sgk1d into pCMV-SPORT6 was carried out without any problems. However, the initial approach to clone Sgk1c following the same procedure as for Sgk1b failed for unknown reasons. This led to the use of combinatorial PCR to clone Sgk1c from mouse genomic DNA isolated from mpkCCD<sub>cl4</sub> cells.

Future cloning of the mouse Sgk1 could add alternative epitope or fluorescent tags to the isoforms. The data in this chapter also provides insight for future studies into the promoter regions for each isoform. Additional cloning could include the 5' and 3' untranslated regions in order to study their regulatory properties for each isoform. Cloning of the mouse Sgk1 isoforms enabled size comparison of overexpressed with endogenous proteins

to reinforce their identification. These vectors were also used to aid detection of phosphorylated Sgk1 isoforms and in verification of isoform specific antibodies.

### **3.3.4 Identification of multiple aldosterone-stimulated endogenous Sgk1 isoforms in mpkCCD<sub>cl4</sub> cells**

Aldosterone treatment of starved mpkCCD<sub>cl4</sub> cells stimulated expression of Sgk1a, b, and c in a time-dependent manner, whereas Sgk1d showed little induction by aldosterone, but was expressed at a much higher basal level. These data therefore suggest that Sgk1a, b, c, and d are differentially regulated by aldosterone in mouse cortical collecting duct cells. At concentrations above 30 nM, aldosterone had a detrimental effect on Sgk1 expression, possibly due to off-target effects that would occur at this concentration. The high concentrations of aldosterone are much greater than cells would experience physiologically and this may be having a detrimental effect on expression of Sgk1.

The results described in this study are supported by Flores et al. (2005), which showed that three Sgk1 bands of estimated sizes; 49, 47, and 45 kDa become detectable after 1 hour of 1  $\mu$ M aldosterone treatment and increase in density, in a time-dependent manner, peaking at 3 hours, before decreasing slightly at 6 hours. Similar results have also been reported by Gonzalez-Rodriguez et al. (2007). This work showed multiple endogenous Sgk1 bands in mCCD<sub>cl1</sub> cells that were maximally induced by combined aldosterone plus insulin or IGF-1 (Gonzalez-Rodriguez et al., 2007). Three aldosterone-induced Sgk1 bands of estimated sizes; 49, 51, 53 kDa were not removed by lambda phosphatase treatment.

The high basal expression of Sgk1d that was found in mpkCCD<sub>cl4</sub> cells (Figure 3.7) may, in part, be explained by the findings in Raikwar et al. (2008), which showed that human SGK1D had a much longer half-life than SGK1A in HEK293 cells ( $t_{1/2}$  = SGK1A: 16 min,

SGK1D: 119 min), but, despite this, latent Sgk1d would still be degraded after 24 hours of starvation. The data from Raikwar et al. (2008) and the limited sensitivity of Sgk1d to aldosterone treatment also suggest that Sgk1d is regulated differently to the other Sgk1 isoforms. The differential regulation of expression of multiple Sgk1 isoforms by aldosterone highlights the need to re-evaluate the existing model of regulation of ENaC in principal cells.

### **3.3.5 Co-migration of overexpressed Sgk1 isoform proteins with endogenous and synthesised Sgk1 isoform proteins**

Three aldosterone-induced Sgk1 bands of estimated sizes; 51, 49, and 48 kDa, co-migrated with overexpressed Sgk1 isoform bands corresponding to the full-length isoforms. An endogenous Sgk1 band at 60 kDa also co-migrated with the overexpressed Sgk1 band corresponding to full-length Sgk1d. Additional Sgk1 bands were detected in overexpressed isoform lanes that corresponded to smaller Sgk1 isoforms, but although some of these co-migrated with endogenous bands, the bands did not appear to be induced by aldosterone. To improve identification of which Sgk1 bands originated from which Sgk1 variant mRNA, synthesised Sgk1 isoform plasmid protein was also analysed for co-migration. An unexpected Sgk1 band was detected in the synthesised Sgk1b protein lane that was estimated to be 56 kDa in size. This 56 kDa band was unexpected as none of the isoforms of Sgk1b are predicted to be above 51 kDa in size. The *in vitro* synthesis of the protein removes post-translational modification and other Sgk1 isoforms as possible origins of the 56 kDa, suggesting an error in cloning. However, cloning was confirmed by plasmid nucleotide sequencing, leaving the identity of the 56 kDa band unknown.

### **3.3.6 Detection of phosphorylated Sgk1 isoforms**

Only overexpressed human SGK1B and C and mouse Sgk1c were detected when overexpressed with PDPK1 in HEK293T cells using phospho-specific Sgk1 antibodies. Attempts to stimulate phosphorylated endogenous or overexpressed Sgk1 in mpkCCD<sub>cl4</sub> cells were unsuccessful despite using phosphatase inhibitors, insulin treatment and co-transfection with PDPK1. Transfected HEK293T cells overexpress protein at a much higher level than mpkCCD<sub>cl4</sub> cells, enabling the weakly-detecting phospho-specific antibodies to detect their target. Not being able to detect all isoforms phosphorylated at threonine 256 suggests there may be differential regulation of phosphorylation between the isoforms. No detectable phosphorylation at threonine 256 may have occurred as a result of different phosphorylation thresholds at the different conserved phosphorylation sites. Also, different activators of Sgk1 such as mTOR may be involved in Sgk1 phosphorylation (Garcia-Martinez et al., 2008; Hong et al., 2008).

Future experiments could use constitutively active/inactive mutants of Sgk1 isoforms to investigate effects of SGK1 phosphorylation on regulation of ENaC. Simple methods to increase the likelihood of detecting phosphorylated SGK1 include: using Ac-Leu-Leu-Nle-CHO (ALLN) to inhibit the proteasome and decrease endogenous SGK1 degradation, or using a greater concentration of sample protein in the Western blotting, or immunoprecipitating total or phosphorylated SGK1 before detection.

### **3.3.7 Sensitivity of aldosterone-stimulated Sgk1 isoforms to LY294002**

LY294002 partially inhibited aldosterone + insulin induction of Sgk1 bands of estimated sizes; 51, 49, and 48 kDa, corresponding to Sgk1b, a, and c, respectively. These data therefore imply that PI3K has a role in regulating the expression levels of Sgk1a, b, and c

in mpkCCD<sub>c14</sub> cells. Interestingly, just as Sgk1d was shown to be unresponsive to aldosterone, Sgk1d expression was unchanged after exposure of cells to LY294002. The present results are supported by the findings of Flores et al. (2005), which showed that aldosterone-induced Sgk1 bands of estimated sizes; 49, 47, and 45 kDa were reduced by exposure of the mpkCCD<sub>c14</sub> cells to 30 min of 50  $\mu$ M LY294002 (Flores et al., 2005). Also, Gonzalez-Rodriguez et al. (2007) showed that aldosterone-induced Sgk1 bands of estimated sizes; 49, 51, 53 kDa were reduced, but not removed by treatment with 50  $\mu$ M LY294002 (Gonzalez-Rodriguez et al., 2007). These results suggest that Sgk1 induction by aldosterone, with or without insulin, is partially dependent on PI3K and mTOR, a conclusion that is not explained by the current model of Sgk1 stimulation. Further work is needed to resolve the roles of PI3K and mTOR in the regulation of expression of Sgk1 in CCD cells.

### **3.3.8 Detection of overexpressed isoforms with isoform-specific antisera**

Although isoform-specific antibodies were created for each of the human SGK1 isoforms (A-F), the SGK1B 3259 and SGK1D 3253 antibodies were the only ones found to be specific for their equivalent mouse Sgk1 isoform targets. The specificity of these antibodies to their target isoform against overexpressed protein further verifies the identity of Sgk1 isoforms b and d. These isoform-specific antibodies provide a method of specifically detecting expression of SGK1B and SGK1D in cell lysate by Western blotting. Also, these antibodies were later used in immunofluorescence studies of Sgk1 expression in native renal tissue. These antibodies could be used in future studies to show localisation or distribution of human or mouse SGK1B and D in other types of tissue or cells.

### 3.4 Summary

- Mouse Sgk1 is expressed as multiple isoforms similar to human SGK1.
- Four distinct Sgk1 isoforms identified in mouse were named Sgk1a, Sgk1b, Sgk1c, and Sgk1d according to their similarity to human SGK1 isoforms.
- mpkCCD<sub>c14</sub> cells and mouse renal tissue express mRNA for Sgk1 isoforms a, b, c and d.
- mpkCCD<sub>c14</sub> cells endogenously express multiple Sgk1 proteins of comparable molecular weights to the predicted proteins of Sgk1a, b, c, and d.
- Endogenously expressed and exogenously expressed Sgk1 isoforms co-migrate in Western blotting.
- Endogenous Sgk1 isoforms are induced by aldosterone.
- Phosphorylated human SGK1 isoform B and C and mouse Sgk1 isoform c are detectable when overexpressed with PDPK1 by Western blotting using phosphothreonine 256-specific antibody.
- Aldosterone stimulation of Sgk isoforms is sensitive to LY294002.
- Sgk1 isoforms b and d are detectable by Western blotting using isoform-specific antibodies.

## **Chapter 4 - Electrophysiological Studies of the Regulation of**

### **Sodium Transport**

#### **4.1 Introduction**

The principal cells of the cortical collecting duct in the kidney mediate hormone-regulated sodium reabsorption required for the essential maintenance of salt homeostasis. Aldosterone acts on principal cells to regulate sodium reabsorption by increasing the synthesis and activities of the epithelial sodium channel (ENaC), the basolateral Na<sup>+</sup>/K<sup>+</sup>-ATPase, and K<sup>+</sup> channels (Ring et al., 2007b; Liang et al., 2006; Flores et al., 2005; Huang et al., 2004; Summa et al., 2004). Aldosterone diffuses into the cell cytosol and binds to the mineralocorticoid receptor (MR) creating a hormone-receptor complex. This complex then translocates from the cytosol to the nucleus where it induces transcription of various genes, including *SGK1* (Verrey et al., 2007). SGK1 itself requires activation to mediate the effects of aldosterone. This occurs by phosphorylation at positions threonine 256 and serine 422, which is mediated by 3-phosphoinositide-dependent protein kinase 1 (PDK1) and mechanistic target of rapamycin complex 2 (mTORC2), respectively (Lu et al., 2010; Park et al., 1999). The activities of PDK1 and mTORC2 are regulated by the phosphoinositide 3-kinase (PI3K) pathway, which is activated by insulin, amongst other agonists (Wang et al., 2001; Park et al., 1999). Activated SGK1 binds, phosphorylates and thus inactivates Nedd4-2, which would otherwise signal ENaC for internalisation and degradation via ubiquitination (Snyder et al., 2002; Staub et al., 2000). This increases the number of ENaC at the apical membrane thus increasing sodium transport (McCormick et al., 2005; Debonneville et al., 2001). There are early and late phases to aldosterone-stimulated sodium transport in the CCD, which begin after ~30 min and ~2 hours of

treatment, respectively (Verrey et al., 2000). The early phase is attributed to increased ENaC activity and redistribution of intracellular ENaC to the apical membrane, whereas the late phase is attributed to stimulated ENaC production to gradually increase channel number in the apical membrane (Butterworth, 2010). An additional level of regulation of ENaC occurs through proteolysis of the alpha and gamma subunits of channels present in the apical membrane, which increases channel activity (Kleyman et al., 2009).

In the previous chapter, four different mouse Sgk1 isoforms were shown to be differentially induced by aldosterone and insulin treatment in renal epithelial cells. The aim of this chapter was to investigate how manipulation of Sgk1 expression and signalling affects ENaC-mediated transepithelial  $\text{Na}^+$  transport by mpkCCD<sub>c14</sub> cells. For these studies, aldosterone and insulin were used as physiological stimulants of  $\text{Na}^+$  transport. In order to determine the ENaC-mediated transepithelial current I have used amiloride to selectively block ENaC. Amiloride blocks ENaC with a  $K_i$  of  $\sim 100$  nM, therefore,  $1 \mu\text{M}$  amiloride was used in an attempt to completely block ENaC without inhibiting other ion channels such as the cyclic nucleotide-gated channel A3 (CNG-A3), which amiloride blocks with a  $K_i$  of  $\sim 50 \mu\text{M}$  (Novaira et al., 2004; Rossier, 2003).

Transepithelial short-circuit current ( $I_{sc}$ ) is a measure of the charge flow per time associated with ion transport across an epithelial cell monolayer (Li et al., 2004). This transepithelial flow of charge is dependent on two factors: resistance of the cell monolayer; and transepithelial potential difference. Resistance of epithelia is determined by the polarity of the cells and the permeability of the tight-junctions between adjacent cells. Transepithelial potential difference is equivalent to the voltage generated by the net movement of ions across a monolayer. Monolayers of mpkCCD<sub>c14</sub> cells were tested under open-circuit conditions (where transepithelial voltage ( $V_{te}$ ) is not clamped) using an epithelial volt and ohmmeter (EVOMeter) (World Precision Instruments, Sarasota, FL,

USA) to measure the transepithelial resistance ( $R_{te}$ ) and  $V_{te}$ . From these two values, the equivalent  $I_{sc}$  ( $I_{eq}$ ) can be calculated using the following equation that is based on Ohm's Law:  $I_{eq} = V_{te}/R_{te}$ .  $I_{eq}$  represents a measure of actual transepithelial flow of ions across the cell monolayer, a positive value corresponding to a net movement of positively charged ions apically to basolaterally (epithelial absorption) or negatively charged ions basolaterally to apically (epithelial secretion) (for negative values this net flow would be *vice versa* for each ion).

## **4.2 Results**

### **4.2.1 Aldosterone and insulin stimulate ENaC-mediated sodium transport**

In chapter 3, Western blotting results demonstrated that 24 hours treatment of serum-starved mpkCCD<sub>cl4</sub> cells with 3-30 nM aldosterone gave a maximal induction of Sgk1 isoforms (Figure 3.6). Results also showed that 10 nM aldosterone induced Sgk1a, b, c, and d expression in a time-dependent manner that was detectable at 1 hour and maximal at 6 hours (Figure 3.7). Bens et al. (1999) have shown previously that 10 nM aldosterone induced ENaC-mediated transepithelial sodium transport in mpkCCD<sub>cl4</sub> cells in a similar time-dependent manner. These studies indicated that 10 nM aldosterone gave a time-dependent increase in  $I_{eq}$ , from a basal level of  $\sim 10 \mu\text{A}/\text{cm}^2$ , that was significantly above control from 2 hours and maximal (4-fold) at 6 hours.

To investigate if the changes in Sgk1 isoform expression were linked to increases in  $\text{Na}^+$  transport required a reliable assay to measure  $I_{eq}$ . To this end, the EVOMeter electrophysiology assay and mpkCCD<sub>cl4</sub> cell growth conditions described by Bens et al. (1999) were employed. In order to ensure the maximum  $I_{eq}$  response of the mpkCCD<sub>cl4</sub> cells to aldosterone treatment, 1  $\mu\text{M}$  insulin was also included in the treatment assay.

Insulin is known to activate a pathway that leads to the phosphorylation and activation of SGK1 and was shown previously to produce a maximal  $I_{eq}$  response when combined with another mineralocorticoid, dexamethasone (Wang et al., 2001).

Aldosterone plus insulin treatment of serum and hormone-starved mpkCCD<sub>cl4</sub> cells stimulated time-dependent changes in  $R_{te}$ ,  $V_{te}$  and calculated  $I_{eq}$  as well as the calculated amiloride-sensitive  $I_{eq}$  at 6 hours (Figure 4.1). Transepithelial resistance ( $R_{te}$ ) had immediately dropped after 1 hour of treatment for both control and aldosterone plus insulin (A+I) treated cells (Figure 4.1A). The initial  $R_{te}$  of  $\sim 3400 \pm 200 \Omega\text{cm}^2$  had dropped by  $\sim 1000 \Omega\text{cm}^2$  for control cells and by  $\sim 1500 \Omega\text{cm}^2$  for A+I treated cells following 1 hour of treatment. After 1 hour, the reduction in  $R_{te}$  gradually slowed, but the  $\sim 500 \Omega\text{cm}^2$  difference between the control and A+I treated cells was maintained (Figure 4.1A). Control cell  $R_{te}$  continued to decrease, reaching  $\sim 1500 \pm 100 \Omega\text{cm}^2$  at 6 hours, whereas A+I treated cells stabilised at  $\sim 1000 \pm 100 \Omega\text{cm}^2$  at 4 hours, which was maintained up to 6 hours. After 6 hours, cells were exposed to  $1 \mu\text{M}$  amiloride to selectively block ENaC. This resulted in an increase in resistance of  $\sim 300 \Omega\text{cm}^2$  for control cells and  $\sim 400 \Omega\text{cm}^2$  for A+I treated cells from 6 to 6.5 hours (Figure 4.1A). The large initial drop in  $R_{te}$  is probably due to a reaction of the cells to the addition of treatment solutions and to the short removal of the cells from a  $37^\circ\text{C}$ , 5%  $\text{CO}_2$  atmosphere for EVOM measurement.

Transepithelial potential difference ( $V_{te}$ ), which had a basal value of  $\sim 85 \pm 3 \text{ mV}$  at 0 hours, also showed a large initial decrease of  $\sim 30 \text{ mV}$  by 1 hour (Figure 4.1B). As with the  $R_{te}$ , the decrease slowed after 1 hour and stabilised at  $\sim 50 \text{ mV}$  for A+I treated cells and  $\sim 25 \text{ mV}$  for control cells after 3 hours. Amiloride treatment after 6 hours caused the potential difference to drop to  $\sim 11 \pm 2 \text{ mV}$  for control cells and to  $\sim 35 \pm 4 \text{ mV}$  for A+I treated cells.

Polarised mpkCCD<sub>cl4</sub> cells exhibited a basal level of net ion absorption giving an  $I_{eq}$  of  $26.0 \pm 2.2 \mu\text{A}/\text{cm}^2$  (Figure 4.1C). Aldosterone plus insulin stimulated significant  $I_{eq}$  above control cells at 1 hour, which continued to increase in a time-dependent manner up to 6 hours. This response paralleled the aldosterone-induced time-dependent increase in Sgk1 expression shown in Figure 3.7. After 6 hours, aldosterone plus insulin  $I_{eq}$  had increased in a time-dependent manner to  $50.9 \pm 3.8 \mu\text{A}/\text{cm}^2$ , 2.5-fold above the control  $I_{eq}$  of  $19.0 \pm 2.0 \mu\text{A}/\text{cm}^2$ . Treatment with 1  $\mu\text{M}$  amiloride removed the majority of the  $I_{eq}$  for both vehicle and A+I treated cells, which was expected, as the majority of ion transport by these cells occurs via ENaC (Bens et al., 1999).  $I_{eq}$  in vehicle treated cells was reduced to  $5.2 \pm 0.8 \mu\text{A}/\text{cm}^2$ , whereas  $I_{eq}$  in A+I treated cells was reduced to  $23.7 \pm 2.4 \mu\text{A}/\text{cm}^2$ , a reduction of just over half for the A+I treated cells. This suggests that there was a significant amount of current that was not due to functional ENaC. However, the identity of this amiloride-insensitive  $I_{eq}$  was not investigated further.

Calculation of the amiloride-sensitive equivalent short circuit current allowed comparison of the treatment effects on ENaC-mediated sodium transport. At 6 hours, control cells displayed around half the amiloride-sensitive  $I_{eq}$  compared to A+I treated cells (Control:  $13.3 \pm 1.6 \mu\text{A}/\text{cm}^2$ ; A+I:  $27.2 \pm 1.9 \mu\text{A}/\text{cm}^2$ ,  $P = <0.001$ ) (Figure 4.1D). This indicated that A+I treatment significantly stimulated ENaC-mediated sodium transport, but also that around half of the sodium transport was not dependent on hormone stimulation.

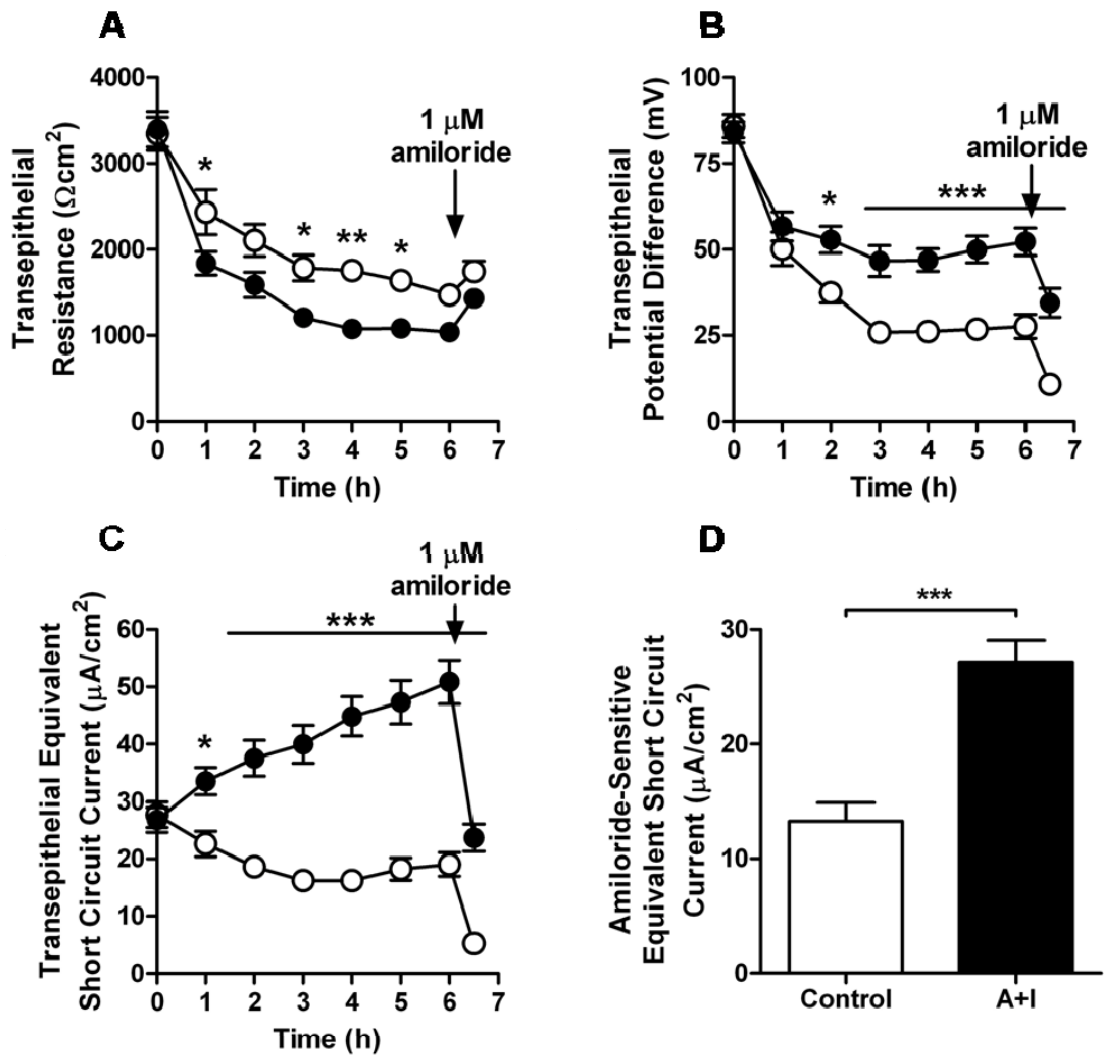


**Figure 4.1 Effect of aldosterone plus insulin on electrophysiology measurements of ion transport in mpkCCD<sub>cl4</sub> cells.** A and B show parallel electrophysiology measurements of transepithelial resistance ( $R_{te}$ ) and transepithelial potential difference ( $V_{te}$ ) over 6.5 hours of treatment of mpkCCD<sub>cl4</sub> monolayers. Cells which had been pre-starved for 24 hours were then exposed to 10 nM aldosterone plus 1  $\mu\text{M}$  insulin (closed circles) or vehicle (open circles). C shows the equivalent short circuit current ( $I_{eq}$ ) calculated from the  $R_{te}$  and  $V_{te}$  values. D shows the amiloride-sensitive  $I_{eq}$ , calculated from the difference in  $I_{eq}$  before and 30 min after treatment with 1  $\mu\text{M}$  amiloride at 6 hours. Values are means  $\pm$  sem,  $n = 18$ . \*, \*\*, and \*\*\* represent P values of  $<0.05$ ,  $<0.01$ , and  $<0.001$  compared with control cells.

This experiment was repeated using the hormones individually or together, in order to investigate if aldosterone and insulin had a synergistic effect on  $I_{eq}$ , as shown by Wang et al. (2008). In order to investigate previously reported early and late actions of aldosterone, cells were prepared in duplicate to allow one set to be used to assess the amiloride-

sensitive  $I_{eq}$  at 2 hours and one set to assess amiloride-sensitive  $I_{eq}$  at 6 hours (McCormick et al., 2005; Verrey et al., 2000).

After 1 hour of treatment, insulin  $I_{eq}$  was significantly greater than control cells and aldosterone treated cells (Ins:  $17.3 \pm 0.4 \mu\text{A}/\text{cm}^2$ ; Control:  $11.2 \pm 0.3 \mu\text{A}/\text{cm}^2$ ; and Aldo:  $13.5 \pm 0.7 \mu\text{A}/\text{cm}^2$ ,  $P = <0.01$ ) (Figure 4.2). By 2 hours, however, the insulin  $I_{eq}$  had dropped slightly ( $16.0 \pm 1.9 \mu\text{A}/\text{cm}^2$ ), whilst the aldosterone  $I_{eq}$  had increased ( $17.2 \pm 1.2 \mu\text{A}/\text{cm}^2$ ). Insulin  $I_{eq}$  remained significantly above control  $I_{eq}$  ( $9.9 \pm 0.3 \mu\text{A}/\text{cm}^2$ ,  $P = <0.001$ ), but this was not maintained beyond 2 hours (Figure 4.2B). These data show that the  $I_{eq}$  response to insulin is short lived ( $<2$  hours) under these conditions.

Aldosterone plus insulin had additive stimulation of  $I_{eq}$ , compared to individual aldosterone and insulin treatments (Figure 4.2). A+I-stimulated  $I_{eq}$  was significantly greater than control and aldosterone  $I_{eq}$  by 1 hour and insulin  $I_{eq}$  by 2 hours ( $P = <0.05$ ). Overall, A+I-stimulated  $I_{eq}$  showed the greatest sustained elevation (Figure 4.2B). These data indicate that the different treatments altered the ion transport properties of the cell monolayer over time. To find out if this was caused by an increase in ENaC activity, the amiloride-sensitive  $I_{eq}$  was calculated for each condition at 2 hours and 6 hours (Figure 4.3).

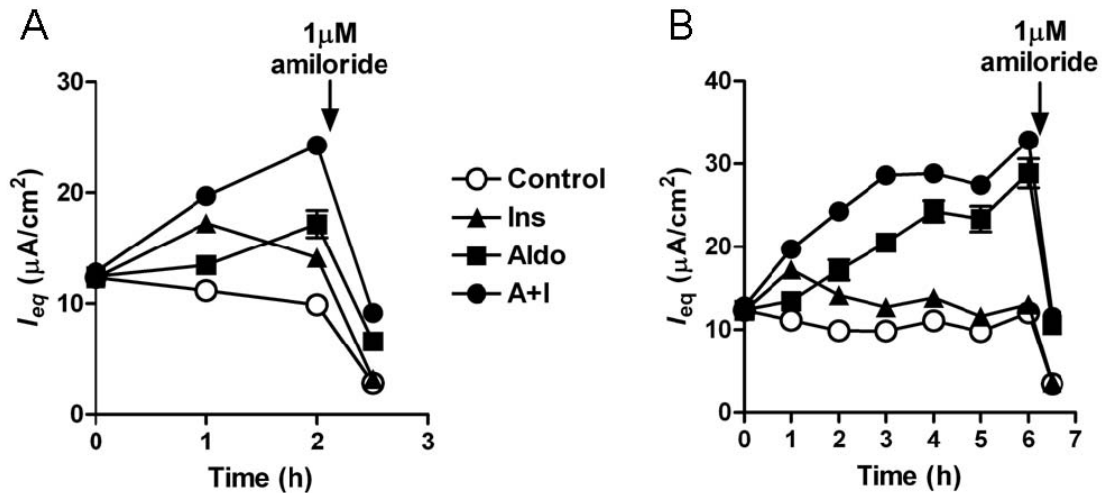


**Figure 4.2 Insulin stimulates a small and short-lived increase in transepithelial equivalent short circuit current, whereas aldosterone stimulates a larger and more sustained increase that peaks earlier when aldosterone is combined with insulin.**

Total equivalent short circuit current ( $I_{eq}$ ) calculated for mpkCCD<sub>cl4</sub> cells treated as described in Figure 4.1, but including 10 nM aldosterone (Aldo) and 1  $\mu$ M insulin (Ins) treatments alone. A shows  $I_{eq}$  calculated for cells treated up to 2 hours before treatment with 1  $\mu$ M amiloride. B shows  $I_{eq}$  calculated for cells treated up to 6 hours before treatment with 1  $\mu$ M amiloride. Values are means  $\pm$  sem,  $n = 6$  from 0-2 hours and  $n = 3$  from 2.5-6 hours.

At 2 hours, insulin and aldosterone-stimulated amiloride-sensitive  $I_{eq}$  were significantly greater than control  $I_{eq}$  (Ins:  $11.0 \pm 0.6 \mu\text{A}/\text{cm}^2$ ; Aldo:  $11.4 \pm 1.1 \mu\text{A}/\text{cm}^2$ ; Control:  $7.1 \pm 0.3 \mu\text{A}/\text{cm}^2$ ,  $P = <0.001$ ) (Figure 4.3A). A+I amiloride-sensitive  $I_{eq}$  at 2 hours was significantly greater than that of all other treatments (A+I:  $15.1 \pm 0.4 \mu\text{A}/\text{cm}^2$ ,  $P = <0.01$ ). Insulin and aldosterone-stimulated  $I_{eq}$  was  $\sim 4 \mu\text{A}/\text{cm}^2$  higher than control  $I_{eq}$ , whereas A+I-stimulated  $I_{eq}$  was  $\sim 8 \mu\text{A}/\text{cm}^2$  higher than control  $I_{eq}$  at 2 hours. These data show that the  $I_{eq}$  response to A+I was additive, but not synergistic.

A 6 hours, only aldosterone and aldosterone plus insulin-stimulated amiloride-sensitive  $I_{eq}$  were above control cells (Control:  $8.6 \pm 0.4 \mu\text{A}/\text{cm}^2$ ; Ins:  $9.5 \pm 0.3 \mu\text{A}/\text{cm}^2$ ; Aldo:  $18.3 \pm 1.0 \mu\text{A}/\text{cm}^2$ ; and A+I:  $21.4 \pm 0.6 \mu\text{A}/\text{cm}^2$ ,  $P = <0.001$ ) (Figure 4.3B). The disappearance of insulin-stimulated amiloride-sensitive  $I_{eq}$  from 2 to 6 hours, further suggests that the effect of insulin on sodium transport is short lived. Also, A+I-stimulated amiloride-

sensitive  $I_{eq}$  was still significantly greater than that of individual aldosterone or insulin at 6 hours, but insulin no longer induced significant amiloride-sensitive  $I_{eq}$ , suggesting a synergistic effect of combined aldosterone plus insulin.

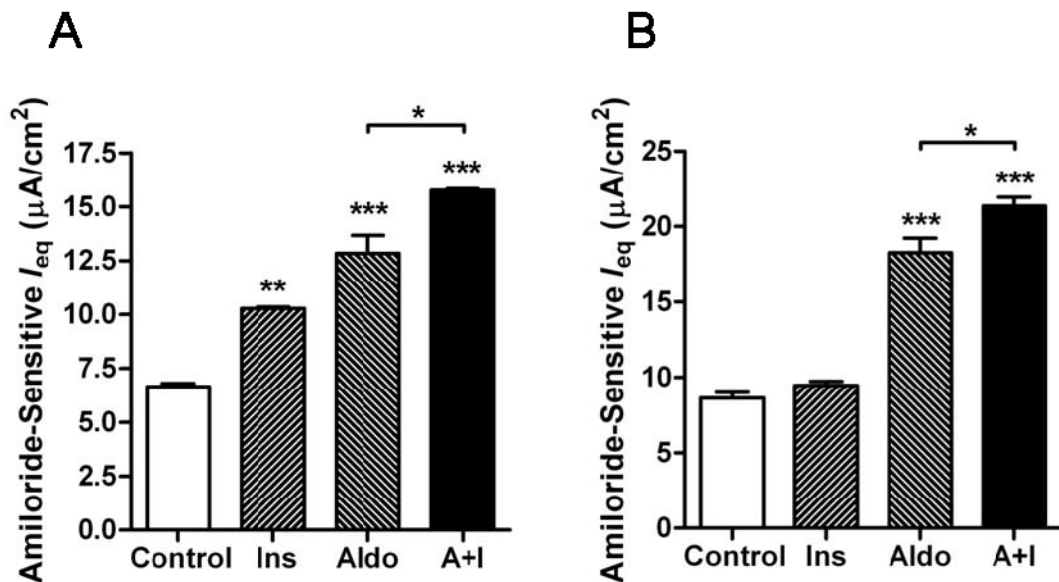


**Figure 4.3** Aldosterone and aldosterone plus insulin stimulate significant ENaC-mediated sodium transport at 2 hours and 6 hours, whereas insulin did so only at 2 hours. A and B show amiloride-sensitive  $I_{eq}$  calculated from the difference between  $I_{eq}$  values before and after 1  $\mu\text{M}$  amiloride treatment of mpkCCD<sub>cl4</sub> cells treated for 2 hours (A) or 6 hours (B) as described in Figure 4.2. Values are means  $\pm$  sem, n = 3. \*, \*\*, and \*\*\* represent P values of <0.05, <0.01, and <0.001.

In a separate experiment, stimulation of amiloride-sensitive  $I_{eq}$  by A+I was compared between 2 hours and 6 hours exposure (Figure 4.4). A+I-stimulated amiloride-sensitive  $I_{eq}$  was significantly above control at both 2 hours (Control:  $7.9 \pm 0.6 \mu\text{A}/\text{cm}^2$ ; A+I:  $18.3 \pm 1.2 \mu\text{A}/\text{cm}^2$ ,  $P = <0.001$ ) and 6 hours (Control:  $8.6 \pm 0.3 \mu\text{A}/\text{cm}^2$ ; A+I:  $22.0 \pm 0.5 \mu\text{A}/\text{cm}^2$ ,  $P = <0.01$ ). This showed that A+I-stimulated amiloride-sensitive  $I_{eq}$  lasted up to 6 hours and suggested a further increase beyond 6 hours. To investigate how long the response was maintained and what the peak response was, this experiment was repeated including time points at 24 and 48 hours (Figure 4.5).

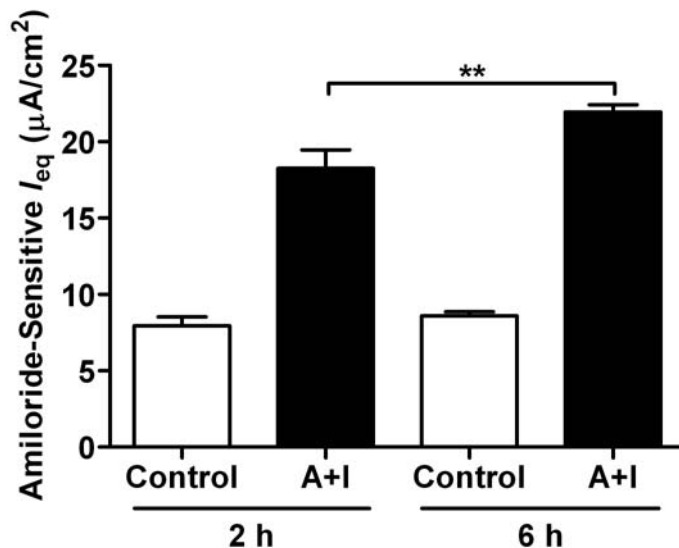


**Figure 4.4 Aldosterone plus insulin-stimulated ENaC-mediated sodium transport was greater at 6 hours than at 2 hours of exposure.** Amiloride-sensitive  $I_{eq}$  at 2 and 6 hours, of mpkCCD<sub>cl4</sub> cells that were treated as described in Figure 4.2. Values are means  $\pm$  sem,  $n = 6$ . \*\* represents  $P = <0.01$ .

A+I-stimulated amiloride-sensitive  $I_{eq}$  was maintained at around double control cell level at 2 hours (Control:  $15.5 \pm 0.3 \mu\text{A}/\text{cm}^2$ ; A+I:  $31.8 \pm 0.3 \mu\text{A}/\text{cm}^2$ ,  $P = <0.001$ ), 6 hours (Control:  $14.2 \pm 0.6 \mu\text{A}/\text{cm}^2$ ; A+I:  $36.4 \pm 1.1 \mu\text{A}/\text{cm}^2$ ,  $P = <0.001$ ) and 24 hours (Control:  $9.2 \pm 0.5 \mu\text{A}/\text{cm}^2$ ; A+I:  $19.2 \pm 1.2 \mu\text{A}/\text{cm}^2$ ,  $P = <0.001$ ), but was completely abolished at

48 hours (Control:  $4.3 \pm 0.5 \mu\text{A}/\text{cm}^2$ ; A+I:  $3.2 \pm 0.6 \mu\text{A}/\text{cm}^2$ ) (Figure 4.5). For this experiment, the same lot of cells was treated multiple times with amiloride at the indicated time points. Amiloride was then washed off and fresh treatment medium replaced. The decrease in vehicle treated control values over time suggests that the cells gradually lost their sodium transport capabilities under these experimental conditions. This transport decrease was probably due to the cells being kept in starvation medium throughout the experiment, which would have a negative impact on cells due to lack of the essential additives in growth medium. Alternatively, the ion transport capabilities of the cells may have been impacted by the repeated treatment with amiloride. In addition, A+I-stimulated amiloride-sensitive  $I_{\text{eq}}$  was maintained to at least 24 hours and was maximal at 6 hours (Figure 4.5). These data parallel results in chapter 3, which showed aldosterone-induced Sgk1 expression peak at 6 hours and maintained for 24 hours (Figure 3.7).

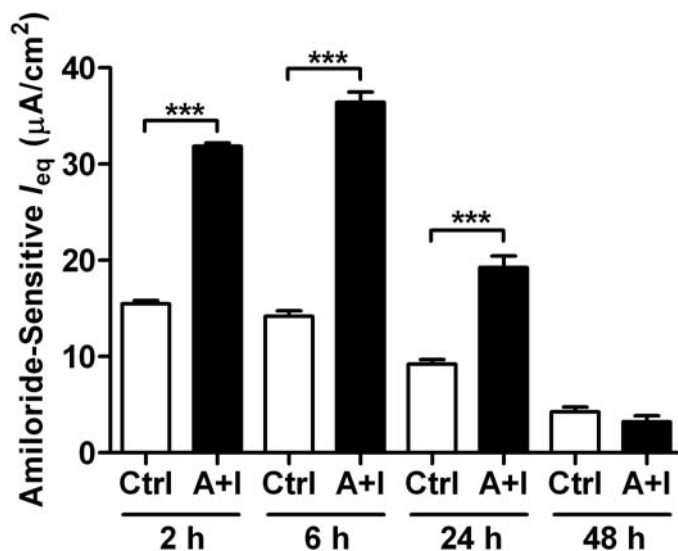


**Figure 4.5 Aldosterone plus insulin-stimulated ENaC-mediated  $I_{\text{eq}}$  is maintained for at least 24 hours and is maximal at 6 hours.** Amiloride-sensitive  $I_{\text{eq}}$  calculated from the difference between  $I_{\text{eq}}$  values before and after  $1 \mu\text{M}$  amiloride treatment of mpkCCD<sub>cl4</sub> cells grown on permeable membrane supports that were starved for 24 hours then treated with vehicle control (Ctrl) or aldosterone plus insulin (A+I). Values are means  $\pm$  sem, n = 3. \*\*\* represents  $P < 0.001$ .

#### **4.2.2 LY294002 reduces aldosterone and aldosterone plus insulin -stimulated sodium transport**

The response of mpkCCD<sub>cl4</sub> cells to aldosterone and insulin has previously been shown to be sensitive to the phosphoinositide 3-kinase (PI3K) and mechanistic target of rapamycin (mTOR) inhibitor LY294002 (Wang et al., 2008; Flores et al., 2005; Wang et al., 2001). To extend information for the time-dependent effects of PI3K and mTOR-dependent  $I_{eq}$  stimulation, the effect of LY294002 on A+I-stimulated amiloride-sensitive  $I_{eq}$  was investigated. Cells were pre-treated with 10  $\mu$ M LY294002 or vehicle control for 30 min before treatment with A+I or vehicle control.  $I_{eq}$  was then measured hourly to 7 hours. At 7 hours, 1  $\mu$ M amiloride was added to cells for 30 min then finally measured to calculate the amiloride-sensitive  $I_{eq}$ .

A+I-stimulated  $I_{eq}$  was significantly greater than control and LY294002-treated cells from 1 hour ( $P = <0.01$ ) (Figure 4.6). LY294002 treatment caused the overall A+I response to decrease, indicating that LY294002 partially inhibited A+I-stimulated  $I_{eq}$ , and caused a sub-maximal stimulation.

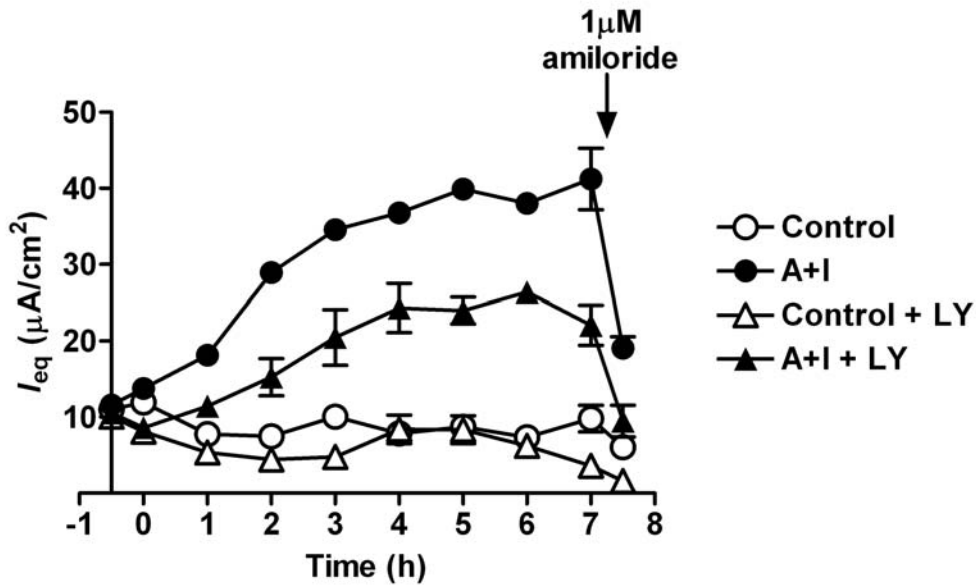


**Figure 4.6 LY294002 causes a lesser magnitude  $I_{eq}$  response to aldosterone plus insulin.**  $I_{eq}$  of polarised mpkCCD<sub>c14</sub> cells grown on permeable membrane supports that were starved for 24 hours then pre-treated with vehicle control or 10  $\mu$ M LY294002 for 30 min. Cells were then treated for 7 hours with vehicle control (Control) or aldosterone + insulin (A+I). After 7 hours of hourly measurement, cells were treated with 1  $\mu$ M amiloride to assess ENaC-mediated  $I_{eq}$ . Values are means  $\pm$  sem, n = 6.

The partial inhibition of A+I-stimulated  $I_{eq}$  by LY294002 was also observed in the amiloride-sensitive  $I_{eq}$  of aldosterone treated cells. LY294002 caused a significant drop in aldosterone-stimulated amiloride-sensitive  $I_{eq}$  at 7 hours (Aldo:  $20.2 \pm 1.0 \mu\text{A}/\text{cm}^2$ ; Aldo + LY:  $9.4 \pm 0.9 \mu\text{A}/\text{cm}^2$ ,  $P = <0.001$ ) (Figure 4.7). This was also observed in A+I treated cells (A+I:  $22.1 \pm 2.9 \mu\text{A}/\text{cm}^2$ ; A+I + LY:  $12.6 \pm 0.7 \mu\text{A}/\text{cm}^2$ ,  $P = <0.001$ ). As a result of this partial inhibition by LY294002, only A+I treated cells, and not aldosterone treated cells, showed significantly increased amiloride-sensitive  $I_{eq}$  above control cells at 7 hours (Ctrl + LY:  $2.3 \pm 1.4 \mu\text{A}/\text{cm}^2$ ,  $P = <0.01$ ). These data parallel the Western blot data in chapter 3 that showed partial inhibition of aldosterone and aldosterone plus insulin-stimulated Sgk1a, b, and c expression by LY294002 (Figure 3.13).

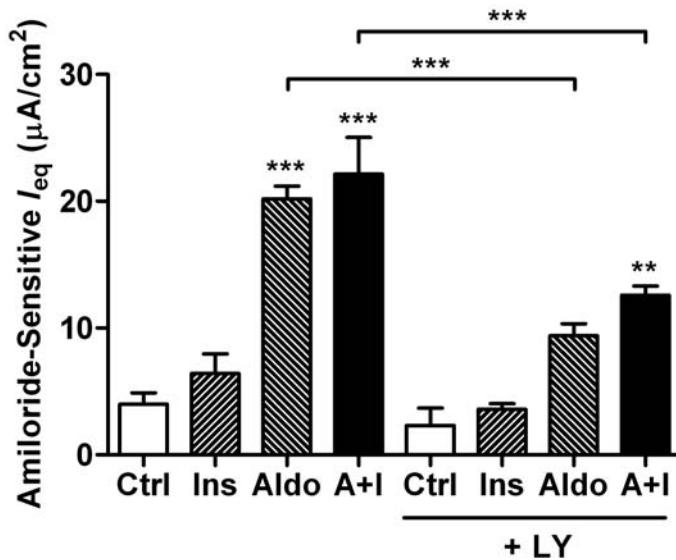


**Figure 4.7 LY294002 causes a significant decrease in aldosterone and aldosterone plus insulin-stimulated ENaC-mediated  $I_{eq}$  at 7 hours.** Amiloride-sensitive  $I_{eq}$  calculated from the difference between  $I_{eq}$  values before and after 1  $\mu\text{M}$  amiloride treatment of mpkCCD<sub>c14</sub> cells grown on permeable membrane supports. Cells were starved for 24 hours then pre-treated with vehicle or 10  $\mu\text{M}$  LY294002 before treatment with vehicle control (Ctrl), aldosterone (Aldo), insulin (Ins) or aldosterone + insulin (A+I). Values are means  $\pm$  sem, n = 6. \*\* and \*\*\* represent P values of <0.01 and <0.001.

#### 4.2.3 Rapamycin reduces aldosterone plus insulin-stimulated sodium transport

Mechanistic target of rapamycin (mTOR) has been identified as a key activator of SGK1 and therefore of ENaC. There is, however, conflicting evidence that suggests either functional complex of mTOR (mTORC1 or mTORC2) may be responsible for phosphorylation of SGK1 (Garcia-Martinez and Alessi, 2008b; Hong et al., 2008). Rapamycin is considered a selective inhibitor of mTORC1 (Loewith et al., 2002), but Sarbassov et al. (2006) showed that prolonged rapamycin treatment also inhibits mTORC2 (Sarbassov et al., 2006). Others also suggest that rapamycin may not completely inhibit mTORC1 activities (Thoreen et al., 2009; Thoreen and Sabatini, 2009). In an attempt to assess the dependence of aldosterone plus insulin-stimulated  $I_{eq}$  on mTOR, the equivalent short circuit current assay was repeated in the presence and absence of 20 nM rapamycin.

This concentration of rapamycin specifically inhibits mTORC1, whereas exposure to 100 nM rapamycin only inhibited formation of mTORC2 after 24 hours (Sarbasov et al., 2006; Sarbasov et al., 2004). Cells were pre-treated for 1 hour with 20 nM rapamycin or vehicle control, and then treated with aldosterone plus insulin at 0 hours.

As expected, A+I-stimulated  $I_{eq}$  was significantly above control cells from 1 hour (Figure 4.8). Rapamycin treatment caused the overall A+I response to decrease. This meant that A+I-stimulated  $I_{eq}$  was only significantly above control from 2 hours ( $P = <0.001$ ), compared to 1 hour without rapamycin ( $P = <0.01$ ). Rapamycin also significantly reduced the peak A+I-stimulated  $I_{eq}$  at 6 hours (A+I:  $74.6 \pm 3.8 \mu\text{A}/\text{cm}^2$ ; A+I + Rapa:  $59.3 \pm 3.0 \mu\text{A}/\text{cm}^2$ ,  $P = <0.001$ ). This significant, but small inhibition of A+I-stimulated  $I_{eq}$  by rapamycin, suggests that mTORC1 plays a small role in A+I-stimulated sodium transport.

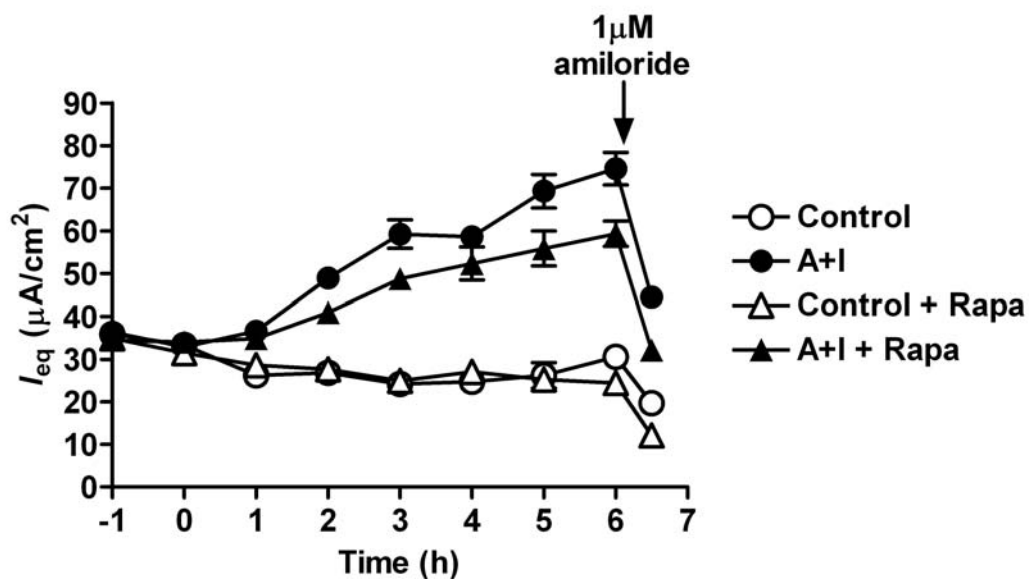


**Figure 4.8 Rapamycin lowers the transepithelial equivalent short circuit current response to aldosterone plus insulin.** mpkCCD<sub>c14</sub> cell monolayers were treated with 20 nM rapamycin (Rapa) or vehicle for 1 hour prior to treatment with aldosterone plus insulin (A+I) or vehicle (Control) at 0 hours. Hourly measurements of  $R_{te}$  and  $V_{te}$  were taken, which were then used to calculate  $I_{eq}$ . At 6 hours, cells were treated with 1  $\mu\text{M}$  amiloride to calculate amiloride-sensitive  $I_{eq}$ . Values are means  $\pm$  sem,  $n = 9$ .

A+I-stimulated amiloride-sensitive  $I_{eq}$  was significantly greater than control cells at 6 hours, both in the presence and absence of rapamycin (A+I + Rapamycin:  $32.4 \pm 0.8 \mu\text{A}/\text{cm}^2$ ; Control + Rapamycin:  $13.5 \pm 1.6 \mu\text{A}/\text{cm}^2$ ,  $P = <0.001$ ) (A+I:  $39.1 \pm 1.9 \mu\text{A}/\text{cm}^2$ ; Control:  $13.5 \pm 1.4 \mu\text{A}/\text{cm}^2$ ,  $P = <0.001$ ) (Figure 4.9). However, rapamycin caused a significant reduction in A+I-stimulated amiloride-sensitive  $I_{eq}$  compared to A+I treatment alone ( $P = <0.05$ ). This shows that the inhibition of  $I_{eq}$  by rapamycin was partially due to inhibition of amiloride-sensitive  $I_{eq}$  and suggests that A+I-stimulated, ENaC-mediated  $\text{Na}^+$  transport is partially dependent on mTORC1.

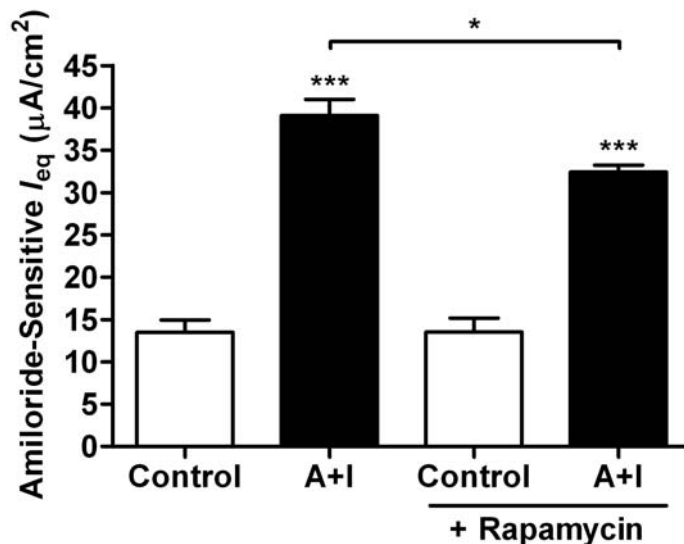


**Figure 4.9 Rapamycin significantly reduced aldosterone plus insulin-stimulated ENaC-mediated  $I_{eq}$  at 6 hours.** Amiloride-sensitive or ENaC-mediated  $I_{eq}$  displayed by the control and A+I-treated mpkCCD<sub>cl4</sub> cell monolayers in the experiment described in Figure 4.8. Values are means  $\pm$  sem,  $n = 9$ . \* and \*\*\* represent  $P = <0.05$  and  $<0.001$ , respectively.

#### **4.2.4 Effect of overexpressing individual mouse Sgk1 isoforms a-d on ENaC-mediated sodium transport**

To this point, the data in this study suggests all Sgk1 isoforms have the potential to regulate ENaC-mediated sodium transport. However, the functional specialisations of each isoform in regulation of ENaC required further investigation. In order to identify the effect of each isoform on ENaC-mediated Na<sup>+</sup> transport required mpkCCD<sub>c14</sub> cells that only express one Sgk1 isoform. In order to achieve this, each Sgk1 isoform was overexpressed in mpkCCD<sub>c14</sub> cells by transient transfection coupled with siRNA knockdown of endogenous Sgk1 isoforms. This section focuses on assessing the effect of overexpressing individual Sgk1 isoforms on sodium transport.

Two approaches were used in an attempt to transfect mpkCCD<sub>c14</sub> cells for use on permeable membrane supports. The first approach used Lipofectamine 2000 transfection reagent following the manufacturer's protocol for cells grown on a 24-well plate, but applied the transfection mix onto the upper (apical) side of cells seeded on permeable membrane supports. In an attempt to optimise this protocol, cells were seeded for 2 and 6 days prior to transfection. The  $I_{eq}$  was then calculated for mpkCCD<sub>c14</sub> cells that were transfected after 2 and 6 days of growth (Figure 4.10). Once cells had been seeded for the appropriate amount of time, resistance and potential difference of the monolayer was measured before transfection mix was applied (time point -6 h). The transfection mix was incubated on the cells for 6 hours, then monolayer measurements were taken again before the growth medium was replaced (time point 0 h). Measurements were then taken every 6 hours to assess the stability of the cell monolayer, with growth medium being replaced again after 2 days. Cells were transfected with either human FLAG tagged SGK1a (HsSGK1aFLAG), a kinase-dead mutant of the human SGK1a (HsSGK1akdFLAG), a

control vector (Vector), or with DNA absent (Untransfected). Human constructs were used because mouse constructs were unavailable at the time.

After 2 days of growth, mpkCCD<sub>cl4</sub> cell monolayers displayed negligible  $I_{eq}$ , which was unaltered by exposure of the cells to transfection solution for 6 hours ( $I_{eq} = \sim 2 \mu\text{A}/\text{cm}^2$  at -6 hours and  $\sim 3 \mu\text{A}/\text{cm}^2$  at 0 hours) (Figure 4.10A). This negligible  $I_{eq}$  showed that the cells had yet to form a polarised monolayer. At 0 hours, cells were given fresh growth medium and, subsequently,  $I_{eq}$  immediately increased by  $\sim 5 \mu\text{A}/\text{cm}^2$  from 0 to 6 hours. This increase continued, but gradually slowed, stabilising at  $\sim 10 \mu\text{A}/\text{cm}^2$  at  $\sim 24$  hours. The  $I_{eq}$  remained stabilised up to 42 hours, when cells were again given fresh growth medium. This caused another rapid increase in  $I_{eq}$ , reaching the peak  $I_{eq}$  of  $\sim 28 \mu\text{A}/\text{cm}^2$  at 54 hours, but, from that point,  $I_{eq}$  steadily decreased in a time-dependent manner to  $\sim 15 \mu\text{A}/\text{cm}^2$  at 90 hours, when cells were treated with  $1 \mu\text{M}$  amiloride. Treatment with amiloride revealed that all cells showed an ENaC-mediated  $I_{eq}$  of  $\sim 10 \mu\text{A}/\text{cm}^2$  at 90 hours, post-transfection.

In contrast to the cells transfected after 2 days, the initial  $I_{eq}$  of cells grown for 6 days, prior to transfection, was at a basal level of  $\sim 10 \mu\text{A}/\text{cm}^2$  (Figure 4.10B). This higher value was probably due to the additional time the cell monolayers were allowed to polarise and form stabilised resistance. As with the cells transfected after 2 days, transfection had a negligible effect on  $I_{eq}$ , which remained at  $\sim 10 \mu\text{A}/\text{cm}^2$  after 6 hours exposure of the cells to transfection solution. The cells were given fresh growth medium at 6 hours and, which stimulated a rapid increase in  $I_{eq}$  to between 30 and  $40 \mu\text{A}/\text{cm}^2$  at 18 hours. This time point showed the greatest variation in  $I_{eq}$  between cells of the different transfections suggesting an effect of transfection, but with no significant difference. The cells then regained very similar values causing the variation to disappear and the  $I_{eq}$  of all cells to rapidly decrease in a time-dependent manner. This decrease in  $I_{eq}$  continued until cells were given fresh growth medium at 42 hours. This caused another rapid increase in  $I_{eq}$  to a peak of  $\sim 50$

$\mu\text{A}/\text{cm}^2$  at 54 hours, the same time-point that 2-day cells peaked at. From this point,  $I_{\text{eq}}$  of all cells decreased in a time-dependent manner reaching between 0-10  $\mu\text{A}/\text{cm}^2$  at 90 hours. At 90 hours,  $I_{\text{eq}}$  was so low that amiloride treatment had little effect and revealed no significant differences.

Collectively, these data show that, whilst cells transfected in this way did demonstrate growth medium-stimulated  $I_{\text{eq}}$ , cells transfected with Sgk1 failed to show any significant deviation from control  $I_{\text{eq}}$ , suggesting that transfection was unsuccessful. To test whether cells were overexpressing any SGK1 protein, cells were lysed after the experiment prior to Western blotting to investigate SGK1 protein expression. The test Western blot showed no difference between overexpressed SGK1 and control lanes (Figure 4.10C), it was therefore unlikely that the transfection procedure was successful.

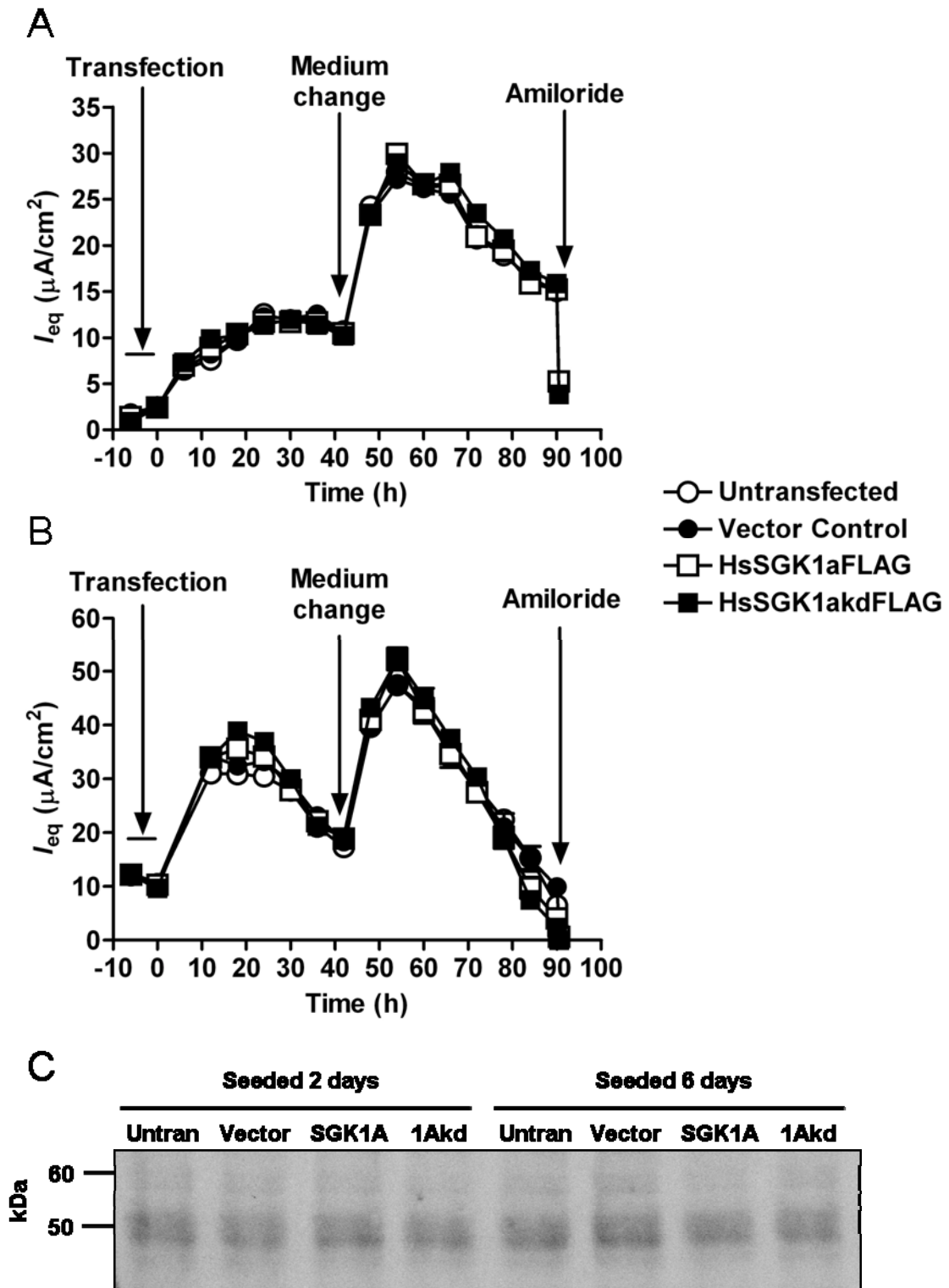


**Figure 4.10** Transepithelial equivalent short circuit current failed to stabilise after transfection of mpkCCD<sub>c14</sub> cell monolayers. A shows  $I_{eq}$  of unpolarised (seeded 2 days) mpkCCD<sub>c14</sub> cells transfected on permeable filter supports. B shows  $I_{eq}$  of polarised (seeded 6 days) mpkCCD<sub>c14</sub> cells transfected on permeable filter supports. Cells were given fresh growth medium at 0 and 42 hours. C shows a Western blot to detect Sgk1 protein expression in the cell lysates produced. Values are means  $\pm$  sem, n = 3.

The second transfection protocol was adapted from a method previously described by Hallows et al. (2009), which used Lipofectamine 2000 to transfect mpkCCD<sub>c14</sub> cells with siRNA for use on permeable membrane supports (Hallows et al., 2009). This method involved transfecting cells while seeded on plastic. These cells were then incubated for 24 hours to allow vector protein expression prior to cells being detached using trypsin, and re-seeded onto permeable filter supports. This allowed the transfected cells to attach to the permeable membrane and generate a cell monolayer for use in the  $I_{eq}$  assay. The method was adapted for use with plasmid DNA according to the Lipofectamine 2000 handbook. Once re-seeded, cell monolayer resistance was monitored and culture medium changed every 2 days until stable resistance of  $>3$  k $\Omega$  was achieved after  $\sim 6$  days. Once stable, monolayers were starved for 24 hours prior to hormone/vehicle treatment and hourly resistance and potential difference measurement. Monolayers did not show any significant differences in  $I_{eq}$  between vector and Sgk1 transfected cells before starvation.

A+I treatment failed to induce any significant amiloride-sensitive  $I_{eq}$  above that of vehicle control at 6 hours, suggesting that the cells had lost their responsiveness to aldosterone plus insulin (Figure 4.11A). Treatment with A+I should have stimulated a maximal increase in amiloride-sensitive  $I_{eq}$  of at least double that of vehicle control cells such as seen in Figure 4.5. To test whether the A+I treatment had stimulated Sgk1 protein expression, cells were lysed and analysed by Western blotting. A+I treatment had stimulated expression of Sgk1 isoforms as expected, but the Sgk1d ( $\sim 59$  kDa) band did not show any elevation in transfected cells compared to control cells (Figure 4.11B). This suggested that: either the transfection was unsuccessful, or that overexpression had subsided during the cell treatment process after transfection. This experiment was then repeated using Sgk1a instead of Sgk1d, to see if switching isoforms made any difference to the outcome (Figure 4.12).

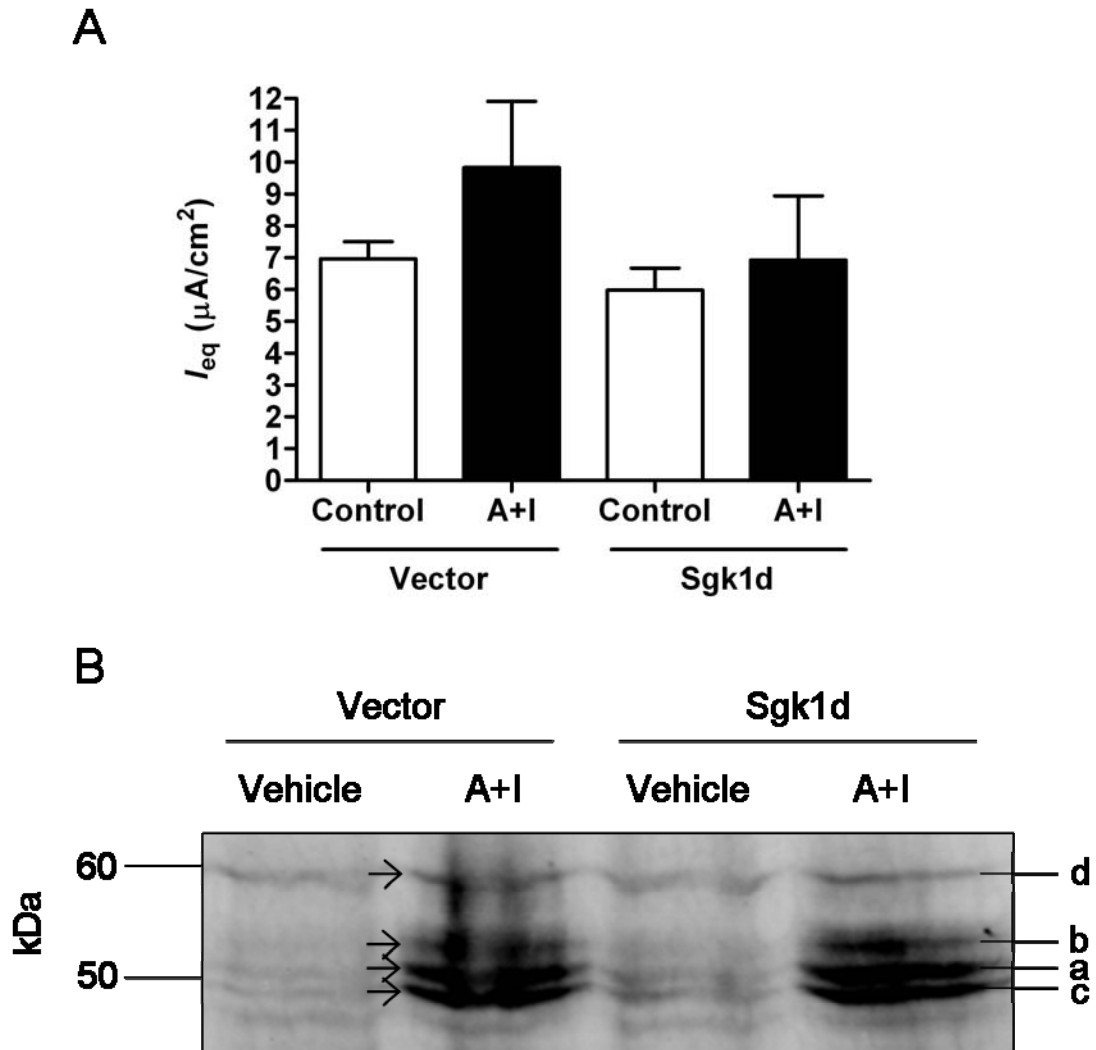


**Figure 4.11** Transiently transfected and then re-seeded mpkCCD<sub>cl4</sub> cell monolayers failed to show both aldosterone plus insulin-stimulated ENaC-mediated equivalent short circuit current and Sgk1d overexpression. mpkCCD<sub>cl4</sub> cells seeded on plastic were transiently transfected with Sgk1d or vector control using Lipofectamine 2000 transfection reagent. Cells were then re-seeded onto permeable filter supports and grown until transepithelial resistance stabilised at  $\geq 3$  k $\Omega$ . Polarised monolayers were incubated with starvation medium for 24 hours then given 10 nM aldosterone plus 1  $\mu\text{M}$  insulin. Hourly  $R_{te}$  and  $V_{te}$  measurements were taken to calculate  $I_{eq}$  until application of 1  $\mu\text{M}$  at 6 hours. A shows the amiloride-sensitive  $I_{eq}$  at 6 hours. After amiloride treatment cells were lysed and SGK1 expression analysed by Western blotting. B shows the SGK1 protein expression of the mpkCCD<sub>cl4</sub> cells monolayers following treatments. SGK1 isoform bands are indicated by arrows. Values are means  $\pm$  sem,  $n = 3$ .

Results derived were similar to those from the experiment using Sgk1d, with no significant stimulation of amiloride-sensitive  $I_{eq}$  by A+I treatment and no variation between vector control and Sgk1a transfected cells. For this experiment, however, cells failed to show any

induction of Sgk1 expression caused by either transfection or treatment with A+I (Figure 4.12B). This suggested that maybe it was the entire treatment process of transfection, trypsinisation, re-seeding and starvation that led cells to be non-responsive. This experiment was then repeated again, including cells for which no DNA was added to the transfection, to test whether the presence of foreign DNA was causing the lack of A+I stimulation (Figure 4.13).

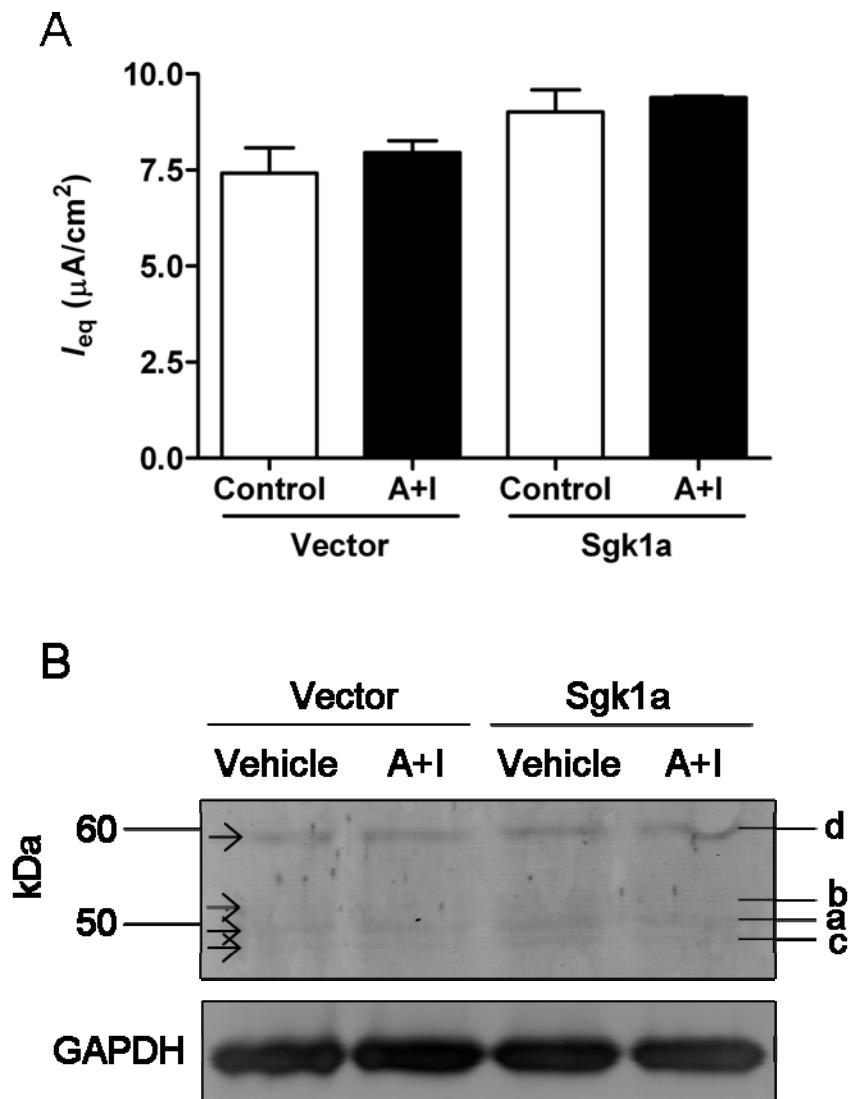


**Figure 4.12** Transiently transfected and then re-seeded mpkCCD<sub>cl4</sub> cell monolayers failed to show aldosterone plus insulin-stimulated ENaC-mediated equivalent short circuit current, Sgk1a overexpression, and induction of Sgk1 expression. Cells were treated identically as described in Figure 4.11, except using Sgk1a. A shows the ENaC-mediated  $I_{eq}$  at 6 hours. B shows the SGK1 expression in mpkCCD<sub>cl4</sub> cell monolayers following current measurement. Values are means  $\pm$  sem, n = 3.

For this experiment alone, transfection with Sgk1a enabled A+I treated cells to show an amiloride-sensitive  $I_{eq}$  that was significantly greater than the respective control (Sgk1a A+I:  $10.1 \pm 0.6 \mu\text{A}/\text{cm}^2$ ; Ctrl:  $7.8 \pm 0.3 \mu\text{A}/\text{cm}^2$ ,  $P = <0.05$ ) (Figure 4.13A). A+I-stimulated amiloride-sensitive  $I_{eq}$ , although significant, was still far below expectations based on previous results (Figure 4.1D). The small induction of amiloride-sensitive  $I_{eq}$  was

paralleled by little or no visible difference between treatments upon examination of Sgk1 expression by Western blotting (Figure 4.13B). This further suggests that cells subjected to this transfection protocol become unresponsive to A+I treatment, as evidenced by both the amiloride-sensitive  $I_{eq}$  and Sgk1 expression data.

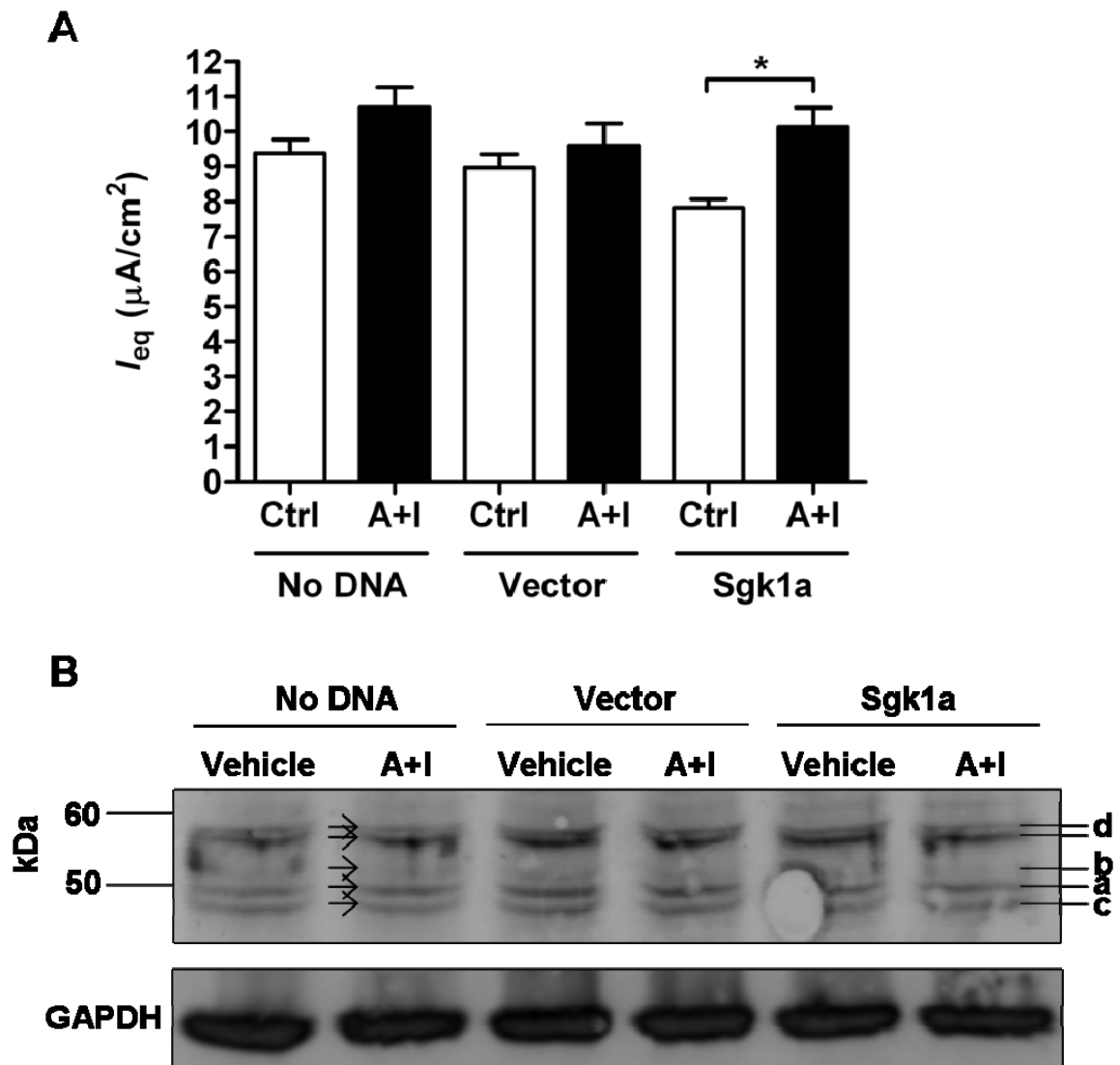


**Figure 4.13 Untransfected control cells also failed to show aldosterone plus insulin-stimulated ENaC-mediated equivalent short circuit current and induction of Sgk1 expression.** Cells were treated identically as described in Figure 4.12, except including a No DNA control. A shows the amiloride-sensitive  $I_{eq}$  at 6 hours. B shows the SGK1 expression in mpkCCD<sub>c14</sub> cell monolayers following current measurement. Values are means  $\pm$  sem, n = 3. \* represents  $P = <0.05$ .

#### **4.2.5 Effect of Sgk1 knockdown using siRNA on transepithelial amiloride-sensitive equivalent short circuit current**

A second approach to investigate the functional specialisations of each isoform in regulation of ENaC involved siRNA knockdown of endogenous Sgk1 isoforms. mpkCCD<sub>c14</sub> cells were transfected with siRNA targeted against Sgk1 to produce knockdown of endogenous Sgk1 expression in order to determine its role in A+I-stimulated amiloride-sensitive  $I_{eq}$ . For these experiments, the transfection protocol described by Hallows et al. (2009) was employed for transfection of mpkCCD<sub>c14</sub> cells with siRNA using Lipofectamine 2000 (Hallows et al., 2009). Commercially available pan-SGK1 specific and scrambled control siRNA were used. The amiloride-sensitive  $I_{eq}$  was calculated for cells that were transiently transfected with either Sgk1 siRNA or scrambled control siRNA and treated with vehicle or A+I (Figure 4.14). The first attempt at this experiment showed significantly reduced A+I-stimulated amiloride-sensitive  $I_{eq}$  in cells transfected with Sgk1 siRNA compared to cells transfected with scrambled siRNA (Figure 4.14A). However, this result was not repeatable in the second attempt (Figure 4.14B). An additional experiment was then conducted, where untransfected cells and no siRNA transfected cells were included as additional controls. The results of this experiment indicated that it was the re-seeding procedure that removed the ability of mpkCCD<sub>c14</sub> cell monolayers to show significant A+I-stimulated amiloride-sensitive  $I_{eq}$  (Figure 4.14C).

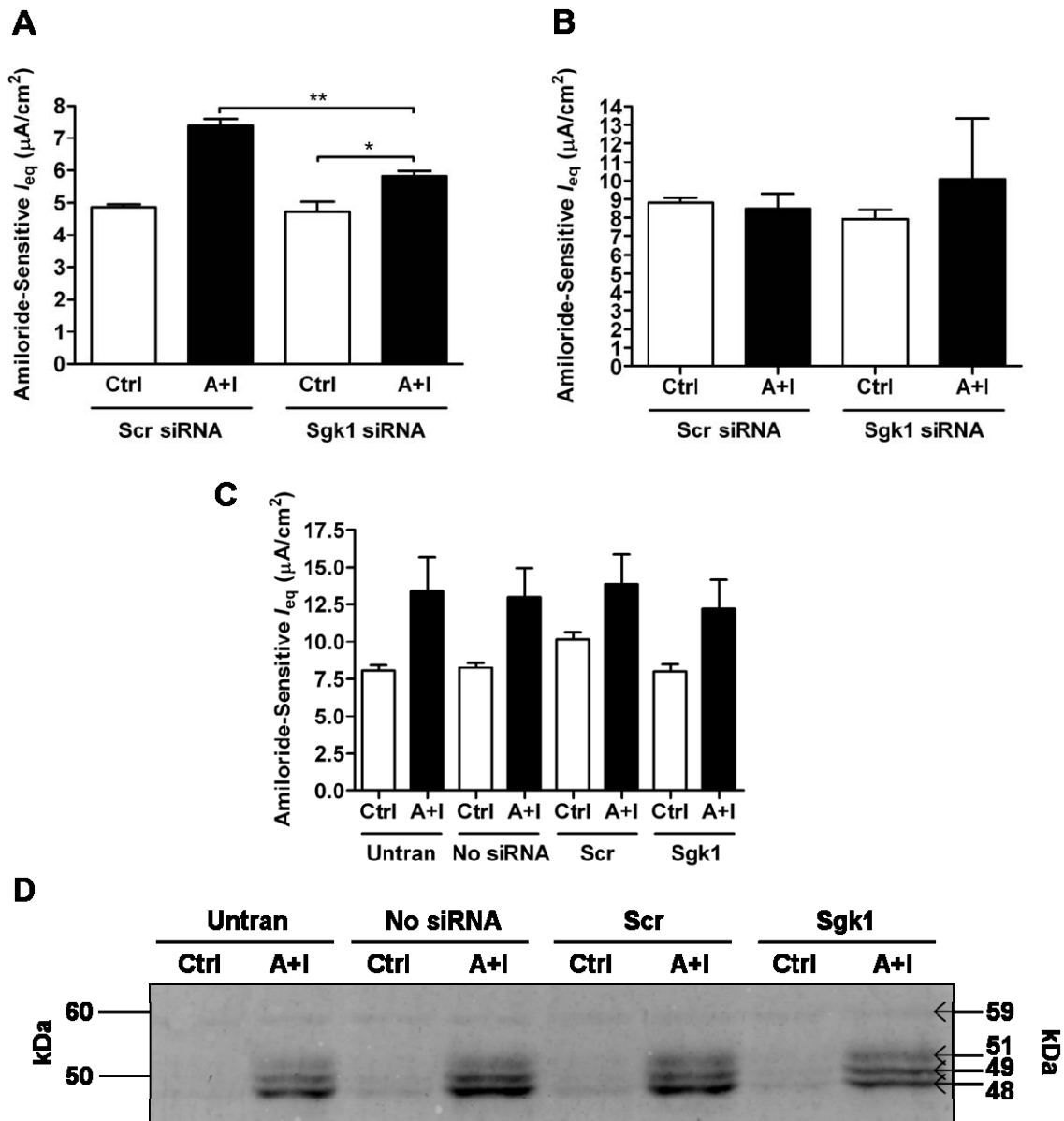


**Figure 4.14** mpkCCD<sub>cl4</sub> cells that were transiently transfected with SGK1 siRNA failed to show aldosterone plus insulin-stimulated ENaC-mediated equivalent short circuit current. Cells that were seeded on plastic were transfected with scrambled control siRNA (Scr), Sgk1 siRNA (Sgk1) or siRNA buffer only (No siRNA) plus control untransfected cells. Following 24 hours growth to allow plasmid expression, cells were re-seeded onto permeable filter supports and grown until monolayers displayed stabilised transepithelial resistance of >3 k $\Omega$ . Monolayers were incubated with starvation medium for 24 hours prior to treatment with 10 nM aldosterone plus 1  $\mu$ M insulin (A+I) or vehicle (Ctrl). After 6 hours of  $I_{eq}$  measurement, cells were given 1  $\mu$ M amiloride in order to calculate ENaC-mediated current. A and B show ENaC-mediated  $I_{eq}$  of two separate experiments, for each n = 3. C shows ENaC-mediated  $I_{eq}$  for experiments including all controls, n = 9. D shows a representative Western blot of cell lysates from cells lysates after the experiment described in C. Sgk1 expression is detected using anti-SGK1 antibody. Values are means  $\pm$  sem. \* and \*\* represent P = <0.05 and 0.01.

## 4.3 Discussion

### 4.3.1 Aldosterone and insulin stimulate amiloride-sensitive equivalent short circuit current

Whilst similar data showing stimulation of sodium current in renal cortical collecting duct cells by aldosterone, insulin and combined aldosterone plus insulin has been reported in several previous studies (de Seigneux et al., 2008; Wang et al., 2008; Michlig et al., 2004; Auberson et al., 2003; Summa et al., 2001; Bens et al., 1999), it was important to ensure that the cells used in this study retained their responsiveness to these agents. Results obtained support those described in Bens et al. (1999), which showed starved mpkCCD<sub>cl4</sub> cell monolayers exhibited aldosterone-stimulated  $I_{eq}$  in a dose- and time-dependent manner. Further results from the study by Bens et al. (1999) showed that 10 nM aldosterone significantly increased  $I_{eq}$  above control cells at 2 hours, which increased to the maximum  $I_{eq}$  (four-fold above control cells) at 6 hours, and was maintained up to 8 hours. Data derived from the present study furthered the study by Bens et al. (1999) by demonstrating the effect of insulin and aldosterone plus insulin treatments, such as seen in Wang et al. (2008), and extending the experiment duration to 48 hours. Data discussed in this chapter which show changes in ENaC-mediated  $I_{eq}$  at 2, 6, 24, and 48 hours exposure to aldosterone also expand on existing data. The  $I_{eq}$  response to insulin observed in this study was comparable to a rapid, but short-lived insulin-stimulated increase in  $I_{eq}$  described for A6 cells, which similarly peaked after 1 hour, but then subsided (Markadieu et al., 2004). A6 and mpkCCD<sub>cl4</sub> cells showed great similarity in  $I_{eq}$  insulin dose-response curves, linking the study of A6 cells to the present data (Nofziger et al., 2005). In A6-S2 cells (an A6 clone that is responsive to aldosterone), similar data showing aldosterone and aldosterone plus insulin stimulation of  $I_{eq}$  was further increased by transfection with wild-

type or a constitutively active mutant SGK1, but was not increased by transfection with a constitutively inactive mutant SGK1 (Alvarez de la Rosa and Canessa, 2003). Naray-Fejes-Toth et al (2004) showed that transfection of primary cultures of rabbit CCD cells with SGK1 antisense oligonucleotides removed a 3-3.5-fold increase in  $I_{eq}$  that was stimulated by 10 nM aldosterone after 24 hours starvation (Naray-Fejes-Toth et al., 2004a). Aldosterone also significantly increased SGK1 mRNA abundance in microselected connecting tubules/cortical collecting ducts compared to untreated tissue (Fakitsas et al., 2007). Collectively, these data suggest that the stimulation of ENaC-mediated  $I_{eq}$  in mouse cortical collecting duct cells by aldosterone and insulin is mediated by Sgk1.

In related Western blotting data, aldosterone induced Sgk1a, b, and c expression as soon as 1 hour and maximally induced all isoforms at 6 hours, which was maintained for 24 hours (Figure 3.7). Insulin failed to induce Sgk1 expression at 24 hours, whereas aldosterone and aldosterone plus insulin differentially induced Sgk1 isoforms (Figure 3.13). These Western blot data, considered with the data discussed above, suggest that aldosterone and aldosterone plus insulin may stimulate ENaC-mediated  $\text{Na}^+$  transport through increasing expression of Sgk1a, b, and c.

Throughout this chapter, data demonstrate a highly variable basal level of  $I_{eq}$  after 24 hours starvation, ranging between  $\sim 10\text{-}35 \mu\text{A}/\text{cm}^2$ , suggesting that, although cells were allowed to stabilise and form similar resistance before starvation, their transport properties varied between experiments. This variation was also evident, although to a lesser extent, with the basal level of amiloride-sensitive  $I_{eq}$ , which ranged between  $\sim 4\text{-}14 \mu\text{A}/\text{cm}^2$ . Western blotting results in chapter 3 showed that only mouse Sgk1d expression was detectable in serum and hormone-starved mpkCCD<sub>cl4</sub> cells, suggesting that this isoform may be responsible for the basal  $I_{eq}$  (Figures 3.6, 3.7, and 3.13). Although data in the present study showed consistent amiloride-insensitive  $I_{eq}$  of  $\sim 30\%$ , the study by Bens et al. (1999)

showed that increasing amiloride concentration to 10  $\mu\text{M}$  reduced amiloride-insensitive  $I_{\text{eq}}$  to  $\sim 10\%$ . This suggests that 1  $\mu\text{M}$  amiloride may be unsuitable to completely block ENaC, but may also indicate a role of other 10  $\mu\text{M}$  amiloride-sensitive channels in aldosterone-stimulated  $I_{\text{eq}}$ . The remaining  $\sim 10\%$  of  $I_{\text{eq}}$  that is 10  $\mu\text{M}$  amiloride-insensitive was probably due to non-ENaC-mediated  $\text{Na}^+$  transport or transport of other ions such as  $\text{Cl}^-$  (Van Huyen et al., 2001).

These findings could have significant implications for other investigations involving SGK1, particularly where studies do not take into consideration the existence of more than one SGK1 isoform. This could also have implications for the use of clinical SGK1 inhibitors, particularly for aldosterone-sensitive therapies, as inhibitors may not be effective against all SGK1 isoforms (Lang and Gorch, 2010). Furthermore, different aldosterone-sensitive SGK1 isoforms may also be linked or associated with the development of hypertension or other conditions through their mutation or dysregulation.

#### **4.3.2 Sensitivity of aldosterone and insulin-stimulated ENaC-mediated sodium transport to inhibition of activators of SGK1**

Exposing cells to LY294002 and rapamycin reduced the response to aldosterone plus insulin in mpkCCD<sub>cl4</sub> cells. Both of these agents also caused aldosterone plus insulin-stimulated ENaC-mediated  $\text{Na}^+$  transport to be significantly lower after 6 hours (sections 4.2.2 and 4.2.3). LY294002 had similar effects on the  $I_{\text{eq}}$  and ENaC-mediated  $I_{\text{eq}}$  responses to aldosterone alone and also abolished the short-term response to insulin. This pattern of inhibition suggests stimulation of  $I_{\text{eq}}$  by aldosterone, insulin, or aldosterone plus insulin is partially mediated by the PI3K/mTOR pathway and mTORC1. This supports the generally accepted hypothesis that aldosterone and insulin stimulate ENaC-mediated  $\text{Na}^+$

transport via PI3K and SGK1 (Lee et al., 2008). In support of the data in section 4.2.2, previous publications have also shown that LY294002 inhibits aldosterone and insulin-stimulated  $I_{eq}$  in A6 (Wang et al., 2001; Record et al., 1996) and mpkCCD<sub>c14</sub> cells (Wang et al., 2008; Flores et al., 2005). These studies, however, did not include identification of individually upregulated and inhibited SGK1 isoforms. LY294002 has been shown to inhibit both PI3K and mTOR kinase activities at similar concentrations (Brunn et al., 1996), suggesting that the effect seen is perhaps due to inhibition of mTOR rather than PI3K. However, use of PIK-90, an inhibitor of the p110- $\alpha$  subunit of PI3K that does not inhibit mTOR had an identical effect to LY294002 on aldosterone, insulin and aldosterone plus insulin stimulated  $I_{eq}$  (Wang et al., 2008), therefore demonstrating that PI3K is a key mediator of aldosterone and aldosterone plus insulin stimulation of  $I_{eq}$ . This may be redundant, as mTOR is part of the PI3K pathway (Liu et al., 2009).

Phosphorylation and activation of SGK1 has been shown to be elicited by 3-phosphoinositide-dependent protein kinase-1 (PDK1) at the T-loop (threonine 256) and by mTOR at the hydrophobic motif (serine 422) (Garcia-Martinez and Alessi, 2008b; Mora et al., 2004). mTOR is present in cells in two different active complexes; mTORC1 and mTORC2, which have both been implicated in activation of SGK1 (Garcia-Martinez and Alessi, 2008b; Hong et al., 2008). It has recently been shown that mTORC2, rather than mTORC1, phosphorylates serine 422 of SGK1 (Dowling et al., 2010; Alessi et al., 2009; Garcia-Martinez et al., 2009; Yan et al., 2008), however, data in the present study suggests that regulation of ENaC-mediated sodium transport is still partially dependent on the rapamycin-sensitive mTORC1. However, the actions of mTORC1 cannot be completely ruled out in the presence of rapamycin as some of its functions have been shown to be rapamycin-insensitive (Foster and Fingar, 2010). In conflict with the present data, Lu et al. (2010) showed 0.1  $\mu$ M rapamycin had no effect on 1  $\mu$ M aldosterone plus 100 nM insulin-

stimulated  $I_{eq}$  in mpkCCD<sub>c14</sub> cells (Lu et al., 2010). This is probably due to the much higher concentration of aldosterone used in Lu et al. (2010) compared to the 10 nM aldosterone used in this study. Aldosterone binds to the mineralocorticoid receptor (MR) with a  $K_d$  of 0.6 nM and the glucocorticoid receptor (GR) with a  $K_d$  of 85 nM (Gaeggeler et al., 2005), therefore, treatment with 1  $\mu$ M aldosterone would cause stimulation of  $I_{eq}$  through a GR-independent pathway.

Related Western blot data in section 3.2.10 showed that LY294002 partially inhibits aldosterone and aldosterone plus insulin-stimulated Sgk1a, b, and c expression. These findings support the hypothesis that PI3K/mTOR-dependent expression of Sgk1a, b, and c may be involved in mediating aldosterone and aldosterone plus insulin-stimulated ENaC-mediated Na<sup>+</sup> transport, however, this is not explained by the current pathway hypothesis. These findings extend upon the current knowledge of Sgk1 isoforms and their regulation by the PI3K and mTOR pathway. Increased knowledge about the effects and dependencies of the individual isoforms may therefore lead to the identification of novel therapeutic targets for treatment of hypertension or other SGK1 linked conditions.

### **4.3.3 Overexpression and knockdown of Sgk1 in mpkCCD<sub>c14</sub> cells grown on permeable filter supports**

Two different protocols were used in the present study in an attempt to achieve overexpression of Sgk1 isoforms in mpkCCD<sub>c14</sub> cells grown on permeable filter supports. The first protocol was adapted for cells grown on permeable filter supports from the protocol used when transfecting cells grown on plastic. This protocol was tested on cells grown for 2 days and 6 days, but, in both cases, failed to modulate aldosterone plus insulin-stimulated  $I_{eq}$  or produce Sgk1 isoform overexpression. The second protocol,

previously described by Hallows et al. (2009) to show successful transfection of mpkCCD<sub>c14</sub> cells grown on permeable filter supports, also failed to produce cells that showed modulated aldosterone plus insulin-stimulated  $I_{eq}$  or Sgk1 overexpression. Furthermore, the protocol of Hallows et al. (2009) also failed to produce reduced aldosterone plus insulin-stimulated  $I_{eq}$  or knockdown of endogenous Sgk1 when used with pan-Sgk1 siRNA. This repeated failure to show Sgk1 overexpression, or effect of siRNA by transient transfection, suggests that either the protocol was unsuitable, that the plasmid or siRNA expression had subsided by the time of detection, or that the methods of detection were unsuitable. Data derived by the present study and by Hallows et al. (2009) suggest that the protocols were suitable for transient transfection. The methods of detection were also suitable, as both effects on  $I_{eq}$  and Sgk1 expression were tested for. Alternatively, since it was necessary to grow the cells on the permeable filter supports for several days after transfection in order to allow a polarised monolayer to form, transient overexpression could have subsided within this time period.

Several studies have nevertheless shown the effects of overexpressing certain human or mouse SGK1 isoforms on ENaC-mediated sodium transport. Arteaga et al. (2007) showed that inducing overexpression of wild-type 49 kDa or constitutively active mutants of 49 or 42 kDa isoforms of Sgk1 in A6 cells caused increased amiloride-sensitive  $I_{eq}$ , suggesting that only the full-length, 49 kDa isoform of Sgk1a is able to induce ENaC activity *in vivo* (Arteaga et al., 2007). Studies using *Xenopus* oocytes showed that coexpression of ENaC with human SGK1A increased sodium uptake, but coexpression of ENaC with human SGK1D did not (Arteaga et al., 2008; Chen et al., 1999). Arteaga et al (2008) showed that mouse Sgk1d had a much longer half life in mouse brain tissue than mouse Sgk1a, consistent with data from the present study showing the presence of mouse Sgk1d in mpkCCD<sub>c14</sub> cells at a consistently higher basal level than the other mouse Sgk1 isoforms

(Figures 3.6, 3.7, and 3.13) (Arteaga et al., 2008). Raikwar et al. (2008) showed enhanced stability and reduced susceptibility of human SGK1D to ubiquitination compared to human SGK1A, and increased expression of  $\alpha$ ENaC in cells transfected with either isoform.

Under salt wasting, Sgk1-knockout mice showed impaired ability to retain renal sodium (Wulff et al., 2002). Furthermore, Sgk1-knockout mice also showed resistance to high-fat diet-induced hypertension due to an inability to retain salt (Huang et al., 2006). Huang et al. (2004) showed that an sgk1-knockout mouse had limited ability to eliminate renal  $K^+$  and had significantly impaired amiloride-sensitive transepithelial potential difference across isolated collecting ducts, suggesting that the removal of Sgk1 limits the ability of ENaC to transport  $Na^+$  (Huang et al., 2004). The knockout of Sgk1 can therefore have significant effects on ENaC-mediated sodium transport, highlighting a need to show which Sgk1 isoform(s) cause(s) this effect.

The different isoforms may well perform different roles in the regulation of ENaC-mediated sodium transport, but further work is needed in order to show the effects of individual SGK1 isoforms on  $Na^+$  transport. Stable or specific expression of single SGK1 isoforms in cells at physiological levels would create a more *in vivo*-like model for study, but would require production of stably transfected cells. Only a few studies have shown overexpression of individual SGK1 isoforms and to date none have shown their individual knockdown or knockout. Future work to achieve this would allow comparison between human and mouse SGK1s and identification of their individual roles in regulation of sodium transport. This could show the predisposition or involvement of one or more of the expressed isoforms in many diseases and conditions, including hypertension.

## 4.4 Summary

- Insulin treatment of mpkCCD<sub>cl4</sub> cell monolayers stimulates a significant ~1.5-fold increase in  $I_{eq}$  above control  $I_{eq}$  by 1 hour that lasts until 2 hours.
- Aldosterone treatment of mpkCCD<sub>cl4</sub> cell monolayers stimulates a time-dependent increase in  $I_{eq}$  from 2 hours that continues to ~2.5-fold above control  $I_{eq}$  at 6 hours.
- Aldosterone plus insulin treatment of mpkCCD<sub>cl4</sub> cell monolayers stimulates a time-dependent increase in  $I_{eq}$  from 1 hour that continues to ~3-fold above control  $I_{eq}$  at 6 hours.
- Insulin stimulated ENaC-mediated Na<sup>+</sup> transport ~1.5-fold at 2 hours, but not after 6 hours.
- Aldosterone stimulated ENaC-mediated Na<sup>+</sup> transport ~2-fold at 2 hours and ~2.5-fold at 6 hours.
- Aldosterone plus insulin stimulated ENaC-mediated Na<sup>+</sup> transport ~2.5-fold at 2 hours and ~3-fold at 6 hours.
- Aldosterone plus insulin stimulated ENaC-mediated Na<sup>+</sup> transport remained significantly above control for 24 hours.
- LY294002 partially inhibits aldosterone plus insulin stimulated  $I_{eq}$  and ENaC-mediated Na<sup>+</sup> transport.
- Rapamycin partially inhibits aldosterone plus insulin stimulated  $I_{eq}$  and ENaC-mediated Na<sup>+</sup> transport.

## **Chapter 5 - Localisation and Co-Immunoprecipitation Studies**

### **as Clues to Regulation of SGK1**

#### **5.1 Introduction**

This thesis and past publications by others have shown that SGK1 is present in multiple isoforms in both human and mouse and that these isoforms vary in their N-termini (Figure 3.1) (Arteaga et al., 2008; Raikwar et al., 2008; Arteaga et al., 2007; Hall, 2007; Simon et al., 2007). These studies also showed that the differing N-termini confer targeted intracellular localisation and/or functional specificity to SGK1 isoforms. For example, Raikwar et al. (2008) showed that FLAG-tagged SGK1A was expressed diffusely in the cytosol of HEK293 cells grown on plastic, whereas FLAG-tagged SGK1D localised to the plasma membrane. Raikwar et al. (2008) also showed that SGK1D stimulated greater ENaC activity than SGK1A in Fisher rat thyroid (FRT) epithelial cells, when cotransfected with the SGK1 isoforms and  $\alpha\beta\gamma$ -ENaC, suggesting that SGK1 needed to be targeted to the plasma membrane in order to alter ENaC activity (Raikwar et al., 2008). The mouse Sgk1 isoforms described in this thesis each have different N-termini that are unique in size and sequence (section 3.2.3), whereas the majority of their amino acid sequences are identical (77% of the largest isoform Sgk1d and 97% of the smallest isoform Sgk1c).

The aim of this chapter was, therefore, to investigate differences in intracellular localisation between SGK1 isoforms, which may be due to their different N-termini and may impart differential regulation of ENaC. To this aim, the subcellular localisation of endogenous SGK1 isoforms in native mouse and human renal collecting duct tissue was investigated by immunofluorescence microscopy using isoform-specific antibodies and fluorescent secondary antibodies. Due to the limited success observed when using the

isoform-specific antibodies to detect SGK1 isoforms by Western blotting (section 3.2.11), the intracellular localisation of overexpressed FLAG-tagged SGK1 isoforms in transiently transfected HEK293T cells was also observed.

In order to further characterise differences in function between SGK1 isoforms, a co-immunoprecipitation assay was adapted from a study by Soundararajan et al. (2009) to determine the recruitment of SGK1 isoforms to glucocorticoid-induced leucine zipper protein 1 (GILZ1). Phosphorylated SGK1 was shown to be recruited to a complex of ENaC-Raf1-Nedd4-2 by GILZ1, which produced a cooperative reduction in the inhibition of ENaC by MAPK/ERK and Nedd4-2 (Soundararajan et al., 2009).

## **5.2 Results**

### **5.2.1 Fluorescence microscopy of SGK1D in human renal tissue**

In chapter 3, results demonstrated that only isoform-specific antibodies for SGK1B and SGK1D were able to detect mouse protein by Western blotting (section 3.2.11). However, in immunofluorescence studies using native human and mouse renal tissue, only the SGK1D-specific antibody gave positive immunostaining. This result may be because Sgk1d is more easily detected, due to being expressed at a higher basal level than Sgk1b in serum and hormone-starved cells, as shown by Western blotting in Figures 3.6, 3.7, and 3.13.

In order to visualise SGK1D localisation in human collecting duct epithelia, healthy human kidney tissue sections were co-immunostained using anti-SGK1D 3253 and anti-aquaporin-2 (AQP2) antibodies. AQP2 was used as a marker of renal principal cells in order to distinguish collecting ducts from other kidney tubules (Leng et al., 2006). Appropriate fluorophore-coupled secondary antibodies were used to examine the

immunostaining of SGK1D using Alexa Fluor 488 immunofluorescence and AQP2 by Alexa Fluor 568 immunofluorescence. Nuclei were stained using Hoechst 33258 (blue), SGK1D staining was coloured green, and AQP2 coloured red, indicating that SGK1D staining is sub-apical and/or perinuclear and appears in a punctate pattern as intracellular accumulations in collecting duct epithelia (Figure 5.1).

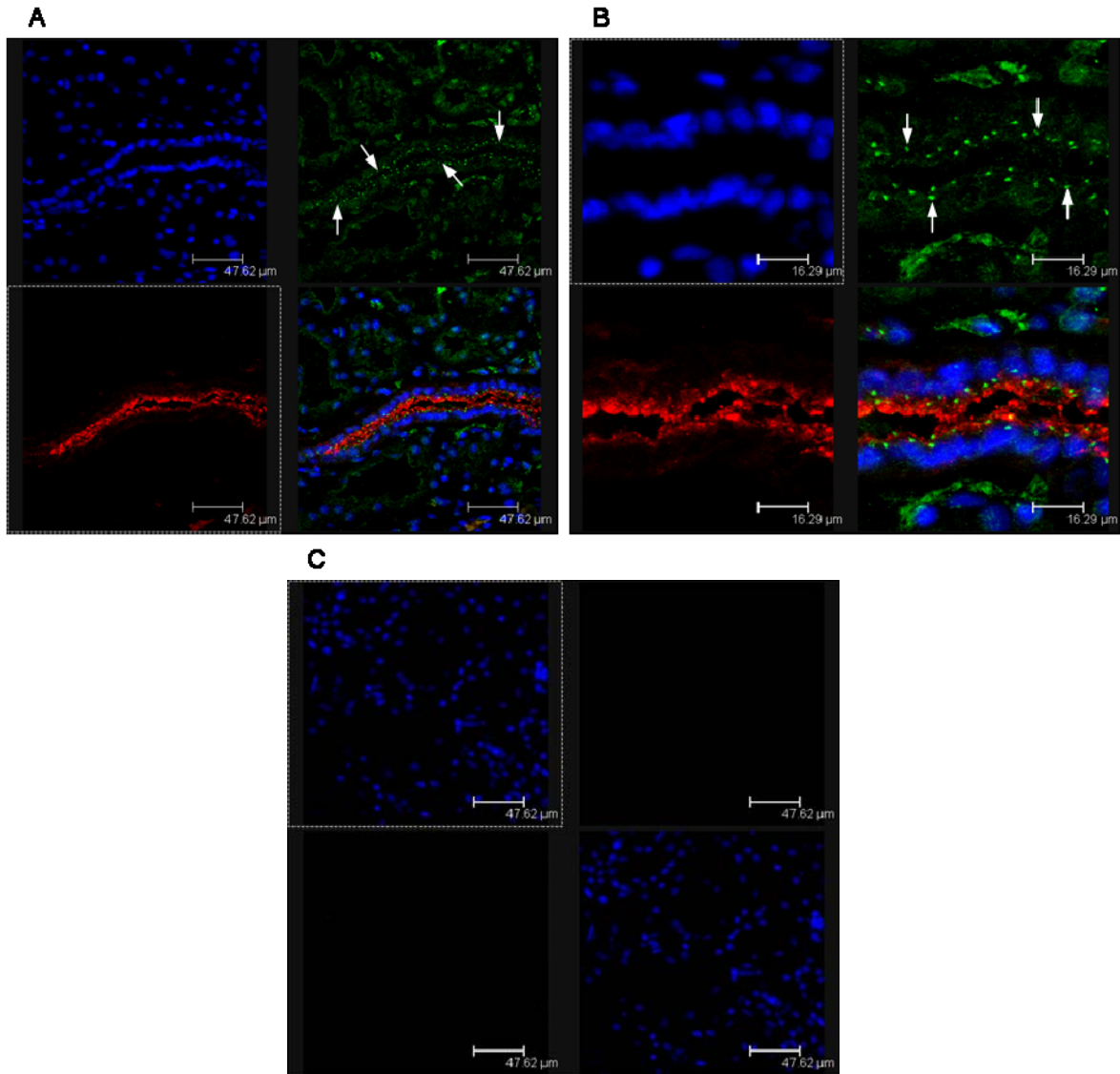


**Figure 5.1 Immunofluorescence of SGK1D sub-apical intracellular accumulations in human renal collecting duct epithelia.** Confocal microscopy images showing Hoechst 33258 staining of DNA (nuclei) in blue, anti-SGK1D 3253 staining in green, and anti-aquaporin-2 (AQP2) staining in red. A shows low power magnification images of the three coloured channels, plus a merged image, of a collecting duct, identified by AQP2 apical membrane staining, with SGK1D intracellular accumulations indicated on the green channel image by white arrows. B shows higher power magnification images, of the same human collecting duct in A, again with SGK1D intracellular accumulations, all in the sub-apical region of the collecting duct epithelium, indicated on the green channel image by white arrows. C shows images of a no primary antibodies control section. All human tissue sections are from the same source kidney.

In a repeat experiment, with SGK1D shown in green and AQP2 in red, SGK1D localised in similar intracellular accumulations within the collecting duct epithelia, but also appears at the cell-cell junctions (Figure 5.2). To investigate what the intracellular punctate pattern of staining may represent, human tissue was co-stained for SGK1D plus markers for mitochondria, basal bodies, microtubules and endoplasmic reticulum, individually. Despite the use of the different intracellular markers, the quality of tissue staining obtained did not allow any definitive conclusions to be made about the identity of the SGK1D intracellular accumulations. Confirmation of the cell-cell junction localisation was also attempted through staining for ZO-1, a marker of tight-junctions. However, due to degradation of the human kidney tissue used for this staining, the result was inconclusive. In order to make conclusions about exactly where SGK1D localised to in the human collecting duct epithelia requires positive identification of the structures shown by the intracellular accumulations and cell-cell junction staining.

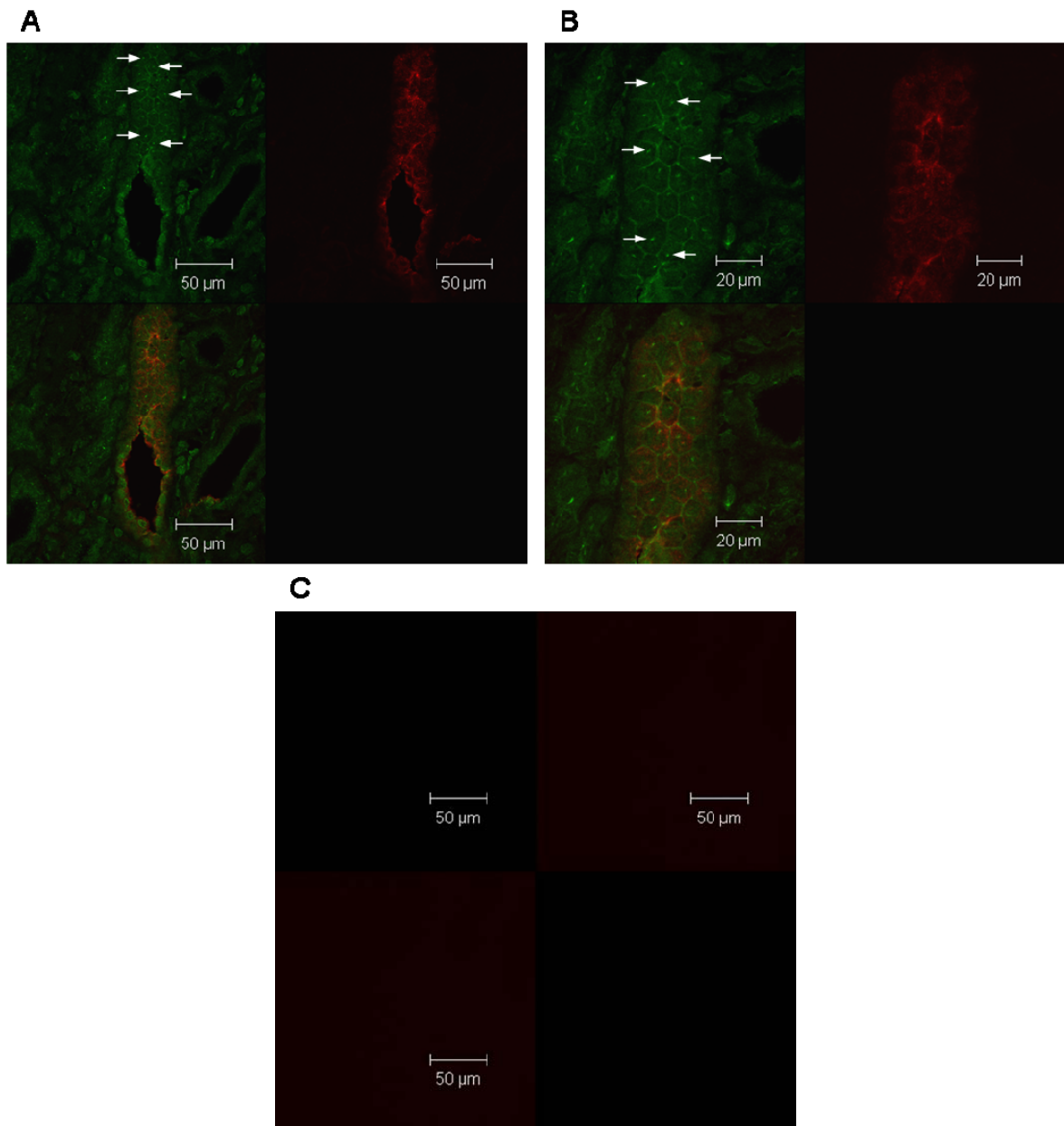


**Figure 5.2 Immunofluorescence of SGK1D sub-apical intracellular accumulations and cell-cell junction localisation in human renal collecting duct epithelia.**

Microscopy images showing anti-SGK1D 3253 staining in green, and anti-aquaporin-2 (AQP2) staining in red. A shows low power magnification images of the two coloured channels, plus a merged image, of a collecting duct, identified by AQP2 apical membrane staining, with SGK1D intracellular accumulations indicated on the green channel image by white arrows and cell-cell junction staining at the boundaries between the cells. B shows the same view in higher power magnification images with the same intracellular accumulations near the stained cell boundaries indicated as in A. C shows images of a no primary antibodies control section.

### **5.2.2 Fluorescence microscopy of Sgk1d in mouse renal tissue**

The mouse and human SGK1D amino acid sequences share 93% identity, a level of similarity that suggests the intracellular localisation of SGK1D in collecting duct epithelia might be conserved between species. To test this hypothesis, immunostaining of Sgk1d in mouse kidney tissue was performed in parallel with the staining of SGK1D in human tissue. Mouse kidney cortex tissue dissected from healthy adult mice was prepared and sectioned identically to the human kidney tissue. Sgk1d in the mouse kidney tissue was detected using the same anti-SGK1D 3253 antibody (Cambridge Biosciences) used with the human tissue, which was shown to detect mouse Sgk1d previously, by Western blotting (Figure 3.14). Surprisingly, Sgk1d was found to be localised to the basolateral membrane of collecting ducts and was also expressed in AQP2-negative tubules (Figure 5.3). This means that mouse Sgk1d in mouse collecting duct tissue shows a completely different localisation compared to human SGK1D in human collecting duct tissue.

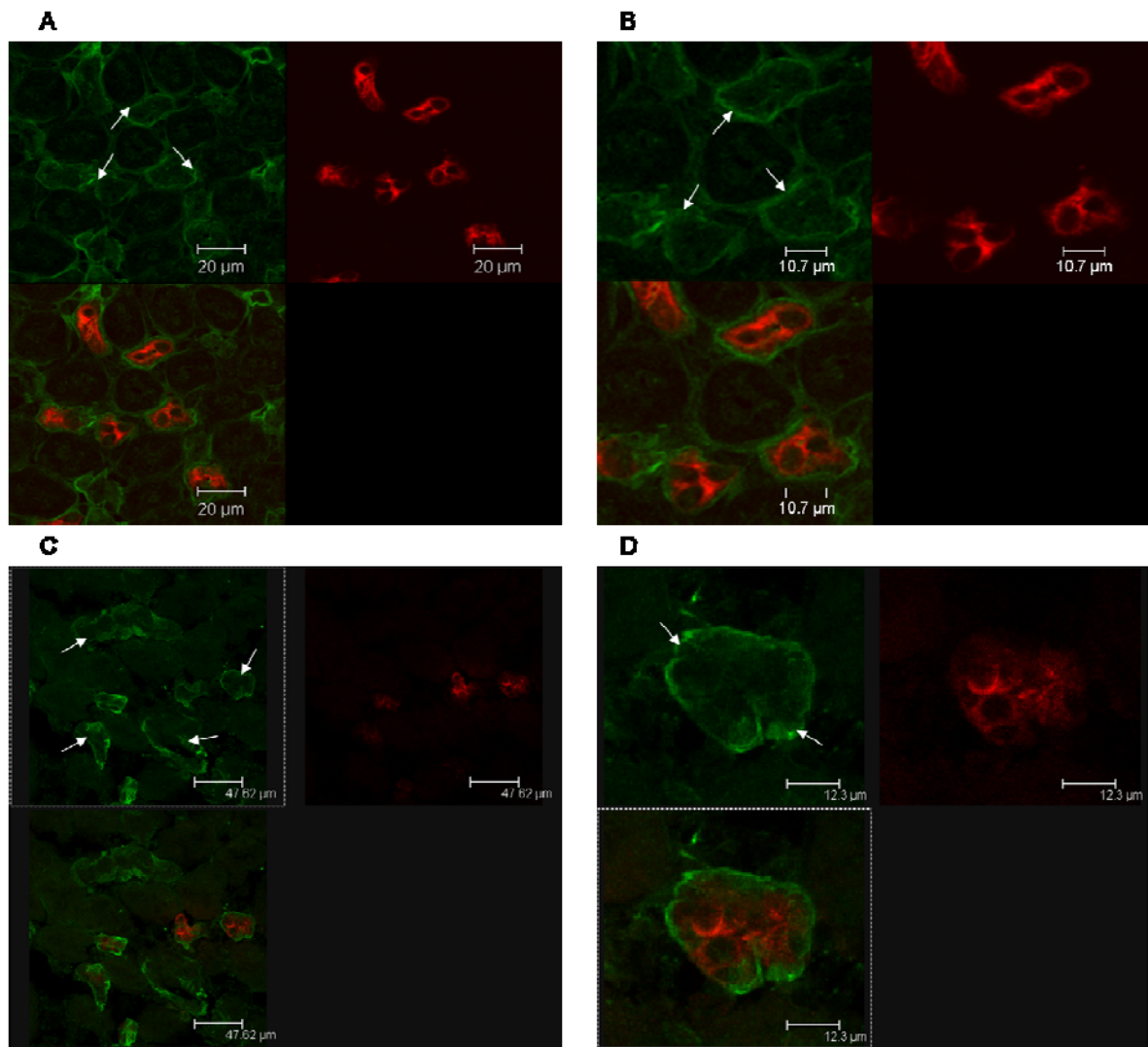


**Figure 5.3 Immunofluorescence of Sgk1d basolateral membrane localisation in mouse renal tubule epithelia.** Microscopy images showing anti-SGK1D 3253 staining in green, and anti-aquaporin-2 (AQP2) staining in red. A and C show low power magnification images of multiple collecting ducts in the two coloured channels, plus a merged image. Sgk1d was found to localise to the basolateral membrane of many tubules, indicated on the green channel image by white arrows. B and D show the same views as A and C, but in higher power magnification, showing that collecting ducts and other tubules display basolateral Sgk1d staining indicated by white arrows.

### **5.2.3 Fluorescence microscopy of immunostained FLAG-tagged human SGK1 isoforms in HEK293T cells**

The limitation of only being able to observe SGK1D specific staining in tissue, meant that the localisation of human SGK1 isoforms A, B, C and F and mouse Sgk1 isoforms a, b and c would have to be examined by other means. HEK293T cells were transiently transfected with human FLAG-tagged SGK1 isoforms, which were then visualised by immunofluorescence following their detection using anti-FLAG antibodies. To try and identify the specific localisation of the different SGK1 isoforms, various cellular compartment markers were employed, some of which were shown previously to colocalise with SGK1. One such study by Cordas et al. (2007) showed that human SGK1A, tagged with autofluorescent fusion protein, colocalised with mitochondria in transfected rabbit cortical collecting tubule cell line (RCCT-28A) cells (Cordas et al., 2007). Also, previous work by Hall (2007), showed colocalisation of human SGK1A, B, and D with mitochondria in human keratinocytes (Hall, 2007). These studies were therefore extended in the present study to include mouse Sgk1 isoforms using HEK293T cells.

HEK293T cells were co-transfected with human FLAG-tagged SGK1 isoforms and pDsRed-mito (BD Biosciences), which expresses a red fluorescent protein (RFP)-tagged target sequence of subunit 8 of human cytochrome c oxidase (COX), and is a marker of mitochondria. Intracellular expression of FLAG-tagged SGK1 isoforms was detected, in relation to red fluorescent mitochondria, by confocal microscopy following staining using anti-FLAG and fluorescent secondary antibodies. To compare images, FLAG staining was coloured green whilst mitochondrial fluorescence was coloured red, and nuclei, labelled using Hoechst 33258, were coloured blue (Figure 5.4). Results showed that none of the SGK1 isoforms appeared to distinctly colocalise with mitochondria, instead, the

yellow/orange colouring seen in the merged images, where green and red combine, seems to be due to incidental overlapping of the cytosolic network-like SGK1 isoform staining with the mitochondria. The images in Figure 5.4 show that human SGK1A and B were localised to an unidentified cytosolic network-like structure (Figure 5.4A and B), whilst SGK1C and D were localised diffusely in the cytoplasm (Figure 5.4C and D), and SGK1F showed predominantly nuclear localisation, but with some weak cytosolic network-like staining (Figure 5.4E).

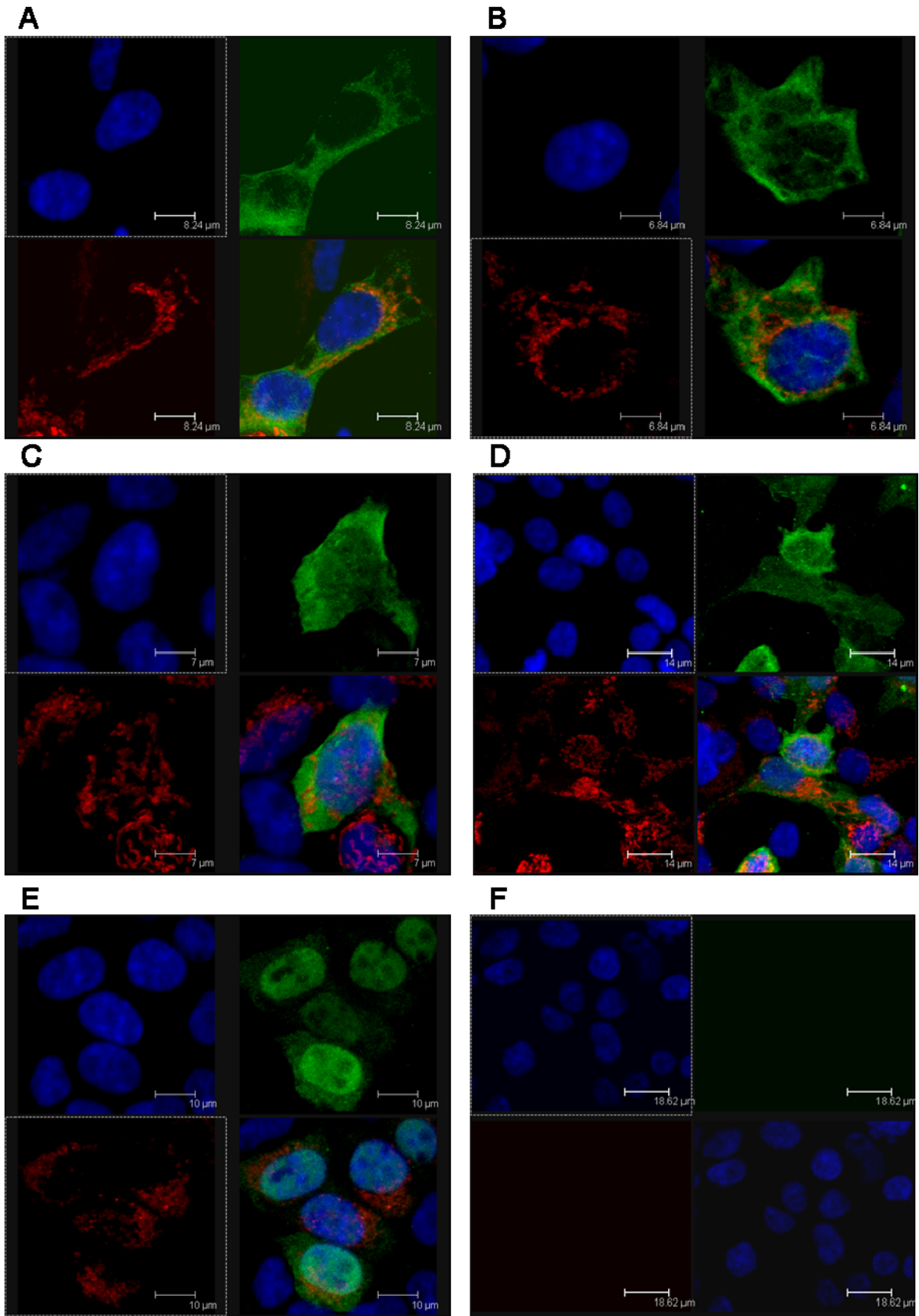


**Figure 5.4 Intracellular localisation of FLAG-tagged human SGK1 isoforms A, B, C, D and F compared with red fluorescent protein (RFP)-labelled mitochondria in HEK293T cells.** A-F each show an image of nuclei staining in blue, FLAG-tagged SGK1 isoform staining in green, and RFP-mitochondria fluorescence in red, plus a merged image of the three colours. A shows cells cotransfected with FLAG-tagged SGK1A and RFP-mitochondria. B shows cells cotransfected with FLAG-tagged SGK1B and RFP-mitochondria. C shows cells cotransfected with FLAG-tagged SGK1C and RFP-mitochondria. D shows cells cotransfected with FLAG-tagged SGK1D and RFP-mitochondria. E shows cells cotransfected with FLAG-tagged SGK1F and RFP-mitochondria. F shows the equivalent images for untransfected control cells.

HEK293T cells grown on glass coverslips were transiently transfected with FLAG-tagged SGK1 isoforms then fixed for immunostaining. Intracellular expression of FLAG-tagged SGK1 isoforms was detected by immunofluorescence microscopy following staining using anti-FLAG and fluorescent secondary antibodies. Cells were co-stained for actin cytoskeleton using Alexa Fluor 633 Phalloidin and nuclei using Hoechst 33258. Anti-FLAG staining is coloured green, whilst cytoskeleton staining is coloured red and nuclei staining coloured blue (Figure 5.5). SGK1C is not shown for this experiment because the FLAG-tagged SGK1C-transfected cells repeatedly failed to show immunostaining. These images showed that none of the SGK1 isoforms A, B, D or F colocalised with actin cytoskeleton, as there was little, or no, overlapping green and red staining (yellow) in any of the merged images. However, this experiment did show that the different SGK1 isoforms localise to specific regions of the cell, with SGK1A, B and D showing cytosolic network-like staining (Figure 5.5A-C), but also some plasma membrane staining for SGK1D (Figure 5.5C), and SGK1F showing predominantly nuclear with some weak cytosolic network-like staining (Figure 5.5D).

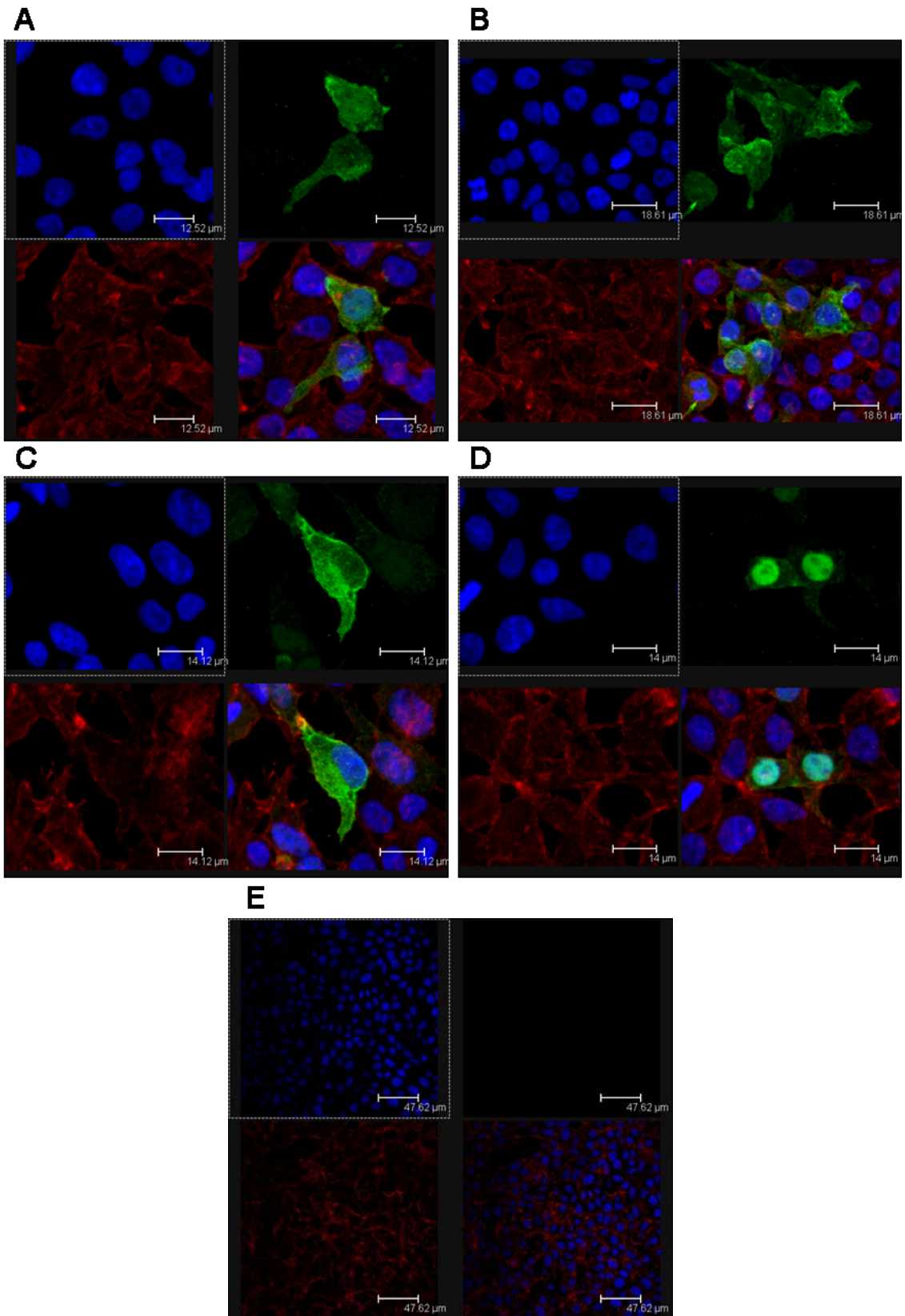


**Figure 5.5 Subcellular localisation of FLAG-tagged human SGK1 isoforms A, B, D and F compared with phalloidin-stained actin cytoskeleton in HEK293T cells.** A-E show images in the same colours and layout as shown in Figure 5.4, but with phalloidin-stained actin cytoskeleton in red. A shows cells transfected with SGK1A. B shows cells transfected with SGK1B. C shows cells transfected with SGK1D. D shows cells transfected with SGK1F. E shows the equivalent images for untransfected control cells.

Previous studies by Bogusz et al. (2006) and Arteaga et al. (2006) showed that green fluorescent protein (GFP)-tagged Sgk1a and hemagglutinin (HA)-tagged Sgk1a colocalised with the endoplasmic reticulum (ER) in COS7 cells, using an anti-calnexin antibody (Arteaga et al., 2006; Bogusz et al., 2006). To further investigate the possibility of this localisation for any of the SGK1 isoforms, transfected HEK293T cells were co-stained for FLAG-tagged SGK1 isoforms and the ER marker calnexin. FLAG-tagged SGK1 isoform staining is shown in green, calnexin staining of ER in red, and nuclei stained with Hoechst 33258 in blue, with results demonstrating that none of the SGK1 isoforms distinctly colocalised with the ER (Figure 5.6). As with the previous imaging data, the incidental overlap of green and red staining produced yellow/orange regions in some of the merged images. Isoform localisations were similar to those shown in Figure 5.5 and Figure 5.4, with SGK1A and SGK1B showing cytosolic network-like localisation (Figure 5.6A & B). SGK1D was an exception, showing ruffle-like plasma membrane staining in some cells and unidentified specks on other cells (Figure 5.6C). SGK1F showed predominantly nuclear localisation with some weak cytosolic network-like staining, as before (Figure 5.6D).

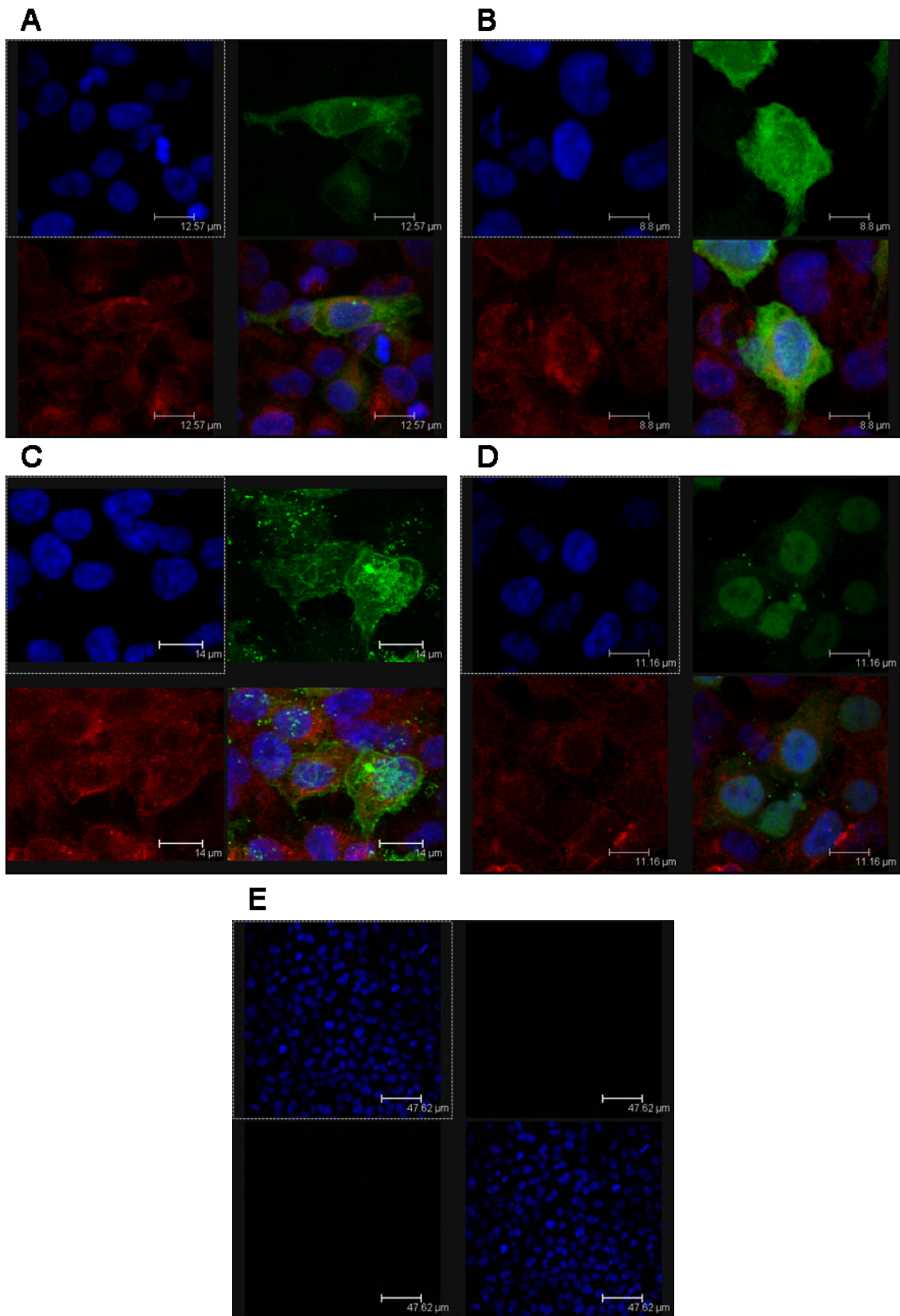


**Figure 5.6 Subcellular localisation of FLAG-tagged human SGK1 isoforms A, B, C, D and F compared with calnexin in HEK293T cells.** A-E show images in the same colours and layout as shown in Figure 5.4, but with calnexin (endoplasmic reticulum) staining in red. A shows cells transfected with SGK1A. B shows cells transfected with SGK1B. C shows cells transfected with SGK1D. D shows cells transfected with SGK1F. E shows the equivalent images for untransfected control cells.

#### **5.2.4 Fluorescence microscopy of immunostained FLAG-tagged mouse Sgk1 isoforms in HEK293T cells**

To investigate the localisation of mouse Sgk1 isoforms a, b, c and d, similar experiments to those for human SGK1 isoform localisation were performed. This also allowed a direct comparison of the mouse Sgk1 and human SGK1 isoform localisations to see if any differences occurred as a result of amino acid sequence variation between the species. HEK293T cells were cotransfected with FLAG-tagged Sgk1 isoforms and pDsRed-mito to test for colocalisation of the mouse Sgk1 isoforms with mitochondria. Mouse FLAG-tagged Sgk1 isoform staining is shown in green, mitochondria in red, and nuclei in blue (Figure 5.7). Mouse Sgk1 isoforms showed no distinct colocalisation with mitochondria. The yellow/orange colouring in the merged images for isoforms a, c and d was, most likely, due to incidental overlap of the diffuse/plasma membrane isoform staining and the red mitochondria. However, this experiment did show a specific staining pattern for each of the four isoforms. Mouse Sgk1a showed cytosolic network-like localisation (Figure 5.7A), whereas Sgk1b showed predominantly nuclear with some cytosolic network-like localisation (Figure 5.7B). Sgk1c showed was diffuse throughout the cell (Figure 5.7C), whilst Sgk1d showed predominantly plasma membrane localisation, but also weaker diffuse staining throughout the cell (Figure 5.7D).

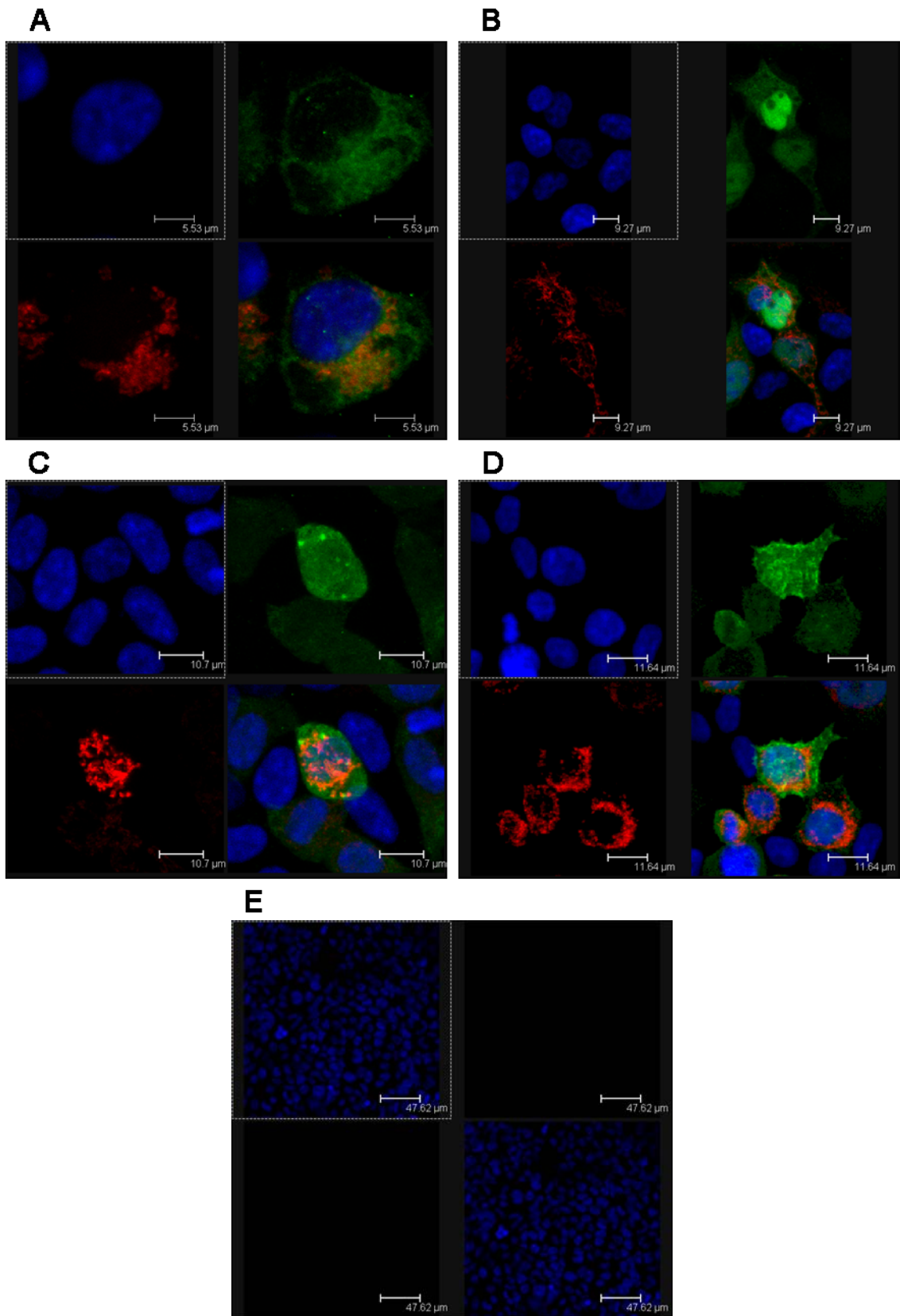


**Figure 5.7 Intracellular localisation of FLAG-tagged mouse Sgk1 isoforms a, b, c, and d compared with red fluorescent protein (RFP)-labelled mitochondria in HEK293T cells.** A-E show images in the same colours and layout as shown in Figure 5.4. A shows cells cotransfected with FLAG-tagged Sgk1a and RFP-mitochondria. B shows cells cotransfected with FLAG-tagged Sgk1b and RFP-mitochondria. C shows cells cotransfected with FLAG-tagged Sgk1c and RFP-mitochondria. D shows cells cotransfected with FLAG-tagged Sgk1d and RFP-mitochondria. E shows the equivalent images for untransfected control cells.

These experiments were subsequently repeated with the ER marker calnexin. FLAG-tagged Sgk1 staining is indicated in green, calnexin staining in red, and nuclei in blue (Figure 5.8). Again, no distinct colocalisation was revealed for any Sgk1 isoforms with calnexin. Sgk1 isoform localisations were very similar to those shown in Figure 5.7, with Sgk1a showing cytosolic network-like localisation, Sgk1b showing predominantly nuclear with some weaker cytosolic network-like staining. Slight differences were observed the other isoforms in that Sgk1c showed cytosolic network-like localisation similar to Sgk1a, and Sgk1d showed predominantly plasma membrane localisation in ruffle-like staining across the cell surface. The SGK1 isoform localisation data is summarised in Table 5.1.

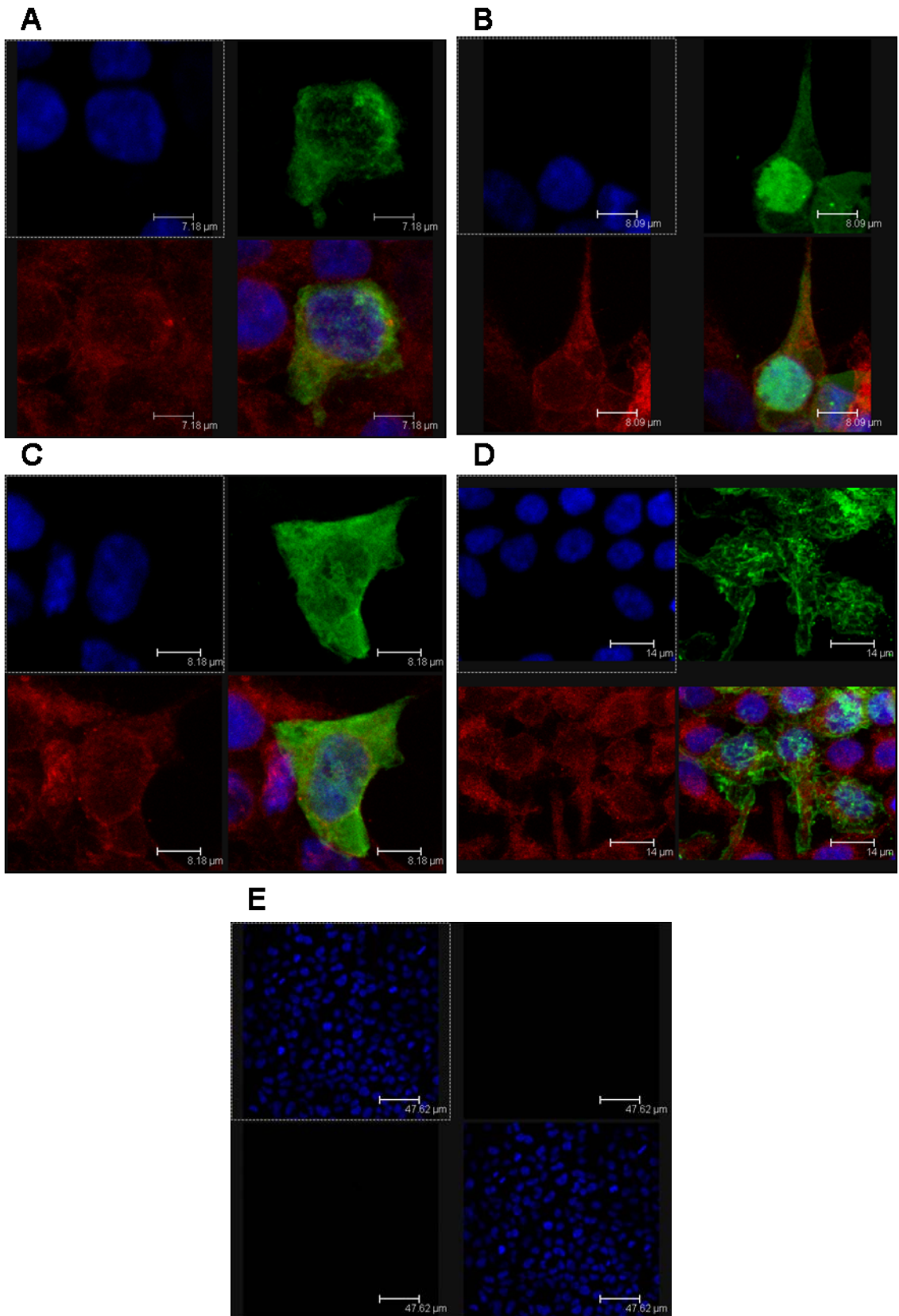


**Figure 5.8 Intracellular localisation of FLAG-tagged mouse Sgk1 isoforms a, b, c, and d compared with red fluorescent protein (RFP)-labelled mitochondria in HEK293T cells.** A-E show images in the same colours and layout as shown in Figure 5.4, but with calnexin staining in red. A shows cells cotransfected with FLAG-tagged Sgk1a and RFP-mitochondria. B shows cells cotransfected with FLAG-tagged Sgk1b and RFP-mitochondria. C shows cells cotransfected with FLAG-tagged Sgk1c and RFP-mitochondria. D shows cells cotransfected with FLAG-tagged Sgk1d and RFP-mitochondria. E shows the equivalent images for untransfected control cells.

<b>SGK1 isoform</b>	<b>Localisation in HEK293T cells</b>	<b>No colocalisation with the following structures</b>
Human A	Cytosolic network-like	Mitochondria, Actin cytoskeleton, Endoplasmic reticulum.
Human B	Cytosolic network-like	As A
Human C	Diffuse cytosolic	Mitochondria
Human D	Predominantly plasma membrane with some diffuse cytosolic	As A
Human F	Predominantly nuclear with some cytosolic network-like	As A
Mouse a	Cytosolic network-like	Mitochondria, Endoplasmic reticulum.
Mouse b	Predominantly nuclear with some cytosolic network-like	As a
Mouse c	Diffuse with cytosolic network-like	As a
Mouse d	Predominantly plasma membrane with some diffuse cytosolic	As a

**Table 5.1 SGK1 isoform localisation summary.**

### **5.2.5 Co-immunoprecipitation of human SGK1 with GILZ1**

SGK1 and GILZ1 have been shown to be upregulated in renal cortical collecting duct cells in response to treatment with aldosterone (Soundararajan et al., 2005; Muller et al., 2003; Robert-Nicoud et al., 2001). Of the four GILZ isoforms that are upregulated by aldosterone, only GILZ1 stimulates increased ENaC-mediated Na<sup>+</sup> transport in renal cortical collecting duct cells (Soundararajan et al., 2007). Both SGK1 and GILZ1 have been shown to negatively regulate the inhibition of ENaC through acting on Nedd4-2 and

ERK, respectively (Bhalla et al., 2006). However, it has been shown recently that SGK1 and GILZ1 interact to stimulate ENaC and that this interaction is dependent on SGK1 being activated and having an intact N-terminus (Soundararajan et al., 2009). In light of this, the assay used in this study was adapted to include the mouse and human SGK1 isoforms as a method of examining: (1) impact of the different N-termini of the SGK1 isoforms on their interaction with GILZ1 and (2) any differences in phosphorylation status between expressed SGK1 isoforms.

HEK293T cells were cotransfected with FLAG-tagged SGK1 isoforms plus GILZ1 or GFP control. GILZ1 was then immunoprecipitated from lysates and the presence of SGK1 isoforms bound to the precipitated GILZ1 protein was determined by Western blotting (Figure 5.9). Arrows indicate the FLAG-tagged SGK1 bands, whereas other bands are probably due to nonspecific binding of the anti-FLAG antibody. FLAG-tagged SGK1 bands in the precipitate lanes demonstrated that human SGK1 isoforms A, B, C, D and F all co-immunoprecipitated with GILZ1, but, based on band intensity, isoforms A and B co-immunoprecipitated in the greatest amounts. This result suggests that, of the human SGK1 isoforms, A and B bind to GILZ1 the most. The doublet band seen for SGK1F is most likely caused by co-detection of a post-translationally modified form of the protein.

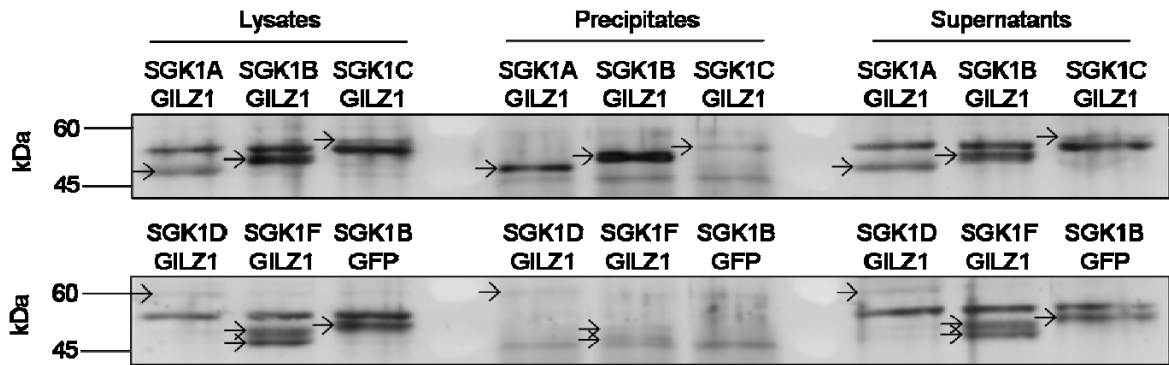


**Figure 5.9 Human SGK1 isoforms A-F all co-immunoprecipitate with GILZ1, but SGK1A and SGK1B show the greatest amount of binding.** HEK293T cell lysates, from cells cotransfected with FLAG-tagged SGK1 isoforms plus GILZ1 or GFP control, were used in co-immunoprecipitation of SGK1 bound to GILZ1 using an anti-GILZ1 antibody. Original lysates, the supernatants and precipitated protein were analysed for FLAG-tagged SGK1 isoforms by Western blotting using an anti-FLAG antibody (Abcam). Arrows indicate the FLAG-tagged SGK1 bands detected, whereas other bands present are due to nonspecific anti-FLAG antibody binding. This experiment was repeated with similar results.

This experiment was repeated using a different anti-FLAG antibody for detection of co-immunoprecipitated FLAG-tagged SGK1 isoforms to verify the result and to obtain fewer nonspecific bands. However, nonspecific protein bands are again detected in the precipitate lanes of the Western blots, but precipitated protein bands for each of the human SGK1 isoforms A, B, C, D and F can still be identified (Figure 5.10). This result again suggests that SGK1A and B co-immunoprecipitate with GILZ1 in a greater amount than the other isoforms, shown by the FLAG bands for these isoforms being overexposed compared with the other isoforms bands. No FLAG bands seen in the GFP transfected control lane confirms that the FLAG-tagged SGK1 bands detected are due to their co-immunoprecipitation with GILZ1.

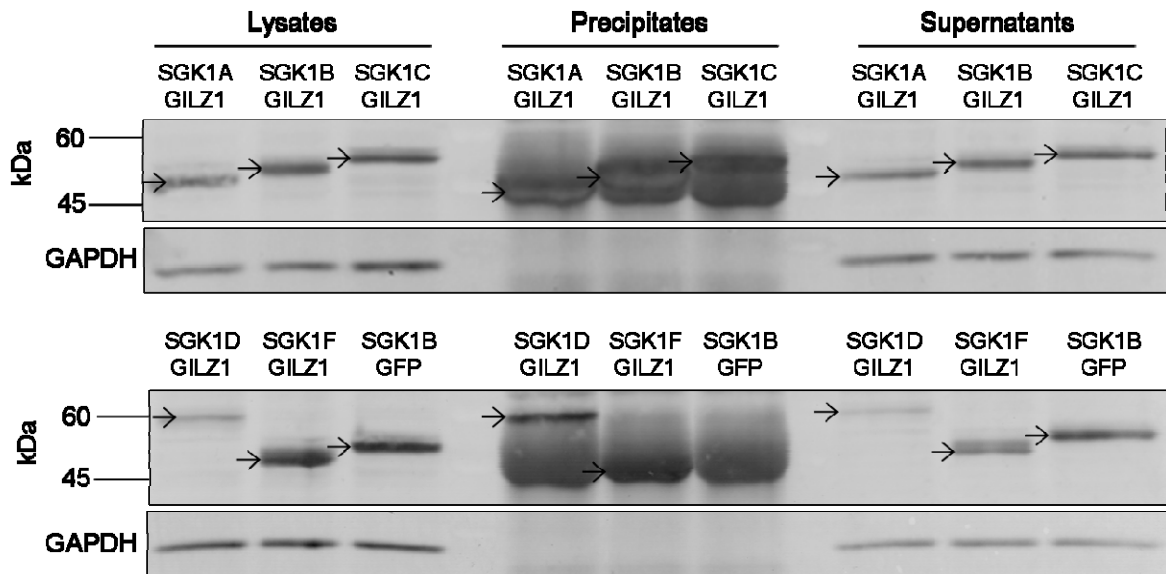


**Figure 5.10 SGK1A and B also appear to co-immunoprecipitate with GILZ1 in greater amounts than SGK1 isoforms C, D and F when detected with a different anti-FLAG antibody.** This experiment used the same procedure as described for Figure 5.9 except for the use of a different anti-FLAG antibody (Chemicon). Negative control (SGK1B with GFP) showed no co-immunoprecipitation.

### 5.2.6 Co-immunoprecipitation of mouse Sgk1 with GILZ1

In order to show relevance of the interaction between human SGK1 isoforms and GILZ1 to mouse Sgk1 isoforms, experiments were repeated using the mouse Sgk1 isoforms and human GILZ1. Mouse Gilz1 could not be used because, when tested by Western blotting, mouse Gilz1-specific antibody failed to detect overexpressed mouse Gilz1 in transfected HEK293T cell lysate. Therefore human GILZ1 was used, which shares 87% amino acid sequence identity with mouse Gilz1. HEK293T cells were cotransfected, as before, with FLAG-tagged mouse Sgk1 isoforms plus GILZ1 or GFP control, followed by their lysis and use in immunoprecipitation of GILZ1. The presence of Sgk1 isoforms bound to the precipitated GILZ1 protein was determined by Western blotting to show FLAG-tagged Sgk1 isoform expression in the precipitated protein fraction, compared with the supernatant or original lysate (Figure 5.11). Arrows indicate the FLAG-tagged SGK1

bands, whereas the other bands are due to nonspecific binding of the anti-FLAG antibody. The Chemicon anti-FLAG antibody could not be used in this experiment because it was raised in mouse and therefore its use would cause secondary antibody cross-reactivity. These data demonstrated that mouse Sgk1 isoforms a, b, c, and d all co-immunoprecipitated with GILZ1, but not GFP and that Sgk1b gave the most intense band in the precipitate, suggesting it bound to GILZ1 the most. These results were similar to those obtained using the human SGK1 isoforms; all the isoforms tested in each species co-immunoprecipitated with GILZ1, but human SGK1A and B and mouse Sgk1b showed the greatest binding.

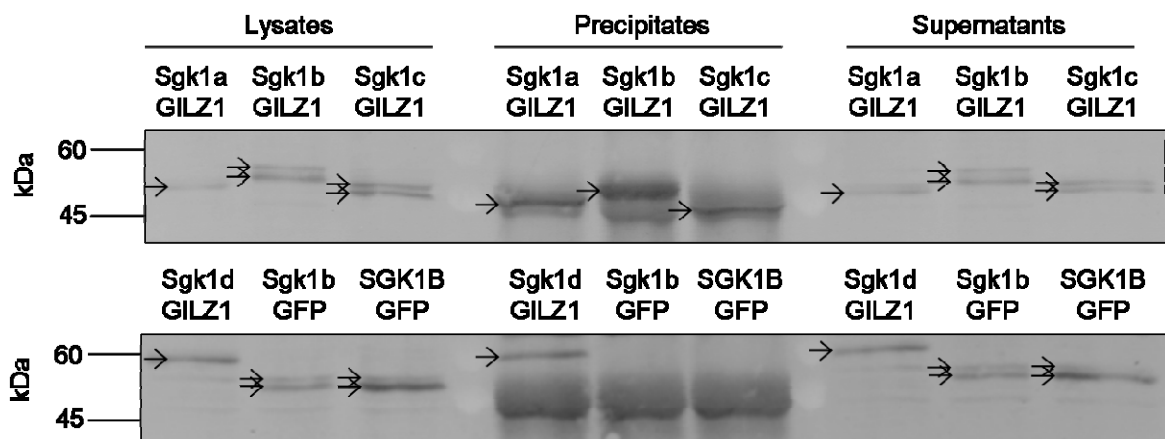


**Figure 5.11 Mouse Sgk1 isoforms a-d all co-immunoprecipitate with GILZ1, but Sgk1b shows the greatest amount of binding.** HEK293T cell lysates, from cells cotransfected with FLAG-tagged Sgk1 isoforms plus GILZ1 or GFP control, were used in co-immunoprecipitation of Sgk1 bound to GILZ1 using an anti-GILZ1 antibody. Original lysates, the supernatants and precipitated protein were analysed for FLAG-tagged Sgk1 isoforms by Western blotting using an anti-FLAG antibody (Abcam). Arrows indicate the FLAG-tagged Sgk1 bands detected, whereas other bands present are due to nonspecific anti-FLAG antibody binding.

## 5.3 Discussion

### 5.3.1 Fluorescence microscopy of SGK1D in human and mouse renal tissue

To date, there have not been any previous studies that have investigated the localisation of endogenous SGK1D in either human or mouse renal tissue. The sub-apical punctate staining shown in Figure 5.1 of human SGK1D in human renal tissue shows no similarity to any SGK1D localisation seen in cultured cells. The sub-apical intracellular accumulations suggested that SGK1D may be localising to several possible intracellular structures, including basal bodies, intracellular vesicles or mitochondria. Because the co-staining of SGK1D with basal bodies, microtubules and mitochondria failed, no conclusions are possible and the identity of the intracellular structures that SGK1D is localising to still requires clarification. The cell-cell junction staining of SGK1D (Figure 5.2), could be explained by the plasma membrane localisation of SGK1D observed in cultured HEK293T cells (Figure 5.6) and in publications by others (Raikwar et al., 2008; Hall, 2007). Verification of this staining, through colocalisation with ZO-1 was not possible, however, due to degradation of the human kidney tissue. Therefore identification of the cell-cell junction structure also requires further verification.

The basolateral membrane localisation of mouse Sgk1d is comparable to plasma membrane staining seen in cultured cells both in this chapter and publications by others (Arteaga et al., 2008). Mouse Sgk1 was also shown to localise to the basolateral membrane of collecting ducts in rat kidney, although this study did not distinguish between Sgk1 isoforms (Alvarez de la Rosa et al., 2003). This localisation at the basolateral surface suggests that mouse Sgk1d may have a function associated with the Na<sup>+</sup>/K<sup>+</sup>-ATPase transporter, which is present at the basolateral membrane of collecting duct epithelia, as opposed to an effect on ENaC, which is present at the apical membrane. Several previous

studies have shown that aldosterone stimulates  $\text{Na}^+/\text{K}^+$ -ATPase activity and also that SGK1, or what is now known to be SGK1A, stimulated  $\text{Na}^+/\text{K}^+$ -ATPase activity when co-expressed in *Xenopus* oocytes (Zecevic et al., 2004; Verrey et al., 2003; Setiawan et al., 2002). However, in epithelial cells, the basolateral localisation of Sgk1d coupled with the conserved catalytic domain between Sgk1 isoforms, suggest that Sgk1d may alone, or in combination with Sgk1a, mediate aldosterone-stimulated  $\text{Na}^+/\text{K}^+$ -ATPase activity. Experiments to show aldosterone-stimulated Sgk1d activity and colocalisation with  $\text{Na}^+/\text{K}^+$ -ATPase would be needed to verify this hypothesis.

The images in Figure 5.1 and Figure 5.2 demonstrated that SGK1D expression was not confined to the collecting duct, but was also present in other renal tubules. This was not entirely unexpected as SGK1A is reported to have many roles in addition to regulation of ENaC, including regulation of NCC in the DCT (Vallon et al., 2009; Lang et al., 2006). However, SGK1D is reported to have a greater effect on ENaC than SGK1A, suggesting that this isoform may play the prominent role in regulation of ENaC (Raikwar et al., 2008). This staining therefore provides insight into the relative distribution of SGK1D in renal tissue. The only relevant previous investigation into the relative tissue distribution of SGK1D has been limited to qRT-PCR of a broad range of mouse tissues and immunoprecipitation of tagged protein from transgenic mouse whole organ lysates, not including kidney (Arteaga et al., 2008). This investigation concluded that mouse Sgk1d was expressed exclusively in brain tissue, despite only examining expression of tagged protein in brain, heart, colon, and lung.

### **5.3.2 Fluorescence microscopy of FLAG-tagged SGK1 isoforms in HEK293T cells**

No previous studies have investigated the localisation of overexpressed human and mouse SGK1 isoforms. The findings in the present study showing immunostaining of overexpressed FLAG-tagged human and mouse SGK1 isoforms in transiently transfected HEK293T cells are summarised in Table 5.1. The majority of the human SGK1 isoforms and the equivalent mouse Sgk1 isoforms showed distinct similarity in their localisation. Human SGK1A and mouse Sgk1a displayed similar cytosolic network-like localisation. Human SGK1C and mouse Sgk1c both displayed similar diffuse localisation. Human SGK1D and mouse Sgk1d, both localised predominantly to the plasma membrane. Interestingly, human SGK1B and mouse Sgk1b were the only isoforms conserved between species that didn't show similar localisation. Human SGK1B showed cytosolic network-like localisation similar to human SGK1A and mouse Sgk1a. In contrast, mouse Sgk1b displayed a predominantly nuclear localisation that was similar to human SGK1F, the only human isoform that is not conserved in mouse. These different localisations of SGK1 isoforms within species, yet similar localisations of equivalent SGK1 isoforms between species, suggest that they may have specific and conserved functional roles.

Although no previous studies have compared the localisation of all SGK1 isoforms before, several have investigated and found similar localisation of SGK1A alone. Naray-Fajes-Toth et al. (2004) showed that yellow fluorescent protein-tagged human SGK1A transfected into RCCT-28 cells (a rabbit CCD cell line) displayed a diffuse cytosolic localisation (Naray-Fejes-Toth et al., 2004a). Also, Menniti et al. (2005) showed that antibody detection of Myc-tagged human SGK1A transfected into COS7 cells also revealed a diffuse cytosolic localisation (Menniti et al., 2005). In a similar experiment, Arteaga et al. (2007) showed cytosolic localisation of HA-tagged mouse Sgk1a in A6 cells

(Arteaga et al., 2007). These three previous studies all used N-terminally tagged SGK1A constructs, but, in another study by Raikwar et al. (2008), comparable diffuse cytosolic localisation was shown of C-terminally FLAG-tagged human SGK1A in HEK293 cells (Raikwar et al., 2008). This study also showed that the regulated localisation of SGK1A to the cytosol is dependent on its N-terminus, as a 60 amino acid-truncated human SGK1A showed diffuse localisation throughout the cell (Raikwar et al., 2008). Raikwar et al (2008) also showed plasma membrane localisation of C-terminally FLAG-tagged human SGK1D in HEK293 cells (Raikwar et al., 2008). This shows that N-terminally and C-terminally FLAG-tagged human SGK1D localised identically in a similar cell type, suggesting that tag location did not affect localisation. The plasma membrane localisation of SGK1D may be due to its putative PX domain, which confers affinity for phosphoinositide binding. Arteaga et al. (2008) also described the localisation of mouse Sgk1d in transfected CHO cells as plasma membrane and showed that this was due to being bound to PI(4,5)P<sub>2</sub> (Arteaga et al., 2008). This paper also found that removal of three positive residues in the mouse Sgk1d N-terminus by K21N/K22N/R23G mutations caused its translocation from the plasma membrane to the cytosol. Furthermore, F19A/F20A and W27A mutations caused Sgk1d translocation to the nucleus. This suggests that residues at positions 19-23 and 27 of Sgk1d, which are thought to be within the PX domain, are critical for its plasma membrane localisation. The plasma membrane localisation and/or phosphoinositide binding of SGK1D may confer its functional specificity.

Data from the present study showed that, although SGK1 isoform localisation in cultured cells can be similar to in native tissue (e.g. mouse Sgk1d), it can also be very different (e.g. human SGK1D). This may be because HEK293T cells are not representative of CCD cells, but could also be because cells were unpolarised, protein was overexpressed, or

isoforms were tagged. The attachment of any protein tag to the SGK1 isoforms may also interfere with their correct localisation. However, FLAG-tagging has the advantage that it involves the attachment of a relatively small epitope compared to fluorescent tags such as a green fluorescent protein, whose larger size would increase the likelihood of localisation interference. A possible improvement to this investigation is to use polarised mpkCCD<sub>cl4</sub> cells instead of HEK293T cells. Polarised mpkCCD<sub>cl4</sub> cells would show the SGK1 isoform localisations that are specific to polarised CCD cells. Although both HEK293T cells and mpkCCD<sub>cl4</sub> cells were used in this study, mpkCCD<sub>cl4</sub> cells did not show high enough transfection efficiency for localisation experiments. HEK293T cells were kept in growth medium containing 10% FCS for SGK1 localisation studies, which should have stimulated SGK1 activity. Future studies into SGK1 isoforms to investigate effects on localisation could test the effects of treating serum-starved HEK and CCD cells with aldosterone on localisation of FLAG-tagged SGK1 isoforms. Investigation of the changes in SGK1 isoform localisation in response to their phosphorylation and activation may reveal more about the changes regarding which isoforms are involved in regulation of ENaC. However, this approach still relies on transient transfection, which floods the cell with overexpressed protein possibly causing altered or dysregulated localisation. Future experiments could target untagged, overexpressed, or endogenous protein, but this requires detection using isoform-specific antibodies. In a previous study, Sahoo et al. (2005) showed that endogenous SGK1 localisation in human breast cancer cells was predominantly cytosolic and network-like, using a pan-SGK1 antibody, suggesting that this staining was accounted for by SGK1A and SGK1B (Sahoo et al., 2005). The human SGK1 isoform-specific antibodies described in this thesis showed decreased specificity when used to detect untagged protein for immunofluorescence. Generation of high-avidity

SGK1 isoform-specific antibodies would allow future investigation of differential isoform regulation and localisation using immunofluorescence.

### **5.3.3 Co-immunoprecipitation of SGK1 isoforms with GILZ1**

The result that SGK1A co-immunoprecipitated with GILZ1 (Figure 5.9 and Figure 5.10) supports the finding of Soundarajan et al. (2009) that showed a 49 kDa SGK1 band protein co-immunoprecipitated with GILZ1 from transfected HEK293T cell lysate (Soundararajan et al., 2009). The results of my experiment using the other human and mouse SGK1 isoforms are novel. GILZ1 has been shown to localise in the cytosol, suggesting that SGK1 isoforms that share this localisation may interact with it the most. Only the human isoforms SGK1A and B, which showed cytosolic localisation, also showed enhanced interaction with GILZ1. Mouse Sgk1b also showed enhanced interaction with GILZ1, despite its predominantly nuclear localisation.

Further investigation is needed to find out why these isoforms preferentially interact with GILZ1 and what role, if any, their intracellular localisation plays. The co-immunoprecipitation of SGK1A with GILZ1 was initially shown by Soundarajan et al. (2009) and revealed to be part of a regulatory complex that enhances ENaC activation. In the same study, GILZ1, FLAG-SGK1, Raf-1, and Nedd4-2 were shown to colocalise in HEK293T cells by fluorescence microscopy, suggesting that both SGK1 action on Nedd4-2 and GILZ1 action on the ERK signalling pathway may be involved (Soundararajan et al., 2009). The MEK1/2 inhibitor, PD98059 has also been shown to partially inhibit aldosterone-stimulated  $I_{eq}$  highlighting the involvement of the Ras-GILZ-ERK pathway (Michlig et al., 2004). As yet, it is unknown what region of SGK1A or the other isoforms interacts with GILZ1. The differential interaction between Sgk1 isoforms and GILZ1 in

cells overexpressing both proteins, suggests that the differing SGK1 isoform N-termini may modulate the interaction. Experiments described in this thesis and experiments in the investigation by Soundarajan et al. (2009) both use tagged SGK1 and, despite showing similar results, the tags could have affected the interaction with GILZ1. Future experiments could include investigating whether the interaction with GILZ1 affects SGK1 isoform localisation. Further work on the interactions of SGK1 isoforms with ENaC regulatory proteins could resolve the identity of a novel ENaC regulatory complex.

## **5.4 Summary**

- SGK1D shows sub-apical/perinuclear punctate and cell-cell junction localisation in human renal collecting duct epithelia.
- Sgk1d shows basolateral membrane localisation in mouse collecting duct and other renal tubule epithelia.
- FLAG-tagged human SGK1 isoforms A, B, C, D and F do not exclusively colocalise with actin cytoskeleton, mitochondria nor endoplasmic reticulum in HEK293T cells.
- FLAG-tagged human SGK1 isoforms A, B, D, and F show cytosolic network-like localisation in HEK293T cells.
- FLAG-tagged human SGK1C shows diffuse cytosolic localisation in HEK293T cells.
- FLAG-tagged human SGK1D shows predominantly plasma membrane localisation in HEK293T cells.

- FLAG-tagged human SGK1F shows predominantly nuclear localisation in HEK293T cells.
- FLAG-tagged mouse Sgk1 isoforms a, b, c and d do not colocalise with mitochondria nor calnexin.
- FLAG-tagged mouse Sgk1a, b, and c show cytosolic network-like localisation in HEK293T cells.
- FLAG-tagged mouse Sgk1b shows predominantly nuclear localisation in HEK293T cells.
- FLAG-tagged mouse Sgk1d shows predominantly plasma membrane localisation in HEK293T cells.
- FLAG-tagged human SGK1 isoforms A, B, C, D and F all bind with GILZ1, but SGK1A and B bind the most.
- FLAG-tagged mouse Sgk1 isoforms a, b, c and d all bind with GILZ1, but Sgk1b binds the most.

## **Chapter 6 - Conclusions**

### **6.1 Achievement of aims**

Data presented in this thesis shows that mouse mpkCCD<sub>c14</sub> cells express four isoforms of Sgk1 (Sgk1a, 1b, 1c, and 1d) and that the expression of these isoforms is regulated by aldosterone. In addition, results from ion transport studies suggest that all four isoforms are involved in aldosterone-dependent regulation of the epithelial sodium channel (ENaC). Additionally, that human and mouse SGK1 isoforms show specific subcellular distribution in both native renal tissue, as well as specific intracellular localisation in cultured HEK293T cells. Overall, this suggests that multiple SGK1 isoforms are involved in the regulation of transepithelial Na<sup>+</sup> transport in cultured CCD cells and native tissue.

### **6.2 Review of research path**

At the start of this PhD the SGK1 gene was considered to code for a single protein, however, work from human skin cells suggested that multiple human SGK1 variants existed. Potential *Sgk1* variant mRNAs were identified by searching the dbEST mouse expressed sequence tag database for alternative *Sgk1* transcripts. Four potential mouse *Sgk1* variant mRNAs were identified that originate from alternative promoter usage and RNA splicing and produce four Sgk1 isoforms, which were named Sgk1a, 1b, 1c, and 1d. Expression of the four *Sgk1* variant mRNAs was confirmed in cultured mouse CCD cells and native mouse renal tissue by whole cell/tissue RNA isolation and RT-PCR using isoform-specific primers. The confirmed *Sgk1* variants were then cloned into an expression vector allowing investigation of their translation products via exogenous overexpression in cultured cells and Western blotting for Sgk1 in the cell lysate. Multiple

Sgk1 protein bands were produced by isoform overexpression, of which the most intense for each isoform corresponded in size with the putative Sgk1 isoform proteins predicted earlier, being ~49 kDa (Sgk1a), ~51 kDa (Sgk1b), ~48 kDa (Sgk1c), and ~60 kDa (Sgk1d). The role of Sgk1 isoforms in regulation of Na<sup>+</sup> transport in mouse CCD cells was investigated firstly by monitoring their induction by aldosterone using different doses and time of exposure to, a hormone known to induce Na<sup>+</sup> transport. Aldosterone increased expression of Sgk1a, 1b, and 1c suggesting these isoforms likely have roles in aldosterone-stimulated Na<sup>+</sup> transport. Aldosterone treatment also revealed the endogenous expression of Sgk1a, 1b, 1c, whilst Sgk1d was expressed at a high basal level in starved mouse CCD cells. Combined aldosterone plus insulin treatment was also used because previous work had shown that combination of hormones induced a larger Na<sup>+</sup> transport increase than aldosterone alone and insulin alone was also known to increase Sgk1 expression (Wang et al., 2008; Gonzalez-Rodriguez et al., 2007). Aldosterone and aldosterone plus insulin induced multiple Sgk1 isoform bands, which were identified by their co-migration with exogenous overexpressed Sgk1 isoforms.

To investigate if changes in Na<sup>+</sup> transport correlated with phosphorylation of Sgk1 isoforms, optimisation of Western blotting using phosphorylated-specific Sgk1 antibodies was attempted, but these antibodies only detected phosphorylated human SGK1B and 1C and mouse Sgk1c. In investigation of the regulation of Sgk1 isoforms, aldosterone-induced Sgk1a, 1b, 1c, and 1d were inhibited by LY294002; an inhibitor of PI3Ks and mTOR. The identity of human and mouse Sgk1b and 1d were further confirmed using isoform-specific antibodies.

In order to relate changes in Sgk1 protein expression to changes in transepithelial Na<sup>+</sup> transport, parallel Western blotting and  $I_{eq}$  measurement were performed, from cells exposed to aldosterone and combined aldosterone plus insulin. Aldosterone treatment

produced a similar time-dependent increase in Na<sup>+</sup> transport as Sgk1 isoform expression. Treatment with amiloride revealed that the Na<sup>+</sup> transport was mostly via ENaC, which is known to be regulated by Sgk1. Inhibition of PI3Ks and mTOR with LY294002 also produced a similar reduction in Na<sup>+</sup> transport as found for the effects of LY294002 on expression of Sgk1 isoforms. Rapamycin, an inhibitor of mTORC1 activity, also produced a small, but significant reduction in Na<sup>+</sup> transport, which was unexpected as mTORC2 has recently been shown to be the mTOR complex responsible for activation of Sgk1. Overexpression and knockdown of Sgk1 in polarised mouse CCD cells was attempted in order to study the effects of individual Sgk1 isoforms, however, these approaches were unsuccessful.

Investigation of the native renal tissue or cultured cells localisation of SGK1 isoforms suggested that SGK1 isoforms have specialised roles. Human SGK1D showed sub-apical punctate staining, as well as cell-cell junction localisation in collecting ducts of human renal tissue. Mouse Sgk1d showed basolateral localisation in the collecting ducts of mouse renal tissue. In HEK293T cells, SGK1A, B and C showed cytosolic localisation, whereas SGK1D showed plasma membrane localisation and SGK1F showed nuclear localisation. In the same cell line, mouse Sgk1a and c showed cytosolic localisation, whereas Sgk1b showed nuclear localisation and Sgk1d showed plasma membrane localisation. These data showing isoform-specific intracellular localisation, together with the differential stimulation of Sgk1 isoforms expression by hormones, as well as the temporal change in Na<sup>+</sup> transport, collectively suggest that Sgk1 isoforms perform different roles in regulation of Na<sup>+</sup> transport. However, these data were not able to measure phosphorylated (active) Sgk1 expression due to the failure of detecting phosphorylated Sgk1 by Western blotting. Therefore, a co-immunoprecipitation assay was adapted from a study by Soundararajan et al. (2009) to look for the recruitment of phosphorylated Sgk1 by GILZ1 to a complex of

ENaC-Raf1-Nedd4-2, which was shown to cooperatively reduce the inhibitory effect of MAPK/ERK and Nedd4-2 on ENaC activity, respectively. All SGK1 isoforms interacted with GILZ1, but the greatest levels of interaction were between GILZ1 and human SGK1 isoforms A and B and mouse Sgk1 isoform b, suggesting these isoforms are the most active or are selective for the role of cooperative regulation of ENaC with GILZ1.

### **6.3 Final discussion**

Aldosterone was also found to induce isoforms equivalent to Sgk1a, 1b, and 1c in the study by Gonzalez-Rodriguez et al. (2007). This study also showed that Sgk1 isoform induction was retained after lambda phosphatase treatment, whereas higher bands on the Western blot were removed, indicating that the Sgk1a, 1b, and 1c bands are not phosphorylated forms (Gonzalez-Rodriguez et al., 2007). In the data presented in chapters 3 and 4, Sgk1d was consistently expressed at a higher basal level than the other isoforms in starved mouse CCD cells, as well as not being induced to the same extent by aldosterone. In addition, Sgk1d was less affected by LY294002 than the other isoforms. The apparent greater stability of Sgk1d compared to Sgk1a in mouse CCD cells was quantified in the study by Raikwar et al. (2008), which showed Sgk1d had a longer half-life than Sgk1a ( $t_{1/2}$  of SGK1A: 16 min, and SGK1D: 119 min). Therefore, stimulation of cells with hormones such as aldosterone would first lead to a selective increase in Sgk1d activity, followed by later increase in other isoforms.

In Sgk1 isoform overexpression studies the unidentified 56 kDa Sgk1 band present in the Western blot of synthesised Sgk1b could be a multi-phosphorylated Sgk1b protein with an increase in apparent size by 5 kDa, but this would require synthesised protein to potentially become phosphorylated. Overexpressing PDK1 with Sgk1 isoforms to induce their

phosphorylation only worked for human SGK1B and C and mouse Sgk1c, suggesting that the Sgk1 isoforms have different phosphorylation profiles. It has been reported that phosphorylation of serine 422 (by mTORC2) is required for phosphorylation of threonine 256 (by PDPK1) to take place, but my experiments suggest this is not the case for human SGK1B and C and mouse Sgk1c.

Sgk1d contains a putative PX domain, which is characterised by phosphoinositide binding primarily to PtdIns(3)P, although PX domains can also bind other PtdIns forms as well (Vanhaesebroeck et al., 2010). Rab5 has been shown to recruit class III PI3K to early endosomes creating a possible route for Sgk1d recruitment to recycling/degrading ENaC in endosomes (Backer, 2008; Lu et al., 2007). Class III PI3K also interacts with Rab7, which is thought to recruit class III PI3K to late endosomes causing an accumulation of PtdIns(3)P (Backer, 2008). This data presents endosomes as a possible localisation of SGK1D in native human renal tissue, although the intracellular accumulations producing the punctate staining of SGK1D were probably too large to be endosomes.

## **6.4 Relevance of findings**

Research, thus far, has identified many different roles for SGK1 in various tissue types throughout the body, but the research conducted only considered that one isoform of SGK1 was involved. Clearly, the demonstration by my work and others that have now shown that multiple SGK1 isoforms exist makes it important that future research considers more than just SGK1A. This thesis has shown that multiple mouse Sgk1 isoforms are differentially induced by aldosterone in parallel with induced Na<sup>+</sup> transport. The isoforms appear to exhibit different intracellular localisation and interact differentially with GILZ1, indicating that mouse Sgk1 isoforms are likely to have specialised functions in the

regulation of Na<sup>+</sup> transport. It is therefore highly likely that SGK1 isoforms also have specialised functions in the other tissue types where the original SGK1 was only considered before. SGK1 isoforms could therefore be responsible for many as yet unidentified effects in tissues throughout the body.

The identification of multiple SGK1 isoforms involved in regulation of CCD Na<sup>+</sup> transport suggests that several proteins, in addition to the original SGK1 (1A), may be involved or underlie dysregulated Na<sup>+</sup> transport and hypertension. Polymorphisms in SGK1 have already been linked to certain types of hypertension (Lang et al., 2009a) and SGK1 knockout mice produce a phenotype with an inability to retain salt when given a low-salt diet, as well as fail to excrete K<sup>+</sup> when given a high K<sup>+</sup> diet (Fejes-Toth et al., 2008; Huang et al., 2004; Wulff et al., 2002). Dysregulation of SGK1 isoforms could also be implicated in cystic fibrosis as SGK1A has been shown to regulate CFTR (Sato et al., 2007). Additionally, SGK1 isoforms could potentially be involved in development of diabetes as polymorphisms in the *SGK1* gene have been linked to variations in blood pressure and predisposal to obesity and type 2 diabetes (Schwab et al., 2008). SGK1A has also been shown to be upregulated by conditions associated with type 2 diabetes and is thought to be involved in development of diabetic nephropathy (Lang et al., 2009b).

Various pharmacological inhibitors of components of the SGK1 signalling pathway are used in clinical treatment such as sirolimus (rapamycin), which is used as an immunosuppressant particularly in kidney transplants, but it has been shown to cause renal Na<sup>+</sup>, K<sup>+</sup>, and Mg<sup>2+</sup> wasting resulting in hypovolemia (da Silva et al., 2009). LY294002 inhibits class I PI3Ks and its use has provided evidence for targeting PI3K in treatment of tumour cells (Liu et al., 2009). However, LY294002 is not used clinically because of off-target effects, as it inhibits CK2, mTOR, and GSK3β (Gharbi et al., 2007) as well as cAMP phosphodiesterase 2 (PDE2) (Abbott and Thompson, 2004), and valosin-containing protein

(VCP) (Halawani and Latterich, 2006). Heterocyclic indazole derivatives have recently been suggested as inhibitors of SGK1 for the clinical treatment of many conditions including hypertension, diabetes, and kidney, heart, and lung fibrosis (Lang and Gorch, 2010). Mechanistic target of rapamycin (mTOR) inhibitors, temsirolimus and everolimus, are currently approved for treatment of renal cell carcinoma (RCC) (Azim et al., 2010), whereas others such as deforolimus (Mita et al., 2008) are in clinical development. These clinical applications for inhibitors of SGK1 and associated proteins show the importance of the pathway and suggest that multiple SGK1 isoforms may complicate interpretations of the effects of these inhibitors, but also provide potential targets for future pharmacological therapeutics.

## **6.5 Future work**

Further work is required to identify the roles of individual SGK1 isoforms in regulation of ENaC-mediated  $\text{Na}^+$  transport in CCD cells. As discussed in chapter 4, this could be achieved by examining the effects of overexpression of individual Sgk1 isoforms or knockdown of endogenous Sgk1 on amiloride-sensitive equivalent short circuit current in mpkCCD<sub>c14</sub> cell monolayers. However, difficulty to transfect monolayers of mpkCCD<sub>c14</sub> cells grown on Transwells using Lipofectamine 2000 suggests other methods of transfection should be used in future. Transfection methods shown to successfully transfect mpkCCD<sub>c14</sub> cells include Nucleofection with plasmid DNA (Soundararajan et al., 2005) and siRNA (Raikwar et al., 2010), and retroviral transfection (Auberson et al., 2003). Alternatively, stable transfection of cells with an expression vector conferring specific antibiotic resistance could be used to generate stable cell lines expressing individual Sgk1 isoforms. Knockdown of Sgk1 in mpkCCD<sub>c14</sub> cells using siRNA has not

been shown to date, but many studies using different cell types, siRNAs, or transfection methods show siRNA-mediated knockdown of SGK1. Alternative knockdown approaches to siRNA include micro RNA, short hairpin RNA, and antisense RNA.

An additional approach to examining the roles of individual SGK1 isoforms involves their individual knockdown using isoform-specific siRNA or other RNAi technique. Instead of simply overexpressing or knocking down SGK1 isoforms, their individual kinase activity could be modified to allow investigation of their roles. For example, this could involve the creation of kinase dead (K127M), constitutively active (T256D/S422D), or non-phosphorylatable (T256A/S422A) mutant Sgk1 isoforms, such as shown for human and mouse SGK1A (Chang et al., 2007; Leong et al., 2003). Modified Sgk1 isoforms could also be used to investigate the origins of the alternative transcription products using site-directed mutagenesis to individually substitute the alternative start methionines and thus remove and identify Sgk1 isoform Western blot bands. Furthermore, investigation of the functions of SGK1 isoforms would be greatly improved by creation of mouse Sgk1 isoform-specific antibodies, more sensitive human SGK1 isoform-specific antibodies and phosphorylated-isoform-specific antibodies, allowing investigation of isoform-specific expression or localisation changes and subcellular distribution of all SGK1 isoforms in native tissues.

Other potential approaches for SGK1 isoform-specific study include creation of isoform-specific knockout mouse models to assess dependence on different isoforms *in vivo*. Also, quantitative RT-PCR could be used to show variations in the relative level of different isoform mRNA expression and further investigate the effects of hormone stimulation. Coexpression of individual SGK1 isoforms with ENaC in *Xenopus* oocytes could show the direct isoform-specific effects on ENaC activity. This study into isoforms of SGK1 could

also be extended to consider possible isoforms and roles of the paralogues SGK2 and SGK3.

## References

- Abbott, B. M. and Thompson, P. E. (2004) 'PDE2 inhibition by the PI3 kinase inhibitor LY294002 and analogues', *Bioorg Med Chem Lett*, 14, (11), pp. 2847-51.
- Abriel, H., Loffing, J., Rebhun, J. F., Pratt, J. H., Schild, L., Horisberger, J. D., Rotin, D. and Staub, O. (1999) 'Defective regulation of the epithelial Na<sup>+</sup> channel by Nedd4 in Liddle's syndrome', *Journal of Clinical Investigation*, 103, (5), pp. 667-73.
- Abriel, H. and Staub, O. (2005) 'Ubiquitylation of ion channels', *Physiology*, 20, pp. 398-407.
- Ahmad, N., Pratt, J. R., Potts, D. J. and Lodge, J. P. (2006) 'Comparative efficacy of renal preservation solutions to limit functional impairment after warm ischemic injury', *Kidney Int*, 69, (5), pp. 884-93.
- Alessi, D. R., Andjelkovic, M., Caudwell, B., Cron, P., Morrice, N., Cohen, P. and Hemmings, B. A. (1996) 'Mechanism of activation of protein kinase B by insulin and IGF-1', *EMBO Journal*, 15, (23), pp. 6541-51.
- Alessi, D. R., Pearce, L. R. and Garcia-Martinez, J. M. (2009) 'New insights into mTOR signaling: mTORC2 and beyond', *Sci Signal*, 2, (67), pp. pe27.
- Alvarez de la Rosa, D. and Canessa, C. M. (2003) 'Role of SGK in hormonal regulation of epithelial sodium channel in A6 cells', *American Journal of Physiology - Cell Physiology*, 284, (2), pp. C404-14.
- Alvarez de la Rosa, D., Coric, T., Todorovic, N., Shao, D., Wang, T. and Canessa, C. M. (2003) 'Distribution and regulation of expression of serum- and glucocorticoid-induced kinase-1 in the rat kidney', *Journal of Physiology*, 551, (Pt 2), pp. 455-66.
- Alvarez de la Rosa, D., Gimenez, I., Forbush, B. and Canessa, C. M. (2006) 'SGK1 activates Na<sup>+</sup>-K<sup>+</sup>-ATPase in amphibian renal epithelial cells', *American Journal of Physiology - Cell Physiology*, 290, (2), pp. C492-8.
- Alvarez de la Rosa, D., Li, H. and Canessa, C. M. (2002) 'Effects of aldosterone on biosynthesis, traffic, and functional expression of epithelial sodium channels in A6 cells.[see comment]', *Journal of General Physiology*, 119, (5), pp. 427-42.
- Amato, R., Menniti, M., Agosti, V., Boito, R., Costa, N., Bond, H. M., Barbieri, V., Tagliaferri, P., Venuta, S. and Perrotti, N. (2007) 'IL-2 signals through Sgk1 and inhibits proliferation and apoptosis in kidney cancer cells', *J Mol Med*, 85, (7), pp. 707-21.

- Andreasen, D., Vuagniaux, G., Fowler-Jaeger, N., Hummler, E. and Rossier, B. C. (2006) 'Activation of epithelial sodium channels by mouse channel activating proteases (mCAP) expressed in *Xenopus* oocytes requires catalytic activity of mCAP3 and mCAP2 but not mCAP1', *Journal of the American Society of Nephrology*, 17, (4), pp. 968-76.
- Aoyama, T., Matsui, T., Novikov, M., Park, J., Hemmings, B. and Rosenzweig, A. (2005) 'Serum and glucocorticoid-responsive kinase-1 regulates cardiomyocyte survival and hypertrophic response', *Circulation*, 111, (13), pp. 1652-9.
- Arteaga, M. F., Alvarez de la Rosa, D., Alvarez, J. A. and Canessa, C. M. (2007) 'Multiple translational isoforms give functional specificity to serum- and glucocorticoid-induced kinase 1', *Mol Biol Cell*, 18, (6), pp. 2072-80.
- Arteaga, M. F., Coric, T., Straub, C. and Canessa, C. M. (2008) 'A brain-specific SGK1 splice isoform regulates expression of ASIC1 in neurons', *Proc Natl Acad Sci U S A*, 105, (11), pp. 4459-64.
- Arteaga, M. F., Wang, L., Ravid, T., Hochstrasser, M. and Canessa, C. M. (2006) 'An amphipathic helix targets serum and glucocorticoid-induced kinase 1 to the endoplasmic reticulum-associated ubiquitin-conjugation machinery', *Proceedings of the National Academy of Sciences of the United States of America*, 103, (30), pp. 11178-83.
- Artunc, F., Nasir, O., Amann, K., Boini, K. M., Haring, H. U., Risler, T. and Lang, F. (2008) 'Serum- and glucocorticoid-inducible kinase 1 in doxorubicin-induced nephrotic syndrome', *Am J Physiol Renal Physiol*, 295, (6), pp. F1624-34.
- Auberson, M., Hoffmann-Pochon, N., Vandewalle, A., Kellenberger, S. and Schild, L. (2003) 'Epithelial Na<sup>+</sup> channel mutants causing Liddle's syndrome retain ability to respond to aldosterone and vasopressin', *American Journal of Physiology - Renal Physiology*, 285, (3), pp. F459-71.
- Azim, H., Azim, H. A., Jr. and Escudier, B. (2010) 'Targeting mTOR in cancer: renal cell is just a beginning', *Target Oncol*.
- Bachhuber, T., Almaca, J., Aldehni, F., Mehta, A., Amaral, M. D., Schreiber, R. and Kunzelmann, K. (2008) 'Regulation of the epithelial Na<sup>+</sup> channel by the protein kinase CK2', *J Biol Chem*, 283, (19), pp. 13225-32.
- Bachmann, S., Bostanjoglo, M., Schmitt, R. and Ellison, D. H. (1999) 'Sodium transport-related proteins in the mammalian distal nephron - distribution, ontogeny and functional aspects', *Anatomy & Embryology*, 200, (5), pp. 447-68.
- Backer, J. M. (2008) 'The regulation and function of Class III PI3Ks: novel roles for Vps34', *Biochem J*, 410, (1), pp. 1-17.
- Beevers, G., Lip, G. Y. and O'Brien, E. (2001) 'ABC of hypertension: The pathophysiology of hypertension', *BMJ*, 322, (7291), pp. 912-6.

- BelAiba, R. S., Djordjevic, T., Bonello, S., Artunc, F., Lang, F., Hess, J. and Gorlach, A. (2006) 'The serum- and glucocorticoid-inducible kinase Sgk-1 is involved in pulmonary vascular remodeling: role in redox-sensitive regulation of tissue factor by thrombin', *Circulation Research*, 98, (6), pp. 828-36.
- Belova, L., Sharma, S., Brickley, D. R., Nicolarsen, J. R., Patterson, C. and Conzen, S. D. (2006) 'Ubiquitin-proteasome degradation of serum- and glucocorticoid-regulated kinase-1 (SGK-1) is mediated by the chaperone-dependent E3 ligase CHIP', *Biochemical Journal*, 400, (2), pp. 235-44.
- Bens, M., Vallet, V., Cluzeaud, F., Pascual-Letallec, L., Kahn, A., Rafestin-Oblin, M. E., Rossier, B. C. and Vandewalle, A. (1999) 'Corticosteroid-dependent sodium transport in a novel immortalized mouse collecting duct principal cell line', *Journal of the American Society of Nephrology*, 10, (5), pp. 923-34.
- Berdiev, B. K., Qadri, Y. J. and Benos, D. J. (2009) 'Assessment of the CFTR and ENaC association', *Mol Biosyst*, 5, (2), pp. 123-7.
- Bhalla, V., Daidie, D., Li, H., Pao, A. C., LaGrange, L. P., Wang, J., Vandewalle, A., Stockand, J. D., Staub, O. and Pearce, D. (2005) 'Serum- and glucocorticoid-regulated kinase 1 regulates ubiquitin ligase neural precursor cell-expressed, developmentally down-regulated protein 4-2 by inducing interaction with 14-3-3', *Molecular Endocrinology*, 19, (12), pp. 3073-84.
- Bhalla, V. and Hallows, K. R. (2008) 'Mechanisms of ENaC Regulation and Clinical Implications', *J Am Soc Nephrol*.
- Bhalla, V., Soundararajan, R., Pao, A. C., Li, H. and Pearce, D. (2006) 'Disinhibitory pathways for control of sodium transport: regulation of ENaC by SGK1 and GILZ', *American Journal of Physiology - Renal Physiology*, 291, (4), pp. F714-21.
- Bhargava, A., Fullerton, M. J., Myles, K., Purdy, T. M., Funder, J. W., Pearce, D. and Cole, T. J. (2001) 'The serum- and glucocorticoid-induced kinase is a physiological mediator of aldosterone action', *Endocrinology*, 142, (4), pp. 1587-94.
- Boehmer, C., Embark, H. M., Bauer, A., Palmada, M., Yun, C. H., Weinman, E. J., Endou, H., Cohen, P., Lahme, S., Bichler, K. H. and Lang, F. (2004) 'Stimulation of renal Na<sup>+</sup> dicarboxylate cotransporter 1 by Na<sup>+</sup>/H<sup>+</sup> exchanger regulating factor 2, serum and glucocorticoid inducible kinase isoforms, and protein kinase B', *Biochemical & Biophysical Research Communications*, 313, (4), pp. 998-1003.
- Boehmer, C., Laufer, J., Jeyaraj, S., Klaus, F., Lindner, R., Lang, F. and Palmada, M. (2008a) 'Modulation of the voltage-gated potassium channel Kv1.5 by the SGK1 protein kinase involves inhibition of channel ubiquitination', *Cell Physiol Biochem*, 22, (5-6), pp. 591-600.

- Boehmer, C., Palmada, M., Klaus, F., Jeyaraj, S., Lindner, R., Laufer, J., Daniel, H. and Lang, F. (2008b) 'The peptide transporter PEPT2 is targeted by the protein kinase SGK1 and the scaffold protein NHERF2', *Cell Physiol Biochem*, 22, (5-6), pp. 705-14.
- Boehmer, C., Wilhelm, V., Palmada, M., Wallisch, S., Henke, G., Brinkmeier, H., Cohen, P., Pieske, B. and Lang, F. (2003) 'Serum and glucocorticoid inducible kinases in the regulation of the cardiac sodium channel SCN5A', *Cardiovascular Research*, 57, (4), pp. 1079-84.
- Boguski, M. S., Lowe, T. M. and Tolstoshev, C. M. (1993) 'dbEST--database for "expressed sequence tags"', *Nature Genetics*, 4, (4), pp. 332-3.
- Bogusz, A. M., Brickley, D. R., Pew, T. and Conzen, S. D. (2006) 'A novel N-terminal hydrophobic motif mediates constitutive degradation of serum- and glucocorticoid-induced kinase-1 by the ubiquitin-proteasome pathway', *FEBS Journal*, 273, (13), pp. 2913-28.
- Bohmer, C., Palmada, M., Kenngott, C., Lindner, R., Klaus, F., Laufer, J. and Lang, F. (2007) 'Regulation of the epithelial calcium channel TRPV6 by the serum and glucocorticoid-inducible kinase isoforms SGK1 and SGK3', *FEBS Lett*, 581, (29), pp. 5586-90.
- Booth, R. E., Tong, Q., Medina, J., Snyder, P. M., Patel, P. and Stockand, J. D. (2003) 'A region directly following the second transmembrane domain in  $\gamma$ ENaC is required for normal channel gating', *Journal of Biological Chemistry*, 278, (42), pp. 41367-79.
- Brennan, F. E. and Fuller, P. J. (2000) 'Rapid upregulation of serum and glucocorticoid-regulated kinase (sgk) gene expression by corticosteroids in vivo', *Molecular & Cellular Endocrinology*, 166, (2), pp. 129-36.
- Brickley, D. R., Mikosz, C. A., Hagan, C. R. and Conzen, S. D. (2002) 'Ubiquitin modification of serum and glucocorticoid-induced protein kinase-1 (SGK-1)', *Journal of Biological Chemistry*, 277, (45), pp. 43064-70.
- Brunet, A., Park, J., Tran, H., Hu, L. S., Hemmings, B. A. and Greenberg, M. E. (2001) 'Protein kinase SGK mediates survival signals by phosphorylating the forkhead transcription factor FKHRL1 (FOXO3a)', *Molecular & Cellular Biology*, 21, (3), pp. 952-65.
- Brunn, G. J., Williams, J., Sabers, C., Wiederrecht, G., Lawrence, J. C., Jr. and Abraham, R. T. (1996) 'Direct inhibition of the signaling functions of the mammalian target of rapamycin by the phosphoinositide 3-kinase inhibitors, wortmannin and LY294002', *Embo J*, 15, (19), pp. 5256-67.

- Busjahn, A., Aydin, A., Uhlmann, R., Krasko, C., Bähring, S., Szelestei, T., Feng, Y., Dahm, S., Sharma, A. M., Luft, F. C. and Lang, F. (2002) 'Serum- and glucocorticoid-regulated kinase (SGK1) gene and blood pressure', *Hypertension*, 40, (3), pp. 256-60.
- Busjahn, A. and Luft, F. C. (2003) 'Twin studies in the analysis of minor physiological differences between individuals', *Cellular Physiology & Biochemistry*, 13, (1), pp. 51-8.
- Busjahn, A., Seebohm, G., Maier, G., Toliat, M. R., Nurnberg, P., Aydin, A., Luft, F. C. and Lang, F. (2004) 'Association of the serum and glucocorticoid regulated kinase (sgk1) gene with QT interval', *Cellular Physiology & Biochemistry*, 14, (3), pp. 135-42.
- Butterworth, M. B. (2010) 'Regulation of the epithelial sodium channel (ENaC) by membrane trafficking', *Biochim Biophys Acta*.
- Butterworth, M. B., Edinger, R. S., Ovaa, H., Burg, D., Johnson, J. P. and Frizzell, R. A. (2007) 'The deubiquitinating enzyme, UCH-L3 regulates the apical membrane recycling of the epithelial sodium channel (ENaC)', *J Biol Chem*.
- Butterworth, M. B. and Johnson, J. P. (2008) 'USP10: the nexus between nexin and vasopressin', *Am J Physiol Renal Physiol*, 295, (4), pp. F888.
- Butterworth, M. B., Weisz, O. A. and Johnson, J. P. (2008) 'Some assembly required: putting the epithelial sodium channel together', *J Biol Chem*, 283, (51), pp. 35305-9.
- Canessa, C. M., Merillat, A. M. and Rossier, B. C. (1994a) 'Membrane topology of the epithelial sodium channel in intact cells', *American Journal of Physiology*, 267, (6 Pt 1), pp. C1682-90.
- Canessa, C. M., Schild, L., Buell, G., Thorens, B., Gautschi, I., Horisberger, J. D. and Rossier, B. C. (1994b) 'Amiloride-sensitive epithelial Na<sup>+</sup> channel is made of three homologous subunits.[see comment]', *Nature*, 367, (6462), pp. 463-7.
- Carattino, M. D., Hughey, R. P. and Kleyman, T. R. (2008) 'Proteolytic processing of the epithelial sodium channel gamma subunit has a dominant role in channel activation', *J Biol Chem*.
- Carattino, M. D., Liu, W., Hill, W. G., Satlin, L. M. and Kleyman, T. R. (2007) 'Lack of a role of membrane-protein interactions in flow-dependent activation of ENaC', *Am J Physiol Renal Physiol*, 293, (1), pp. F316-24.
- Chang, C. T., Wu, M. S., Tian, Y. C., Chen, K. H., Yu, C. C., Liao, C. H., Hung, C. C. and Yang, C. W. (2007) 'Enhancement of epithelial sodium channel expression in renal cortical collecting ducts cells by advanced glycation end products', *Nephrology Dialysis Transplantation*, 22, (3), pp. 722-31.

- Chen, S. Y., Bhargava, A., Mastroberardino, L., Meijer, O. C., Wang, J., Buse, P., Firestone, G. L., Verrey, F. and Pearce, D. (1999) 'Epithelial sodium channel regulated by aldosterone-induced protein sgk', *Proceedings of the National Academy of Sciences of the United States of America*, 96, (5), pp. 2514-9.
- Chen, W., Chen, Y., Xu, B. E., Juang, Y. C., Stippec, S., Zhao, Y. and Cobb, M. H. (2009) 'Regulation of a third conserved phosphorylation site in SGK1', *J Biol Chem*, 284, (6), pp. 3453-60.
- Cheng, C., Prince, L. S., Snyder, P. M. and Welsh, M. J. (1998) 'Assembly of the epithelial Na<sup>+</sup> channel evaluated using sucrose gradient sedimentation analysis', *Journal of Biological Chemistry*, 273, (35), pp. 22693-700.
- Choate, K. A., Kahle, K. T., Wilson, F. H., Nelson-Williams, C. and Lifton, R. P. (2003) 'WNK1, a kinase mutated in inherited hypertension with hyperkalemia, localizes to diverse Cl<sup>-</sup>-transporting epithelia', *Proceedings of the National Academy of Sciences of the United States of America*, 100, (2), pp. 663-8.
- Chraïbi, A. and Horisberger, J. D. (2002) 'Na<sup>+</sup> self inhibition of human epithelial Na<sup>+</sup> channel: temperature dependence and effect of extracellular proteases', *Journal of General Physiology*, 120, (2), pp. 133-45.
- Chraïbi, A., Schnizler, M., Clauss, W. and Horisberger, J. D. (2001) 'Effects of 8-cpt-cAMP on the epithelial sodium channel expressed in *Xenopus* oocytes', *Journal of Membrane Biology*, 183, (1), pp. 15-23.
- Chun, J., Kwon, T., Lee, E., Suh, P. G., Choi, E. J. and Sun Kang, S. (2002) 'The Na<sup>+</sup>/H<sup>+</sup> exchanger regulatory factor 2 mediates phosphorylation of serum- and glucocorticoid-induced protein kinase 1 by 3-phosphoinositide-dependent protein kinase 1', *Biochemical & Biophysical Research Communications*, 298, (2), pp. 207-15.
- Chun, J., Kwon, T., Lee, E. J., Kim, C. H., Han, Y. S., Hong, S. K., Hyun, S. and Kang, S. S. (2004) '14-3-3 Protein mediates phosphorylation of microtubule-associated protein tau by serum- and glucocorticoid-induced protein kinase 1', *Mol Cells*, 18, (3), pp. 360-8.
- Cordas, E., Naray-Fejes-Toth, A. and Fejes-Toth, G. (2007) 'Subcellular location of serum- and glucocorticoid-induced kinase-1 in renal and mammary epithelial cells', *American Journal of Physiology - Cell Physiology*, 292, (5), pp. C1971-81.
- da Silva, C. A., de Braganca, A. C., Shimizu, M. H., Sanches, T. R., Fortes, M. A., Giorgi, R. R., Andrade, L. and Seguro, A. C. (2009) 'Rosiglitazone prevents sirolimus-induced hypomagnesemia, hypokalemia, and downregulation of NKCC2 protein expression', *Am J Physiol Renal Physiol*, 297, (4), pp. F916-22.

- de Seigneux, S., Leroy, V., Ghzili, H., Rousselot, M., Nielsen, S., Rossier, B. C., Martin, P. Y. and Feraille, E. (2008) 'NF- $\kappa$ B inhibits sodium transport via down-regulation of SGK1 in renal collecting duct principal cells', *J Biol Chem*, 283, (37), pp. 25671-81.
- Debonneville, C., Flores, S. Y., Kamynina, E., Plant, P. J., Tauxe, C., Thomas, M. A., Munster, C., Chraïbi, A., Pratt, J. H., Horisberger, J. D., Pearce, D., Löffing, J. and Staub, O. (2001) 'Phosphorylation of Nedd4-2 by Sgk1 regulates epithelial Na<sup>+</sup> channel cell surface expression', *EMBO Journal*, 20, (24), pp. 7052-9.
- Dehner, M., Hadjihannas, M., Weiske, J., Huber, O. and Behrens, J. (2008) 'Wnt signaling inhibits Forkhead box O3a-induced transcription and apoptosis through up-regulation of serum- and glucocorticoid-inducible kinase 1', *J Biol Chem*, 283, (28), pp. 19201-10.
- Dieter, M., Palmada, M., Rajamanickam, J., Aydin, A., Busjahn, A., Boehmer, C., Luft, F. C. and Lang, F. (2004) 'Regulation of glucose transporter SGLT1 by ubiquitin ligase Nedd4-2 and kinases SGK1, SGK3, and PKB', *Obesity Research*, 12, (5), pp. 862-70.
- Dowling, R. J., Topisirovic, I., Fonseca, B. D. and Sonenberg, N. (2010) 'Dissecting the role of mTOR: lessons from mTOR inhibitors', *Biochim Biophys Acta*, 1804, (3), pp. 433-9.
- Duc, C., Farman, N., Canessa, C. M., Bonvalet, J. P. and Rossier, B. C. (1994) 'Cell-specific expression of epithelial sodium channel alpha, beta, and gamma subunits in aldosterone-responsive epithelia from the rat: localization by in situ hybridization and immunocytochemistry', *Journal of Cell Biology*, 127, (6 Pt 2), pp. 1907-21.
- Edelheit, O., Hanukoglu, I., Shriki, Y., Tfilin, M., Dascal, N., Gillis, D. and Hanukoglu, A. (2010) 'Truncated beta epithelial sodium channel (ENaC) subunits responsible for multi-system pseudohypoaldosteronism support partial activity of ENaC', *J Steroid Biochem Mol Biol*.
- Edinger, R. S., Lebowitz, J., Li, H., Alzamora, R., Wang, H., Johnson, J. P. and Hallows, K. R. (2009) 'Functional regulation of the epithelial Na<sup>+</sup> channel by I $\kappa$ B kinase- $\beta$  occurs via phosphorylation of the ubiquitin ligase Nedd4-2', *J Biol Chem*, 284, (1), pp. 150-7.
- Ellson, C. D., Andrews, S., Stephens, L. R. and Hawkins, P. T. (2002) 'The PX domain: a new phosphoinositide-binding module', *J Cell Sci*, 115, (Pt 6), pp. 1099-105.
- Embark, H. M., Setiawan, I., Poppendieck, S., van de Graaf, S. F., Boehmer, C., Palmada, M., Wieder, T., Gerstberger, R., Cohen, P., Yun, C. C., Bindels, R. J. and Lang, F. (2004) 'Regulation of the epithelial Ca<sup>2+</sup> channel TRPV5 by the NHE regulating factor NHERF2 and the serum and glucocorticoid inducible kinase isoforms SGK1 and SGK3 expressed in *Xenopus* oocytes', *Cellular Physiology & Biochemistry*, 14, (4-6), pp. 203-12.

- Fajac, I., Viel, M., Gaitch, N., Hubert, D. and Bienvenu, T. (2009) 'Combination of ENaC and CFTR mutations may predispose to cystic fibrosis-like disease', *Eur Respir J*, 34, (3), pp. 772-3.
- Fakitsas, P., Adam, G., Daidie, D., van Bemmelen, M. X., Fouladkou, F., Patrignani, A., Wagner, U., Warth, R., Camargo, S. M., Staub, O. and Verrey, F. (2007) 'Early aldosterone-induced gene product regulates the epithelial sodium channel by deubiquitylation', *Journal of the American Society of Nephrology*, 18, (4), pp. 1084-92.
- Fejes-Toth, G., Frindt, G., Naray-Fejes-Toth, A. and Palmer, L. G. (2008) 'Epithelial Na<sup>+</sup> channel activation and processing in mice lacking SGK1', *Am J Physiol Renal Physiol*.
- Fels, J., Oberleithner, H. and Kusche-Vihrog, K. (2010) 'Ménage à trois: Aldosterone, sodium and nitric oxide in vascular endothelium', *Biochim Biophys Acta*.
- Feng, Y., Wang, Q., Wang, Y., Yard, B. and Lang, F. (2005) 'SGK1-mediated fibronectin formation in diabetic nephropathy', *Cell Physiol Biochem*, 16, (4-6), pp. 237-44.
- Fenton, R. A. and Knepper, M. A. (2007) 'Mouse models and the urinary concentrating mechanism in the new millennium', *Physiol Rev*, 87, (4), pp. 1083-112.
- Feraille, E., Mordasini, D., Gonin, S., Deschenes, G., Vinciguerra, M., Doucet, A., Vandewalle, A., Summa, V., Verrey, F. and Martin, P. Y. (2003) 'Mechanism of control of Na<sup>+</sup>,K<sup>+</sup>-ATPase in principal cells of the mammalian collecting duct', *Annals of the New York Academy of Sciences*, 986, pp. 570-8.
- Firsov, D., Gautschi, I., Merillat, A. M., Rossier, B. C. and Schild, L. (1998) 'The heterotetrameric architecture of the epithelial sodium channel (ENaC)', *EMBO Journal*, 17, (2), pp. 344-52.
- Flores, S. Y., Loffing-Cueni, D., Kamynina, E., Daidie, D., Gerbex, C., Chabanel, S., Dudler, J., Loffing, J. and Staub, O. (2005) 'Aldosterone-induced serum and glucocorticoid-induced kinase 1 expression is accompanied by Nedd4-2 phosphorylation and increased Na<sup>+</sup> transport in cortical collecting duct cells', *Journal of the American Society of Nephrology*, 16, (8), pp. 2279-87.
- Foster, K. G. and Fingar, D. C. (2010) 'Mammalian target of rapamycin (mTOR): conducting the cellular signaling symphony', *J Biol Chem*, 285, (19), pp. 14071-7.
- Fuller, P. J. and Young, M. J. (2005) 'Mechanisms of mineralocorticoid action', *Hypertension*, 46, (6), pp. 1227-35.
- Fuster, D. G., Bobulescu, I. A., Zhang, J., Wade, J. and Moe, O. W. (2007) 'Characterization of the regulation of renal Na<sup>+</sup>/H<sup>+</sup> exchanger NHE3 by insulin', *American Journal of Physiology - Renal Physiology*, 292, (2), pp. F577-85.

- Gaeggeler, H. P., Gonzalez-Rodriguez, E., Jaeger, N. F., Loffing-Cueni, D., Norregaard, R., Loffing, J., Horisberger, J. D. and Rossier, B. C. (2005) 'Mineralocorticoid versus glucocorticoid receptor occupancy mediating aldosterone-stimulated sodium transport in a novel renal cell line', *Journal of the American Society of Nephrology*, 16, (4), pp. 878-91.
- Gamper, N., Fillon, S., Huber, S. M., Feng, Y., Kobayashi, T., Cohen, P. and Lang, F. (2002) 'IGF-1 up-regulates K<sup>+</sup> channels via PI3-kinase, PDK1 and SGK1', *Pflugers Archiv - European Journal of Physiology*, 443, (4), pp. 625-34.
- Garcia-Caballero, A., Rasmussen, J. E., Gaillard, E., Watson, M. J., Olsen, J. C., Donaldson, S. H., Stutts, M. J. and Tarran, R. (2009) 'SPLUNC1 regulates airway surface liquid volume by protecting ENaC from proteolytic cleavage', *Proc Natl Acad Sci U S A*, 106, (27), pp. 11412-7.
- Garcia-Martinez, J. M. and Alessi, D. R. (2008) 'mTOR complex 2 (mTORC2) controls hydrophobic motif phosphorylation and activation of serum- and glucocorticoid-induced protein kinase 1 (SGK1)', *Biochem J*, 416, (3), pp. 375-85.
- Garcia-Martinez, J. M., Moran, J., Clarke, R. G., Gray, A., Cosulich, S. C., Chresta, C. M. and Alessi, D. R. (2009) 'Ku-0063794 is a specific inhibitor of the mammalian target of rapamycin (mTOR)', *Biochem J*, 421, (1), pp. 29-42.
- Garty, H. and Palmer, L. G. (1997) 'Epithelial sodium channels: function, structure, and regulation', *Physiological Reviews*, 77, (2), pp. 359-96.
- Gharbi, S. I., Zvelebil, M. J., Shuttleworth, S. J., Hancox, T., Saghir, N., Timms, J. F. and Waterfield, M. D. (2007) 'Exploring the specificity of the PI3K family inhibitor LY294002', *Biochem J*, 404, (1), pp. 15-21.
- Gomez-Sanchez, E. P. (2010) 'The mammalian mineralocorticoid receptor: tying down a promiscuous receptor', *Exp Physiol*, 95, (1), pp. 13-8.
- Gonin, S., Deschenes, G., Roger, F., Bens, M., Martin, P. Y., Carpentier, J. L., Vandewalle, A., Doucet, A. and Feraille, E. (2001) 'Cyclic AMP increases cell surface expression of functional Na<sup>+</sup>,K<sup>+</sup>-ATPase units in mammalian cortical collecting duct principal cells', *Molecular Biology of the Cell*, 12, (2), pp. 255-64.
- Gonzalez-Robayna, I. J., Falender, A. E., Ochsner, S., Firestone, G. L. and Richards, J. S. (2000) 'Follicle-Stimulating hormone (FSH) stimulates phosphorylation and activation of protein kinase B (PKB/Akt) and serum and glucocorticoid-induced kinase (Sgk): evidence for A kinase-independent signaling by FSH in granulosa cells', *Molecular Endocrinology*, 14, (8), pp. 1283-300.
- Gonzalez-Rodriguez, E., Gaeggeler, H. P. and Rossier, B. C. (2007) 'IGF-1 vs insulin: Respective roles in modulating sodium transport via the PI-3 kinase/Sgk1 pathway in a cortical collecting duct cell line', *Kidney International*, 71, (2), pp. 116-25.

- Goulet, C. C., Volk, K. A., Adams, C. M., Prince, L. S., Stokes, J. B. and Snyder, P. M. (1998) 'Inhibition of the epithelial Na<sup>+</sup> channel by interaction of Nedd4 with a PY motif deleted in Liddle's syndrome', *Journal of Biological Chemistry*, 273, (45), pp. 30012-7.
- Greger, R. (2000) 'Physiology of renal sodium transport', *Am J Med Sci*, 319, (1), pp. 51-62.
- Halawani, D. and Latterich, M. (2006) 'p97: The cell's molecular purgatory?' *Mol Cell*, 22, (6), pp. 713-7.
- Hall, B. A. (2007) *The identification and characterisation of novel serum and glucocorticoid regulated kinase 1 (SGK1) isoforms in human skin*. PhD thesis. Newcastle University.
- Hallows, K. R., Bhalla, V., Oyster, N. M., Wijngaarden, M. A., Lee, J. K., Li, H., Chandran, S., Xia, X., Huang, Z., Chalkley, R. J., Burlingame, A. L. and Pearce, D. (2010) 'Phosphopeptide screen uncovers novel Nedd4-2 phosphorylation sites that potentiate its inhibition of the epithelial Na<sup>+</sup> channel', *J Biol Chem*.
- Hallows, K. R., Wang, H., Edinger, R. S., Butterworth, M. B., Oyster, N. M., Li, H., Buck, J., Levin, L. R., Johnson, J. P. and Pastor-Soler, N. M. (2009) 'Regulation of epithelial Na<sup>+</sup> transport by soluble adenylyl cyclase in kidney collecting duct cells', *J Biol Chem*.
- Harris, M., Garcia-Caballero, A., Stutts, M. J., Firsov, D. and Rossier, B. C. (2008) 'Preferential assembly of ENaC subunits in Xenopus oocyte: Role of furin-mediated endogenous proteolysis', *J Biol Chem*.
- Hayashi, M., Tapping, R. I., Chao, T. H., Lo, J. F., King, C. C., Yang, Y. and Lee, J. D. (2001) 'BMK1 mediates growth factor-induced cell proliferation through direct cellular activation of serum and glucocorticoid-inducible kinase', *Journal of Biological Chemistry*, 276, (12), pp. 8631-4.
- Heise, C. J., Xu, B. E., Deaton, S. L., Cha, S. K., Cheng, C. J., Sengupta, S., Juang, Y. C., Stippec, S., Xu, Y., Zhao, Y., Huang, C. L. and Cobb, M. H. (2010) 'Serum and glucocorticoid-induced kinase (SGK) 1 and the epithelial sodium channel are regulated by multiple with no lysine (WNK) family members', *J Biol Chem*.
- Higgins, B. and Williams, B. (2007) 'Pharmacological management of hypertension', *Clin Med*, 7, (6), pp. 612-6.
- Hills, C. E., Bland, R., Bennett, J., Ronco, P. M. and Squires, P. E. (2006) 'High glucose up-regulates ENaC and SGK1 expression in HCD-cells', *Cellular Physiology & Biochemistry*, 18, (6), pp. 337-46.
- Hollenberg, N. K., Stevanovic, R., Agarwal, A., Lansang, M. C., Price, D. A., Laffel, L. M., Williams, G. H. and Fisher, N. D. (2004) 'Plasma aldosterone concentration in the patient with diabetes mellitus', *Kidney Int*, 65, (4), pp. 1435-9.

- Hong, F., Larrea, M. D., Doughty, C., Kwiatkowski, D. J., Squillace, R. and Slingerland, J. M. (2008) 'mTOR-raptor binds and activates SGK1 to regulate p27 phosphorylation', *Mol Cell*, 30, (6), pp. 701-11.
- Hong, G., Lockhart, A., Davis, B., Rahmoune, H., Baker, S., Ye, L., Thompson, P., Shou, Y., O'Shaughnessy, K., Ronco, P. and Brown, J. (2003) 'PPAR $\gamma$  activation enhances cell surface ENaC $\alpha$  via up-regulation of SGK1 in human collecting duct cells', *FASEB Journal*, 17, (13), pp. 1966-8.
- Huang, D. Y., Boini, K. M., Osswald, H., Friedrich, B., Artunc, F., Ullrich, S., Rajamanickam, J., Palmada, M., Wulff, P., Kuhl, D., Vallon, V. and Lang, F. (2006) 'Resistance of mice lacking the serum- and glucocorticoid-inducible kinase SGK1 against salt-sensitive hypertension induced by a high-fat diet', *American Journal of Physiology - Renal Physiology*, 291, (6), pp. F1264-73.
- Huang, D. Y., Wulff, P., Volkl, H., Loffing, J., Richter, K., Kuhl, D., Lang, F. and Vallon, V. (2004) 'Impaired regulation of renal K<sup>+</sup> elimination in the sgk1-knockout mouse', *J Am Soc Nephrol*, 15, (4), pp. 885-91.
- Huber, R., Krueger, B., Diakov, A., Korbmacher, J., Haerteis, S., Einsiedel, J., Gmeiner, P., Azad, A. K., Cuppens, H., Cassiman, J. J., Korbmacher, C. and Rauh, R. (2010) 'Functional characterization of a partial loss-of-function mutation of the epithelial sodium channel (ENaC) associated with atypical cystic fibrosis', *Cell Physiol Biochem*, 25, (1), pp. 145-58.
- Inglis, S. K., Gallacher, M., Brown, S. G., McTavish, N., Getty, J., Husband, E. M., Murray, J. T. and Wilson, S. M. (2008) 'SGK1 activity in Na<sup>+</sup> absorbing airway epithelial cells monitored by assaying NDRG1-Thr(346/356/366) phosphorylation', *Pflugers Arch*.
- Itani, O. A., Liu, K. Z., Cornish, K. L., Campbell, J. R. and Thomas, C. P. (2002) 'Glucocorticoids stimulate human sgk1 gene expression by activation of a GRE in its 5'-flanking region', *American Journal of Physiology - Endocrinology & Metabolism*, 283, (5), pp. E971-9.
- Ji, H. L., Su, X. F., Kedar, S., Li, J., Barbry, P., Smith, P. R., Matalon, S. and Benos, D. J. (2006) ' $\delta$ -subunit confers novel biophysical features to  $\alpha\beta\gamma$ -human epithelial sodium channel (ENaC) via a physical interaction', *J Biol Chem*, 281, (12), pp. 8233-41.
- Jin, H. S., Hong, K. W., Lim, J. E., Hwang, S. Y., Lee, S. H., Shin, C., Park, H. K. and Oh, B. (2010) 'Genetic Variations in the Sodium Balance-Regulating Genes ENaC, NEDD4L, NDFIP2 and USP2 Influence Blood Pressure and Hypertension', *Kidney Blood Press Res*, 33, (1), pp. 15-23.
- Kabra, R., Knight, K. K., Zhou, R. and Snyder, P. M. (2008) 'Nedd4-2 induces endocytosis and degradation of proteolytically cleaved epithelial Na<sup>+</sup> channels', *J Biol Chem*, 283, (10), pp. 6033-9.

- Kahle, K. T., Rinehart, J., Ring, A., Gimenez, I., Gamba, G., Hebert, S. C. and Lifton, R. P. (2006) 'WNK protein kinases modulate cellular Cl<sup>-</sup> flux by altering the phosphorylation state of the Na<sup>+</sup>-K<sup>+</sup>-Cl<sup>-</sup> and K<sup>+</sup>-Cl<sup>-</sup> cotransporters', *Physiology*, 21, pp. 326-35.
- Kahle, K. T., Wilson, F. H. and Lifton, R. P. (2005) 'Regulation of diverse ion transport pathways by WNK4 kinase: a novel molecular switch', *Trends in Endocrinology & Metabolism*, 16, (3), pp. 98-103.
- Kamynina, E. and Staub, O. (2002) 'Concerted action of ENaC, Nedd4-2, and Sgk1 in transepithelial Na<sup>+</sup> transport', *American Journal of Physiology - Renal Physiology*, 283, (3), pp. F377-87.
- Ke, Y., Butt, A. G., Swart, M., Liu, Y. F. and McDonald, F. J. (2010) 'COMMD1 down-regulates the epithelial sodium channel through Nedd4-2', *Am J Physiol Renal Physiol*.
- Kleyman, T. R., Carattino, M. D. and Hughey, R. P. (2009) 'ENaC at the cutting edge: Regulation of epithelial sodium channels by proteases', *J Biol Chem*.
- Knight, K. K., Olson, D. R., Zhou, R. and Snyder, P. M. (2006) 'Liddle's syndrome mutations increase Na<sup>+</sup> transport through dual effects on epithelial Na<sup>+</sup> channel surface expression and proteolytic cleavage', *Proceedings of the National Academy of Sciences of the United States of America*, 103, (8), pp. 2805-8.
- Kobayashi, T. and Cohen, P. (1999) 'Activation of serum- and glucocorticoid-regulated protein kinase by agonists that activate phosphatidylinositide 3-kinase is mediated by 3-phosphoinositide-dependent protein kinase-1 (PDK1) and PDK2', *Biochemical Journal*, 339, (Pt 2), pp. 319-28.
- Kobayashi, T., Deak, M., Morrice, N. and Cohen, P. (1999) 'Characterization of the structure and regulation of two novel isoforms of serum- and glucocorticoid-induced protein kinase', *Biochemical Journal*, 344 Pt 1, pp. 189-97.
- Komander, D., Fairservice, A., Deak, M., Kular, G. S., Prescott, A. R., Peter Downes, C., Safrany, S. T., Alessi, D. R. and van Aalten, D. M. (2004) 'Structural insights into the regulation of PDK1 by phosphoinositides and inositol phosphates', *EMBO Journal*, 23, (20), pp. 3918-28.
- Kumar, J. M., Brooks, D. P., Olson, B. A. and Laping, N. J. (1999) 'Sgk, a putative serine/threonine kinase, is differentially expressed in the kidney of diabetic mice and humans', *Journal of the American Society of Nephrology*, 10, (12), pp. 2488-94.
- Kyriakis, J. M. (2007) 'The integration of signaling by multiprotein complexes containing Raf kinases', *Biochim Biophys Acta*, 1773, (8), pp. 1238-47.

- Lang, F., Artunc, F. and Vallon, V. (2009a) 'The physiological impact of the serum and glucocorticoid-inducible kinase SGK1', *Curr Opin Nephrol Hypertens*, 18, (5), pp. 439-48.
- Lang, F., Bohmer, C., Palmada, M., Seebohm, G., Strutz-Seebohm, N. and Vallon, V. (2006) '(Patho)physiological significance of the serum- and glucocorticoid-inducible kinase isoforms', *Physiological Reviews*, 86, (4), pp. 1151-78.
- Lang, F. and Gorlach, A. (2010) 'Heterocyclic indazole derivatives as SGK1 inhibitors, WO2008138448', *Expert Opin Ther Pat*, 20, (1), pp. 129-35.
- Lang, F., Gorlach, A. and Vallon, V. (2009b) 'Targeting SGK1 in diabetes', *Expert Opin Ther Targets*.
- Lang, F., Henke, G., Embark, H. M., Waldegger, S., Palmada, M., Bohmer, C. and Vallon, V. (2003) 'Regulation of channels by the serum and glucocorticoid-inducible kinase - implications for transport, excitability and cell proliferation', *Cellular Physiology & Biochemistry*, 13, (1), pp. 41-50.
- Lang, F., Klingel, K., Wagner, C. A., Stegen, C., Warntges, S., Friedrich, B., Lanzendorfer, M., Melzig, J., Moschen, I., Steuer, S., Waldegger, S., Sauter, M., Paulmichl, M., Gerke, V., Risler, T., Gamba, G., Capasso, G., Kandolf, R., Hebert, S. C., Massry, S. G. and Broer, S. (2000) 'Deranged transcriptional regulation of cell-volume-sensitive kinase hSGK in diabetic nephropathy.[see comment]', *Proceedings of the National Academy of Sciences of the United States of America*, 97, (14), pp. 8157-62.
- Lang, F., Strutz-Seebohm, N., Seebohm, G. and Lang, U. E. (2010) 'Significance of SGK1 in the regulation of neuronal function', *J Physiol*.
- Laufer, J., Boehmer, C., Jeyaraj, S., Knuwer, M., Klaus, F., Lindner, R., Palmada, M. and Lang, F. (2009) 'The C-terminal PDZ-binding motif in the Kv1.5 potassium channel governs its modulation by the Na<sup>+</sup>/H<sup>+</sup> exchanger regulatory factor 2', *Cell Physiol Biochem*, 23, (1-3), pp. 25-36.
- Lawes, C. M., Vander Hoorn, S. and Rodgers, A. (2008) 'Global burden of blood-pressure-related disease, 2001', *Lancet*, 371, (9623), pp. 1513-8.
- Lee, I. H., Campbell, C. R., Cook, D. I. and Dinudom, A. (2008) 'Regulation of epithelial Na<sup>+</sup> channels by aldosterone: role of Sgk1', *Clin Exp Pharmacol Physiol*, 35, (2), pp. 235-41.
- Leenen, F. H. (2010) 'The central role of the brain aldosterone - "ouabain" pathway in salt-sensitive hypertension', *Biochim Biophys Acta*.
- Leng, Q., Kahle, K. T., Rinehart, J., MacGregor, G. G., Wilson, F. H., Canessa, C. M., Lifton, R. P. and Hebert, S. C. (2006) 'WNK3, a kinase related to genes mutated in hereditary hypertension with hyperkalaemia, regulates the K<sup>+</sup> channel ROMK1 (Kir1.1)', *Journal of Physiology*, 571, (Pt 2), pp. 275-86.

- Leong, M. L., Maiyar, A. C., Kim, B., O'Keeffe, B. A. and Firestone, G. L. (2003) 'Expression of the serum- and glucocorticoid-inducible protein kinase, Sgk, is a cell survival response to multiple types of environmental stress stimuli in mammary epithelial cells', *Journal of Biological Chemistry*, 278, (8), pp. 5871-82.
- Leroy, V., De Seigneux, S., Agassiz, V., Hasler, U., Rafestin-Oblin, M. E., Vinciguerra, M., Martin, P. Y. and Feraille, E. (2008) 'Aldosterone Activates NF- $\kappa$ B in the Collecting Duct', *J Am Soc Nephrol*.
- Lester, D. S., Asher, C. and Garty, H. (1988) 'Characterization of cAMP-induced activation of epithelial sodium channels', *American Journal of Physiology*, 254, (6 Pt 1), pp. C802-8.
- Li, H., Sheppard, D. N. and Hug, M. J. (2004) 'Transepithelial electrical measurements with the Ussing chamber', *J Cyst Fibros*, 3 Suppl 2, pp. 123-6.
- Li, K., Guo, D., Zhu, H., Hering-Smith, K. S., Hamm, L. L., Ouyang, J. and Dong, Y. (2010) 'Interleukin-6 Stimulates Epithelial Sodium Channels in Mouse Cortical Collecting Duct Cells', *Am J Physiol Regul Integr Comp Physiol*.
- Liang, X., Peters, K. W., Butterworth, M. B. and Frizzell, R. A. (2006) '14-3-3 isoforms are induced by aldosterone and participate in its regulation of epithelial sodium channels', *Journal of Biological Chemistry*, 281, (24), pp. 16323-32.
- Liu, P., Cheng, H., Roberts, T. M. and Zhao, J. J. (2009) 'Targeting the phosphoinositide 3-kinase pathway in cancer', *Nat Rev Drug Discov*, 8, (8), pp. 627-44.
- Lizcano, J. M., Deak, M., Morrice, N., Kieloch, A., Hastie, C. J., Dong, L., Schutkowski, M., Reimer, U. and Alessi, D. R. (2002) 'Molecular basis for the substrate specificity of NIMA-related kinase-6 (NEK6). Evidence that NEK6 does not phosphorylate the hydrophobic motif of ribosomal S6 protein kinase and serum- and glucocorticoid-induced protein kinase in vivo', *J Biol Chem*, 277, (31), pp. 27839-49.
- Loewith, R., Jacinto, E., Wullschleger, S., Lorberg, A., Crespo, J. L., Bonenfant, D., Oppliger, W., Jenoe, P. and Hall, M. N. (2002) 'Two TOR complexes, only one of which is rapamycin sensitive, have distinct roles in cell growth control', *Mol Cell*, 10, (3), pp. 457-68.
- Loffing, J., Pietri, L., Aregger, F., Bloch-Faure, M., Ziegler, U., Meneton, P., Rossier, B. C. and Kaissling, B. (2000) 'Differential subcellular localization of ENaC subunits in mouse kidney in response to high- and low-Na<sup>+</sup> diets', *American Journal of Physiology - Renal Physiology*, 279, (2), pp. F252-8.
- Loffing, J., Zecevic, M., Feraille, E., Kaissling, B., Asher, C., Rossier, B. C., Firestone, G. L., Pearce, D. and Verrey, F. (2001) 'Aldosterone induces rapid apical translocation of ENaC in early portion of renal collecting system: possible role of SGK', *American Journal of Physiology - Renal Physiology*, 280, (4), pp. F675-82.

- Lu, C., Pribanic, S., Debonneville, A., Jiang, C. and Rotin, D. (2007) 'The PY Motif of ENaC, Mutated in Liddle Syndrome, Regulates Channel Internalization, Sorting and Mobilization from Subapical Pool', *Traffic*.
- Lu, M., Wang, J., Jones, K. T., Ives, H. E., Feldman, M. E., Yao, L. J., Shokat, K. M., Ashrafi, K. and Pearce, D. (2010) 'mTOR Complex-2 Activates ENaC by Phosphorylating SGK1', *J Am Soc Nephrol*.
- Mall, M. (2008) 'Role of ENaC in the pathogenesis and as a therapeutic target for cystic fibrosis lung disease', *Exp Physiol*.
- Marieb, E. N. (2000) *Human anatomy & physiology*. Benjamin Cummings.
- Markadieu, N., Blero, D., Boom, A., Erneux, C. and Beauwens, R. (2004) 'Phosphatidylinositol 3,4,5-trisphosphate: an early mediator of insulin-stimulated sodium transport in A6 cells', *Am J Physiol Renal Physiol*, 287, (2), pp. F319-28.
- McCormick, J. A., Bhalla, V., Pao, A. C. and Pearce, D. (2005) 'SGK1: a rapid aldosterone-induced regulator of renal sodium reabsorption', *Physiology*, 20, pp. 134-9.
- McEneaney, V., Dooley, R., Yusef, Y. R., Keating, N., Quinn, U., Harvey, B. J. and Thomas, W. (2010) 'Protein kinase D1 modulates aldosterone-induced ENaC activity in a renal cortical collecting duct cell line', *Mol Cell Endocrinol*.
- McManus, E. J., Collins, B. J., Ashby, P. R., Prescott, A. R., Murray-Tait, V., Armit, L. J., Arthur, J. S. and Alessi, D. R. (2004) 'The in vivo role of PtdIns(3,4,5)P3 binding to PDK1 PH domain defined by knockin mutation', *EMBO Journal*, 23, (10), pp. 2071-82.
- Meneton, P., Jeunemaitre, X., de Wardener, H. E. and MacGregor, G. A. (2005) 'Links between dietary salt intake, renal salt handling, blood pressure, and cardiovascular diseases', *Physiol Rev*, 85, (2), pp. 679-715.
- Meneton, P., Loffing, J. and Warnock, D. G. (2004) 'Sodium and potassium handling by the aldosterone-sensitive distal nephron: the pivotal role of the distal and connecting tubule', *Am J Physiol Renal Physiol*, 287, (4), pp. F593-601.
- Menniti, M., Iuliano, R., Amato, R., Boito, R., Corea, M., Le Pera, I., Gulletta, E., Fuiano, G. and Perrotti, N. (2005) 'Serum and glucocorticoid-regulated kinase Sgk1 inhibits insulin-dependent activation of phosphomannomutase 2 in transfected COS-7 cells', *Am J Physiol Cell Physiol*, 288, (1), pp. C148-55.
- Michlig, S., Mercier, A., Doucet, A., Schild, L., Horisberger, J. D., Rossier, B. C. and Firsov, D. (2004) 'ERK1/2 controls Na<sup>+</sup>,K<sup>+</sup>-ATPase activity and transepithelial sodium transport in the principal cell of the cortical collecting duct of the mouse kidney', *Journal of Biological Chemistry*, 279, (49), pp. 51002-12.

- Mick, V. E., Itani, O. A., Loftus, R. W., Husted, R. F., Schmidt, T. J. and Thomas, C. P. (2001) 'The  $\alpha$ -subunit of the epithelial sodium channel is an aldosterone-induced transcript in mammalian collecting ducts, and this transcriptional response is mediated via distinct cis-elements in the 5'-flanking region of the gene', *Molecular Endocrinology*, 15, (4), pp. 575-88.
- Mies, F., Spriet, C., Heliot, L. and Sariban-Sohraby, S. (2007) 'Epithelial Na<sup>+</sup> Channel Stimulation by n-3 Fatty Acids Requires Proximity to a Membrane-bound A-kinase-anchoring Protein Complexed with Protein Kinase A and Phosphodiesterase', *Journal of Biological Chemistry*, 282, (25), pp. 18339-47.
- Mikosz, C. A., Brickley, D. R., Sharkey, M. S., Moran, T. W. and Conzen, S. D. (2001) 'Glucocorticoid receptor-mediated protection from apoptosis is associated with induction of the serine/threonine survival kinase gene, *sgk-1*', *Journal of Biological Chemistry*, 276, (20), pp. 16649-54.
- Mita, M., Sankhala, K., Abdel-Karim, I., Mita, A. and Giles, F. (2008) 'Deforolimus (AP23573) a novel mTOR inhibitor in clinical development', *Expert Opin Investig Drugs*, 17, (12), pp. 1947-54.
- Mizuno, H. and Nishida, E. (2001) 'The ERK MAP kinase pathway mediates induction of SGK (serum- and glucocorticoid-inducible kinase) by growth factors', *Genes to Cells*, 6, (3), pp. 261-8.
- Mora, A., Komander, D., van Aalten, D. M. and Alessi, D. R. (2004) 'PDK1, the master regulator of AGC kinase signal transduction', *Seminars in Cell & Developmental Biology*, 15, (2), pp. 161-70.
- Moriguchi, T., Urushiyama, S., Hisamoto, N., Iemura, S., Uchida, S., Natsume, T., Matsumoto, K. and Shibuya, H. (2005) 'WNK1 regulates phosphorylation of cation-chloride-coupled cotransporters via the STE20-related kinases, SPAK and OSR1', *J Biol Chem*, 280, (52), pp. 42685-93.
- Morris, D. J., Souness, G. W., Brem, A. S. and Oblin, M. E. (2000) 'Interactions of mineralocorticoids and glucocorticoids in epithelial target tissues', *Kidney International*, 57, (4), pp. 1370-3.
- Muller, O. G., Parnova, R. G., Centeno, G., Rossier, B. C., Firsov, D. and Horisberger, J. D. (2003) 'Mineralocorticoid effects in the kidney: correlation between  $\alpha$ ENaC, GILZ, and *Sgk-1* mRNA expression and urinary excretion of Na<sup>+</sup> and K<sup>+</sup>', *Journal of the American Society of Nephrology*, 14, (5), pp. 1107-15.
- Murray, J. T., Campbell, D. G., Morrice, N., Auld, G. C., Shpiro, N., Marquez, R., Peggie, M., Bain, J., Bloomberg, G. B., Grahammer, F., Lang, F., Wulff, P., Kuhl, D. and Cohen, P. (2004) 'Exploitation of KESTREL to identify NDRG family members as physiological substrates for SGK1 and GSK3', *Biochem J*, 384, (Pt 3), pp. 477-88.

- Mustafa, S. B., Castro, R., Falck, A. J., Petershack, J. A., Henson, B. M., Mendoza, Y. M., Choudary, A. and Seidner, S. R. (2008) 'Protein kinase A and mitogen-activated protein kinase pathways mediate cAMP induction of alpha-epithelial Na<sup>+</sup> channels (alpha-ENaC)', *J Cell Physiol*, 215, (1), pp. 101-10.
- Myerburg, M. M., Harvey, P. R., Heidrich, E. M., Pilewski, J. M. and Butterworth, M. (2010) 'Acute Regulation of ENaC in Airway Epithelia by Proteases and Trafficking', *Am J Respir Cell Mol Biol*.
- Nagaki, K., Yamamura, H., Shimada, S., Saito, T., Hisanaga, S., Taoka, M., Isobe, T. and Ichimura, T. (2006) '14-3-3 Mediates phosphorylation-dependent inhibition of the interaction between the ubiquitin E3 ligase Nedd4-2 and epithelial Na<sup>+</sup> channels', *Biochemistry*, 45, (21), pp. 6733-40.
- Naray-Fejes-Toth, A., Canessa, C., Cleaveland, E. S., Aldrich, G. and Fejes-Toth, G. (1999) 'sgk is an aldosterone-induced kinase in the renal collecting duct. Effects on epithelial Na<sup>+</sup> channels', *Journal of Biological Chemistry*, 274, (24), pp. 16973-8.
- Naray-Fejes-Toth, A. and Fejes-Toth, G. (2000) 'The sgk, an aldosterone-induced gene in mineralocorticoid target cells, regulates the epithelial sodium channel', *Kidney Int*, 57, (4), pp. 1290-4.
- Naray-Fejes-Toth, A., Helms, M. N., Stokes, J. B. and Fejes-Toth, G. (2004a) 'Regulation of sodium transport in mammalian collecting duct cells by aldosterone-induced kinase, SGK1: structure/function studies', *Molecular & Cellular Endocrinology*, 217, (1-2), pp. 197-202.
- Naray-Fejes-Toth, A., Snyder, P. M. and Fejes-Toth, G. (2004b) 'The kidney-specific WNK1 isoform is induced by aldosterone and stimulates epithelial sodium channel-mediated Na<sup>+</sup> transport', *Proceedings of the National Academy of Sciences of the United States of America*, 101, (50), pp. 17434-9.
- Nesterov, V., Dahlmann, A., Bertog, M. and Korbmacher, C. (2008) 'Trypsin can activate the epithelial sodium channel (ENaC) in microdissected mouse distal nephron', *Am J Physiol Renal Physiol*, 295, (4), pp. F1052-62.
- Nofziger, C., Chen, L., Shane, M. A., Smith, C. D., Brown, K. K. and Blazer-Yost, B. L. (2005) 'PPARgamma agonists do not directly enhance basal or insulin-stimulated Na<sup>+</sup> transport via the epithelial Na<sup>+</sup> channel', *Pflugers Arch*, 451, (3), pp. 445-53.
- Novaira, H. J., Botelho, B. F., Goldenberg, R. C., Guggino, S. E. and Morales, M. M. (2004) 'Modulation of renal CNG-A3 sodium channel in rats subjected to low- and high-sodium diets', *Biochim Biophys Acta*, 1665, (1-2), pp. 101-10.
- O'Neil, R. G. and Hayhurst, R. A. (1985) 'Functional differentiation of cell types of cortical collecting duct', *American Journal of Physiology*, 248, (3 Pt 2), pp. F449-53.

- O'Reilly, M., Marshall, E., Macgillivray, T., Mittal, M., Xue, W., Kenyon, C. J. and Brown, R. W. (2006) 'Dietary electrolyte-driven responses in the renal WNK kinase pathway in vivo', *J Am Soc Nephrol*, 17, (9), pp. 2402-13.
- O'Reilly, M., Marshall, E., Speirs, H. J. and Brown, R. W. (2003) 'WNK1, a gene within a novel blood pressure control pathway, tissue-specifically generates radically different isoforms with and without a kinase domain', *Journal of the American Society of Nephrology*, 14, (10), pp. 2447-56.
- O'Shaughnessy, K. M. and Karet, F. E. (2006) 'Salt handling and hypertension', *Annu Rev Nutr*, 26, pp. 343-65.
- Palmada, M., Boehmer, C., Akel, A., Rajamanickam, J., Jeyaraj, S., Keller, K. and Lang, F. (2006) 'SGK1 kinase upregulates GLUT1 activity and plasma membrane expression', *Diabetes*, 55, (2), pp. 421-7.
- Palmada, M., Dieter, M., Boehmer, C., Waldegger, S. and Lang, F. (2004a) 'Serum and glucocorticoid inducible kinases functionally regulate ClC-2 channels', *Biochemical & Biophysical Research Communications*, 321, (4), pp. 1001-6.
- Palmada, M., Dieter, M., Speil, A., Bohmer, C., Mack, A. F., Wagner, H. J., Klingel, K., Kandolf, R., Murer, H., Biber, J., Closs, E. I. and Lang, F. (2004b) 'Regulation of intestinal phosphate cotransporter NaPi IIb by ubiquitin ligase Nedd4-2 and by serum- and glucocorticoid-dependent kinase 1', *American Journal of Physiology - Gastrointestinal & Liver Physiology*, 287, (1), pp. G143-50.
- Palmada, M., Poppendieck, S., Embark, H. M., van de Graaf, S. F., Boehmer, C., Bindels, R. J. and Lang, F. (2005) 'Requirement of PDZ domains for the stimulation of the epithelial Ca<sup>2+</sup> channel TRPV5 by the NHE regulating factor NHERF2 and the serum and glucocorticoid inducible kinase SGK1', *Cellular Physiology & Biochemistry*, 15, (1-4), pp. 175-82.
- Pao, A. C., McCormick, J. A., Li, H., Siu, J., Govaerts, C., Bhalla, V., Soundararajan, R. and Pearce, D. (2007) 'NH2 terminus of serum and glucocorticoid-regulated kinase 1 binds to phosphoinositides and is essential for isoform-specific physiological functions', *American Journal of Physiology - Renal Physiology*, 292, (6), pp. F1741-50.
- Park, J., Leong, M. L., Buse, P., Maiyar, A. C., Firestone, G. L. and Hemmings, B. A. (1999) 'Serum and glucocorticoid-inducible kinase (SGK) is a target of the PI3Kinase-stimulated signaling pathway', *EMBO Journal*, 18, (11), pp. 3024-33.
- Pearce, L. R., Komander, D. and Alessi, D. R. (2010) 'The nuts and bolts of AGC protein kinases', *Nat Rev Mol Cell Biol*, 11, (1), pp. 9-22.
- Perlewitz, A., Nafz, B., Skalweit, A., Fahling, M., Persson, P. B. and Thiele, B. J. (2010) 'Aldosterone and vasopressin affect  $\alpha$ - and  $\gamma$ -ENaC mRNA translation', *Nucleic Acids Res.*

- Perrotti, N., He, R. A., Phillips, S. A., Haft, C. R. and Taylor, S. I. (2001) 'Activation of serum- and glucocorticoid-induced protein kinase (Sgk) by cyclic AMP and insulin', *J Biol Chem*, 276, (12), pp. 9406-12.
- Planes, C., Randrianarison, N. H., Charles, R. P., Frateschi, S., Cluzeaud, F., Vuagniaux, G., Soler, P., Clerici, C., Rossier, B. C. and Hummler, E. (2010) 'ENaC-mediated alveolar fluid clearance and lung fluid balance depend on the channel-activating protease 1', *EMBO Mol Med*, 2, (1), pp. 26-37.
- Pochynyuk, O., Rieg, T., Bugaj, V., Schroth, J., Fridman, A., Boss, G. R., Insel, P. A., Stockand, J. D. and Vallon, V. (2010) 'Dietary Na<sup>+</sup> inhibits the open probability of the epithelial sodium channel in the kidney by enhancing apical P2Y2-receptor tone', *Faseb J*, 24, (6), pp. 2056-65.
- Pochynyuk, O., Staruschenko, A., Tong, Q., Medina, J. and Stockand, J. D. (2005) 'Identification of a functional phosphatidylinositol 3,4,5-trisphosphate binding site in the epithelial Na<sup>+</sup> channel', *Journal of Biological Chemistry*, 280, (45), pp. 37565-71.
- Raikwar, N. S., Snyder, P. M. and Thomas, C. P. (2008) 'An evolutionarily conserved N-terminal Sgk1 variant with enhanced stability and improved function', *Am J Physiol Renal Physiol*, 295, (5), pp. F1440-8.
- Raikwar, N. S., Vandewalle, A. and Thomas, C. P. (2010) 'Nedd4-2 interacts with occludin to inhibit tight junction formation and enhance paracellular conductance in collecting duct epithelia', *Am J Physiol Renal Physiol*.
- Rauh, R., Diakov, A., Tzschoppe, A., Korbmacher, J., Azad, A. K., Cuppens, H., Cassiman, J. J., Dotsch, J., Sticht, H. and Korbmacher, C. (2010) 'A mutation of the epithelial sodium channel associated with atypical cystic fibrosis increases channel open probability and reduces Na<sup>+</sup> self inhibition', *J Physiol*, 588, (Pt 8), pp. 1211-25.
- Rauh, R., Dinudom, A., Fotia, A. B., Paulides, M., Kumar, S., Korbmacher, C. and Cook, D. I. (2006) 'Stimulation of the epithelial sodium channel (ENaC) by the serum- and glucocorticoid-inducible kinase (Sgk) involves the PY motifs of the channel but is independent of sodium feedback inhibition', *Pflugers Archiv - European Journal of Physiology*, 452, (3), pp. 290-9.
- Record, R. D., Johnson, M., Lee, S. and Blazer-Yost, B. L. (1996) 'Aldosterone and insulin stimulate amiloride-sensitive sodium transport in A6 cells by additive mechanisms', *Am J Physiol*, 271, (4 Pt 1), pp. C1079-84.
- Reisenauer, M. R., Wang, S. W., Xia, Y. and Zhang, W. (2010) 'Dot1a contains three nuclear localization signals and regulates epithelial Na<sup>+</sup> channel (ENaC) at multiple levels', *Am J Physiol Renal Physiol*.
- Riepe, F. G. (2009) 'Clinical and molecular features of type 1 pseudohypoaldosteronism', *Horm Res*, 72, (1), pp. 1-9.

- Ring, A. M., Cheng, S. X., Leng, Q., Kahle, K. T., Rinehart, J., Lalioti, M. D., Volkman, H. M., Wilson, F. H., Hebert, S. C. and Lifton, R. P. (2007a) 'WNK4 regulates activity of the epithelial Na<sup>+</sup> channel *in vitro* and *in vivo*', *Proceedings of the National Academy of Sciences of the United States of America*, 104, (10), pp. 4020-4.
- Ring, A. M., Leng, Q., Rinehart, J., Wilson, F. H., Kahle, K. T., Hebert, S. C. and Lifton, R. P. (2007b) 'An SGK1 site in WNK4 regulates Na<sup>+</sup> channel and K<sup>+</sup> channel activity and has implications for aldosterone signaling and K<sup>+</sup> homeostasis', *Proceedings of the National Academy of Sciences of the United States of America*, 104, (10), pp. 4025-9.
- Robert-Nicoud, M., Flahaut, M., Elalouf, J. M., Nicod, M., Salinas, M., Bens, M., Doucet, A., Wincker, P., Artiguenave, F., Horisberger, J. D., Vandewalle, A., Rossier, B. C. and Firsov, D. (2001) 'Transcriptome of a mouse kidney cortical collecting duct cell line: effects of aldosterone and vasopressin', *Proceedings of the National Academy of Sciences of the United States of America*, 98, (5), pp. 2712-6.
- Rollins, B. M., Garcia-Caballero, A., Stutts, M. J. and Tarran, R. (2010) 'SPLUNC1 expression reduces surface levels of the epithelial sodium channel (ENaC) in *Xenopus laevis* oocytes', *Channels (Austin)*, 4, (4).
- Ronzaud, C., Loffing, J., Bleich, M., Gretz, N., Grone, H. J., Schutz, G. and Berger, S. (2007) 'Impairment of sodium balance in mice deficient in renal principal cell mineralocorticoid receptor', *Journal of the American Society of Nephrology*, 18, (6), pp. 1679-87.
- Rossier, B. C. (2003) 'The epithelial sodium channel (ENaC): new insights into ENaC gating', *Pflugers Archiv - European Journal of Physiology*, 446, (3), pp. 314-6.
- Rozen Steve, S. H. J. (2000) *Primer3 on the WWW for general users and for biologist programmers*. Available at: <http://frodo.wi.mit.edu/primer3/input.htm> (Accessed: October 16th).
- Sahoo, S., Brickley, D. R., Kocherginsky, M. and Conzen, S. D. (2005) 'Coordinate expression of the PI3-kinase downstream effectors serum and glucocorticoid-induced kinase (SGK-1) and Akt-1 in human breast cancer', *European Journal of Cancer*, 41, (17), pp. 2754-9.
- Sanchez-Perez, A., Kumar, S. and Cook, D. I. (2007) 'GRK2 interacts with and phosphorylates Nedd4 and Nedd4-2', *Biochemical & Biophysical Research Communications*, 359, (3), pp. 611-5.
- Sarbassov, D. D., Ali, S. M., Kim, D. H., Guertin, D. A., Latek, R. R., Erdjument-Bromage, H., Tempst, P. and Sabatini, D. M. (2004) 'Rictor, a novel binding partner of mTOR, defines a rapamycin-insensitive and raptor-independent pathway that regulates the cytoskeleton', *Curr Biol*, 14, (14), pp. 1296-302.

- Sarbassov, D. D., Ali, S. M., Sengupta, S., Sheen, J. H., Hsu, P. P., Bagley, A. F., Markhard, A. L. and Sabatini, D. M. (2006) 'Prolonged rapamycin treatment inhibits mTORC2 assembly and Akt/PKB', *Mol Cell*, 22, (2), pp. 159-68.
- Sato, J. D., Chapline, M. C., Thibodeau, R., Frizzell, R. A. and Stanton, B. A. (2007) 'Regulation of Human Cystic Fibrosis Transmembrane Conductance Regulator (CFTR) by Serum- and Glucocorticoid-Inducible Kinase (SGK1)', *Cell Physiol Biochem*, 20, (1-4), pp. 91-8.
- Saxena, S. K., Singh, M., Kaur, S. and George, C. (2007) 'Distinct domain-dependent effect of syntaxin1A on amiloride-sensitive sodium channel (ENaC) currents in HT-29 colonic epithelial cells', *Int J Biol Sci*, 3, (1), pp. 47-56.
- Schild, L., Lu, Y., Gautschi, I., Schneeberger, E., Lifton, R. P. and Rossier, B. C. (1996) 'Identification of a PY motif in the epithelial Na<sup>+</sup> channel subunits as a target sequence for mutations causing channel activation found in Liddle syndrome', *EMBO Journal*, 15, (10), pp. 2381-7.
- Schoenebeck, B., Bader, V., Zhu, X. R., Schmitz, B., Lubbert, H. and Stichel, C. C. (2005) 'Sgk1, a cell survival response in neurodegenerative diseases', *Mol Cell Neurosci*, 30, (2), pp. 249-64.
- Schwab, M., Lupescu, A., Mota, M., Mota, E., Frey, A., Simon, P., Mertens, P. R., Floege, J., Luft, F., Asante-Poku, S., Schaeffeler, E. and Lang, F. (2008) 'Association of SGK1 Gene Polymorphisms with Type 2 Diabetes', *Cell Physiol Biochem*, 21, (1-3), pp. 151-60.
- Segditsas, S., Sieber, O., Deheragoda, M., East, P., Rowan, A., Jeffery, R., Nye, E., Clark, S., Spencer-Dene, B., Stamp, G., Poulson, R., Suraweera, N., Silver, A., Ilyas, M. and Tomlinson, I. (2008) 'Putative direct and indirect Wnt targets identified through consistent gene expression changes in APC-mutant intestinal adenomas from humans and mice', *Hum Mol Genet*, 17, (24), pp. 3864-75.
- Setiawan, I., Henke, G., Feng, Y., Bohmer, C., Vasilets, L. A., Schwarz, W. and Lang, F. (2002) 'Stimulation of Xenopus oocyte Na<sup>+</sup>,K<sup>+</sup>-ATPase by the serum and glucocorticoid-dependent kinase sgk1', *Pflugers Arch*, 444, (3), pp. 426-31.
- Shane, M. A., Nofziger, C. and Blazer-Yost, B. L. (2006) 'Hormonal regulation of the epithelial Na<sup>+</sup> channel: from amphibians to mammals', *Gen Comp Endocrinol*, 147, (1), pp. 85-92.
- Shen, J. P. and Cotton, C. U. (2003) 'Epidermal growth factor inhibits amiloride-sensitive sodium absorption in renal collecting duct cells', *American Journal of Physiology - Renal Physiology*, 284, (1), pp. F57-64.
- Shigaev, A., Asher, C., Latter, H., Garty, H. and Reuveny, E. (2000) 'Regulation of sgk by aldosterone and its effects on the epithelial Na<sup>+</sup> channel', *American Journal of Physiology - Renal Physiology*, 278, (4), pp. F613-9.

- Simon, P., Schneck, M., Hochstetter, T., Koutsouki, E., Mittelbronn, M., Merseburger, A., Weigert, C., Niess, A. and Lang, F. (2007) 'Differential Regulation of Serum- and Glucocorticoid-Inducible Kinase 1 (SGK1) Splice Variants Based on Alternative Initiation of Transcription', *Cell Physiol Biochem*, 20, (6), pp. 715-728.
- Smith, P. K., Krohn, R. I., Hermanson, G. T., Mallia, A. K., Gartner, F. H., Provenzano, M. D., Fujimoto, E. K., Goeke, N. M., Olson, B. J. and Klenk, D. C. (1985) 'Measurement of protein using bicinchoninic acid.[erratum appears in Anal Biochem 1987 May 15;163(1):279]', *Analytical Biochemistry*, 150, (1), pp. 76-85.
- Snyder, P. M., Olson, D. R. and Thomas, B. C. (2002) 'Serum and glucocorticoid-regulated kinase modulates Nedd4-2-mediated inhibition of the epithelial Na<sup>+</sup> channel', *Journal of Biological Chemistry*, 277, (1), pp. 5-8.
- Soundararajan, R., Melters, D., Shih, I. C., Wang, J. and Pearce, D. (2009) 'Epithelial sodium channel regulated by differential composition of a signaling complex', *Proc Natl Acad Sci U S A*.
- Soundararajan, R., Wang, J., Melters, D. P. and Pearce, D. (2007) 'Differential activities of glucocorticoid-induced leucine zipper protein (gilz) isoforms', *J Biol Chem*.
- Soundararajan, R., Zhang, T. T., Wang, J., Vandewalle, A. and Pearce, D. (2005) 'A novel role for glucocorticoid-induced leucine zipper protein in epithelial sodium channel-mediated sodium transport', *Journal of Biological Chemistry*, 280, (48), pp. 39970-81.
- Staessen, J. A., Kuznetsova, T. and Stolarz, K. (2003) 'Hypertension prevalence and stroke mortality across populations', *Jama*, 289, (18), pp. 2420-2.
- Staub, O., Abriel, H., Plant, P., Ishikawa, T., Kanelis, V., Saleki, R., Horisberger, J. D., Schild, L. and Rotin, D. (2000) 'Regulation of the epithelial Na<sup>+</sup> channel by Nedd4 and ubiquitination', *Kidney International*, 57, (3), pp. 809-15.
- Stichel, C. C., Schoenebeck, B., Foguet, M., Siebertz, B., Bader, V., Zhu, X. R. and Lubbert, H. (2005) 'sgk1, a member of an RNA cluster associated with cell death in a model of Parkinson's disease', *Eur J Neurosci*, 21, (2), pp. 301-16.
- Stothard, P. (2000) 'The sequence manipulation suite: JavaScript programs for analyzing and formatting protein and DNA sequences. ' *BioTechniques*, (28), pp. 1102-1104.
- Summa, V., Camargo, S. M., Bauch, C., Zecevic, M. and Verrey, F. (2004) 'Isoform specificity of human Na<sup>+</sup>,K<sup>+</sup>-ATPase localization and aldosterone regulation in mouse kidney cells', *Journal of Physiology*, 555, (Pt 2), pp. 355-64.
- Summa, V., Mordasini, D., Roger, F., Bens, M., Martin, P. Y., Vandewalle, A., Verrey, F. and Feraille, E. (2001) 'Short term effect of aldosterone on Na<sup>+</sup>,K<sup>+</sup>-ATPase cell surface expression in kidney collecting duct cells', *J Biol Chem*, 276, (50), pp. 47087-93.

- Tai, D. J., Su, C. C., Ma, Y. L. and Lee, E. H. (2009) 'SGK1 phosphorylation of I $\kappa$ B Kinase- $\alpha$  and p300 Up-regulates NF- $\kappa$ B activity and increases N-Methyl-D-aspartate receptor NR2A and NR2B expression', *J Biol Chem*, 284, (7), pp. 4073-89.
- Thoreen, C. C., Kang, S. A., Chang, J. W., Liu, Q., Zhang, J., Gao, Y., Reichling, L. J., Sim, T., Sabatini, D. M. and Gray, N. S. (2009) 'An ATP-competitive mammalian target of rapamycin inhibitor reveals rapamycin-resistant functions of mTORC1', *J Biol Chem*, 284, (12), pp. 8023-32.
- Thoreen, C. C. and Sabatini, D. M. (2009) 'Rapamycin inhibits mTORC1, but not completely', *Autophagy*, 5, (5), pp. 725-6.
- Titze, J. and Ritz, E. (2009) 'Salt and its effect on blood pressure and target organ damage: new pieces in an old puzzle', *J Nephrol*, 22, (2), pp. 177-89.
- Trochen, N., Ganapathipillai, S., Ferrari, P., Frey, B. M. and Frey, F. J. (2004) 'Low prevalence of nonconservative mutations of serum and glucocorticoid-regulated kinase (SGK1) gene in hypertensive and renal patients', *Nephrology Dialysis Transplantation*, 19, (10), pp. 2499-504.
- Tyan, S. W., Tsai, M. C., Lin, C. L., Ma, Y. L. and Lee, E. H. (2007) 'Serum- and glucocorticoid-inducible kinase 1 enhances zif268 expression through the mediation of SRF and CREB1 associated with spatial memory formation', *J Neurochem*.
- Uchida, N., Shiohara, M., Miyagawa, S., Yokota, I. and Mori, T. (2009) 'A novel nonsense mutation of the mineralocorticoid receptor gene in the renal form of pseudohypoaldosteronism type 1', *J Pediatr Endocrinol Metab*, 22, (1), pp. 91-5.
- Urbanet, R., Pilon, C., Calcagno, A., Peschechera, A., Hubert, E. L., Giacchetti, G., Gomez-Sanchez, C., Mulatero, P., Toffanin, M., Sonino, N., Zennaro, M. C., Giorgino, F., Vettor, R. and Fallo, F. (2010) 'Analysis of Insulin Sensitivity in Adipose Tissue of Patients with Primary Aldosteronism', *J Clin Endocrinol Metab*.
- Vallon, V. and Lang, F. (2005) 'New insights into the role of serum- and glucocorticoid-inducible kinase SGK1 in the regulation of renal function and blood pressure', *Current Opinion in Nephrology & Hypertension*, 14, (1), pp. 59-66.
- Vallon, V., Schroth, J., Lang, F., Kuhl, D. and Uchida, S. (2009) 'Expression and phosphorylation of the Na<sup>+</sup>-Cl<sup>-</sup> cotransporter NCC in vivo is regulated by dietary salt, potassium, and SGK1', *Am J Physiol Renal Physiol*, 297, (3), pp. F704-12.
- Vallon, V., Wyatt, A. W., Klingel, K., Huang, D. Y., Hussain, A., Berchtold, S., Friedrich, B., Grammer, F., Belaiba, R. S., Gorch, A., Wulff, P., Daut, J., Dalton, N. D., Ross, J., Jr., Fogel, U., Schrader, J., Osswald, H., Kandolf, R., Kuhl, D. and Lang, F. (2006) 'SGK1-dependent cardiac CTGF formation and fibrosis following DOCA treatment', *J Mol Med*, 84, (5), pp. 396-404.

- Van Huyen, J. P., Bens, M., Teulon, J. and Vandewalle, A. (2001) 'Vasopressin-stimulated chloride transport in transimmortalized mouse cell lines derived from the distal convoluted tubule and cortical and inner medullary collecting ducts', *Nephrology Dialysis Transplantation*, 16, (2), pp. 238-45.
- Vanhaesebroeck, B., Guillermet-Guibert, J., Graupera, M. and Bilanges, B. (2010) 'The emerging mechanisms of isoform-specific PI3K signalling', *Nat Rev Mol Cell Biol*, 11, (5), pp. 329-41.
- Vasquez, M. M., Castro, R., Seidner, S. R., Henson, B. M., Ashton, D. J. and Mustafa, S. B. (2008) 'Induction of serum- and glucocorticoid-induced kinase-1 (SGK1) by cAMP regulates increases in alpha-ENaC', *J Cell Physiol*, 217, (3), pp. 632-42.
- Verrey, F., Fakitsas, P., Adam, G. and Staub, O. (2007) 'Early transcriptional control of ENaC (de)ubiquitylation by aldosterone', *Kidney Int*.
- Verrey, F., Pearce, D., Pfeiffer, R., Spindler, B., Mastroberardino, L., Summa, V. and Zecevic, M. (2000) 'Pleiotropic action of aldosterone in epithelia mediated by transcription and post-transcription mechanisms', *Kidney International*, 57, (4), pp. 1277-82.
- Verrey, F., Summa, V., Heitzmann, D., Mordasini, D., Vandewalle, A., Feraille, E. and Zecevic, M. (2003) 'Short-term aldosterone action on Na<sup>+</sup>,K<sup>+</sup>-ATPase surface expression: role of aldosterone-induced SGK1?' *Annals of the New York Academy of Sciences*, 986, pp. 554-61.
- Viengchareun, S., Kamenicky, P., Teixeira, M., Butlen, D., Meduri, G., Blanchard-Gutton, N., Kurschat, C., Lanel, A., Martinerie, L., Sztal-Mazer, S., Blot-Chabaud, M., Ferrary, E., Cherradi, N. and Lombes, M. (2009) 'Osmotic stress regulates mineralocorticoid receptor expression in a novel aldosterone-sensitive cortical collecting duct cell line', *Mol Endocrinol*, 23, (12), pp. 1948-62.
- Vinciguerra, M., Deschenes, G., Hasler, U., Mordasini, D., Rousselot, M., Doucet, A., Vandewalle, A., Martin, P. Y. and Feraille, E. (2003) 'Intracellular Na<sup>+</sup> controls cell surface expression of Na<sup>+</sup>,K<sup>+</sup>-ATPase via a cAMP-independent PKA pathway in mammalian kidney collecting duct cells', *Molecular Biology of the Cell*, 14, (7), pp. 2677-88.
- Vitari, A. C., Deak, M., Morrice, N. A. and Alessi, D. R. (2005) 'The WNK1 and WNK4 protein kinases that are mutated in Gordon's hypertension syndrome phosphorylate and activate SPAK and OSR1 protein kinases', *Biochemical Journal*, 391, (Pt 1), pp. 17-24.
- von Wovorn, F., Berglund, G., Carlson, J., Mansson, H., Hedblad, B. and Melander, O. (2005) 'Genetic variance of SGK-1 is associated with blood pressure, blood pressure change over time and strength of the insulin-diastolic blood pressure relationship', *Kidney International*, 68, (5), pp. 2164-72.

- Vuagniaux, G., Vallet, V., Jaeger, N. F., Pfister, C., Bens, M., Farman, N., Courtois-Coutry, N., Vandewalle, A., Rossier, B. C. and Hummler, E. (2000) 'Activation of the amiloride-sensitive epithelial sodium channel by the serine protease mCAP1 expressed in a mouse cortical collecting duct cell line', *Journal of the American Society of Nephrology*, 11, (5), pp. 828-34.
- Wakida, N., Kitamura, K., Tuyen, D. G., Maekawa, A., Miyoshi, T., Adachi, M., Shiraishi, N., Ko, T., Ha, V., Nonoguchi, H. and Tomita, K. (2006) 'Inhibition of prostatic-induced ENaC activities by PN-1 and regulation of PN-1 expression by TGF- $\beta$ 1 and aldosterone', *Kidney Int*, 70, (8), pp. 1432-8.
- Waldegger, S., Erdel, M., Nagl, U. O., Barth, P., Raber, G., Steuer, S., Utermann, G., Paulmichl, M. and Lang, F. (1998) 'Genomic organization and chromosomal localization of the human SGK protein kinase gene', *Genomics*, 51, (2), pp. 299-302.
- Wang, J., Barbry, P., Maiyar, A. C., Rozansky, D. J., Bhargava, A., Leong, M., Firestone, G. L. and Pearce, D. (2001) 'SGK integrates insulin and mineralocorticoid regulation of epithelial sodium transport', *American Journal of Physiology - Renal Physiology*, 280, (2), pp. F303-13.
- Wang, J., Knight, Z. A., Fiedler, D., Williams, O., Shokat, K. M. and Pearce, D. (2008) 'Activity of the p110- $\alpha$  subunit of phosphatidylinositol-3-kinase is required for activation of epithelial sodium transport', *Am J Physiol Renal Physiol*, 295, (3), pp. F843-50.
- Wang, Q., Zhang, X., Wang, Y., Deng, A., Zhu, Z. and Feng, Y. (2005) 'Significance and expression of serum and glucocorticoid-inducible kinase in kidney of mice with diabetic nephropathy', *J Huazhong Univ Sci Technolog Med Sci*, 25, (2), pp. 170-3.
- Webster, M. K., Goya, L. and Firestone, G. L. (1993a) 'Immediate-early transcriptional regulation and rapid mRNA turnover of a putative serine/threonine protein kinase', *Journal of Biological Chemistry*, 268, (16), pp. 11482-5.
- Webster, M. K., Goya, L., Ge, Y., Maiyar, A. C. and Firestone, G. L. (1993b) 'Characterization of sgk, a novel member of the serine/threonine protein kinase gene family which is transcriptionally induced by glucocorticoids and serum', *Molecular & Cellular Biology*, 13, (4), pp. 2031-40.
- Wheelan, S. J., Church, D. M. and Ostell, J. M. (2001) 'Spidey: a tool for mRNA-to-genomic alignments', *Genome Res*, 11, (11), pp. 1952-7.
- Wiemuth, D., Ke, Y., Rohlfs, M. and McDonald, F. J. (2007) 'Epithelial sodium channel (ENaC) is multi-ubiquitinated at the cell surface', *Biochemical Journal*, 405, (1), pp. 147-55.

- Wilson, F. H., Disse-Nicodeme, S., Choate, K. A., Ishikawa, K., Nelson-Williams, C., Desitter, I., Gunel, M., Milford, D. V., Lipkin, G. W., Achard, J. M., Feely, M. P., Dussol, B., Berland, Y., Unwin, R. J., Mayan, H., Simon, D. B., Farfel, Z., Jeunemaitre, X. and Lifton, R. P. (2001) 'Human hypertension caused by mutations in WNK kinases.[see comment]', *Science*, 293, (5532), pp. 1107-12.
- Wishart, M. J., Taylor, G. S. and Dixon, J. E. (2001) 'Phoxy lipids: revealing PX domains as phosphoinositide binding modules', *Cell*, 105, (7), pp. 817-20.
- Wolf, S. C., Schultze, M., Risler, T., Rieg, T., Lang, F., Schulze-Osthoff, K. and Brehm, B. R. (2006) 'Stimulation of serum- and glucocorticoid-regulated kinase-1 gene expression by endothelin-1', *Biochemical Pharmacology*, 71, (8), pp. 1175-1183.
- Wulff, P., Vallon, V., Huang, D. Y., Volkl, H., Yu, F., Richter, K., Jansen, M., Schlunz, M., Klingel, K., Loffing, J., Kauselmann, G., Bosl, M. R., Lang, F. and Kuhl, D. (2002) 'Impaired renal Na<sup>+</sup> retention in the sgk1-knockout mouse.[see comment]', *Journal of Clinical Investigation*, 110, (9), pp. 1263-8.
- Xu, B. E., Stippec, S., Chu, P. Y., Lazrak, A., Li, X. J., Lee, B. H., English, J. M., Ortega, B., Huang, C. L. and Cobb, M. H. (2005a) 'WNK1 activates SGK1 to regulate the epithelial sodium channel', *Proceedings of the National Academy of Sciences of the United States of America*, 102, (29), pp. 10315-20.
- Xu, B. E., Stippec, S., Lazrak, A., Huang, C. L. and Cobb, M. H. (2005b) 'WNK1 activates SGK1 by a phosphatidylinositol 3-kinase-dependent and non-catalytic mechanism', *Journal of Biological Chemistry*, 280, (40), pp. 34218-23.
- Yan, L., Mieulet, V. and Lamb, R. F. (2008) 'mTORC2 is the hydrophobic motif kinase for SGK1', *Biochem J*, 416, (3), pp. e19-21.
- You, H., Jang, Y., You-Ten, A. I., Okada, H., Liepa, J., Wakeham, A., Zaugg, K. and Mak, T. W. (2004) 'p53-dependent inhibition of FKHRL1 in response to DNA damage through protein kinase SGK1', *Proceedings of the National Academy of Sciences of the United States of America*, 101, (39), pp. 14057-62.
- Yun, C. C., Palmada, M., Embark, H. M., Fedorenko, O., Feng, Y., Henke, G., Setiawan, I., Boehmer, C., Weinman, E. J., Sandrasagra, S., Korbmacher, C., Cohen, P., Pearce, D. and Lang, F. (2002) 'The serum and glucocorticoid-inducible kinase SGK1 and the Na<sup>+</sup>/H<sup>+</sup> exchange regulating factor NHERF2 synergize to stimulate the renal outer medullary K<sup>+</sup> channel ROMK1', *Journal of the American Society of Nephrology*, 13, (12), pp. 2823-30.
- Zagorska, A., Pozo-Guisado, E., Boudeau, J., Vitari, A. C., Rafiqi, F. H., Thastrup, J., Deak, M., Campbell, D. G., Morrice, N. A., Prescott, A. R. and Alessi, D. R. (2007) 'Regulation of activity and localization of the WNK1 protein kinase by hyperosmotic stress', *Journal of Cell Biology*, 176, (1), pp. 89-100.

- Zecevic, M., Heitzmann, D., Camargo, S. M. and Verrey, F. (2004) 'SGK1 increases  $\text{Na}^+$ , $\text{K}^+$ -ATPase cell-surface expression and function in *Xenopus laevis* oocytes', *Pflugers Arch*, 448, (1), pp. 29-35.
- Zhang, B. H., Tang, E. D., Zhu, T., Greenberg, M. E., Vojtek, A. B. and Guan, K. L. (2001) 'Serum- and glucocorticoid-inducible kinase SGK phosphorylates and negatively regulates B-Raf', *J Biol Chem*, 276, (34), pp. 31620-6.
- Zhang, W., Xia, X., Reisenauer, M. R., Rieg, T., Lang, F., Kuhl, D., Vallon, V. and Kone, B. C. (2007) 'Aldosterone-induced Sgk1 relieves Dot1a-Af9-mediated transcriptional repression of epithelial  $\text{Na}^+$  channel  $\alpha$ ', *Journal of Clinical Investigation*, 117, (3), pp. 773-83.
- Zhang, Z. R., Chou, C. F., Wang, J., Liang, Y. Y. and Ma, H. P. (2009) 'Anionic phospholipids differentially regulate the epithelial sodium channel (ENaC) by interacting with  $\alpha$ ,  $\beta$ , and  $\gamma$  ENaC subunits', *Pflugers Arch*.
- Zhou, R. and Snyder, P. M. (2005) 'Nedd4-2 phosphorylation induces serum and glucocorticoid-regulated kinase (SGK) ubiquitination and degradation', *Journal of Biological Chemistry*, 280, (6), pp. 4518-23.

## **Appendix - Raw DNA Sequencing Data**

### **Sgk1 isoform identification RT-PCR products**

#### Mouse Sgk1a:

TTCAC T GCTCCCCTCAGTCTCTTTTGGGCTCTTTCCGGGCATCGGGACGATGACCGTCAAAGCCGAGGCTGCT  
CGAAGCACCCCTTACCTACTCCAGAATGAGGGGAATGGTAGCGATTCTCATCGCTTTTATGAAACAGAGAAGGA  
TGGGCCTGAACGATTTTATTTCAGAAGATTGCCAGCAACACCTATGCATGCAAACACGCTGAAGTTCAGTCCAT  
TTTGAAAATGTCCCATCCTCAGGAGCCGGAGCTTATGAACGCTAACCCCTCTCCTCCGCCAAGTCCCTCTCAA  
CAAATCAACCTGGGTCC

#### Mouse Sgk1b:

GCTCAGAAAAGGAGCGAGTCCGTCTGCTGAGCGGACTGGCTTTTATGAAACAGAGAAGGATGGGCCTGAACG  
ATTTTATTTCAGAAGATTGCCAGCAACACCTATGCATGCAAACACGCTGAAGTTCAGTCCATTTTGAAAATGTC  
CCATCCTCAGGAGCCGGAGCTTATGAACGCTAACCCCTCTCCTCCGCCAAGTCCCTCTCAACAAATCAACCTG  
GGTCCGTCTCCAACCTCACGCCAAACCCCTCCGACTTTTCACTTCTTGAAAGTGATCGGAAAGGG

#### Mouse Sgk1c:

CCCTTCCGATCACTTCAAGAAGTGAAAGTCGGAGGGTTTGGCGTGAGGGTTGGAGGACGGACCCAGGTTGA  
TTTGTGAGAGGGACTTGGCGGAGGAGAGGGGTTAGCGTTCATAAGCTCCGGCTCCTGAGGATGGGACATTTT  
CAAATGGACTGAACCTCAGCGTGTTCATGCATAGGTGTTGCTGGCAATCTTCTGAATAAAAATCGTTCAGG  
CCCATCCTTCTCTGTTTTCATAAAAGCTTTCCAAGGGGATCTTAAGGTCTCCTCTTTTCACTTCTTACAATGCTG  
CAGAGGTGGAGGCTGGGGTTACTTT

#### Mouse Sgk1d:

TGAGGCCATGTGTCAATCATGCCTGGGTGACCATGCTTTCCAAAGGGGGATGCTCCCTCCAGAGGAGTCCTGT  
TCCTGGGAGATCCAACCTGGGTGTGAAGTGAAAGAACAATGTAATCATGCCAACATCCTGACCAAGCCGGACC  
CAAGAACCCTTCTGGACTAATGATGATGCAGCTTTTATGAAACAGAGAAGGATGGGCCTGAACGATTTTATTCA  
GAAGATTGCCAGCAACACCTATGCATGCAAACACGCTGAAGTTCAGTCCATTTTGAAAATGTCCCATCCTCAG  
GAGCCGGAGCTTATGAACGCTAACCCCTCTCCTC

### **Sgk1 isoform cloning into pCMV-SPORT6**

#### Mouse Sgk1a:

ATGACCGTCAAAGCCGAGGCTGCTCGAAGCACCCCTTACCTACTCCAGAATGAGGGGAATGGTAGCGATTCTCA  
TCGCTTTTATGAAACAGAGAAGGATGGGCCTGAACGATTTTATTTCAGAAGATTGCCAGCAACACCTATGCATG  
CAAACACGCTGAAGTTCAGTCCATTTTGAAAATGTCCCATCCTCAGGAGCCGGAGCTTATGAACGCTAACCC  
TCTCCTCCGCCAAGTCCCTCTCAACAAATCAACCTGGGTCCGTCTCCTCCAACCCCTCACGCCAAACCCCTCCGACT  
TTCACCTTCTTGAAAGTGATCGGAAAGGGCAGTTTTTGGAAAGGGTCTTCTGCTAGGCACAAGGCAGAAGA  
AGTATTCTATGCAGTCAAAGTTTTACAGAAGAAAGCCATCCTGAAGAAGAAAGAGGAGAAGCATATTATGTCA  
GAGCGGAATGTTCTGTTGAAGAATGTGAAGCACCCCTTCTGGTGGGCCTTCACTTCTCATTCCAGACCGCTG  
ACAAGCTCTACTTTGTCTGGACTACATTAATGGTGGAGAGCTGTTCTACCATCTCCAGAGGGAGCGCTGCTT  
CCTGGAACCACGGGCTCGCTTCTACGCAGCTGAAATAGCCAGTGCCCTGGGCTATCTGCACTCCCTAAACATC  
GTTTATAGAGACTTAAAACCTGAGAATATTCTCCTAGACTCCAGGGGCACATCGTCCCTCACTGACTTTGGGC  
TCTGCAAAGAGAATATTGAGCATAACGGGACAACATCTACCTTCTGTGGCACGCCTGAGTATCTGGCTCCTGA

GGTCTCCATAAACAGCCGTATGACCGGACGGTGGACTGGTGGTGTCTTGGGGCTGTCTGTATGAGATGCTC  
TACGGCCTGCCCCGTTTTATAGCCGGAACACGGCTGAGATGTACGACAATATTCTGAACAAGCCTCTCCAGT  
TGAAACCAAATATTACAAACTCGGCAAGGCACCTCCTGGAAGGCCTCCTGCAGAAGGACCGGACCAAGAGGCT  
GGGTGCCAAGGATGACTTTATGGAGATTAAGAGTCATATTTCTTCTTTAATTAACCTGGGATGATCTCATC  
AATAAGAAGATTACACCCCCATTTAACCCTAAATGTGAGTGGGCCAGTGACCTTCGGCACTTCGATCCCAGT  
TTACCGAGGAGCCGGTCCCCAGCTCCATCGGCAGGTCCCCTGACAGCATCCTTGTACGGCCAGTGTGAAGGA  
AGCAGCAAAGCCTTCCTCGGCTTCTCCTATGCACCTCCTGTGGATTCTTCTCTGA

### Mouse Sgk1b:

ATGGGCGAGATGCAGGGCGCGCTGGCTCGGGCTCGGCTCGAGTCCCTGCTCCGGCCCCGCCACAAAAAGCGGG  
CGGAGGCTCAGAAAAGGAGCGAGTCCGTCTGCTGAGCGGACTGGCTTTTATGAAACAGAGAAGGATGGGCCT  
GAACGATTTTATTAGAAAGATTGCCAGCAACACCTATGCATGCAAACACGCTGAAGTTTCACTTTTAAAA  
ATGTCCCATCCTCAGGAGCCGGAGCTTATGAACGCTAACCCTCTCCTCCGCCAAGTCCCTCTCAACAAATCA  
ACCTGGGTCCGTCTCCAACCTCACGCCAAACCTCCGACTTTCACCTTCTTGAAGTGTATCGGAAAGGGCAG  
TTTTGGAAAGGTTCTTCTGGCTAGGCACAAGGCAGAAGAAGTATTCTATGCAGTCAAAGTTTTACAGAAGAAA  
GCCATCTGAAGAAGAAAGAGGAGAAGCATATTATGTGAGAGCGGAATGTTCTGTTGAAGAATGTGAAGCACC  
CTTCTCCTGGTGGGCCTTCACTTCTCATTCCAGACCGCTGACAAGCTCTACTTTGTCTGGACTACATTAATGG  
TGGAGAGCTGTTTACCATCTCCAGAGGGAGCGCTGCTTCTGGAACCACGGGCTCGATTCTACGCAGCTGAA  
ATAGCCAGTGCCCTGGGCTATCTGCACTCCCTAAACATCGTTTTATAGAGACTTAAAACTGAGAATATTCTCC  
TAGACTCCCAGGGGCACATCGTCTCCTCACTGACTTTGGGCTCTGCAAAGAGAATATTGAGCATAACGGGACAAC  
ATCTACCTTCTGTGGCACGCTGAGTATCCGGCTCCTGAGGTCTCCATAAGCAGCCGTATGACCGGACGGTG  
GACTGGTGGTGTCTTGGGGCTGTCTGTATGAGATGCTCTACGGCCTGCCCCCGTTTTATAGCCGGAACACGG  
CTGAGATGTACGACAATATTCTGAACAAGCCTCTCCAGTTGAAACCAAATATTACAAACTCGGCAAGGCACCT  
CCTGGAAGGCCTTCTGCAGAAGGACCGGACCAAGAGGCTGGGTGCCAAGGATGACTTTATGGAGATTAAGAGT  
CATATTTCTTCTCTTTAATTAACCTGGGATGATCTCATCAATAAGAAGATTACACCCCCATTTAACCCTAAATG  
TGAGTGGGCCAGTGACCTTCGGCACTTCGATCCCAGTTTTACCGAGGAGCCGGTCCCCAGCTCCATCGGCAG  
GTCCCCCTGACAGCATCCTTGTACGGCCAGTGTGAAGGAAGCAGCAGAAGCCTTCTCCTCGGCTTCTCCTATGCA  
CTCCTGTGGATTCTTCTCTGA

### Mouse Sgk1c:

ATGAAAGAGGAGACCTTAAGATCCCCCTTGGAAAGCTTTTTATGAAACAGAGAAGGATGGGCCTGAACGATTTTA  
TTCAGAAGATTGCCAGCAACACCTATGCATGCAAACACGCTGAAGTTTCACTTTTAAAAATGTCCCATCC  
TCAGGAGCCGGAGCTTATGAACGCTAACCCTCTCCTCCGCCAAGTCCCTCTCAACAAATCAACCTGGGTCCG  
TCCTCCAACCTCACGCCAAACCTCCGACTTTCACCTTCTTGAAGTGTATCGGAAAGGGCAGTTTTGGAAAGG  
TTCTTCTGGCTAGGCACAAGGCAGAAGAAGTATTCTATGCAGTCAAAGTTTTACAGAAGAAAGCCATCCTGAA  
GAAGAAAGAGGAGAAGCATATTATGTGAGAGCGGAATGTTCTGTTGAAGAATGTGAAGCACCCCTTCTGGTG  
GGCCTTCACTTCTCATCCAGACCGCTGACAAGCTCTACTTTGTCTGGACTACATTAATGGTGGAGAGCTGT  
TCTACCATCTCCAGAGGGAGCGCTGCTTCTGGAACCACGGGCTCGATTCTACGCAGCTGAAATAGCCAGTGC  
CCTGGCTATCTGCACCTCCCATAACATCGTTTTATAGAGACTTAAAACTGAGAATATTCTCCTAGACTCCCAG  
GGGCACATCGTCTCACTGACTTTGGGCTCTGCAAAGAGAATATTGAGCATAACGGGACAACATCTACCTTCT  
GTGGCACGCCCTGAGTATCTGGCTCCTGAGGTCTCCATAAGCAGCCGTATGACCGGACGGTGGACTGGTGGTG  
TCTTGGGGCTGTCTGTATGAGATGCTCTACGGCCTGCCCCCGTTTTATAGCCGGAACACGGCTGAGATGTAC  
GACAATATTCTGAACAAGCCTCTCCAGTTGAAACCAAATATTACAAACTCGGCAAGGCACCTCCTGGAAGGCC  
TCCTGCAGAAGGACCGGACCAAGAGGCTGGGTGCCAAGGATGACTTTATGGAGATTAAGAGTCATATTTCTT  
CTCTTTAATTAACCTGGGATGATCTCATCAATAAGAAGATTACACCCCCATTTAACCCTAAATGTGAGTGGGCC  
AGTGACCTTCGGCACTTCGATCCCAGTTTTACCGAGGAGCCGGTCCCCAGCTCCATCGGCAGGTCCCCTGACA  
GCATCCTTGTACGGCCAGTGTGAAGGAAGCAGCAGAAGCCTTCTCCTCGGCTTCTCCTATGCACCTCCTGTGGA  
TTCCTTCTC

### Mouse Sgk1d:

ATGGTAAACAAAGACATGAATGGATTCCCGGTCAAGAAATGCTCAGCGTTCCAATTTTTTAAAGAAACGGGTAC  
GAAGATGGATCAAGAGCCCCATGGTCAGCGTGGACAAGCATCAGAGCCCCAACTTGAAGTACACTGGCCCTGC  
TGGGGTGCATCTTCCCCCTGGGGAGTCAGACTTTGAGGCCATGTGTCAATCATGCCTGGGTGACCATGCTTTC  
CAAAGGGGGATGCTCCCTCCAGAGGAGTCTGTTCTTGGGAGATCCAACCTGGGTGTGAAGTGAAGAACAAT  
GTAATCATGCCAATCCTGACCAAGCCGGACCCAAGAACCTTCTGGACTAATGATGATGCAGCTTTTATGAA  
ACAGAGAAGGATGGGCCTGAACGATTTTATTAGAAAGATTGCCAGCAACACCTATGCATGCAAACACGCTGAA

GTTTCAGTCCATTTTGGAAAATGTCCCATCCTCAGGAGCCGGAGCTTATGAACGCTAACCCCTCTCCTCCGCCAA  
GTCCCTCTCAACAAATCAACCTGGGTCCGTCCTCCAACCCTCACGCCAAACCCTCCGACTTTCCTTCTTGAA  
AGTGATCGGAAAGGGCAGTTTTGGAAAGGTTCTTCTGGCTAGGCACAAGGCAGAAGAAGTATTCTATGCAGTC  
AAAGTTTTACAGAAGAAAGCCATCCTGAAGAAGAAAGAGGAGAAGCATATTATGTGAGAGCGGAATGTTCTGT  
TGAAGAATGTGAAGCACCCTTTCCTGGTGGGCCTTCACTTCTCATTCCAGACCGCTGACAAGCTCTACTTTGT  
CCTGGACTACATTAATGGTGGAGAGCTGTTCTACCATCTCCAGAGGGAGCGCTGCTTCTGGAACCACGGGCT  
CGATTCACGCAGCTGAAATAGCCAGTGCCCTGGGCTATCTGCACTCCCTAAACATCGTTTTATAGAGACTTAA  
AACCTGAGAATATTCCTAGACTCCCAGGGGCACATCGTCTCACTGACTTTGGGCTCTGCAAAGAGAATAT  
TGAGCATAACGGGACAACATCTACCTTCTGTGGCAGCCTGAGTATCTGGCTCCTGAGGCTCCATAAGCAG  
CCGTATGACCGGACGGTGGACTGGTGGTGTCTTGGGGCTGTCTGTATGAGATGCTCTACGGCCTGCCCCCGT  
TTTATAGCCGGAACACGGCTGAGATGTACGACAATATTCTGAACAAGCCTCTCCAGTTGAAACCAAATATTAC  
AAACTCGGCAAGGCACCTCCTGGAAGGCCTCCTGCAGAAGGACCGGACCAAGAGGCTGGGTGCCAAGGATGAC  
TTTATGGAGATTAAGAGTCATATTTCTTCTTTAATTAACTGGGATGATCTCATCAATAAGAAGATTACAC  
CCCCATTTAACCCAAATGTGAGTGGGCCAGTGACCTTCGGCACTTCGATCCCAGTTTACCGAGGAGCCGGT  
CCCCAGCTCCATCGGCAGGTCCCCTGACAGCATCCTTGTACGGCCAGTGTGAAGGAAGCAGCAGAAGCCTTC  
CTCGGCTTCTCCTATGCACCTCCTGTGGATTCTTCTCTGA

## **Sgk1 isoform cloning into p-FLAG-CMV2**

Mouse Sgk1a:

TAGCAGAGCTCGTTTTAGTGACCGTCAGAATTGATCTACCATGGACTACAAAGACGATGAC  
GACAAGCTTGCGGCCGCAGCAACCGTCAAAGCCGAGGCTGCTCGAAGCACCCCTTACCTAC  
TCCAGAATGAGGGGAATGGTAGCGATTCTCATCGCTTTTATGAAACAGAGAAGGATGGGC  
CTGAACGATTTTATTGAGAAGATTGCCAGCAACACCTATGCATGCAAACACGCTGAAGTT  
CAGTCCATTTTGGAAAATGTCCCATCCTCAGGAGCCGGAGCTTATGAACGCTAACCCCTCT  
CCTCCGCCAAGTCCCTCTCAACAAATCAACCTGGGTCCGTCCTCCAACCCTCACGCCAAA  
CCCTCCGACTTTCCTTCTGAAAGTGATCGGAAAGGGCAGTTTTGGAAAGGTTCTTCTG  
GCTAGGCACAAGGCAGAAGAAGTATTCTATGCAGTCAAAGTTTTACAGAAGAAAGCCATC  
CTGAAGAAGAAAGAGGAGAAGCATATTATGTGAGAGCGGAATGTTCTGTTGAAGAATGTG  
AAGCACCCCTTTCCTGGTGGGCCTTCACTTCTCATTCCAGACCGCTGACAAGCTCTACTTT  
GTCTGGACTACATTAATGGTGGAGAGCTGTTCTACCATCTCCAGAGGGAGCGCTGCTTC  
CTGGAACCACGGGCTCGCTTCTACGCAGCTGAAATAGCCAGTGCCCTGGGCTATCTGCAC  
TCCCTAAACATCGTTTTATAGAGACTTAAAACCTGAGAATATTCTCCTAGACTCCCAGGG  
CACATCGTCTCACTGACTTTGGGCTCTGCAAAGAGAATATTGAGCATAACGGGACAACA  
TCTACCTTCTGTGGCAGCCTGAGTATCTGGCTCCTGAGGCTCCTCCATAAACAGCCGAT  
GACCCGGACTGGTGGTGTCTTGGGGCTGTCTGTATGAGATGCTCTACGGCCTG  
CCCCGTTTTTATAGCCGGAACACGGCTGAGATGTACGACAATATTCTGAACAAGCCTCTC  
CAGTTGAAACCAAATATTACAAACTCGGCAAGGCACCTCCTGGAAGGCCTCCTGCAGAAG  
GACCCGGACCAAGAGGCTGGGTGCCAAGGATGACTTTATGGAGATTAAGAGTCATATTTTC  
TTCTCTTTAATTAACTGGGATGATCTCATCAATAAGAAGATTACACCCCCATTTAACC  
AATGTGAGTGGGCCAGTGACCTTCGGCACTTCGATCCCAGTTTACCGAGGAGCCGGT  
CCCAGCTCCATCGGCAGGTCCCCTGACAGCATCCTTGTACGGCCAGTGTGAAGGAAGCA  
GCAGAAGCCTTCTCGGCTTCTCCTATGCACCTCCTGTGGATTCTTCTCTGAGTCGAC  
TCTAGAGGATCCCGGTGGCATCCCTGTGACCCCTCCCAGTGCCTCTCCTGGCCCTGGA  
AGTTGCCACTCCAGTGCCACCAGCCTTGTCTAATAAAATTAAGTTGCATCATTTTGT  
TGACTAGGTGTCTTCTATAATATTATGGGGTGGAGGGGGTGGTATGGAGCAAGGGGCA  
AGTTGGGAAGACAACCTGTAGGGCTGCGGGTCTATTGGGAACCAAGCTGGAGTGCAGT  
GGCACAATCTTGGCTCACTGCAATCTCCGCCTCCTGGGTTCAAGCGATTCTCCTGCCTCA  
GCCTCCCAGTTGTGGGATTCAGGCATGCATGACCAGGCTCAGCTAATTTTTGTTTT  
TTGGTAGAGACGGGTTTTACCATATTGGCCAGGCTGGTCTCCAACCTCTAATCTCAGGT  
GATCTACCCACCTTGGCCTCCCAAATGCTGGGATTACAGGCGTGAACCACTGCTCCCTT  
CCCTGTCTTCTGATTTTAAAATAACTATACCAGCAGGAGGACGTCCAGACACAGCATAG  
GCTACCTGGCCATGCCAACCAGGTGGGACATTTGAGTTGCTTGGCACTGTCTCTC  
ATGCGTTGGGTCCACTCAGTAGATGCCTGTTGAATTGGTAC

Mouse Sgk1b:

AGCAGAGCTCGTTTTAGTGAACCGTCAGAATTGATCTACCATGGACTACAAAGACGATGAC  
GACAAGCTTGCGGCCCGCAGCAGGCGAGTTACAGGGCGCGCTGGCTCGGGCTCGGCTCGAG  
TCCCTGCTCCGGCCCCGCCACAAAAGCGGGCGGAGGCTCAGAAAAGGAGCGAGTCCGTC  
CTGCTGAGCGGACTGGCTTTTTATGAAACAGAGAAGGATGGGCCTGAACGATTTTATTTCAG  
AAGATTGCCAGCAACACCTATGCATGCAAACACGCTGAAGTTCAGTCCATTTTGAAAATG  
TCCCATCCTCAGGAGCCGGAGCTTATGAACGCTAACCCCTCTCCTCCGCCAAGTCCCTCT  
CAACAAATCAACCTGGGTCCGTCCCTCCAACCCCTCACGCCAAACCCCTCCGACTTTCCTTC  
TTGAAAGTGATCGGAAAGGGCAGTTTTTGAAAGGTTCTTCTGGCTAGGCACAAGGCAGAA  
GAAGTATTCTATGCAGTCAAAGTTTTACAGAAGAAAGCCATCCTGAAGAAGAAAGAGGAG  
AAGCATATTATGTCAGAGCGGAATGTTCTGTTGAAGAATGTGAAGCACCCCTTTCCTGGTG  
GGCCTTCACTTCTCATTCCAGACCGCTGACAAGCTCTACTTTGTCTGGACTACATTAAT  
GGTGGAGAGCTGTTCTACCATCTCCAGAGGGAGCGCTGCTTCTGGAACCACGGGCTCGA  
TTCTACGCAGCTGAAATAGCCAGTGCCTGGGCTATCTGCACTCCCTAAACATCGTTTAT  
AGAGACTTAAACCTGAGAATATTCTCCTAGACTCCAGGGGCACATCGTCTCCTACTGAC  
TTTGGGCTCTGCAAAGAGAATATTGAGCATAACGGGACAACATCTACCTTCTGTGGCAGC  
CCTGAGTATCCGGCTCCTGAGGTCTCCATAAGCAGCCGTATGACCGGACGGTGGACTGG  
TGGTGTCTTGGGGCTGTCTGTATGAGATGCTCTACGGCCTGCCCCCGTTTTATAGCCGG  
AACACGGCTGAGATGTACGACAATATTCTGAACAAGCCTCTCCAGTTGAAACCAAATATT  
ACAACTCGGCAAGGCACCTCCTGGAAGGCCTTCTGCAGAAGGACCGGACCAAGAGGCTG  
GGTGCCAAGGATGACTTTATGGAGATTAAGAGTCATATTTTTCTTCTTTAATTAAGTGG  
GATGATCTCATCAATAAGAAGATTACACCCCATTTAACCCAAATGTGAGTGGGCCAGT  
GACCTTCGGCACTTCGATCCCGAGTTTACCGAGGAGCCGGTCCCAGCTCCATCGGCAGG  
TCCCCTGACAGCATCCTTGTACGGCCAGTGTGAAGGAAGCAGCAGAAGCCTTCTCCTGGC  
TTCTCCTATGCACCTCCTGTGGATTCTTCTCCTCTGAGTCGACTCTAGAGGATCCCGGGTG  
GCATCCCTGTGACCCCTCCCAGTGCCTCTCCTGGCCCTGGAAGTTGCCACTCCAGTGCC  
CACCAGCCTTGTCTAATAAAAATTAAGTTGCATCATTTTTGTCTGACTAGGTGTCTTTCTA  
TAATATTATGGGGTGGAGGGGGTGGTATGGAGCAAGGGGCAAGTTGGGAAGACAACCTG  
TAGGGCCTGCGGGTCTATTGGGAACCAAGCTGGAGTGCAGTGGCACAATCTTGGCTCAC  
TGCAATCTCCGCCCTCCTGGGTCAAGCGATTCTCCTGCCTCAGCCTCCCAGTGTGGG  
ATTCAGGCATGCATGACCAGGCTCAGCTAATTTTTGTTTTTTTTGGTAGAGACGGGGTTT  
CACCATATTGGCCAGGCTGGTCTCCAACCTCAATCTCAGGTGATCTACCCACCTTGGCC  
TCCCAAATTGCTGGGATTACAGGCGTGAACACTGCTCCCTTCCCTGTCTTCTGATTTT  
AAAATAACTATAACCAGCAGGAGGACGTCCAGACACAGCATAGGCTACCTGGCCATGCCCA  
ACCGTGGGACATTTGAGTTGCTTGGCTTGGCACTGTCTCTCATGCGTTGGGTCCACTCA  
GTAGATGCCTGTTGAATTGGGTACGCGCCAGCTTGGCTGTGGAA

Mouse Sgk1c:

GGAGAGCTCGTTTTAGTGACCGTCAGAATTGATCTACCATGGACTACAAAGACGATGACGA  
CAAGCTTGCGGCCCGCAGCAAAAAGAGGAGACCTTAAGATCCCCTTGAAAGCTTTTTATGAA  
ACAGAGAAGGATGGGCCTGAACGATTTTATTTCAGAAGATTGCCAGCAACACCTATGCATG  
CAAACACGCTGAAGTTCAGTCCATTTTGAAAATGTCCCATCCTCAGGAGCCGGAGCTTAT  
GAACGCTAACCCCTCTCCTCCGCCAAGTCCCTCTCAACAAATCAACCTGGGTCCGTCCCTC  
CAACCCCTCACGCCAAACCCCTCCGACTTTCCTTCTTGAAGTGATCGGAAAGGGCAGTTT  
TGGAAGGTTCTTCTGGCTAGGCACAAGGCAGAAGAAGTATTCTATGCAGTCAAAGTTTT  
ACAGAAGAAAGCCATCCTGAAGAAGAAAGAGGAGAAGCATATTATGTCAGAGCGGAATGT  
TCTGTTGAAGAATGTGAAGCACCCCTTCTGGTGGGCCTTCACTTCTCATTCCAGACCGC  
TGACAAGCTCTACTTTGTCTGGACTACATTAATGGTGGAGAGCTGTTCTACCATCTCCA  
GAGGGAGCGCTGCTTCTGGAACCACGGGCTCGATTCTACGCAGCTGAAATAGCCAGTGC  
CCTGGGCTATCTGCACCTCCCTAAACATCGTTTTATAGAGACTTAAAACCTGAGAATATTCT  
CCTAGACTCCCAGGGGCACATCGTCTCCTACTGACTTTGGGCTCTGCAAAGAGAATATTGA  
GCATAACGGGACAACATCTACCTTCTGTGGCAGCCTGAGTATCCGGCTCCTGAGGTCTC  
CCATAAGCAGCCGTATGACCGGACGGTGGACTGGTGGTGTCTTGGGGCTGTCTGTATGA  
GATGCTCTACGGCTGCCCCCGTTTTATAGCCGGAACACGGCTGAGATGTACGACAATAT  
TCTGAACAAGCCTCTCCAGTTGAAACCAAATATTACAACTCGGCAAGGCACCTCCTGGA  
AGCCCTTCTGCAGAAGGACCGGACCAAGAGGCTGGGTGCCAAGGATGACTTTATGGAGAT  
TAAGAGTCATATTTCTTCTCTTTAATTAAGTGGGATGATCTCATCAATAAGAAGATTAC

ACCCCCATTTAACCCAAATGTGAGTGGGCCAGTGACCTTCGGCACTTCGATCCCGAGTT  
TACCGAGGAGCCGGTCCCCAGCTCCATCGGCAGGTCCCCTGACAGCATCCTTGTACGGC  
CAGTGTGAAGGAAGCAGCAGAAGCCTTCCCTCGGCTTCTCCTATGCACCTCCTGTGGATT  
CTTCCCTCGAGTCGACTCTAGAGGATCCCGGGTGGCATCCCTGTGACCCCTCCCCAGTGC  
CTCTCCTGGCCCTGGAAGTTGCCACTCCAGTGCCCACCAGCCTTGTCTTAATAAAAATTAA  
GTTGCATCATTTTGTCTGACTAGGTGTCTTCTATAATATTATGGGGTGGAGGGGGGTGG  
TATGGAGCAAGGGGCAAGTTGGGAAGACAACCTGTAGGGCTGCGGGGTCTATTGGGAAC  
CAAGCTGGAGTGCAGTGGCACAATCTTGGCTCACTGCAATCTCCGCCTCCTGGGTCAAG  
CGATTCCTCCCTCAGCCTCCCGAGTTGTTGGGATTCCAGGCATGCATGACCAGGCTCA  
GCTAATTTTTTGTTTTTTTGGTAGAGACGGGGTTTACCATATTGGCCAGGCTGGTCTCCA  
ACTCCTAATCTCAGGTGATCTACCCACCTTGGCCTCCCAAATTGCTGGGATTACAGGCGT  
GAACCACTGCTCCCTTCCCTGTCTTCTGATTTTTAAAATAACTATAACCAGCAGGAGGACG  
TCCAGACACAGCATAGGCTACCTGGCCATGCCCAACCGGTGGGACATTTGAGTTGCTTGC  
TTGGCACTGTCTCTCATGCGTTGGGTCCACTCAGTAGATGCCTGTTGAATTGGGTACGC  
GGCCAGCTTGGCTGTGGAATGTGTGTC

Mouse Sgk1d:

GCAGAGCTCGTTTTAGTGACCGTCAGAATTGATCTACCATGGACTACAAAGACGATGACGA  
CAAGCTTGCGGCCGCAGCAGTAAACAAAGACGCAAATGGATTCCCAGTCAAGAAATGCTC  
AGCGTTCCAATTTTTTAAGAAACGGGTACGAAGATGGATCAAGAGCCCCATGGTCAGCGT  
GGACAAGCATCAGAGCCCCAAGTGAAGTACACTGGCCCTGCTGGGGTGCATCTTCCCC  
TGGGGAGTCAGACTTTGAGGCCATGTGTCAATCATGCCTGGGTGACCATGCTTTCAAAG  
GGGATGCTCCCTCCAGAGGAGTCTGTTCCTGGGAGATCCAACCTGGGTGTGAAGTGAA  
AGAACAATGTAATCATGCCAACATCCTGACCAAGCCGGACCCAAGAACCTTCTGGACTAA  
TGATGATGCAGCTTTTATGAAACAGAGAAGGATGGGCCTGAACGATTTTTATTGAGAAGAT  
TGCCAGCAACACCTATGCATGCAAACACGCTGAAGTTCAGTCCATTTTGAAAATGTCCCA  
TCCTCAGGAGCCGGAGCTTATGAACGCTAACCCCTCTCCTCCGCAAGTCCCTCTCAACA  
AATCAACCTGGGTCCGTCTTCCAACCTCACGCCAAACCCCTCCGACTTTCACCTTCTTGAA  
AGTGATCGGAAAGGGCAGTTTTGGAAAGGTTCTTCTGGCTAGGCACAAGGCAGAAGAAGT  
ATTCATATGCAGTCAAAGTTTTACAGAAGAAAGCCATCCTGAAGAAGAAAGAGGAGAAGCA  
TATTATGTACAGACCGAATGTTCTGTTGAAGAATGTGAAGCACCCCTTCTGGTGGGCCT  
TCACCTTCATCCAGACCGCTGACAAGCTTACTTTGTCTTGACTACATTAATGTTGG  
AGAGCTGTTTACCATCTCCAGAGGGAGCGTCTTCTGGAACCACGGGCTCGATTCTA  
CGCAGCTGAAATAGCCAGTGCCCTGGGCTATCTGCACTCCCTAAACATCGTTTATAGAGA  
CTTAAAACCTGAGAATATTCTCCTAGACTCCCAGGGGCACATCGTCCTCACTGACTTTGG  
GCTCTGCAAAGAGAATATTGAGCATAACGGGACAACATCTACCTTCTGTGGCACGCCTGA  
GTATCTGGCTCCTGAGGTCTCCATAAGCAGCCGTATGACCGGACGGTGGACTGGTGGTG  
TCTTGGGGCTGTCTGTATGAGATGCTCTACGGCCTGCCCCCGTTTTATAGCCGGAACAC  
GGCTGAGATGTACGACAATATTCTGAACAAGCCTCTCCAGTTGAAACCAAATATTACAAA  
CTCGGCAAGGCACCTCCTGGAAGGCCTCCTGCAGAAGGACCGGACCAAGAGGCTGGGTGC  
CAAGGATGACTTTATGGAGATTAAGAGTCATATTTTCTTCTCTTTAATTAAGTGGATGA  
TCTCATCAATAAGAAGATTACACCCCATTTAACCCAAATGTGAGTGGGCCAGTGACCT  
TCGGCACTTCGATCCCGAGTTTACCAGGAGCCGGTCCCAGCTCCATCGGCAGGTCCCC  
TGACAGCATCCTTGTACGGCCAGTGTGAAGGAAGCAGCAGAAGCCTTCCCTCGGCTTCTC  
CTATGCACCTCCTGTGGATTCCCTCCTCTGAGTCGACTCTAGAGGATCCCGGGTGGCATC  
CCTGTGACCCCTCCCCAGTGCCTCTCCTGGCCCTGGAAGTTGCCACTCCAGTGCCACCA  
GCCTTGTCTAATAAAAATTAAGTTGCATCATTTTGTCTGACTAGGTGTCTTCTATAATA  
TTATGGGGTGGAGGGGGTGGTATGGAGCAAGGGGCAAGTTGGGAAGACAACCTGTAGGG  
CCTGCGGGGTCTATTGGGAACCAAGCTGGAGTGCAGTGGCACAATCTTGGCTCACTGCAA  
TCTCCGCTCCTGGGTTCAAGCGATTCTCCTGCCTCAGCCTCCCGAGTTGTTGGGATTCC  
AGCATGCATGACAGGCTCAGCTAATTTTTTGTTTTTTTGGTAGAGACGGGGTTTACCA  
TATTGGCCAGGCTGGTCTCCAACCTAATCTCAGGTGATCTACCCACCTTGGCCTCCCA  
AATTGCTGGGATTACAGGCGTGAACCACCTGCTCCCTTCCCTGTCTTCTGATTTTTAAAAT  
AACTATAACCAGCAGAGGAC

## **Publications and presentations arising from the work presented in this thesis**

**Nigel A. Daniels**, Trevor R. Jackson and Mike A. Gray. *Aldosterone regulates the expression of multiple isoforms of serum and glucocorticoid regulated kinase1 in mouse cortical collecting duct epithelial cells.* Poster presentation at the Physiological Society Themed Meeting "Epithelial form, function and environment", Newcastle upon Tyne - 6-8/Sep/2009.

**Nigel A. Daniels**, Mike A. Gray and Trevor R. Jackson. *Investigation of transcriptional variants of SGK1 in regulation of sodium transport in renal cortical collecting duct cells.* Oral presentation at the Epithelial Biology Meeting, Dundee - 11-12/Sep/2008.

**Nigel A. Daniels**, Mike A. Gray and Trevor R. Jackson. *A Role for PI 3-kinase in Mouse Renal Cortical Collecting Duct Ion Transport.* Poster presentation at the Newcastle University School of Clinical and Laboratory Sciences Research Day - 8/Jul/2008.

**Nigel A. Daniels**, Mike A. Gray and Trevor R. Jackson. *Aldosterone Inducible Expression of Multiple SGK1 Isoforms in a Kidney Cortical Collecting Duct Model Cell Line.* Oral presentation at the Newcastle University Dermatology Research in Progress Meeting - 29/Feb/2008.

**Nigel A. Daniels**, Mike A. Gray and Trevor R. Jackson. *Investigation of the role of novel SGK1 isoforms in regulation of sodium transport in kidney epithelial cells.* Oral presentation at the Newcastle University Epithelial Research Group PhD Student Presentations - 13/Feb/2008.

**Nigel A. Daniels**, Mike A. Gray and Trevor R. Jackson. *Aldosterone-inducible expression of multiple splice variants of Sgk1 in a mouse cortical collecting duct model cell line.* Poster presentation at the Newcastle University School of Clinical and Laboratory

Sciences Postgraduate Poster Night - 21/Nov/2007 (commended) and at the Newcastle University Medical Faculty Graduate School Poster Evening - 10/Mar/2008.

**Nigel A. Daniels**, Mike A. Gray and Trevor R. Jackson. *Investigation of the role of novel SGK1 isoforms in regulation of sodium transport in kidney epithelial cells.* Oral presentation at the Newcastle University Dermatology Group Lab Meeting - 11/May/2007.

**Nigel A. Daniels**, Mike A. Gray and Trevor R. Jackson. *Novel SGK1 Isoforms in Regulation of Renal Sodium Uptake.* Oral presentation at the Newcastle University Dermatology Group Away Day - Dec/2006.